R. C. Bauer

AEDC-TR-82-27

Two-Component Simultaneous LDV Turbulence Measurements in an Axisymmetric Nozzle Afterbody Subsonic Flow Field with a Cold, Underexpanded Supersonic Jet

F. L. Heltsley and F. L. Crosswy
Calspan Field Services, Inc.

June 1983

Final Report for Period October 1, 1980 – September 30, 1982

Approved for public release; distribution unlimited.

ARNOLD ENGINEERING DEVELOPMENT CENTER
ARNOLD AIR FORCE STATION, TENNESSEE
AIR FORCE SYSTEMS COMMAND
UNITED STATES AIR FORCE

APPROVAL STATEMENT

This report has been reviewed and approved.

Robert H. Nichols

ROBERT H. NICHOLS
Directorate of Technology
Deputy for Operations

Approved for publication:

FOR THE COMMANDER

Marion L. Laster

MARION L. LASTER
Director of Technology
Deputy for Operations

UNCLASSIFIED

SECURITY CLASSIFICATION OF THIS PAGE (When Data Entered)

REPORT DOCUMENTATION PAGE		READ INSTRUCTIONS BEFORE COMPLETING FORM
1. REPORT NUMBER AEDC-TR-82-27	2. GOVT ACCESSION NO.	3. RECIPIENT'S CATALOG NUMBER
4. TITLE (and Subtitle) TWO-COMPONENT SIMULTANEOUS LDV TURBULENCE MEASUREMENTS IN AN AXISYMMETRIC NOZZLE AFTERBODY SUBSONIC FLOW FIELD WITH A COLD, UNDEREXPANDED SUPERSONIC JET		5. TYPE OF REPORT & PERIOD COVERED Final Report, October 1, 1980 - September 30, 1982 6. PERFORMING ORG. REPORT NUMBER
7. AUTHOR(s) F. L. Heltsley and F. L. Crosswy, Calspan Field Services, Inc.		8. CONTRACT OR GRANT NUMBER(s)
9. PERFORMING ORGANIZATION NAME AND ADDRESS Arnold Engineering Development Center /DOT Air Force Systems Command Arnold Air Force Station, TN 37389		10. PROGRAM ELEMENT, PROJECT, TASK AREA & WORK UNIT NUMBERS Project No. D202PW
11. CONTROLLING OFFICE NAME AND ADDRESS Arnold Engineering Development Center/DOS Air Force Systems Command Arnold Air Force Staion, TN 37389		12. REPORT DATE June 1983 13. NUMBER OF PAGES 124
14. MONITORING AGENCY NAME & ADDRESS(if different from Controlling Office)		15. SECURITY CLASS. (of this report) UNCLASSIFIED 15a. DECLASSIFICATION/DOWNGRADING SCHEDULE N/A

16. DISTRIBUTION STATEMENT (of this Report)

Approved for public release; distribution unlimited.

17. DISTRIBUTION STATEMENT (of the abstract entered in Block 20, if different from Report)

18. SUPPLEMENTARY NOTES

Available in Defense Technical Information Center (DTIC).

19. KEY WORDS (Continue on reverse side if necessary and identify by block number)

wind tunnel tests
flow fields
turbulent flow
supersonic flow
laser velocimeters
flow separation
static pressure

20. ABSTRACT (Continue on reverse side if necessary and identify by block number)

A test was conducted to obtain nonintrusive measurements in the flow field about an axisymmetric nozzle afterbody with a cold, underexpanded jet, M_j=1.563, in a parallel free stream, M_∞ = 0.6. Reynolds shear stress and two components of mean velocity and turbulence intensity were measured using a two-color Bragg-diffracted laser Doppler velocimeter. Additional experimental data include the afterbody surface pressure distribution and laser vapor screen flow visualization of the jet plume. A multiple seeding technique was used to investigate the bimodal velocity probability distributions observed in the jet mixing region.

DD FORM 1 JAN 73 1473 EDITION OF 1 NOV 65 IS OBSOLETE

UNCLASSIFIED

SECURITY CLASSIFICATION OF THIS PAGE (When Data Entered)

PREFACE

The work reported herein was conducted by the Arnold Engineering Development Center (AEDC), Air Force Systems Command (AFSC). The AEDC project manager was Mr. Robert Nichols. The results were obtained by Calspan Field Services, Inc., AEDC Division, operating contractor for Aerospace Flight Dynamics testing at AEDC, AFSC, Arnold Air Force Station, Tennessee, under Project Number D202PW (P32G-B73). The manuscript was submitted for publication on November 18, 1982.

Appreciation and acknowledgement are extended to R. C. Bauer and Dr. E. M. Kraft for sharing their insight into topics relating to this investigation.

CONTENTS

ILLUSTRATIONS

APPENDIXES

1.0 INTRODUCTION

A significant need has existed for several years to predict the flow fields about nozzle afterbodies in the transonic regime with reliability. Considerable effort has gone into providing computational techniques capable of simulating the afterbody geometry as well as the blockage and entrainment effects of the jet efflux. The lack of accurate experimental data has been a major restriction to the development and subsequent validation of adequate methods. The laser Doppler velocimeter (LDV) has made it possible to obtain nonintrusive measurements in highly turbulent flow fields, often with embedded shock waves, shear surfaces, and/or regions of separated flow (Refs. 1 through 9).

The purpose of this investigation was to measure model surface pressures and flow-field velocities for an axisymmetrical afterbody with an underexpanded supersonic jet exhausting using a two-color two-component Bragg cell-diffracted LDV system in the Arnold Engineering Development Center (AEDC) Aerodynamic Wind Tunnel (1T) of the Propulsion Wind Tunnel (PWT) Facility.

2.0 APPARATUS

2.1 TEST FACILITY

The AEDC Tunnel 1T is a continuous flow, open-circuit wind tunnel that can be operated over a Mach number range from 0.20 to 1.50. The tunnel operates at a constant stagnation presure of approximately 2,850 psfa with a capability of varying the stagnation temperature from 80 to 120°F above ambient temperature. A complete description of the facility is included in Ref. 10.

Standard 6-percent perforated test section top and bottom walls were used during the test. The side wall nearest the LDV was a flat-ground and polished optical quality window. The far side wall was solid aluminum.

A plan view of the Tunnel 1T test area showing the LDV system installation is presented in Fig. 1. Two fluidized bed particle seeders shown in the figure were used to introduce seed particles into the flow and thus provide scatter centers for the LDV. The seeders and their operation are described in Section 2.4.

2.2 TEST ARTICLE AND SUPPORT STRUT

The experimental data were acquired using a 14.697-in.-long axisymmetric body with a maximum diameter of 0.986 in. Afterbody internal and external contours are presented in

Fig. 2. The test article was positioned on the tunnel centerline by a floor-mounted strut as illustrated in Fig. 2b. Channels were provided within the strut for passage of instrumentation and for transmission of high-pressure gas to the (1.268) 1.221 exit-to-throat area ratio nozzle. Figure 3 is a photograph of the model installed in Tunnel 1T. The LDV optical bench can be seen through the test section and plenum windows on the far side of the wind tunnel.

2.3 HIGH-PRESSURE GAS SUPPLY SYSTEM

The piping system shown schematically in Fig. 4 was used during the subject test to supply pressure-controlled, temperature-conditioned, dry nitrogen for the model jet exhaust. The multi-venturi metering station provided three different venturi throat diameters. System operation could thus be optimized by selecting the combination of venturis having a combined throat area nearest the desired value. Primary pressure control was maintained by a pneumatically controlled regulator located between the supply tank and the metering station. The nitrogen tube was brought to operating temperature by heating it in a concentric-tube steam heat exchanger. A rupture disc was installed between the metering station and the test area to protect the model from inadvertent overpressure.

2.4 FLUIDIZED BED PARTICLE SEEDERS

The installation included two fluidized bed particle seeders (Fig. 5) designed to dispense a solid particle aerosol into the airstream. The high pressure configuration (Fig. 5a) was installed in the nitrogen supply system (Fig. 4) for introducing seed into the jet flow. Seeding rate was controlled by diverting a small portion of the already metered high-pressure nitrogen into the seeder, up through the continuously agitated particle bed, and back into the jet supply line (Fig. 1).

Tunnel free-stream seeding was accomplished by passing pressure-regulated dry nitrogen through the low pressure seeder illustrated in Fig. 5b. Particles were either introduced into the tunnel stilling chamber or upstream of the tunnel compressor. The latter procedure provided a uniform particle number density throughout the test section while the former produced a more localized "stream tube" seed pattern with unacceptable lateral density gradients. Although the steam tube technique reduced the seeding material consumption by an estimated 50 to 1, whole tunnel seeding was used during most of the test.

Aluminum oxide powder with a nominal particle diameter of 1μm was used in both seeding devices. Whole tunnel seeding resulted in a powder consumption rate of roughly 0.8 lb per 40 hr of testing. Significantly less consumption was required for jet seeding because of the relatively lower mass flow.

2.5 INSTRUMENTATION

2.5.1 Pressure and Temperature

The test article was instrumented with 32 static pressure orifices distributed over the afterbody external surface, including four at $\ell = 0$ on the aft-facing nozzle lip. Positions of the orifices are given in Fig. 6. These pressures were measured by the standard Tunnel 1T pressure system consisting of five gauged 48-port Scanivalves®, each with a 15-psid transducer.

Four additional static orifices were located within the nozzle plenum chamber. Strain-gage transducers with a range from 0 to 500 psia were used to measure these pressures.

Two copper-constantan thermocouples were located in the gas supply line just upstream of the model to measure gas temperature for computation of nozzle mass flow.

Instrumentation for the venturi metering station included one copper-constantan thermocouple and four strain gage pressure transducers. The thermocouple and a 0 to 2,000 psia transducer measured supply gas conditions, and three 0 to 1,000 psia transducers measured venturi throat static pressure.

2.5.2 Flow Field Velocity

A two-color Bragg cell-diffracted LDV system was used to obtain two-component simultaneous velocity measurements in the model flow field. The optical system shown schematically in Fig. 7 includes a 5-w argon laser, transmitting optics, receiving optics, and photomultiplier photodetectors. The multiline output of the laser was split into its six consituent lines by a multiple prism assembly. Mirrors were used to pick off the two most powerful lines or colors. The blue 488.0-nm and green 514.5-nm lines were used to generate an orthogonal arrangement of interference fringes within a small (0.3-mm by 2.0-mm) ellipsoidal probe volume. Conceptual drawings of the fringe pattern associated with each color and the pattern's orientation relative to the measurement coordinate system are presented in Fig. 8. The x-, y-, and z-axes shown in Figs. 7 and 8 are rectangular Cartesian coordinates which coincide respectively with tunnel axial (positive downstream), the horizontal crossflow (positive left looking downstream), and vertical (positive up) directions. The Bragg cell-induced fringe travel indicated in Fig. 8 permits discrimination of positive and negative particle velocities. A complete description of the LDV data acquisition system and signal processing technique is contained in Ref. 9.

The probe volume was positioned in the flow field by moving the entire optical system on a three degree-of-freedom tranversing table also described in Ref. 9. Probe volume location was expressed in x, y, z coordinates relative to an origin at the model nozzle exit center.

3.0 PROCEDURE

3.1 TEST CONDITIONS

The experiment involved a single test condition at a free-stream Mach number of 0.6 with a tunnel stagnation temperature of 640° R. The Mach 1.563 nozzle was operated with a tunnel matched stagnation temperature of 640° R and at an underexpanded nozzle static pressure ratio of 4.5 (nozzle exit static to tunnel free-stream static).

The test condition was attained by setting the appropriate free-stream Mach number, regulating the nozzle plenum pressure to provide the desired exit static pressure ratio, and adjusting the steam heater for a proper nitrogen stagnation temperature.

3.2 LDV DATA ACQUISITION

3.2.1 Measurement Locations

The test was designed to produce the maximum useful flow-field information within the time allocated. The velocimeter was set up to measure the tunnel axial, x, and vertical, z, components of velocity. With the assumption of axial symmetry, the positive z-component is interchangeable with the r-component in the vertical plane containing the model centerline ($y = 0$). The initial strategy was to obtain a series of well-defined constant x profiles at selected stations along the model axis. Adequate flow-field definition generally required measurements at more frequent intervals in the radial direction than in the axial since stronger gradients were encountered normal to the jet axis. The jet profiles were extended well across the model centerline to verify the assumption of axisymmetric flow.

In addition to the vertical profiles, two constant radius surveys were made within the jet to determine if Mach discs were present and, if so, to record their positions. Another constant radius survey at $r/D = 1.5$ was made to provide data for a relatively far field computational boundary.

3.2.2 Multiple Seeding

The unexpected appearance of bimodal axial velocity histograms (probability distributions) along the jet plume boundary prompted a modification of the LDV aquisition procedure. Either or both modes could be produced by variation of jet to free-stream seeding ratio. One mode was apparently caused by seed particles which were exhausted from the nozzle along with the jet fluid (jet seed). The other mode resulted from seed originating in the tunnel flow (free-stream seed) being drawn toward the jet centerline.

To understand more fully the mechanism involved, three separate velocity measurements were obtained at each point within the affected region. Constant x velocity profiles were first obtained with only the jet seeder operating. These jet seed profiles extended up from below the model centerline until the data rate dropped to less than one percent of the original value. Then, with only the tunnel flow seeder on, free-stream velocity profiles were extended down into the jet until a similar low data rate was encountered. Finally, with both seeders adjusted to provide "equal" particle number density in the jet and free stream, the measurements were repeated and the same points in the region of jet/free-stream profile overlap.

3.3 DATA REDUCTION

Wind tunnel flow conditions were determined using the standard Tunnel 1T calibration equations for closed side walls and perforated top and bottom walls. Nitrogen mass flow through the venturi metering station and the converging-diverging nozzle was calculated using the equations in Ref. 11, as were the jet plume aerodynamic properties.

3.4 UNCERTAINTY OF MEASUREMENT

Estimated uncertainties for various test parameters are as follows:

$M_\infty \pm 0.004$	$V_x \pm 10$ ft/sec
$C_p \pm 0.011$	$V_r \pm 10$ ft/sec
NSPR $\pm$ 0.117	x/D $\pm$ 0.018
$V_e \pm 14$ ft/sec	r/D $\pm$ 0.005
$T_t \pm$	

The ± 10 ft/sec uncertainty quoted for the LDV mean velocity component measurements, V_x and V_r, does not include systematic bias errors which can usually be determined and removed. Each LDV data acquisition session was begun with several velocity measurements at a predetermined "reference point" in the flow field. Day-to-day comparison of these data provided a basis for assessment of long term measurement system variation.

The standard deviation of the radial velocity component probability distribution measured at the reference point was found to be generally higher than that of the corresponding axial data. The instrument broadening discussed in Ref. 3 is thought to be mainly responsible for the effect. However, experimental data obtained during a flow angularity probe dynamic calibration revealed a time dependency in the Tunnel 1T test section vertical velocity. The fluctuation, apparently caused by the orientation of the tunnel's primary compressor, was not detected in either horizontal velocity component.

Since the uncertainty in the actual standard deviation level of the two velocity components has not been resolved, the data are presented as measured.

Two potential mean velocity uncertainties can result from the time dependencies observed within the subject flow field. Both error sources discussed in Ref. 12 are related to temporal variations in particle flux. In the first case the indicated mean velocity is biased toward the high velocity end of the probability distribution because more particles per unit time pass through the probe volume during periods of high velocity than during equally long periods of low speed flow. The resulting error is correctable if the local velocity magnitude is known and if the particle number density is uniform throughout the field.

The second, and often more severe uncertainty, is more difficult to deal with since the changes in particle flux are caused by passage through the focal volume of flow which has a velocity correlated but generally unknown nonuniform particle number density. This situation was observed along the jet plume/free-stream interface. As already discussed in Section 3.2.2, the particle number density was forced to be as uniform as possible by carefully adjusting the seeding rates in the jet and free-stream flows.

Time-dependent characteristics observed in other regions of the flow field were similar. Since they involved only fluid from a single source, however, the nonuniform seeding rate could not be eliminated. The indicated mean velocities in one suspect region, discussed later in Section 4.1.3, are thought to have been biased toward the attached flow values. If so, and if an intermittent separation was present, the fluid which was drawn upstream into the separated region during periods of flow separation would have contained fewer particles than the attached flow. Since both the attached and reversed flow originated in the uniformly seeded free stream, some mechanism must have existed in the flow field which redistributed the particles. The effects of such mechanisms have been observed in standing vortices, steady boundary layers and wake flows, as well as in intermittent boundary-layer separations and vortex streets. Although particle dynamics are responsible, in most instances, for the seed redistribution, the actual level of particle lag error may be too small to detect in the local mean velocity measurements. The particle number density at a point in the flow field is a cumulative function of the differences in particle and fluid velocity upstream of that point. Therefore, significant variation in particle distribution may occur within some flows.

Calculations[7] indicate that direct particle lag uncertainty was less than one percent throughout most of the flow field, including the jet plume. Somewhat larger errors were present immediately downstream of the nozzle exit and the normal shock on the model centerline.

4.0 RESULTS AND DISCUSSION

4.1 AFTERBODY FLOW FIELD

4.1.1 Computational Boundary Measurements

Longitudinal LDV surveys were made at r/D = 1.5 and 1.35 to obtain input boundary condition information for future numerical flow-field computations. Data were taken at both r/D positions for each of the 29 x/D stations in the survey.

The scatter in the resulting velocity distributions shown in Fig. 9 reflects the estimated 1.5-percent uncertainty in the LDV measurements. Some type of smoothing would be required to condition the data for input into a computational code.

4.1.2 Boundary-Layer Profiles and Flow Separation

Radial LDV surveys between the computational boundary and the model surface were made at 13 axial stations along the afterbody. Mean velocity vectors for those over the boattail are illustrated in Fig. 10. Rectangles indicate turbulence intensity levels in the x- and r-directions at that location. The height and width of each rectangle are proportional to the standard deviations (turbulence levels) in the radial and axial velocity measurements, respectively.

The distributions of axial velocity for each constant x/D survey are presented in Fig. 11. The velocity profiles indicate that no large region of mean flow separation was present near the model surface. However, a comparison of the experimental measurements of axial turbulence intensity in Ref. 13 with the present results suggests that separation was present. The axial turbulence intensity at x/D = 0 shown in Fig. 10 increases with decreasing radius to a maximum within the boundary layer. The value then becomes significantly smaller near the surface. In Ref. 13, measurements in a separated flow produced a similar distribution, whereas an attached flow distribution did not include the decrease in intensity near the surface.

In addition, an accumulation of dust similar to that associated with separated flow appeared on the afterbody from x/D = −0.5 to 0 during each test period.

The evidence suggests that a thin separated zone could have existed in the sublayer, so close to the surface that it was undetected by the nearest LDV velocity measurement. The more likely possibility is that an intermittent, time-dependent flow separation was present. A

small region in the flow field immediately downstream of the aft facing model base was found to be "transparent" to the LDV; i.e., the fluid there contained no particles large enough to provide a measurable signal. Experience has shown that an intermittent flow reversal can go undetected if the fluid swept upstream contains relatively few particles. It is reasonable to assume that such an intermittent separation could exist downstream of $x/D = -0.5$, alternately containing either particle-laden fluid from the free stream or "transparent" fluid from the aft facing base region. The LDV would "see" and record only the velocities of the free-stream seed.

In some instances seed can be introduced into the sparsely seeded fluid and thus reduce or correct the biasing effect upon the measurement. Such a flow situation appears to have existed along the boundary of the jet turbulent mixing region and will be discussed in Section 4.2.

4.1.3 Static Pressure Distribution

The afterbody static pressure distribution presented in Fig. 12 rules out any large mean flow separation as do the LDV measurements. The pressure data do not, however, rule out a zone of intermittent or sublayer separation. In fact, a slight positive shift in pressure can be seen in the distribution at $x/D = -0.5$, where the dust deposit begins.

4.2 TURBULENT JET PLUME

4.2.1 Constant r/D Surveys

Two longitudinal LDV surveys were done within the jet plume, one at $r/D = 0.19$ and the other on the model centerline. The resulting mean velocity distributions presented in Fig. 13 are quite different. The data indicate that the centerline flow passed through a normal shock (Mach disc) in the vicinity of $x/D = 1$. The flow along the $r/D = 0.19$ survey line remained fully supersonic. It should be mentioned that the nozzle flow was slightly unsymmetrical with an initial upward flow angle of approximately 3.5 deg at the exit centerline. The angularity decreased to less than half a degree by $x/D = 0.4$ and remained so for the remainder of the survey.

Figure 13b reveals that the probability distributions in the vicinity of the shock wave either are or tend to be bimodal. Based upon available evidence, the shock appears to be oscillating in the axial direction between two discrete locations, namely $x/D = 0.97$ and $x/D = 1.25$, spending minimal time in between. Either the vortex-street structure of a jet boundary described in Ref. 14 or the wave-like contorted boundary of a jet proposed in Ref. 15 could furnish a suitable explanation for the observed shock motion. In both cases, the

fluctuating character of the jet/external flow boundary would tend to modulate the near field pressure. Feeding in all directions via the subsonic free stream, the pressure variations could conceivably influence the flow to either shock down prematurely or sustain the supersonic Mach numbers farther downstream.

4.2.2 Constant x/D Surveys

In addition to the longitudinal surveys, eight radial LDV profiles were made at selected stations along the jet plume. The seeding technique described in Section 3.2 was used, and the surveys were extended from below the jet centerline, across the plume, and well into the external stream. Mean velocity vectors are illustrated separately for the three seeding procedures in Fig. 14. The distribution of mean axial velocity is presented in Fig. 15 for each individual x-station.

The letters on each profile signify certain key characteristics common to most of the data. The $x/D = 3$ distribution in Fig. 15g is a typical example of the profiles aft of the Mach disc. According to the jet seeded measurements, the maximum jet velocity occurred at a point Aj, away from the plume centerline, followed by a sharp decrease in velocity to a plateau somewhat higher than the external stream, and finally followed by another decrease at Bj, to the point Cj, where the data rate became negligible. The free-stream seeded profile exhibited no significant increase in velocity until well within the turbulent mixing region. In fact, the velocity decreased slightly before the rapid increase at point G_{fs}. The region of relatively low velocity appears to have been a remnant of the model boundary layer, thickened by the adverse pressure gradient over the boattail. The point C_{fs} at the end of the profile identifies the extent of free-stream seed penetration into the jet, marked by an extremely low data rate.

The velocity distribution resulting from the dual seeded measurements looked much like a conventional turbulent mixing profile. Dual seeded measurements matched the free-stream seeded measurements at the outer edge of the mixing region, E_{fs}, matched the jet seed measurements deep within the jet, E_j, and smoothly transitioned from one profile to the other in between.

Two additional key profile characteristics which are often used in the discussion of shear flows can be identified in the jet seeded profile. One is the radius at which the maximum gradient in axial velocity with respect to the radial coordinate occurs. Two such maximum gradients are present at $x/D = 3$. The first and primary one, $M1_j$, is near the center of the conventional turbulent mixing profile between points E_{fs}, and A_j. The second, $M2_j$, lies between A_j and the centerline and is associated with a secondary shear layer trailing downstream from the Mach disc near $x/D = 1$.

The other key point on the profile is the half-velocity radius H_j. Defined here in terms of other profile characteristics, it is the radius where the velocity is equal to the average of the velocities at the point A_j, and the free-stream velocity.

Using an alternate definition to determine the half-velocity radius H_j, the free-stream velocity would be replaced by the minimum velocity occurring in the free-stream seeded profile at the radius G_{fs}. This less conventional but perhaps more realistic approach accounts for the residual velocity deficit caused by the body boundary layer. The difference would be significant in the Fig. 15 profiles upstream of x/D = 1 and could result in even larger discrepancies in situations involving major flow separation and/or flow reversal.

4.2.3 Analysis of x/D = 3 Data

The data obtained by the LDV contain significantly more information than the mean velocity values presented in Fig. 15. Simultaneous two-component velocity measurements for a large number of discrete particles passing through the focal volume can provide invaluable insight into the statistical characteristics of the flow. Selected data from x/D = 3 are presented in Figs. 16, 17, and 18. The radial distributions of several sample statistical parameters are shown in Fig. 16. Axial velocity histograms are illustrated in Fig. 17. Individual particle velocities, plotted as two-dimensional velocity distributions, are presented in Fig. 18. The letters introduced in the previous section to identify key profile characteristics have been included where appropriate.

Two relative maxima are present in the Fig. 16a distribution of radial velocity for jet seeding. One corresponds to the point of maximum gradient in the axial velocity profile, $M1_j$, while the other occurs at the point B_j at the outer end of the axial velocity plateau. The jet seeded radial velocity measurements were generaly positive, away from the centerline. The free-stream seeded radial velocities were negative, into the jet, except in the vicinity of the maximum axial velocity gradient.

A primary feature of the Fig. 16b standard deviation distribution is the large peak in S_x/V_∞ for the jet seeded data. This places the maximum axial turbulence intensity at $r/D \approx 0.35$, slightly toward the jet centerline from the half-velocity radius, H_j, at r/D = 0.378. The peak position coincides with the point of maximum slope in the axial velocity distribution, $M1_j$, which is consistent with the experimental data in Ref. 5. The relative maximum at the jet centerline apparently resulted from the oscillation of the Mach disc near x/D = 1.

Another significant observation about the Fig. 16b measurements is the appearance of low turbulence, free-stream flow well within the jet mixing region. At the same time the jet

seeded data indicate that the relatively high axial turbulence levels associated with the jet flow were observed from the jet centerline to the outer edge of the jet, C_j. This implies that the free-stream fluid which penetrated into the jet maintained both its characteristic low turbulence and mean velocity (Fig. 16a). Similarly, jet fluid which reached the outer extremes of the mixing region remained relatively highly turbulent and traveled faster than any free-stream fluid which was observed at the same location.

The same conclusion can be drawn from the Fig. 17 histograms and Fig. 18 velocity distributions. The flow in each regime carries with it a distinct velocity/turbulence "signature." The fact that the signatues from either or both regimes could be observed essentially unaltered over much of the mixing zone suggests a process in which the two fluids were somehow distributed about the region without being "mixed" in the steady state, homogeneous sense. A hypothetical model of such a process will be discussed in the next section.

The Reynolds shear stress and turbulence kinetic energy distributions are presented in Fig. 16c. The shape of the latter distribution is very much like that of the axial turbulence intensity of Fig. 16b, since the radial turbulence intensity variation with radius was small. Both Reynolds shear stress and turbulent kinetic energy reach maximum values near the radius, $M1_j$, where the axial velocity gradient is maximum (Refs. 3 and 5). Another axial velocity gradient-related maximum in Reynolds shear occurs ar $r/D \approx 0.08$ which coincides with the radius, $M2_j$. In this instance the shear stress is negative since the velocity gradient is of opposite sign (Fig. 16a).

The variation of velocity sample skewness at $x/D = 3$ is presented in Fig. 16d. As in Refs. 5 and 6, the values of the axial component skewness, SK_x, are negative from the radius of maximum axial velocity, A_j, outward to the half-velocity radius H_j. At that point the skewness changes sign and remains positive for the remainder of the jet seeded measurements. The dual seeded histograms become significantly more positively skewed in the intermittent region, attaining a maximum value near the edge of the jet. The skewness then abruptly decreases and again changes sign. Finally, the slight negative skewness disappears as the histograms become Gaussian, as evidenced by the free-stream seeded data.

The reason for the differences between the three seeding condition results is clearly shown by the actual histograms in Fig. 17. The jet seeded and free-stream seeded samples produced their characteristic single mode, nearly normal probability distributions except at the extreme ends of their respective surveys, C_j and C_{fs}. The highly skewed, dual seeded distributions appearing between $r/D = 0.45$ and $r/D = 0.65$ were produced by the combination of turbulent, high-speed flow measurements with relatively larger numbers of lower velocity, nonturbulent free-stream seeded flow samples near the jet edge. The typical

resulting histogram was heavily weighted toward the low velocity end of the distribution, producing the classical positively skewed shape (Fig. 17c).

The radial velocity samples were found to have a nearly Gaussian distribution for all radii at x/D = 3.

The computed axial velocity sample kurtosis values presented in Fig. 16e are generally larger than those in Refs. 5 and 6. The trend is somewhat similar, however, with the occurrence of a minimum of the half-velocity radius H_j, and a peak near the jet edge C_j. Again, the dual seeded results are quite different from the single seeded measurements and appear to provide a more accurate description of the jet mixing process.

4.2.4 Shear Flow Model

The observations made in previous sections regarding the intermittent nature of the mixing region flow and the conservation of jet and free-stream properties across the region are consistent with the turbulence shear layer model described in Ref. 15. Outer nonturbulent fluid is separated from an inner turbulent fluid by a moving boundary containing bulges and valleys. Such features are present in the turbulent shear layer photograph (Fig. 19) from Ref. 16.

A fixed observer in the interface region would experience alternating periods of distinctly turbulent and nonturbulent flow as the bulges and valleys moved past his position. Assuming that the turbulence levels in the inner and outer regions were relatively constant, the mean turbulence level would be a function only of the amount of time spent in each region. The ratio of time spent in the turbulent region to the total time is defined as the intermittency factor, Ω, in Ref. 15. Based upon this definition, the average axial velocity of the fluid at a point (V_x^a) in the mixing region can be written

$$V_x^a = \Omega V_x^j + (1 - \Omega) V_x^{fs} \tag{1}$$

where V_x^j and V_x^{fs} are the mean axial velocities obtained from independent jet seeded and free-stream seeded measurements. The average axial velocity can be calculated by assuming a Gaussian distribution of the intermittency across the shear layer as in Ref. 13.

Estimated values of the intermittency factor can be determined for the present data since balanced dual seeded, as well as single seeded measurements were obtained, Substituting the mean axial velocity for dual seeding, V_x^d, for V_x^a in Eq. (1) and rearranging yields an expression for the experimentally determined intermittency,

$$\Omega_e = \frac{V_x^d - V_x^{fs}}{V_x^j = V_x^{fs}} \tag{2}$$

Two alternate techniques for analyzing the shear layer velocity fluctuations can be applied at points where the axial velocity histograms are strongly bimodal and have separate non-overlapping jet and free-stream velocity distributions. In such instances, measurements with all three seeding conditions are not necessary since the required information can be determined from the dual seed histograms. Statistical analyses of the individual parts of the axial velocity probability distribution associated with the jet and free-stream modes provide the respective mean axial velocities, V_x^{jm} and V_x^{fsm}. Substitution into Eq. (2) yields, for the estimated intermittency factor,

$$\Omega_{e1} = \frac{V_x^d - V_x^{fsm}}{V_x^{jm} = V_x^{fsm}} \tag{3}$$

In another technique also involving nonoverlapping bimodal histograms, the intermittency factor is expressed in terms of the area under the axial velocity probability distribution curve as,

$$\Omega_{e2} = \frac{A_x^{jm}}{A_x^{jm} + A_x^{fsm}} \tag{4}$$

where A_x^{jm} and A_x^{fsm} are, respectively, the areas associated with the jet and free-stream modes.

Weighting functions to correct for the Ref. 12 velocity biasing have been omitted from Eqs. (1-4). Such corrections are recommended, however, since the large differences in mean velocity between modes can result in significant errors.

Returning to the discussion of Figs. 15 through 18, we can relate the intermittency factor concept to the LDV measurements. By seeding the flow on only one side of the interface, the fluid on the other side remained "transparent" to the LDV. The instrument recorded either data from the seeded flow or nothing, depending upon which side of the interface the probe volume was on at the time. The single seeding technique effectively forced the intermittency factor to be either 0 or 1.

It follows that properly balanced dual seeding could provide a smooth transition from the nonturbulent to turbulent flow by letting the flow "self-adjust" the intermittency factor

as a function of radius. The dual seeded histograms (Fig. 17c) do, in fact, behave in a manner consistent with the proposed mixing model, resulting in a smooth transition from free-stream to jet velocity (Fig. 15).

The dual seeded mode values which occur in each velocity probability distribution in Fig. 17c closely match the free-stream and jet seeded modes in Fig. 17a and 17b at corresponding radii. The smooth transfer of mean velocity from one mode to the other appears to have been accomplished by time-weighted averages of the two mode values. The weighting function appears to have been similar to the previously mentioned intermittency factor, Ω, going from 0 at the point E_{fs} to 1 at the point E_j.

A conventional analysis (Ref. 17) of the measured (dual seed) mixing zone velocity profile at $x/D = 3$ indicates that the similarity parameter, σ, for turbulent mixing is in the 25 to 35 range. The corresponding similarity parameter for single stream mixing is in the 11 to 15 range which is consistent with other experimental and theoretical values presented in Ref. 18. As a result, conventional turbulence models should adequately predict this mixing region.

The data from $x/D = 1$ were selected for presentation in Fig. 20 because the widely separated modes provide a somewhat clearer definition of the bimodal transition mechanism. The jet seeded survey (Fig. 20b) was terminated prematurely by a seeder malfunction. As a result, the constant velocity plateau portion of the profile was not recorded. Estimated r/D positions for the points B_j, and C_j based on the dual seed measurements have been included in Fig. 20c and other appropriate figures as indicated values.

4.2.5 Axial Variation

The axial velocity probability distribution having an estimated intermittency factor, Ω_e, nearest 0.5 is presented in Fig. 21 for each of the six axial stations. Mean velocities for jet, free-stream, and dual seeding are indicated in the figure. The radial location of each measurement and the estimated intermittency factor have also been included at each axial station.

Based upon the selected examples, the velocity differences between modes, as well as the values of the higher jet seeded mode, are both maximum near the jet exit and decrease with distance downstream. In contrast, the free-stream seeded mode velocity shows an increase. As was stated earlier in this report, the model boattail boundary layer was thought to be responsible for the velocity deficit in the free-stream seeded mode. This hypothesis is reinforced by the relatively wide initial velocity variation about the mode value near the jet

exit. The subsequent decrease in standard deviation is probably attributable to viscous entrainment. The histograms indicate that most of the low velocity, moderately turbulent fluid has been entrained by the jet before x/D = 2. The free-stream seeded modes farther downstream represent low turbulence fluid from beyond the model boundary layer.

Figure 22 illustrates the variation of several of the Fig. 15 velocity profile characteristics along the jet plume centerline. The points C_j and C_{fs} identify the limits of penetration of seed from each region into the other. Their loci in Fig. 22a define the zone at overlap in which both particles from both seed sources could be observed. No overlap could be detected at x/D = 0.1. The wake from the separated base region which trailed downstream contained no detectable particles and was transparent to the LDV.

The loci of the symbols E_j and E_{fs} in Fig. 22b define the observed effective limits of seed penetration as well as the extent of the zone of intermittent flow. Velocity measurements within the region require carefully controlled dual seeding to avoid intermittency biasing.

The inner boundary of the conventional shear layer (Ref. 17) is presented in Fig. 22b as the locus of the maximum velocity radii A_j. The outer boundary coincides with the outer edge of the intermittency zone E_{fs}.

Axial variation in the location of points B_j and G_{fs} is shown in Fig. 22b. The location B_j signifies the appearance of ambient free-stream particles in the jet seeded histograms and marks the outer end of the velocity plateau region. The radius G_{fs} indicates the point in the free-stream seeded profile where jet induced viscous forces begin to dominate the free-stream fluid behavior. According to the Fig. 15, data the point G_{fs} appears to occur consistently at the same radius as the start of the plateau region of the jet-seeded velocity profiles.

Laser vapor screen flow visualization provided a qualitative look at the jet plume turbulent mixing region. A slight reduction of jet total temperature on a high humidity day yielded sufficient condensate. The rings shown in Fig. 23 resulted when a sheet of laser light in the constant x/D plane was directed across the plume at five different axial stations. The condensate appeared only in the inner half of the conventional shear layer shown in Fig. 22b, i.e., the region bounded by the locus of maximum velocity points A_j and the inner edge of the intermittent zone E_j. Since the gas exhausted from the jet was dry nitrogen obtained by boiling liquid nitrogen, the source of the condensate is assumed to be the free-stream air. This implies that the tunnel air penetrated deeper into the jet than did the seed particles. If so, the dual seed measurements in that region may have been biased by an undetected extension of the intermittent region. The introduction of smaller particles into the free-stream flow could improve the results, if such particles could be detected by the LDV.

Additional qualitative flow "visualization" data were obtained using the LDV system oscilloscope. Condensate, invisible to the eye with the proper jet total temperature, could be "seen" on the oscilloscope. The region illustrated in Fig. 24 was defined by systematically traversing the region with the LDV probe volume and observing the output signal. A typical survey into the jet produced an increasingly strong signal with a broad band fluctuation maximum along the line denoted by the diamond symbol. From that point inward toward a second line denoted by triangles the signal was essentially a constant, relatively high d-c level. A maximum narrow band signal was observed in the vicinity of the second line, followed by a gradual decrease in signal strength toward the jet centerline. The outer edges of the regions shown in Figs. 23 and 24 are nearly matched. The oscilloscope defined region (Fig. 24) is wider and extends closer to the jet centerline than does the zone of visible condensate (Fig. 23). This probably indicates that the condensate detected by the oscilloscope was smaller and penetrated farther into the jet than did the condensate which was visible to the eye.

4.2.6 Resolved Mean Velocity Profiles

The velocity measurements for the three seeding conditions were combined to provide an effective mean axial velocity profile at each x/D station. Each profile follows the free-stream data to the outer edge of the intermittent region E_{fs}. The dual seeded results then provide a smooth transition to the jet seeded velocity level on the inner edge of the intermittent region E_j. The remainder of the profile coincides with the jet seeded measurements.

Velocity profiles from the afterbody flow field and jet plume are combined in Fig. 25 to provide an overall picture of the field of interest. The effects of flow acceleration upstream of the model shoulder appear as a slight positive bulge outside the boundary layer in the second profile from the left. This is followed by a marked deceleration and thickening of the boundary layer over the remainder of the afterbody.

The growth of the shear layer can clearly be seen in Fig. 22. As the flow leaves the nozzle exit, the point of maximum velocity gradient moves radially outward at an estimated initial angle of 20 deg with the centerline to a maximum radius of approximately 0.4 D at $x/D \approx 1$.

Simultaneously, the velocity gradient magnitude decays rapidly from the extreme initial value. The decrease continues for another quarter-body diameter and remains relatively constant for the remainder of the axial stations. Shear layer growth appears to continue as the flow moves downstream but at an extremely slow rate.

The velocity deficit caused by the Mach disc on the centerline near x/D = 1 is significant in the x/D = 1.5 profile. Recovery is almost complete, however, at the last axial station.

4.2.7 Tabulated Data

The experimental data are presented in digital form in Appendix B. Measurements along the constant r/D computational boundary are tabulated first, followed by the constant r/D surveys in the jet and the constant x/D surveys. The data from each survey which penetrates the jet plume include separate measurements for the three seeding conditions. Free-stream, jet, and dual seeding are indicated by values of the seeding condition variable SE of 1, 2, and 3, respectively. The resolved profile data presented in Fig. 25 are denoted by a data condition code variable, CC = 1.

5.0 CONCLUDING REMARKS

The flow field about an axisymmetric nozzle afterbody in a subsonic parallel stream has been surveyed, including the flow within the supersonic underexpanded jet plume and the turbulent mixing region. Two-component simultaneous flow-field measurements were obtained using a two-color Bragg-diffracted laser Doppler velocimeter system. LDV measurements include mean velocity, turbulence intensity, Reynolds shear stress, skewness, and kurtosis. Model surface pressures were obtained, as well as qualitative plume data from two types of flow visualization.

The turbulent shear layer was investigated thoroughly. The characteristics of the intermittent interface between the turbulent jet and relatively quiet free stream were defined by seeding the two flow regimes separately and in combination. Measurements obtained from the three seeding conditions provide a new insight into the mechanisms involved in jet entrainment and turbulent mixing. The data clearly show the extreme sensitivity of the LDV measurements to nonuniformity in seeding in such intermittent regions. The injection of seed into both streams is usually recommended to increase the probability of a sufficiently small known particle size. Extreme care must be taken to adjust and maintain the two seeding rates to ensure uniform particle number density at the point of interest.

The present investigation has demonstrated the unique capability of the LDV for providing nonintrusive measurements in an environment hostile to other diagnostic devices. However, the sensitivity of measurement accuracy to the complex character of a given flow field often places application-peculiar constraints upon the design of the LDV system. Care must be exercised in the initial design and setup, as well as the periodic alignment, adjustment, and calibration of each LDV component system to ensure balanced

measurement sensitivity between components and continuity of the data acquired from day to day.

The indicated discrepancy in standard deviation between the two velocity components which was observed in the free-stream flow is thought to have been at least partially a result of instrument broadening in the radial component histograms. Additional data are necessary for resolution of the question. If the indicated level of nonisotropic turbulence does, in fact, exist in the Tunnel 1T test section flow, corrective action would be desirable.

The use of smaller seed particles is recommended for future tests of this type to reduce the particle lag associated with the nozzle and the centerline Mach disc. The small particles should also provide more fluid-like penetration into the jet, as suggested by the condensate data, and thus better define the intermittency region flow.

REFERENCES

1. Cline, V.A. and Lo, C. F. "Application of the Dual-Scatter Laser Velocimeter in Transonic Flow Research." AGARD Meeting on Applications of Nonintrusive Instrumentaion in Fluid Flow Research, Saint-Louis, France, May 1976.

2. Lo, C. F. and Heltsley, F. L. "Interpretation of Laser Velocimeter Measurements in a Transonic Flow Field." 22nd International ISA Aerospace Instrumentation Symposium, San Diego, California, May 1976.

3. Barnett, D. O. and Giel, T. V., Jr. "Application of a Two-Component Bragg-Diffracted Laser Velocimeter to Turbulence Measurement in a Subsonic Jet." AEDC-TR-76-36 (AD-A025355), May 1976.

4. Knott, P. and Mossey, P. "Parametric Laser Velocimeter Studies of High Velocity, High Temperature Turbulent Jets." AFAPL-TR-76-68, Vol. II, Technical Report, July 1976, pp. 390-416.

5. Morris, P. J. "Turbulence Measurements in Subsonic and Supersonic Axisymmetric Jets in a Parallel Stream." *AIAA Journal*, Vol. 14, No. 10, October 1976, pp. 1468-1475.

6. Lau, J. C., Morris, P. J. and Fisher, M. J. "Measurements in Subsonic and Supersonic Free Jets Using a Laser Velocimeter." *Journal of Fluid Mechanics*, Vol. 93, Part 1, pp. 1-27, July 12, 1979.

7. Heltsley, F. L. and Cline, V. A. "Wing/Store Flow-Field Measurement at Transonic Speeds Using a Laser Velocimeter." AEDC-TR-79-5 (AD-A068328), April 1979.

8. Heltsley, F. L., Crosswy, F. L. and Brayton, D. "Transonic Wing/Store Flow-Field Measurement Using a Laser Velocimeter." AEDC-TR-80-54 (AD-A103929), August 1981.

9. Crosswy, F. L., Heltsley, F. L. and Sherrouse, P. M. "Recent Development and Applications of a Three-Component Laser Doppler Velocimeter." 28th ISA International Instrumentation Symposium, Las Vegas, Nevada, May 1982.

10. *Test Facilities Handbook* (Eleventh Edition). "Propulsion Wind Tunnel Facility, Vol. 4." Arnold Engineering Development Center, June 1979.

11. Peters, W. L. "Jet Simulation Techniques: Simulation of Temperature Effects by Alternating Gas Composition." AEDC-TR-78-43 (AD-A067084), March 1979.

12. McLaughlin, D. K. and Tiederman, W. G. "Biasing Correction for Individual Realization of Laser Anemometer Measurements in Turbulent Flows." *Physics of Fluids*, Vol. 16, No. 12, December 1973, pp. 2082-2088.

13. Benek, J. A. "Separated and Nonseparated Turbulent Flows about Axisymmetric Nozzle Afterbody, Part II, Detailed Flow Measurements." AEDC-TR-79-22 (AD-A076458), October 1979.

14. Lau, J. C. "The Vortex-Street Structure of Turbulent Jets, Part 2." *Proceedings of the Royal Society of London*, Vol. 368, No. 1735, November 1979, pp. 547-571.

15. Hinze, J. O. *Turbulence*. McGraw-Hill Book Company, Inc., New York, 1975.

16. Van Dyke, M. *An Album of Fluid Motion*. The Parabolic Press, Stanford, California, 1982.

17. Korst, H. H. and Chow, W. L. "Non-isoenergetic Turbulent ($P_{r\star}$ = 1.0) Jet Mixing Between Two Compressible Streams at Constant Pressure." ME-TN-393-2, Engineering Experiment Station, University of Illinois, Urbana, Illinois, April 1965.

18. Bauer, R. C. "Another Estimate of the Similarity Parameter for Turbulent Mixing." *AIAA Journal*, Vol. 6, No. 5, May 1968, pp. 925-927.

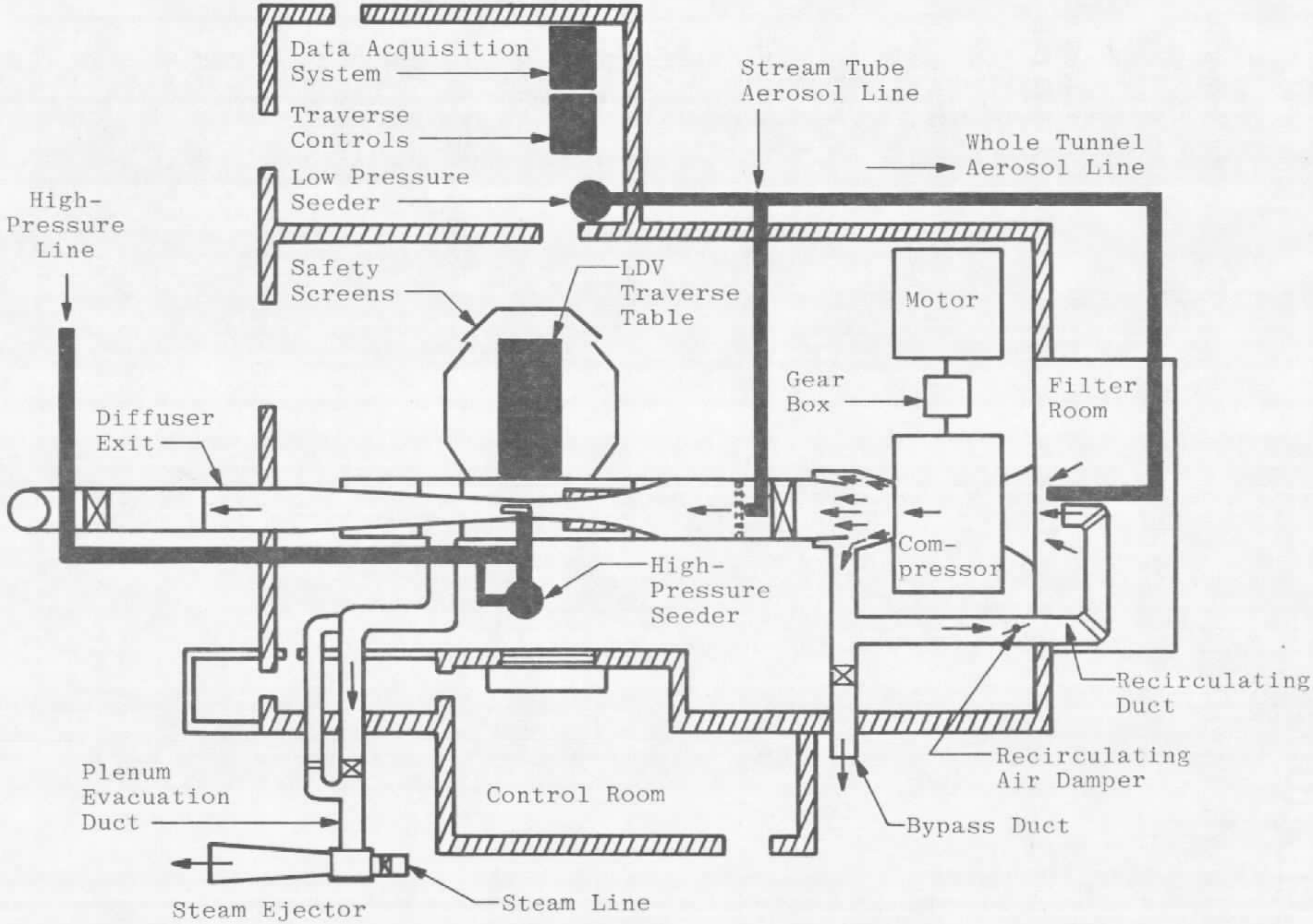

Figure 1. Tunnel 1T layout and LDV system installation.

$\frac{A}{A^*} = 1.2681$

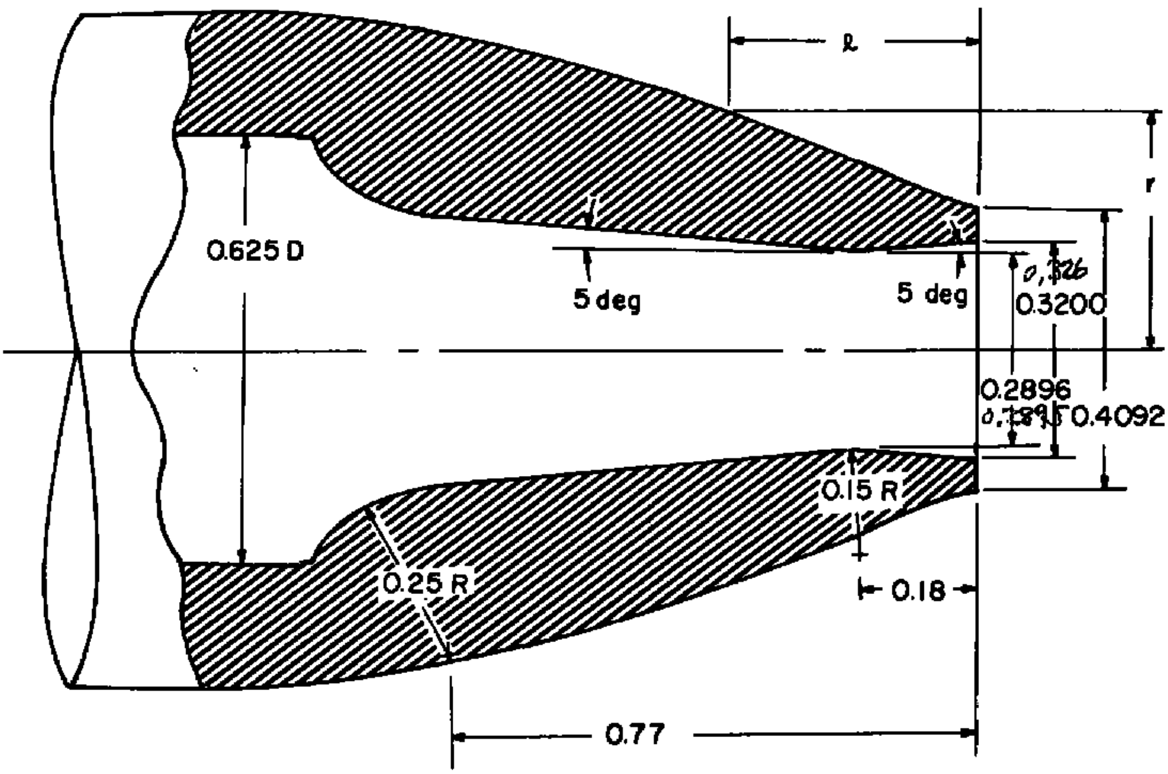

NOTE: ALL DIMENSIONS IN INCHES

ℓ	r	ℓ	r	ℓ	r	ℓ	r
0.0000	0.2046	0.2712	0.3135	0.5423	0.4050	0.8135	0.4677
0.0247	0.2125	0.2958	0.3229	0.5669	0.4120	0.8381	0.4721
0.0493	0.2214	0.3205	0.3321	0.5916	0.4189	0.8628	0.4760
0.0740	0.2315	0.3451	0.3410	0.6163	0.4252	0.8874	0 4795
0.0986	0.2423	0.3698	0.3495	0.6409	0.4313	0.9121	0.4829
0.1233	0.2532	0.3944	0.3579	0.6656	0.4373	0.9367	0.4859
0.1479	0.2641	0.4191	0.3666	0.6902	0.4427	0.9604	0.4884
0 1726	0.2749	0.4437	0.3747	0.7149	0.4479	0.9860	0.4908
0.1972	0.2848	0.4684	0.3826	0.7396	0.4531	1.0107	0.4920
0.2219	0.2946	0.4930	0.3903	0.7642	0.4580	1.0353	0.4930
0.2465	0.3043	0.5177	0.3977	0.7888	0.4629	1.0500	0.4930

a. Afterbody contour
Figure 2. Test article and support strut.

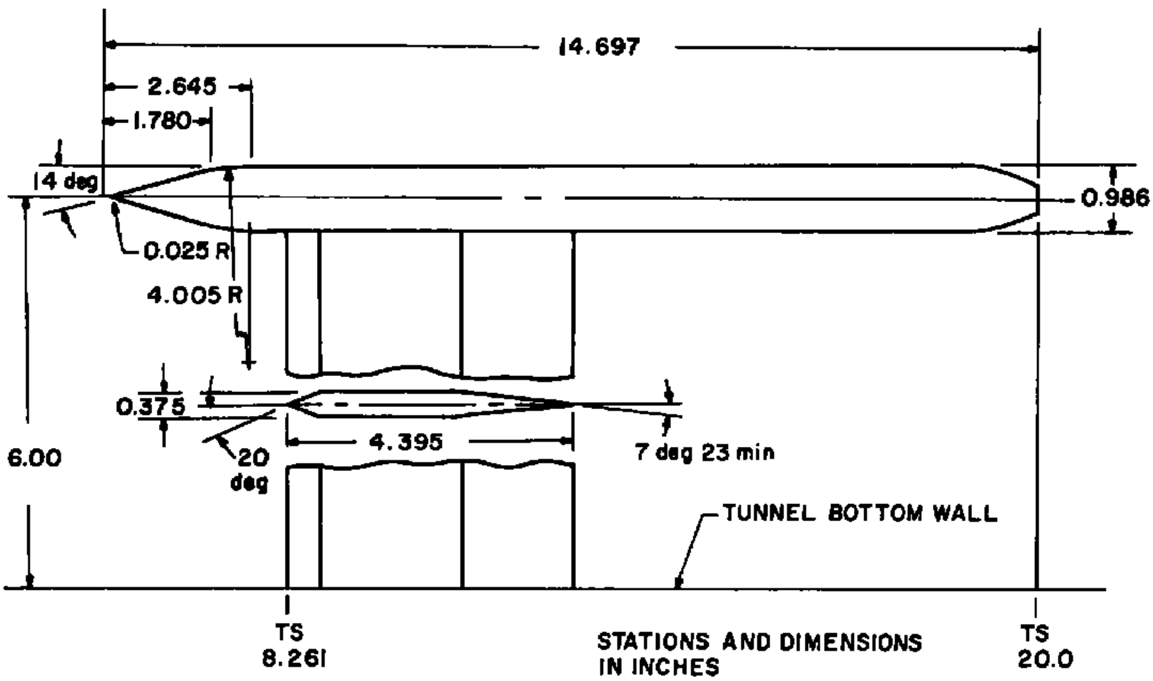

b. Overall dimensions
Figure 2. Concluded.

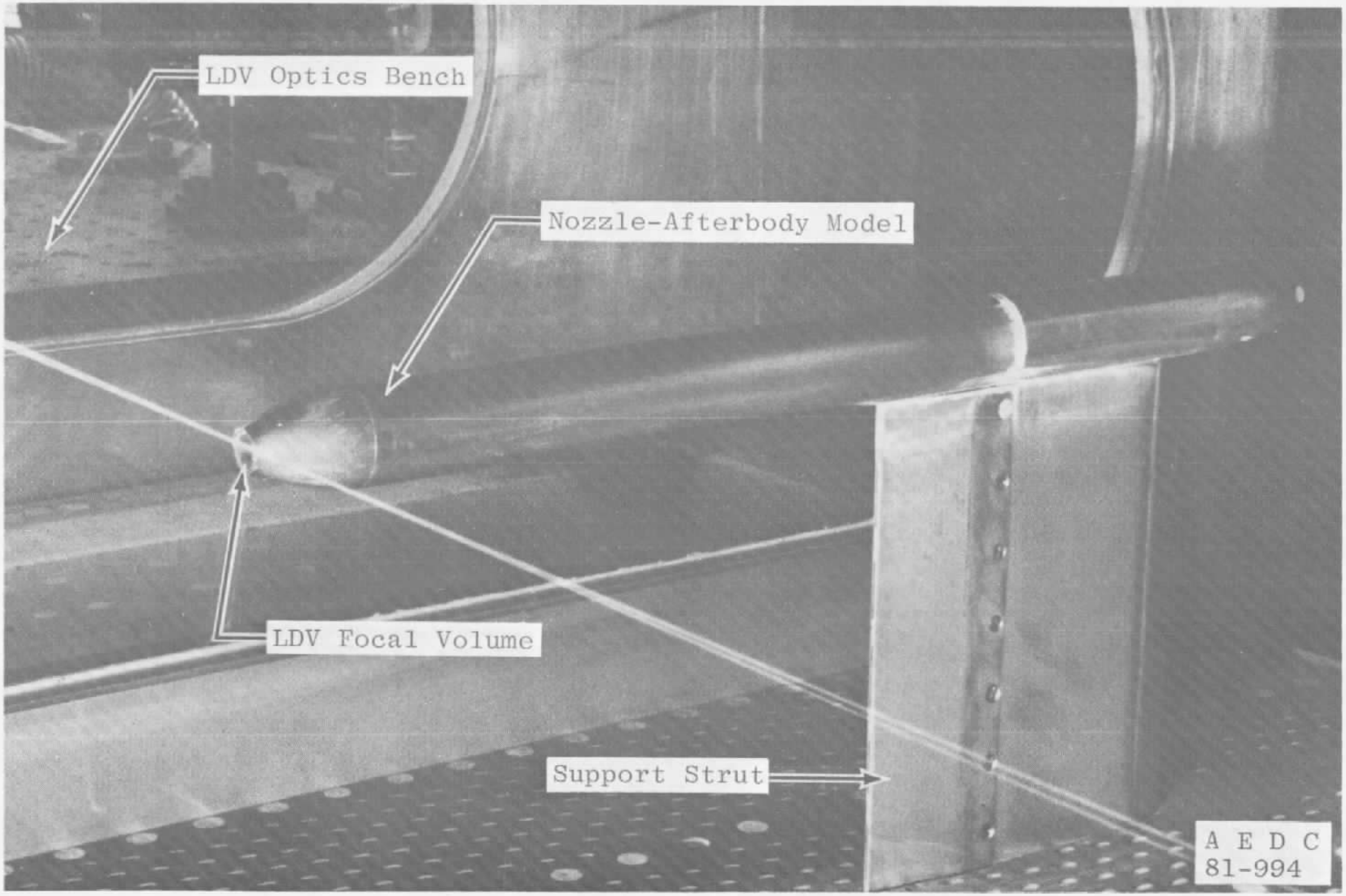

Figure 3. Nozzle-afterbody model in Tunnel 1T.

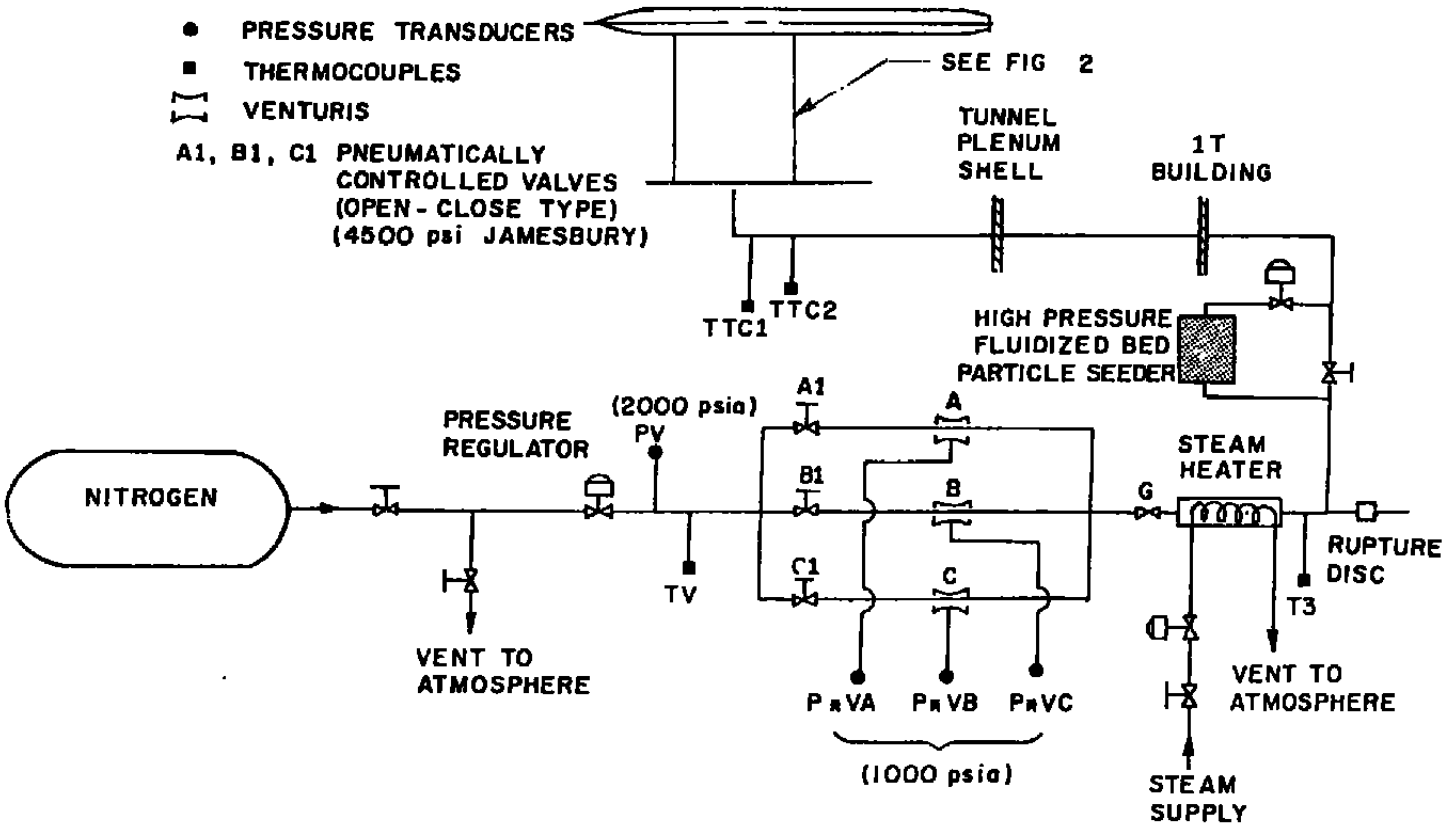

Figure 4. High-pressure gas system schematic.

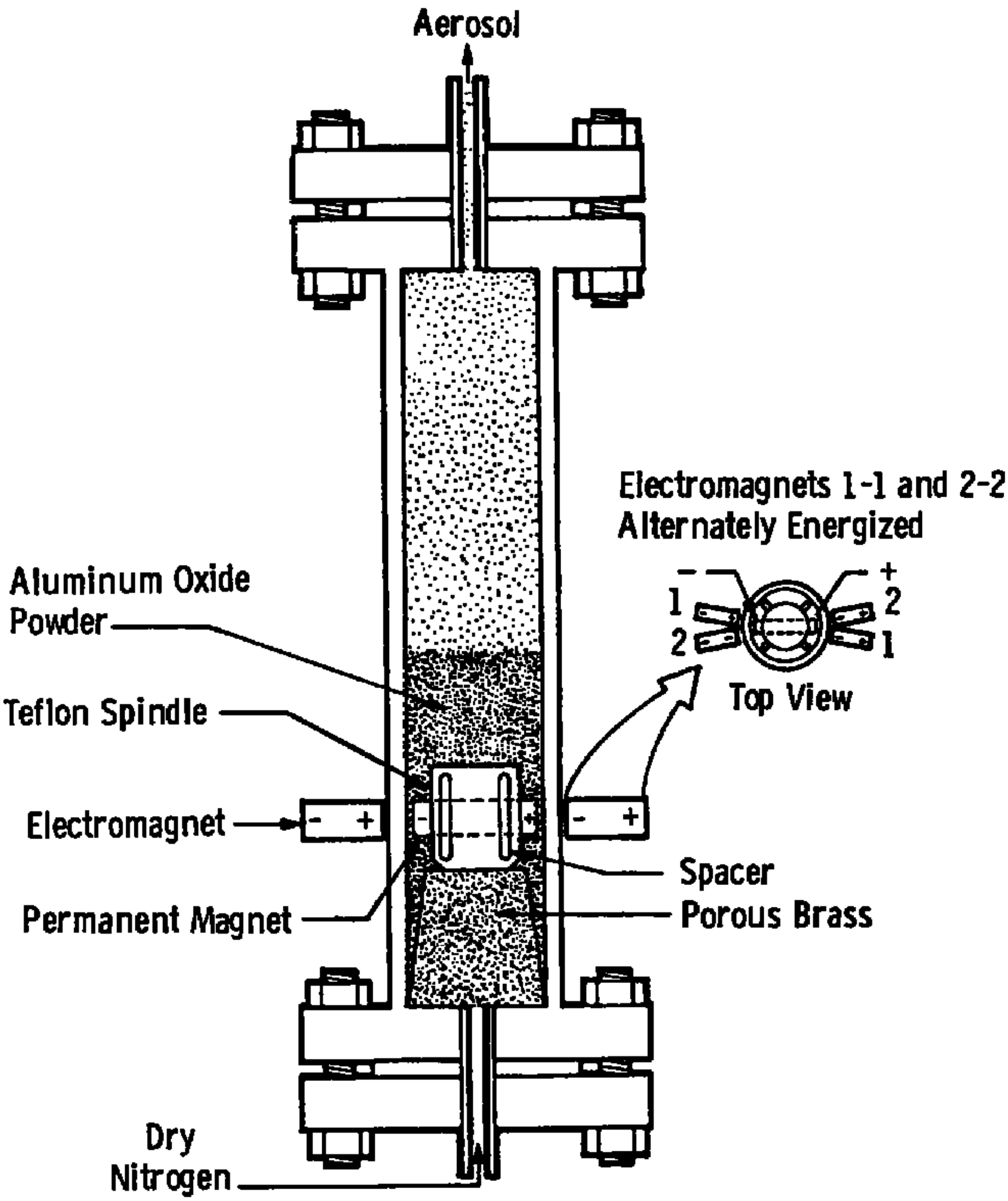

a. High pressure (2,000 psi maximum)
Figure 5. Fluidized bed particle seeders.

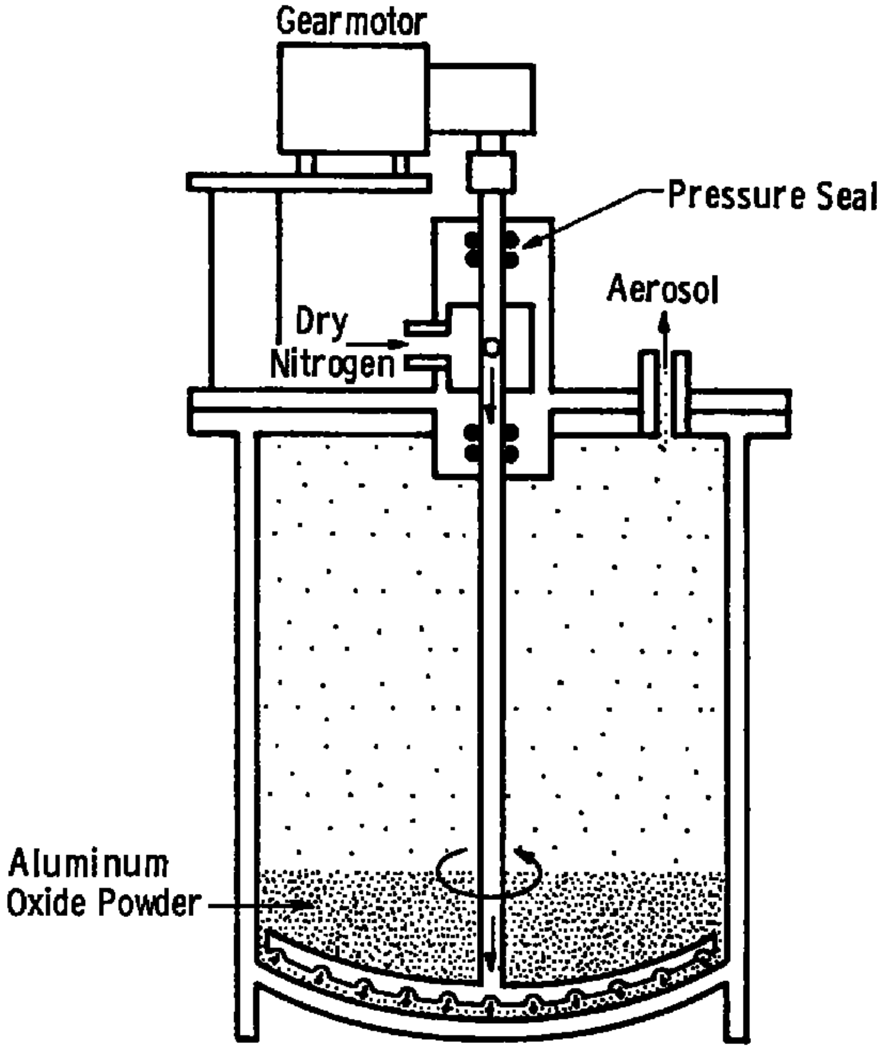

b. Low pressure (60 psi maximum)
Figure 5. Concluded.

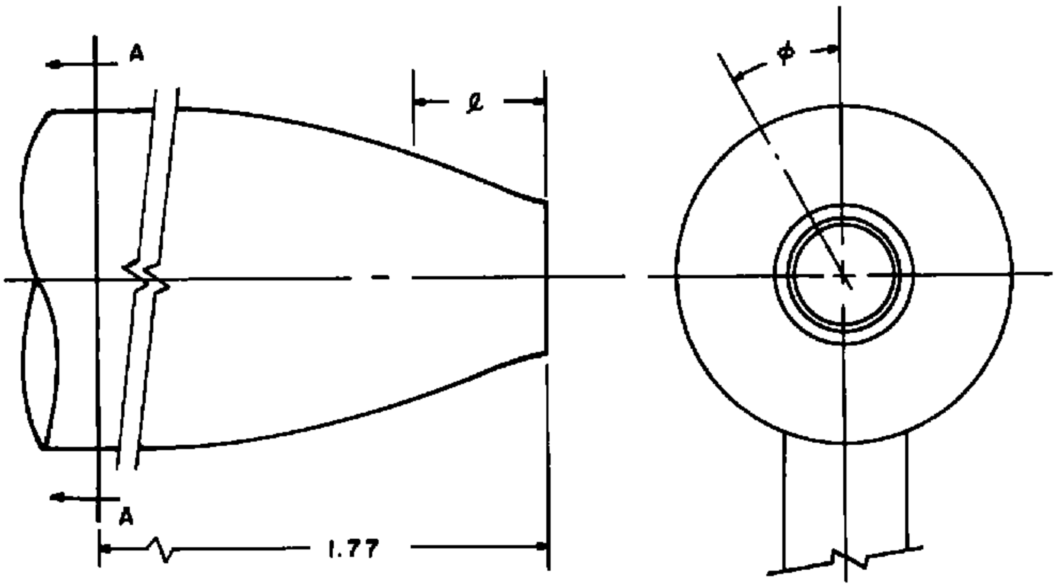

ℓ	ϕ	ℓ	ϕ
0.125	10	0.723	80
0.201	350	0.756	70
0.249	340	0.786	50
0.293	320	0.819	30
0.331	300	0.851	330
0.371	280	0.883	290
0.407	260	0.917	240
0.439	250	0.951	200
0.475	230	0.983	150
0.509	210	1.021	110
0.542	190	1.060	60
0.570	170	1.107	20
0.599	160	0.0	0
0.629	140	0.0	90
0.663	120	0.0	180
0.693	100	0.0	270

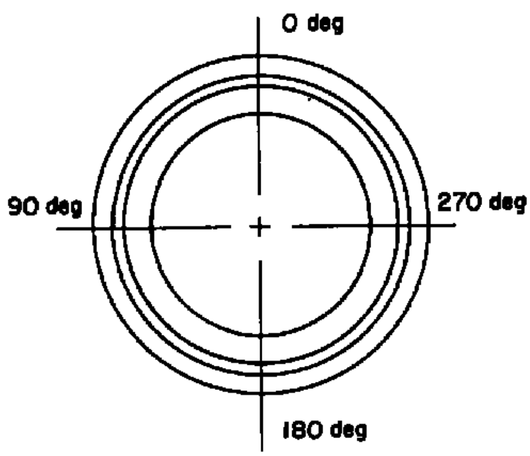

PLENUM STATIC PRESSURE ORIFICES
SECTION AA

Figure 6. Model pressure orifice locations.

1 LASER
2 PRISM ASSEMBLY
3 BEAM SELECTING MIRRORS
4 MODE MATCHING LENSES
5 BRAGG CELLS
6 ANGLE MULTIPLIER LENSES
7 BEAM COMBINING MIRROR
8 TRANSMITTER LENSES
9 PROBE VOLUME
10 RECEIVER LENSES
11 PINHOLE APERTURE
12 INTERFERENCE FILTER
13 PHOTOMULTIPLIER TUBE

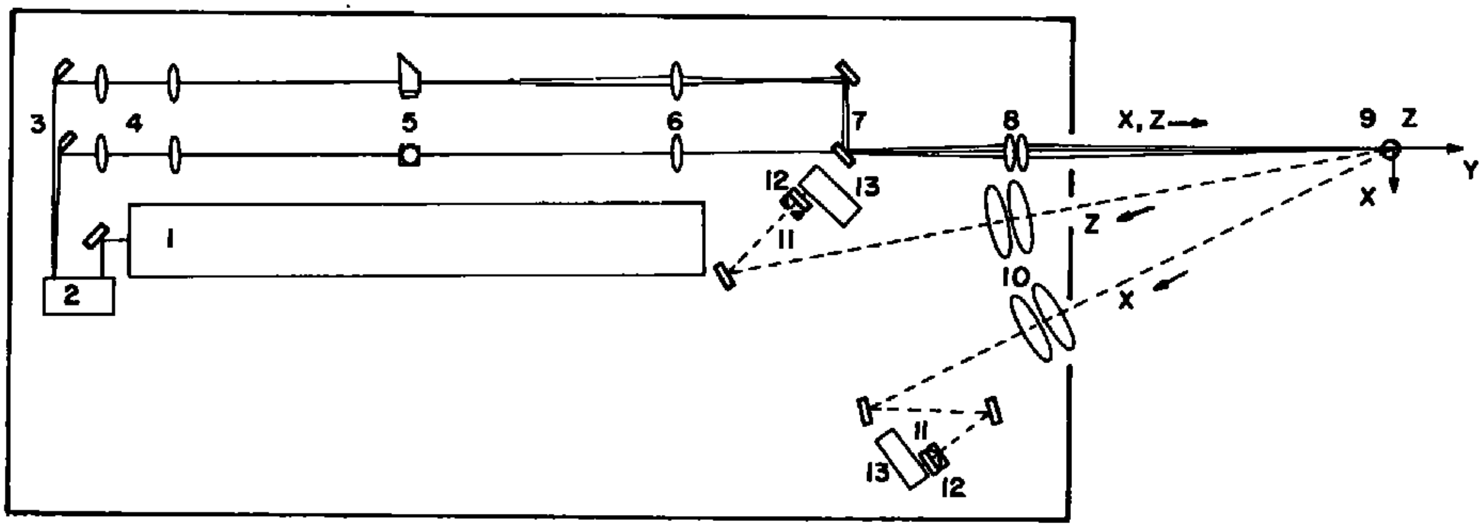

Figure 7. Two-color two-component LDV optical system and measurement coordinates.

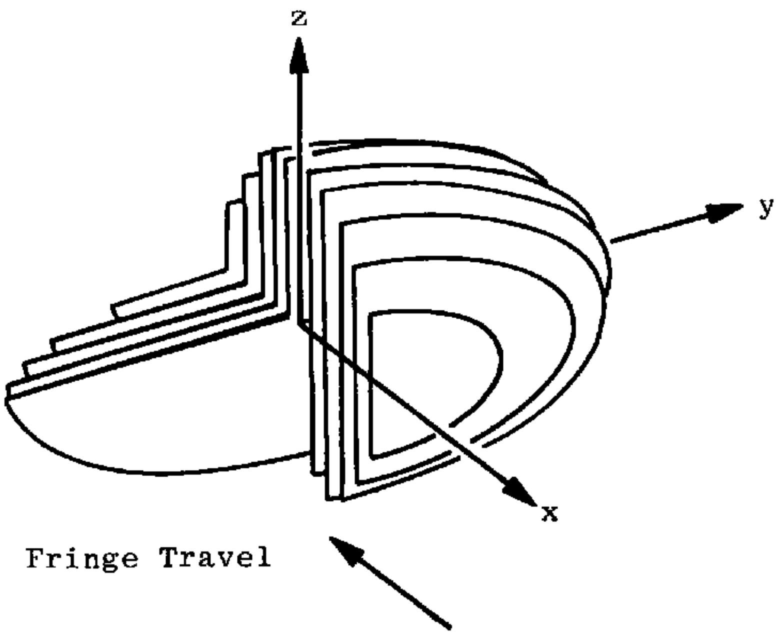

a. 488.0 nm, x-component of velocity

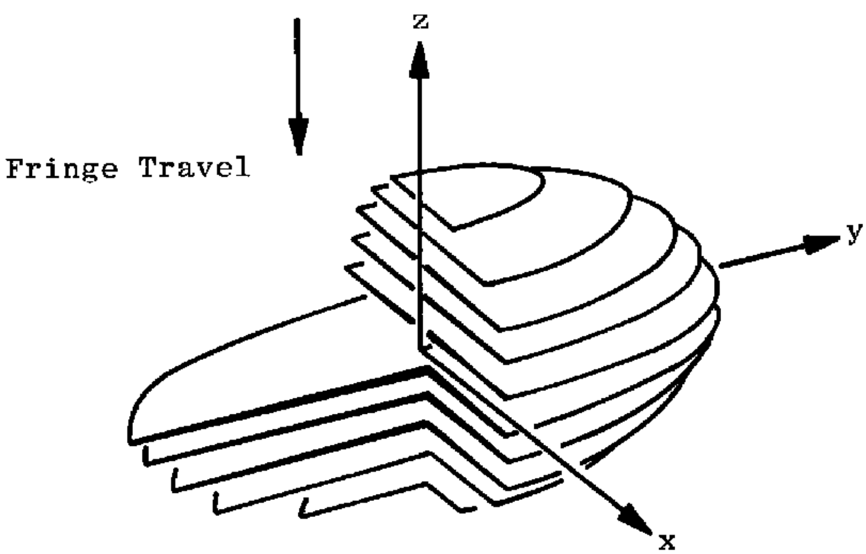

b. 514.5 nm, z-component of velocity

Figure 8. LDV fringe array orientation relative to the measurement coordinate system.

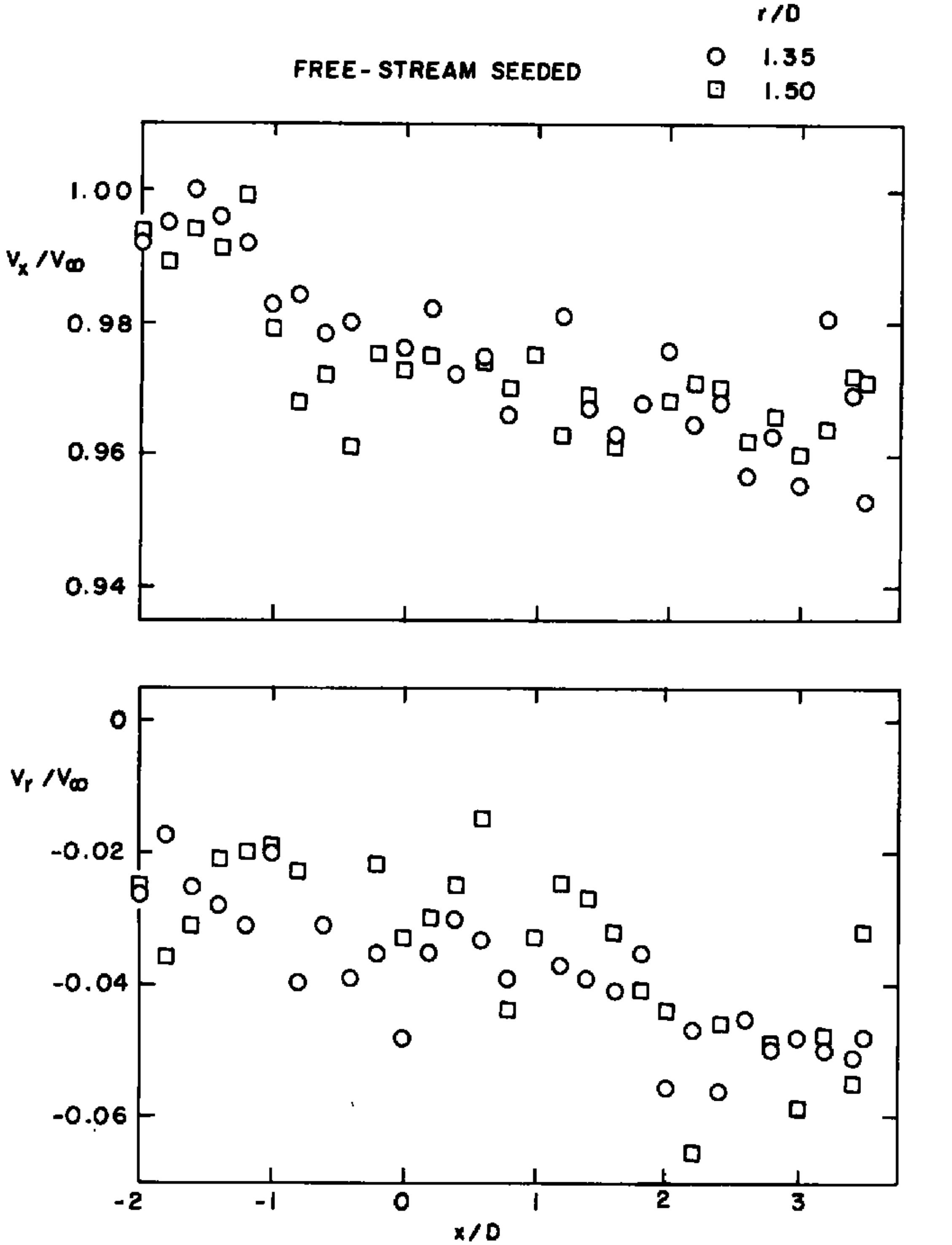

Figure 9. Longitudinal distribution of velocity above the nozzle afterbody.

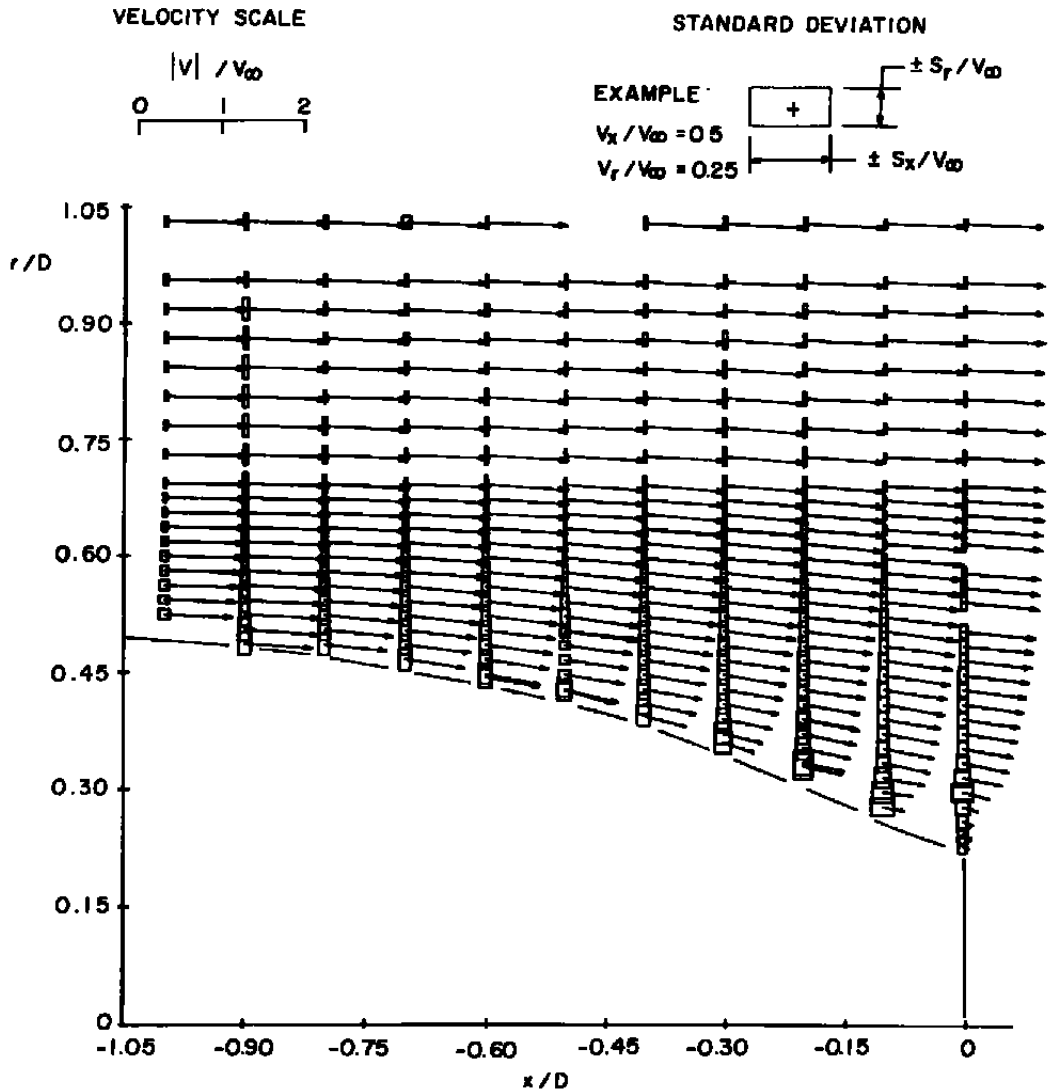

Figure 10. Mean velocity vectors and turbulence intensities near the model base.

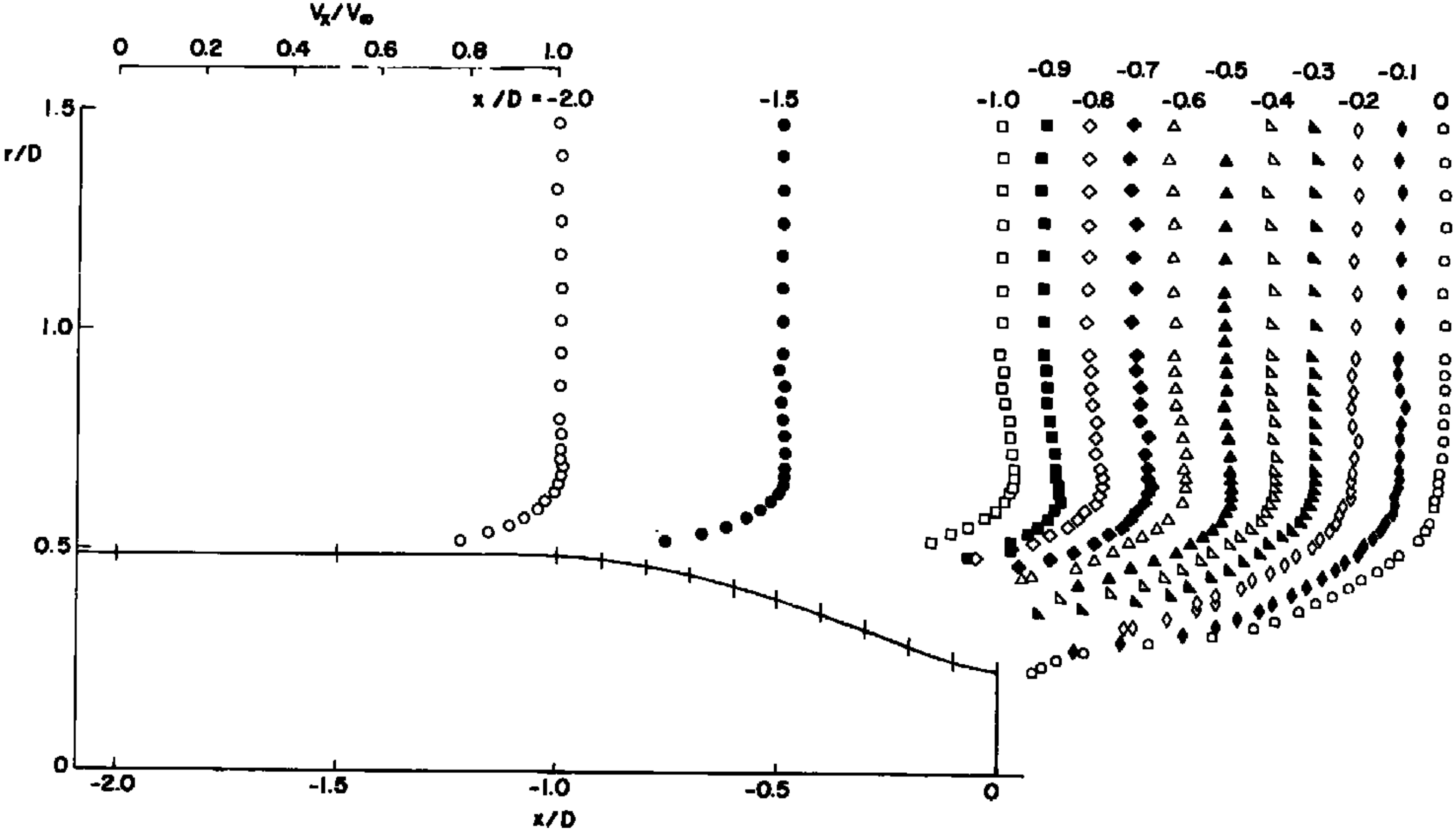

Figure 11. Profiles of mean axial velocity near the afterbody.

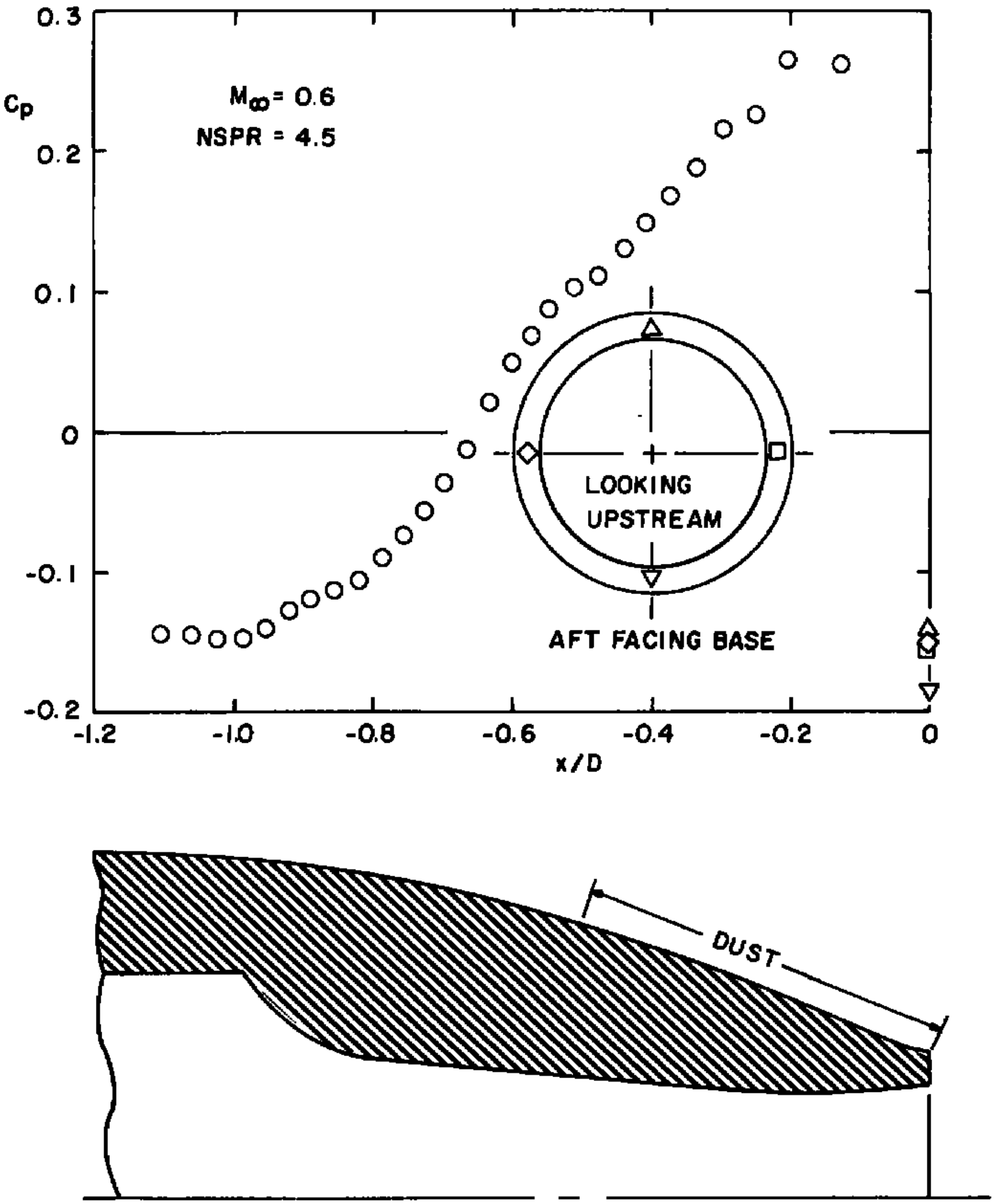

Figure 12. Distribution of static pressure coefficient on the afterbody.

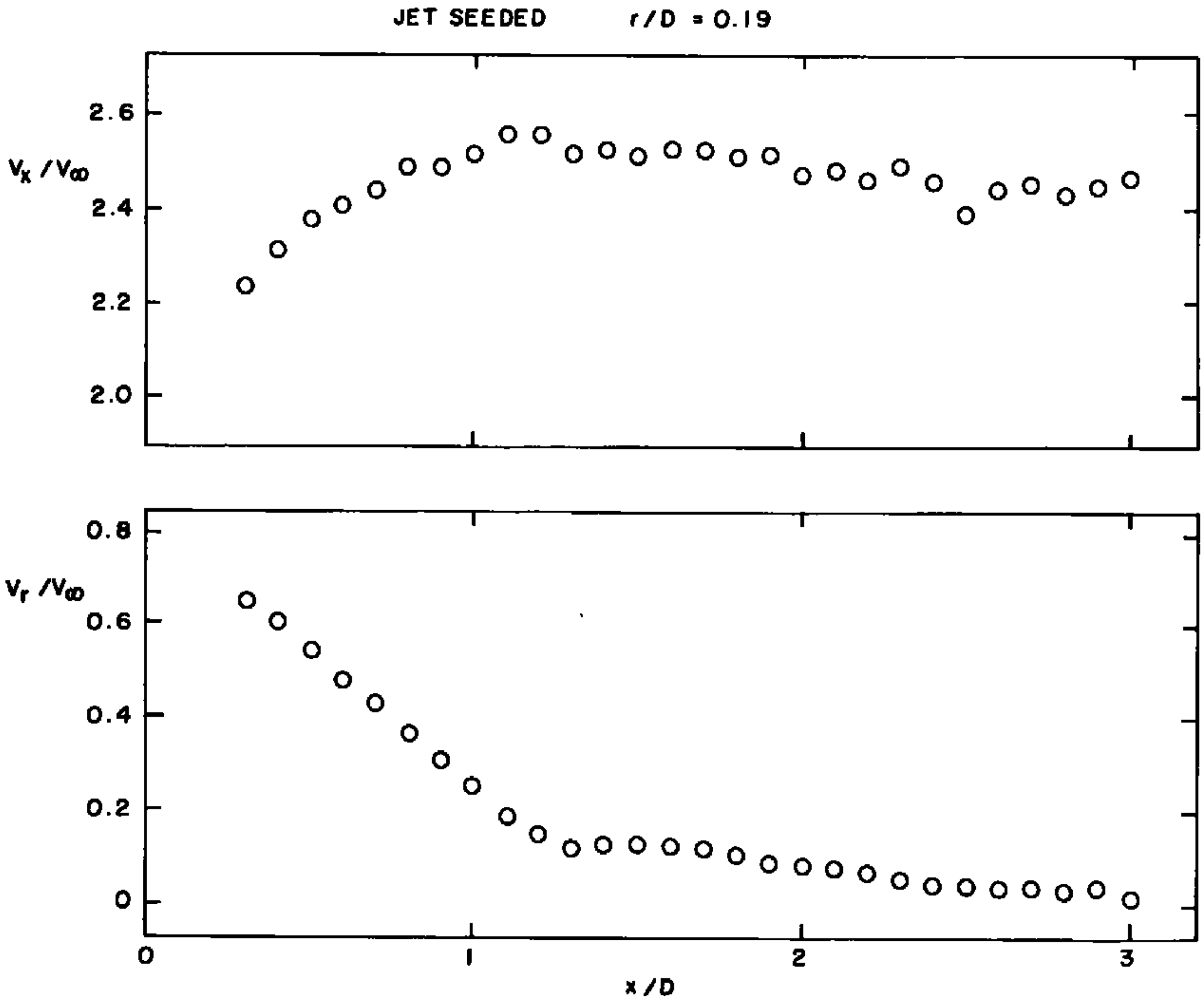

a. r/D = 0.19
Figure 13. Axial distribution of velocity in the jet plume.

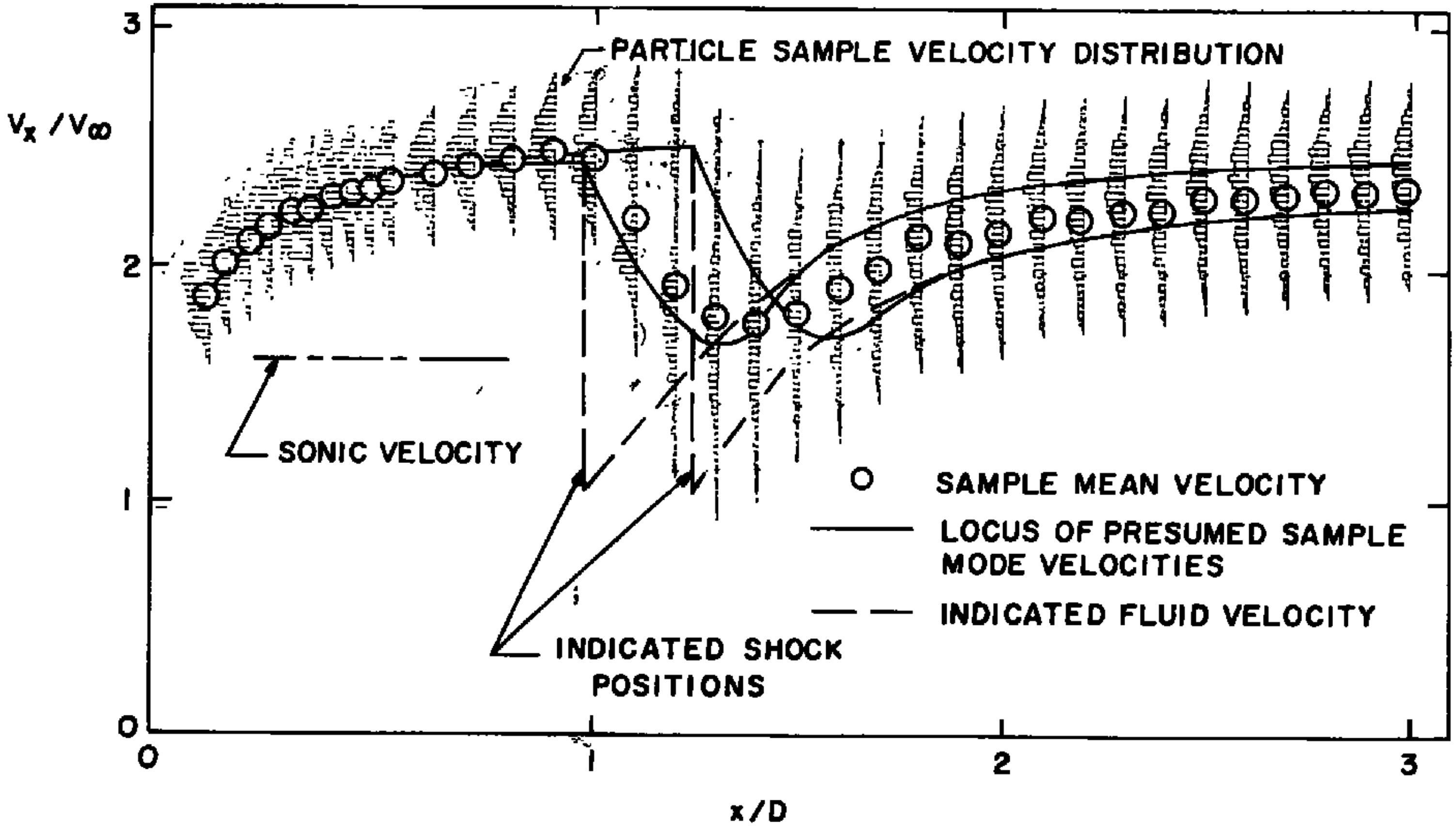

b. r/D = 0

Figure 13. Concluded.

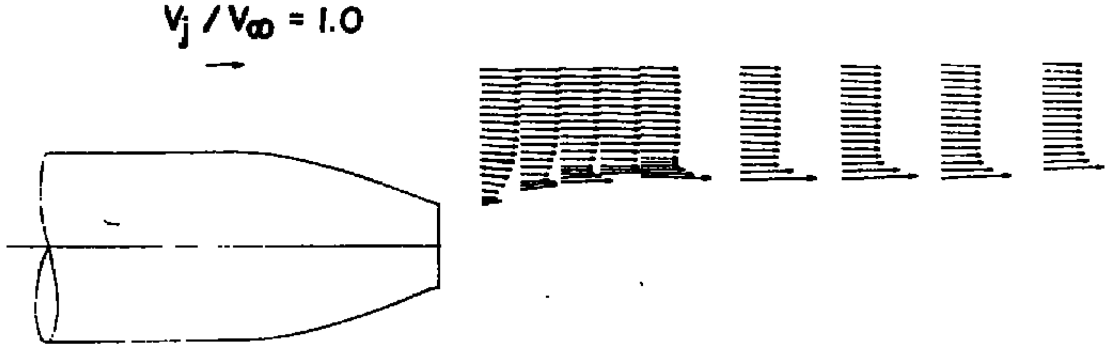

a. Free-stream seeded

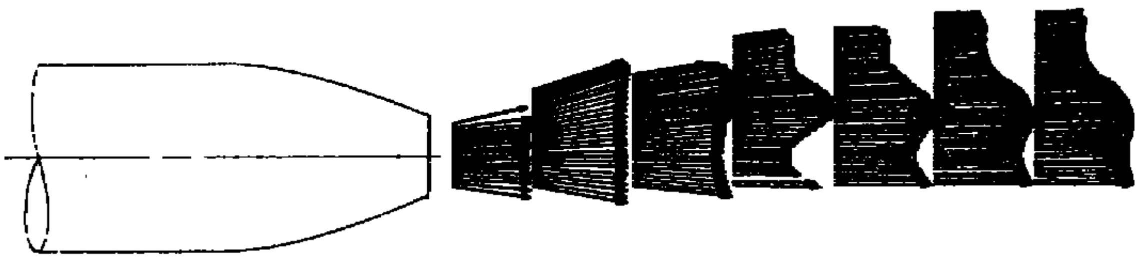

b. Jet seeded

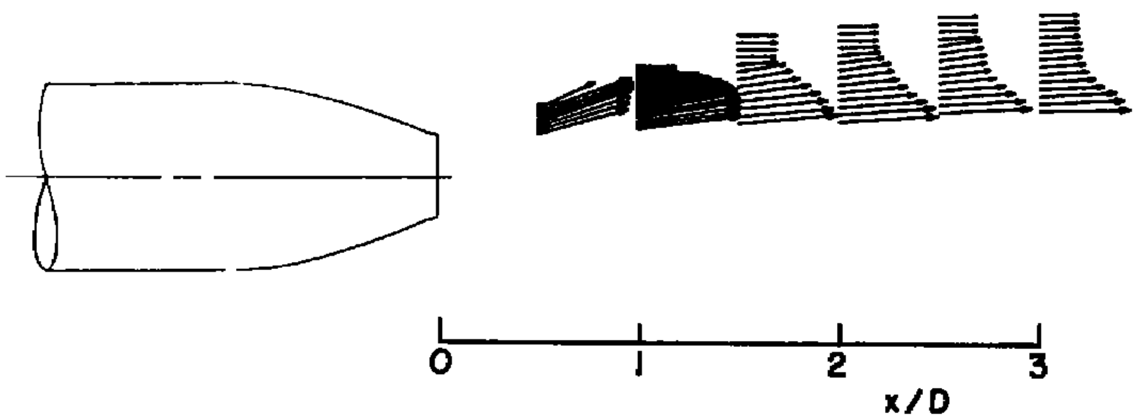

c. Jet and free-stream seeded

Figure 14. Mean velocity vectors in the jet plume region for three seeding conditions.

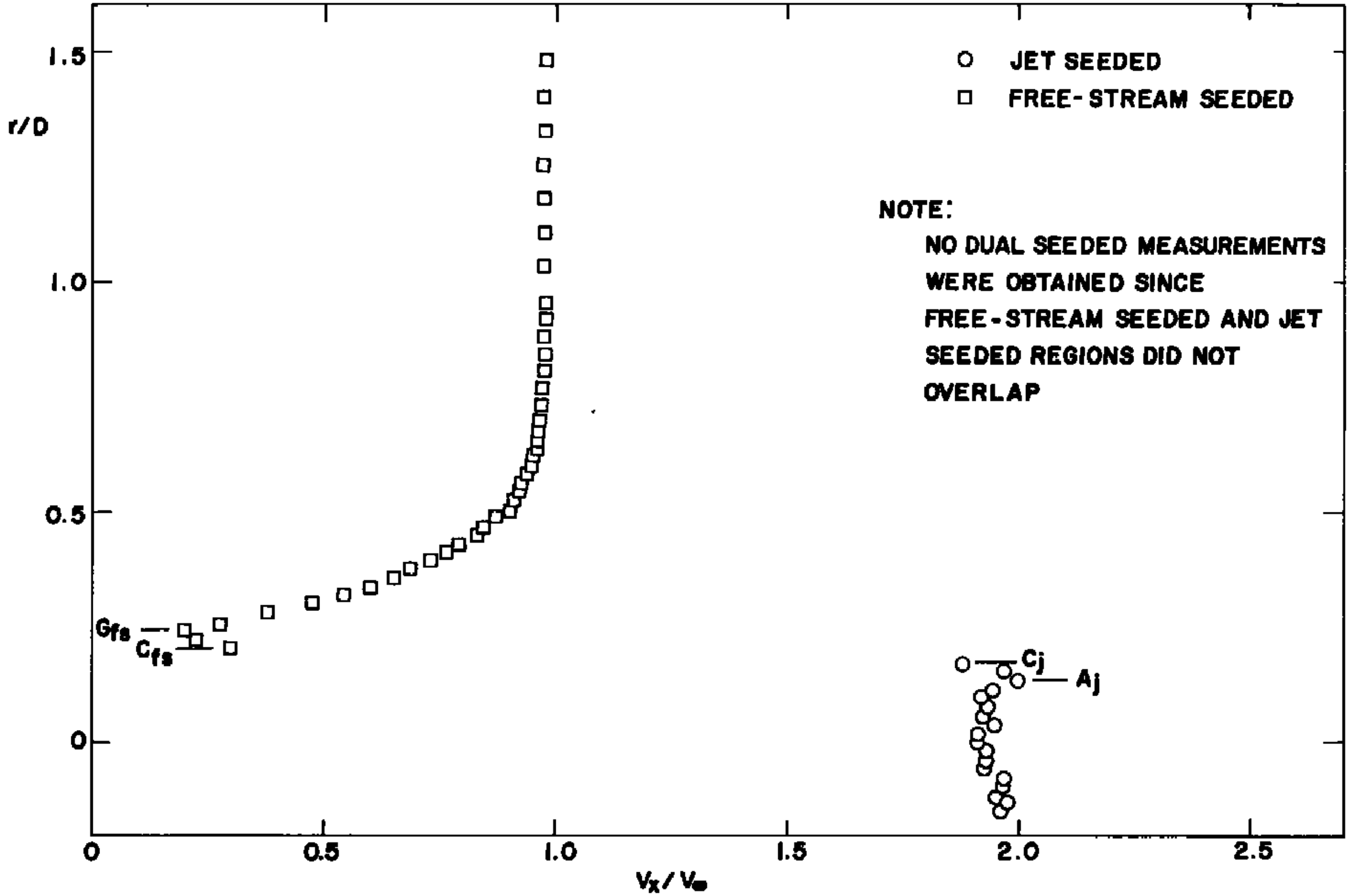

a. x/D = 0.1

Figure 15. Profiles of mean axial velocity in the jet plume region for three seeding conditions.

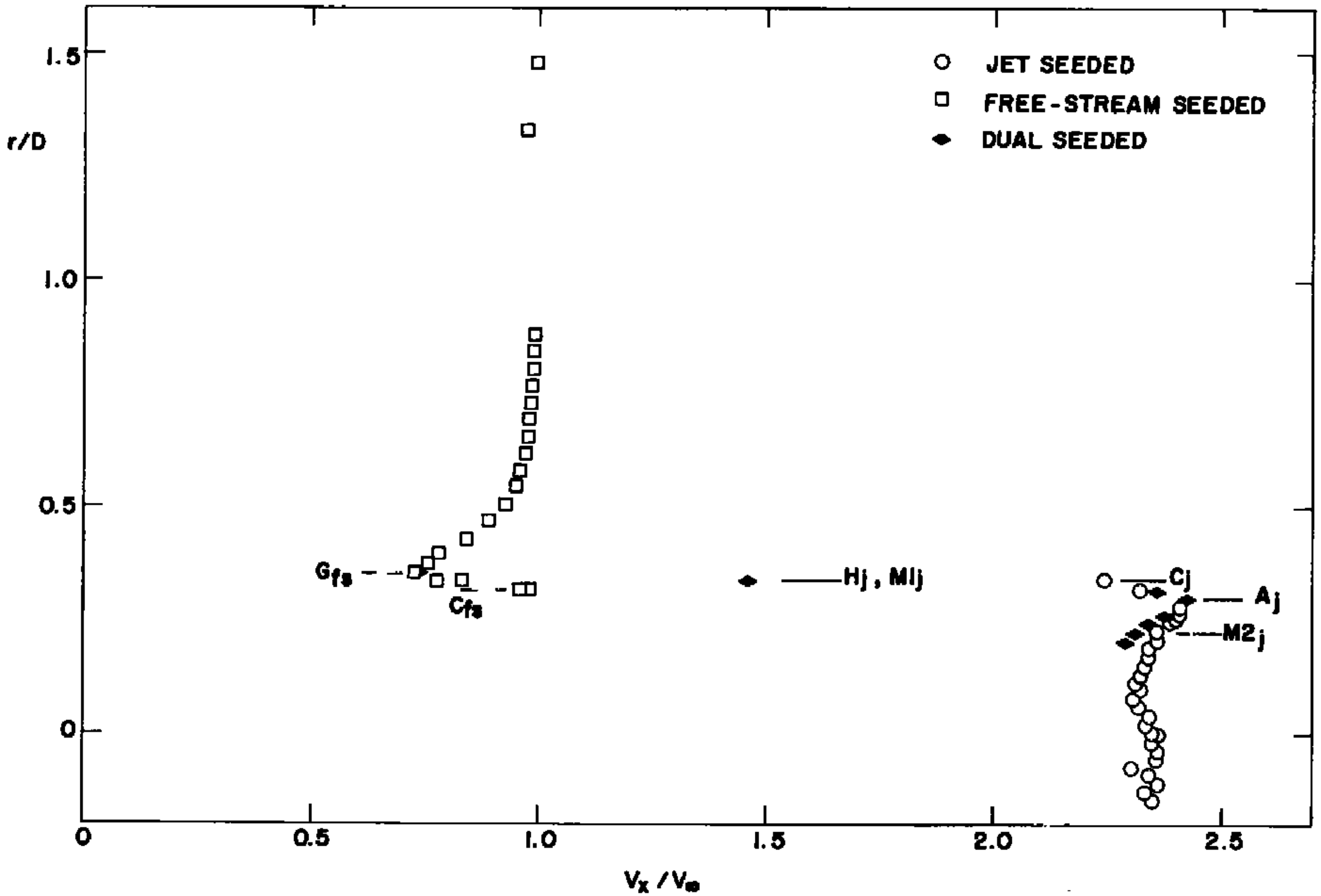

b. x/D = 0.5
Figure 15. Continued.

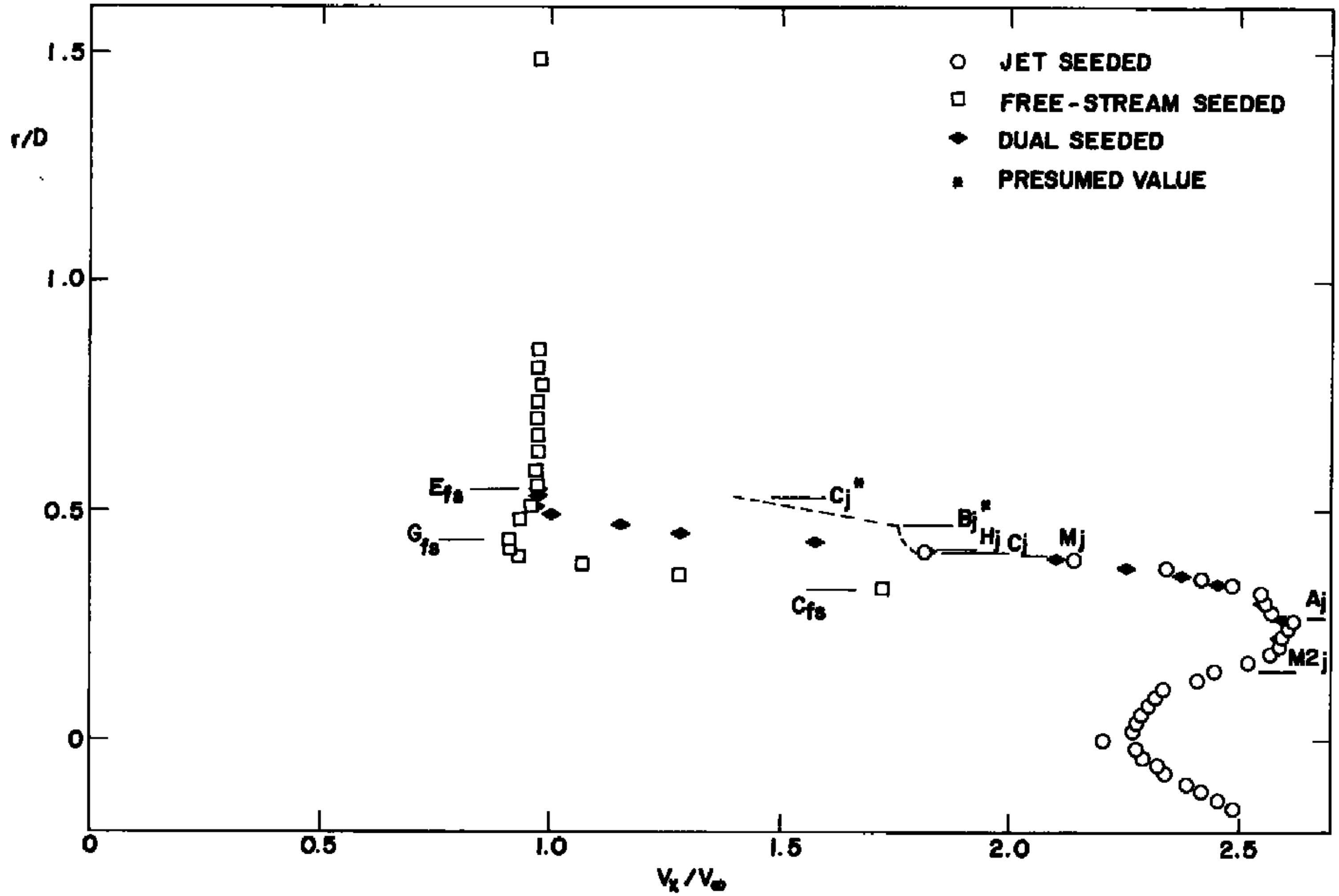

c. x/D = 1.0
Figure 15. Continued.

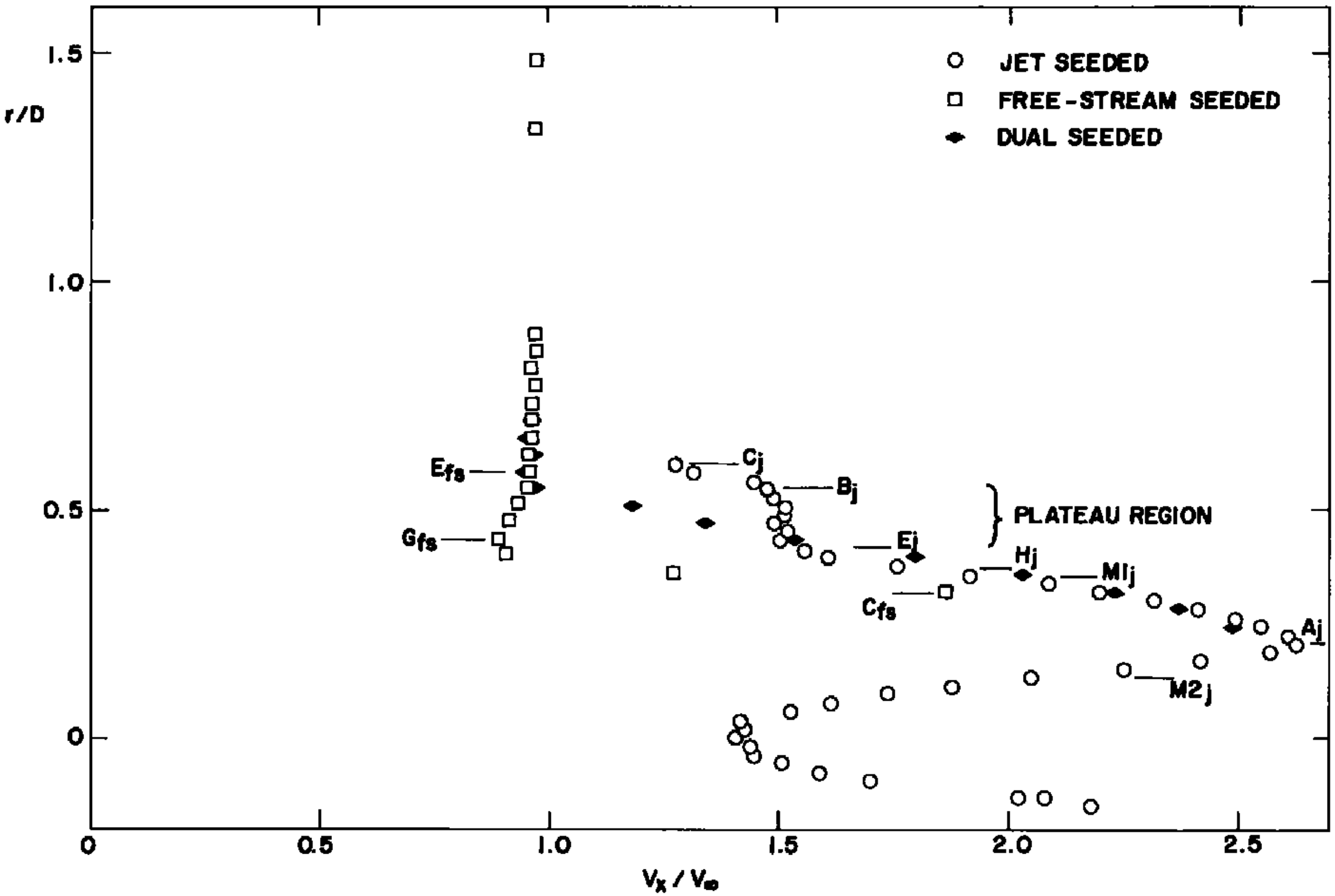

d. x/D = 1.5
Figure 15. Continued.

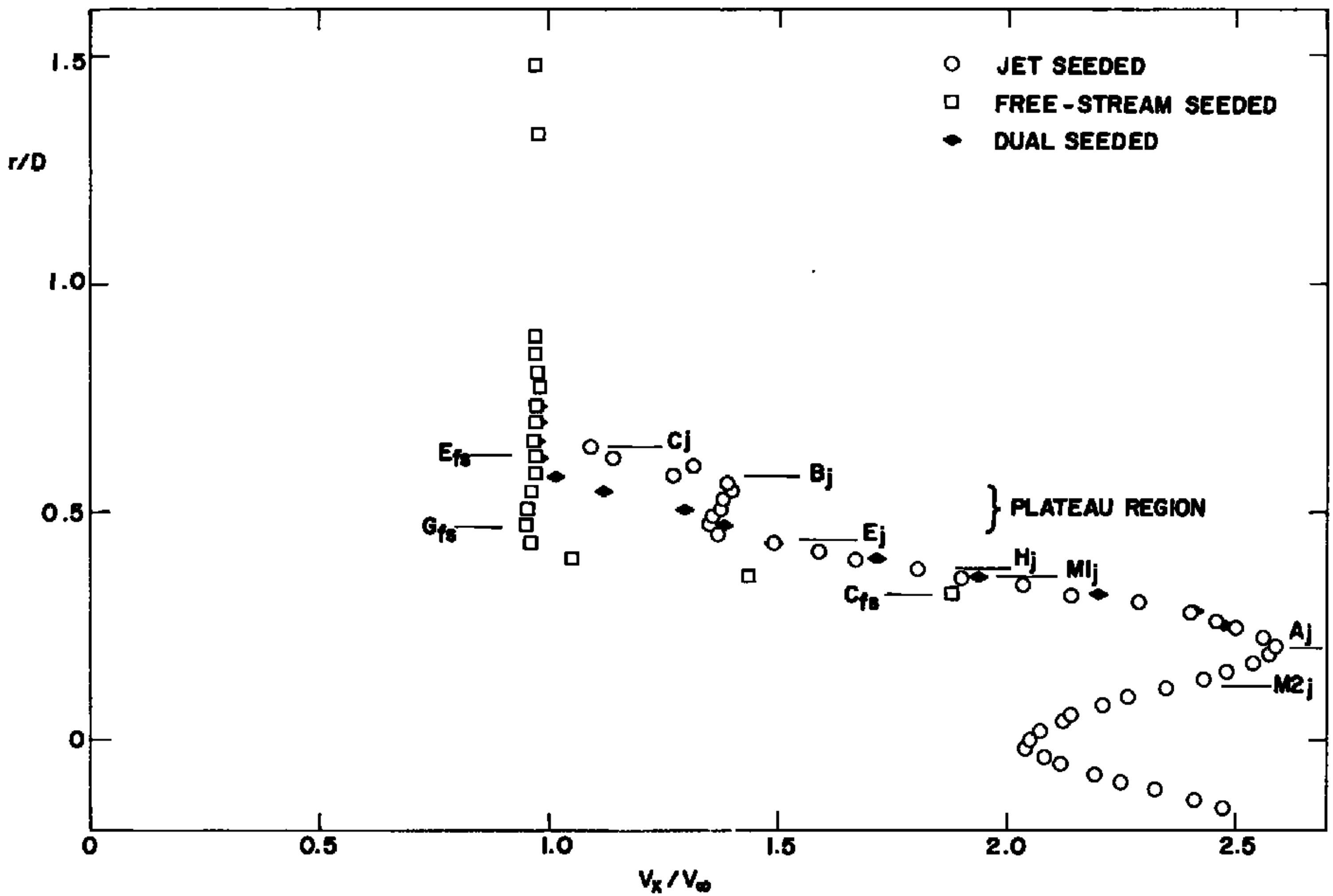

e. x/D = 2.0
Figure 15. Continued.

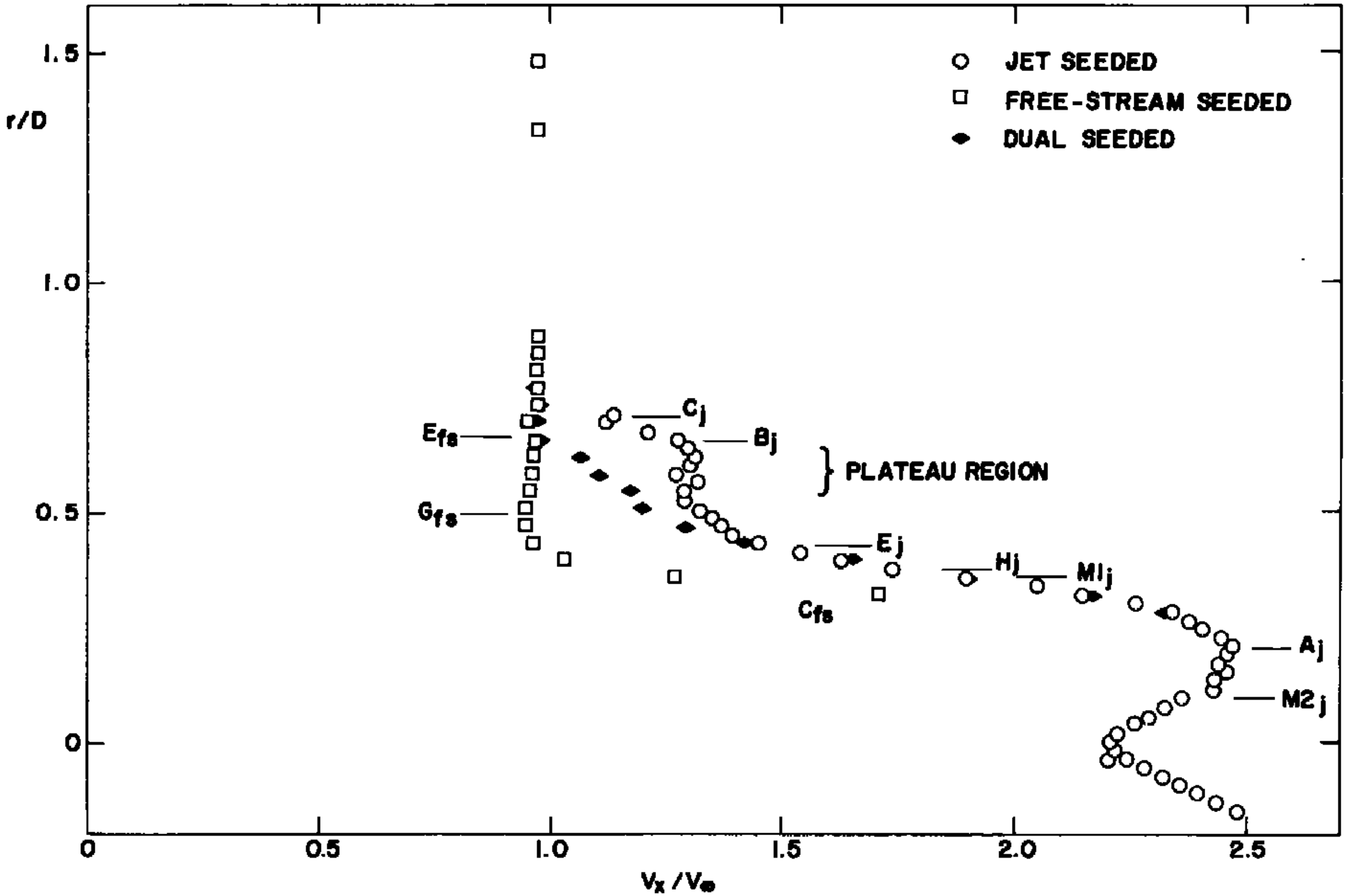

f. x/D = 2.5
Figure 15. Continued.

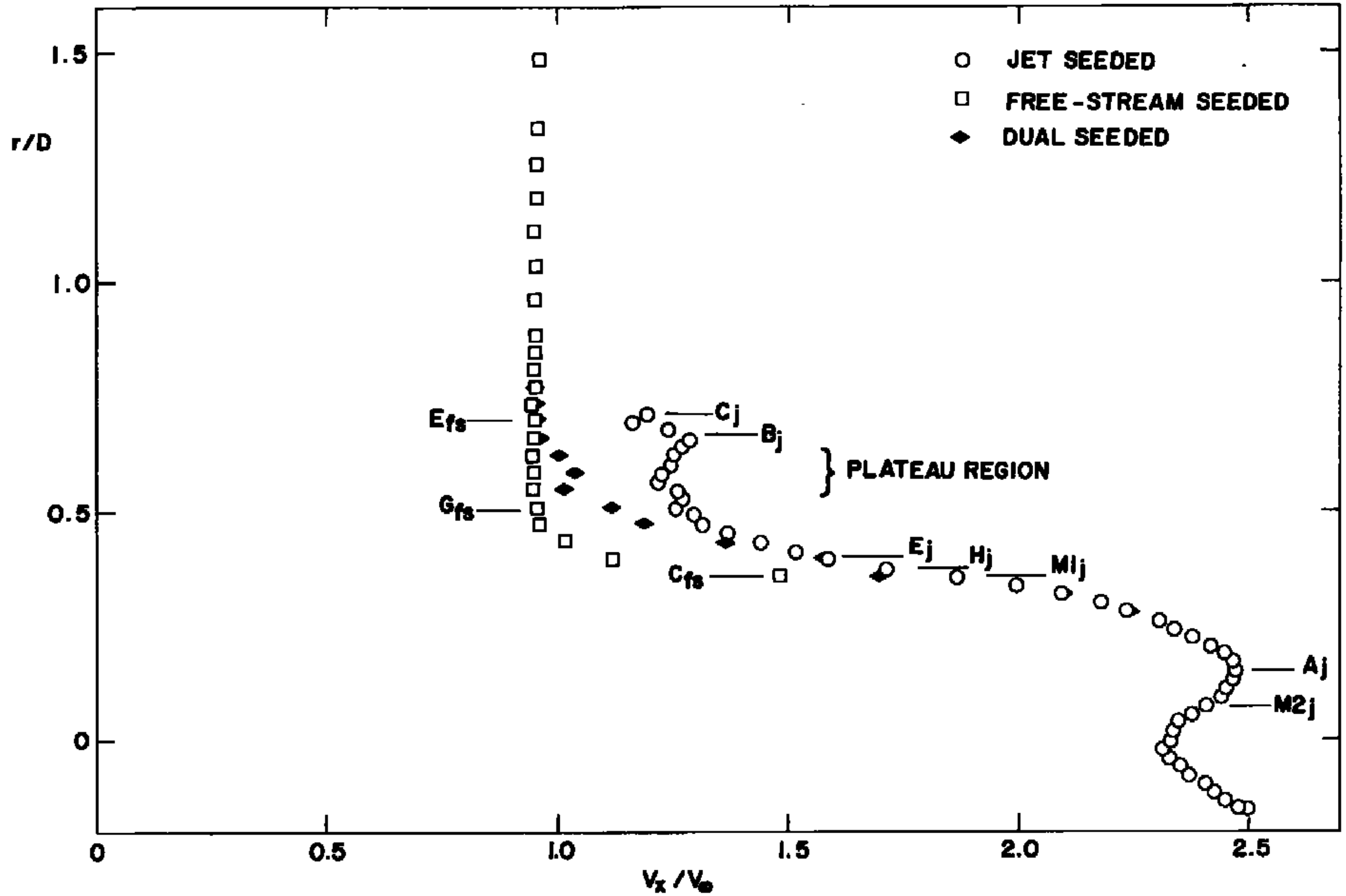

g. x/D = 3.0
Figure 15. Continued.

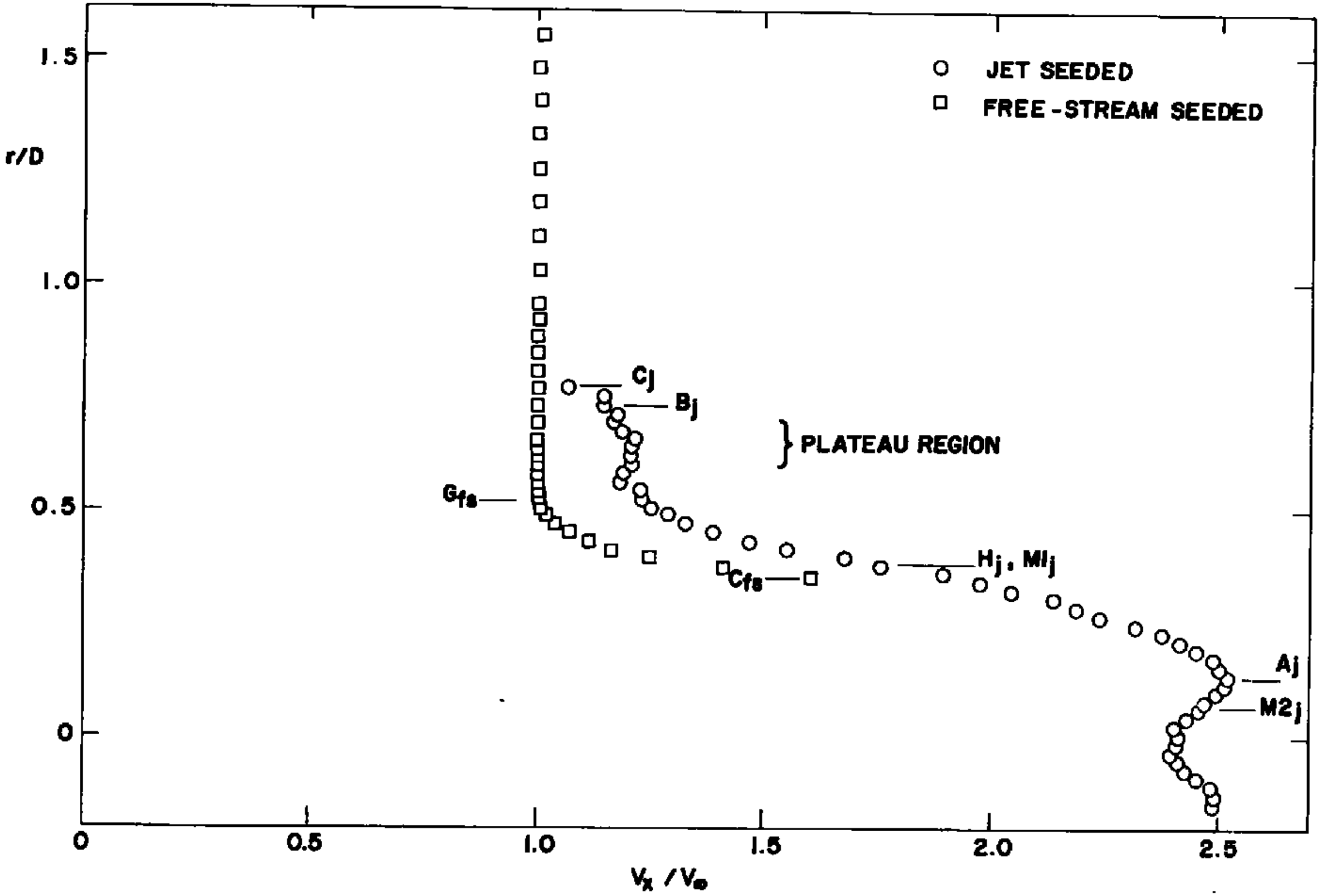

h. x/D = 3.5
Figure 15. Concluded.

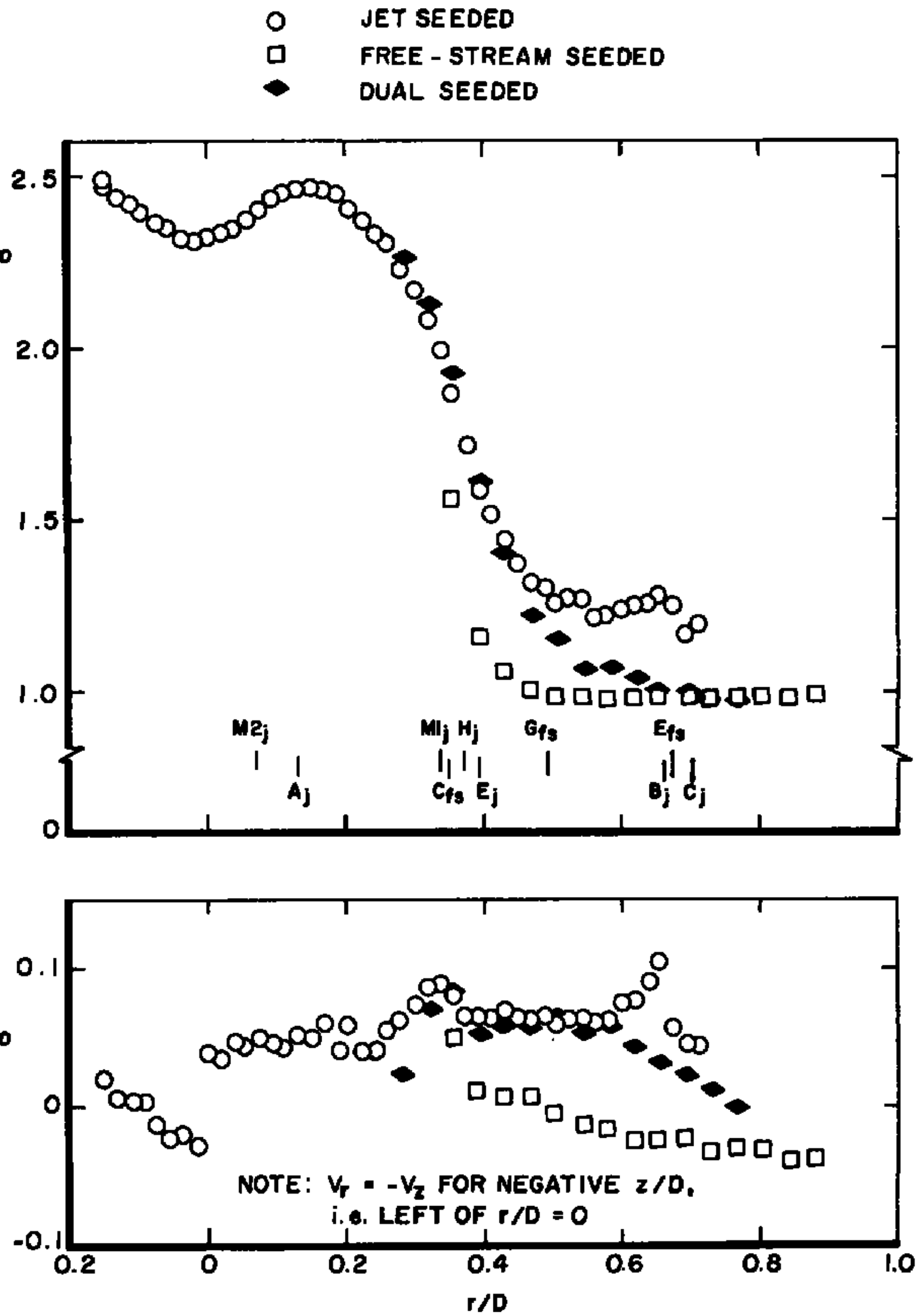

a. Mean velocity

Figure 16. Radial distribution of statistical properties for V_x and V_z component LDV data samples for three seeding conditions, x/D = 3.

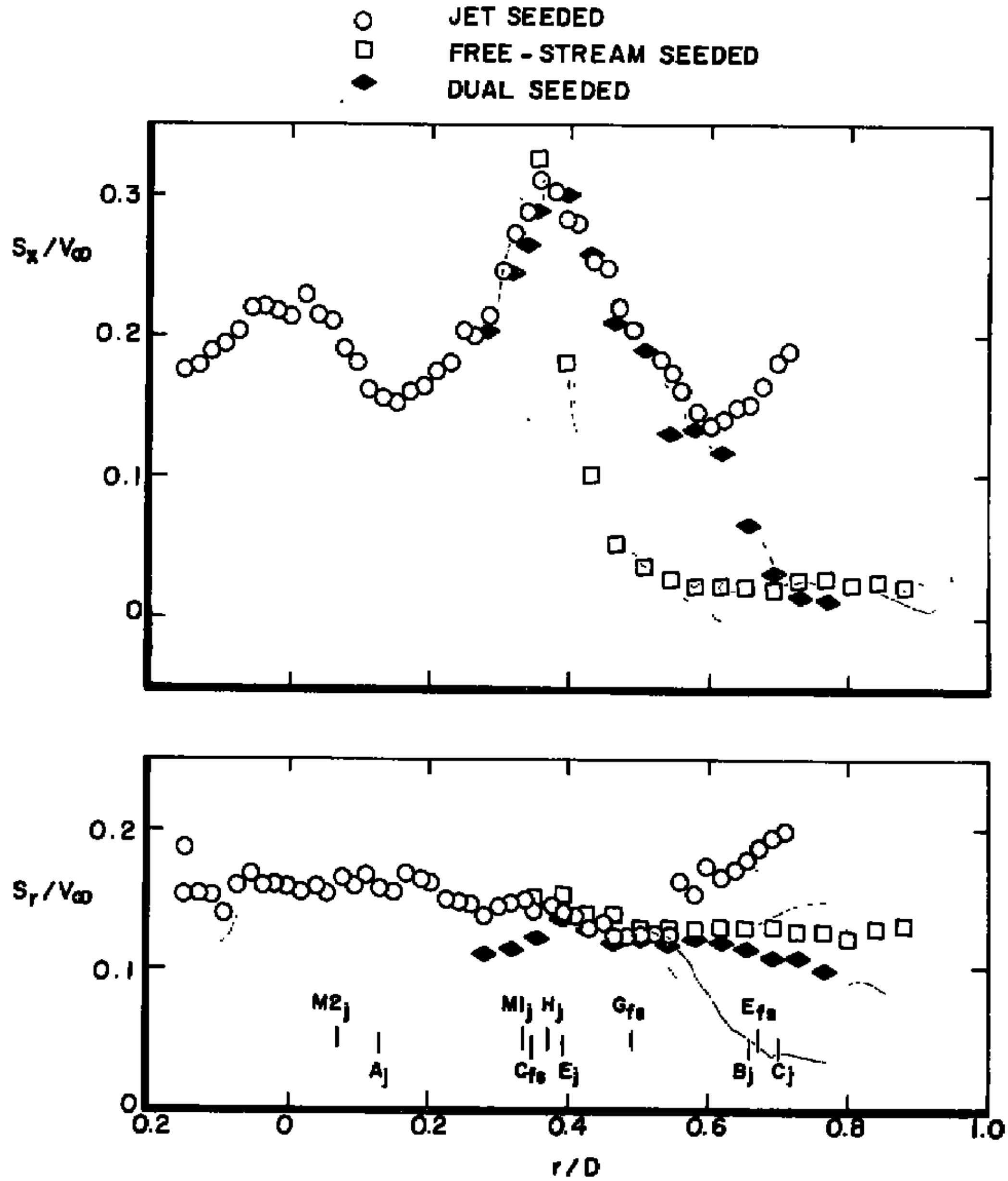

b. Standard deviation (Turbulence intensity)
Figure 16. Continued.

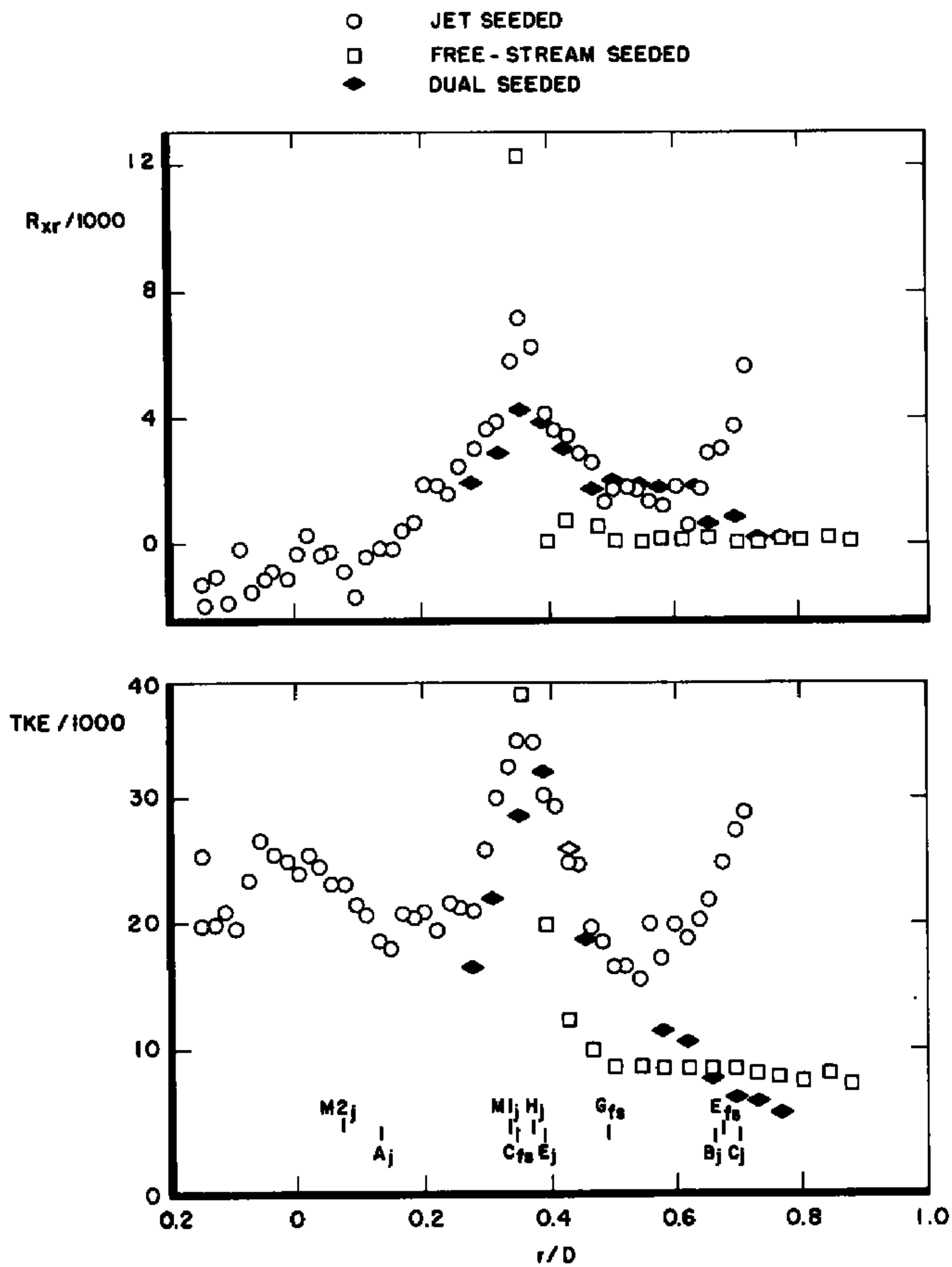

c. Reynolds shear stress and turbulence kinetic energy
Figure 16. Continued.

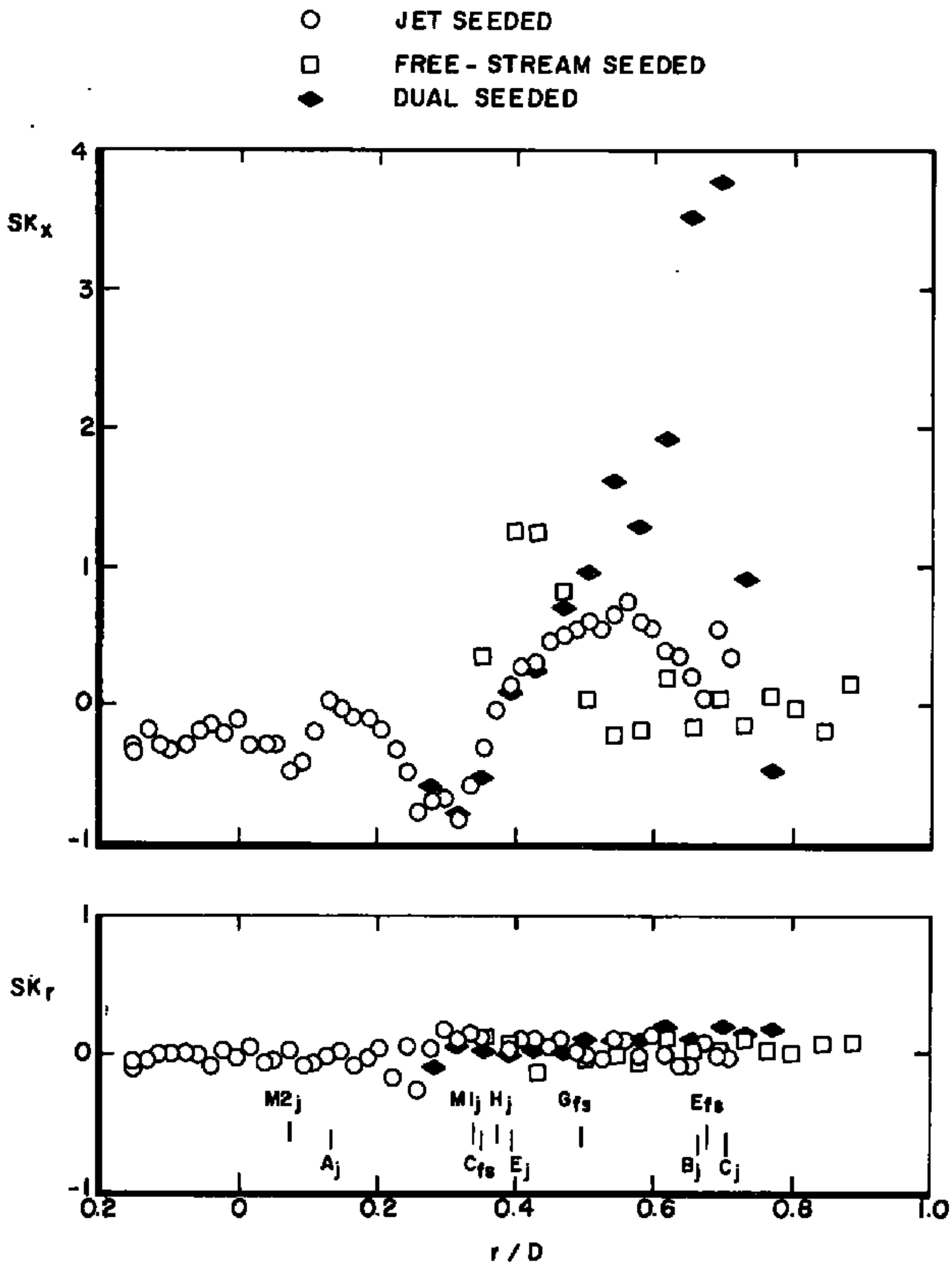

d. Skewness
Figure 16. Continued.

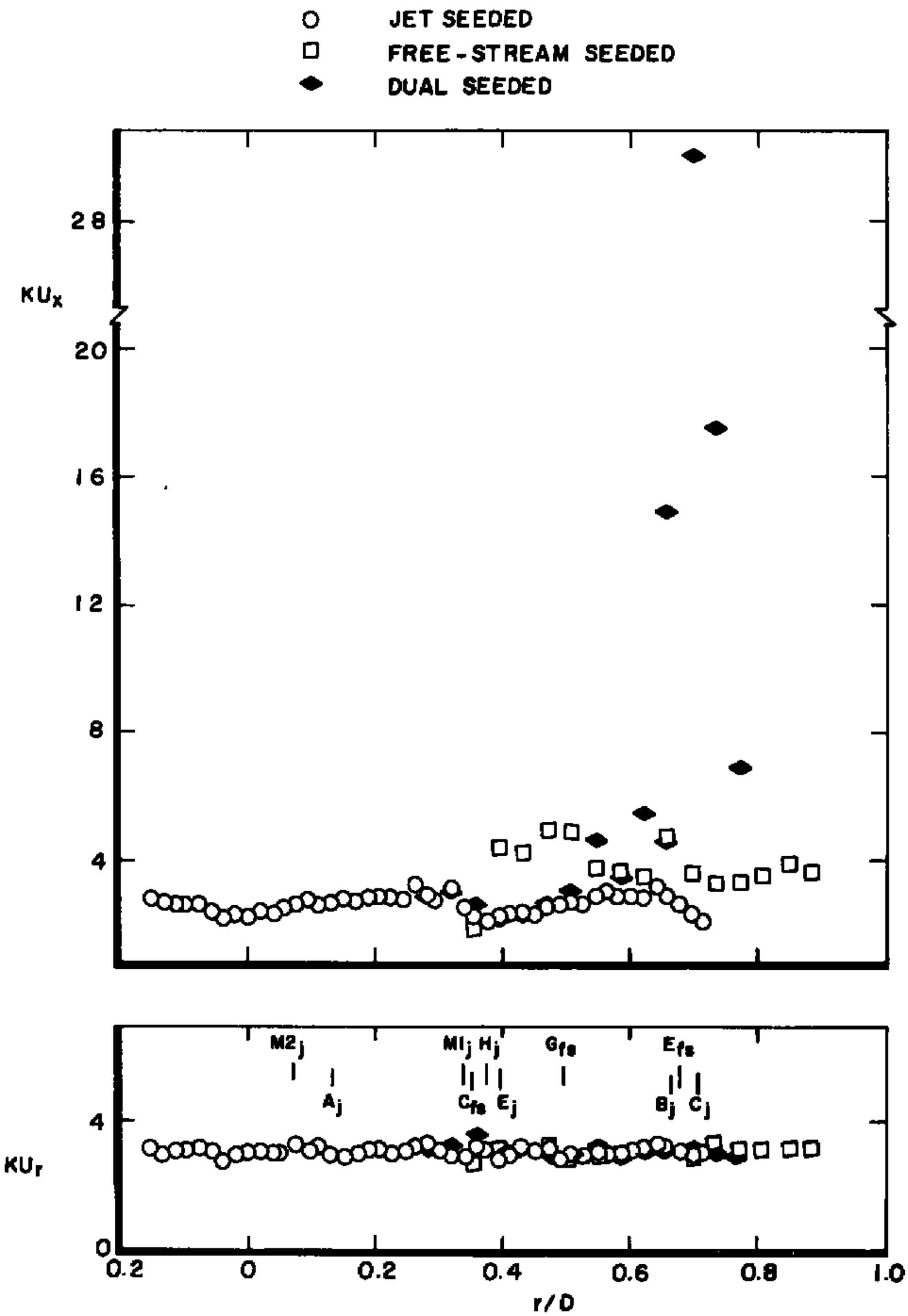

e. Kurtosis
Figure 16. Concluded.

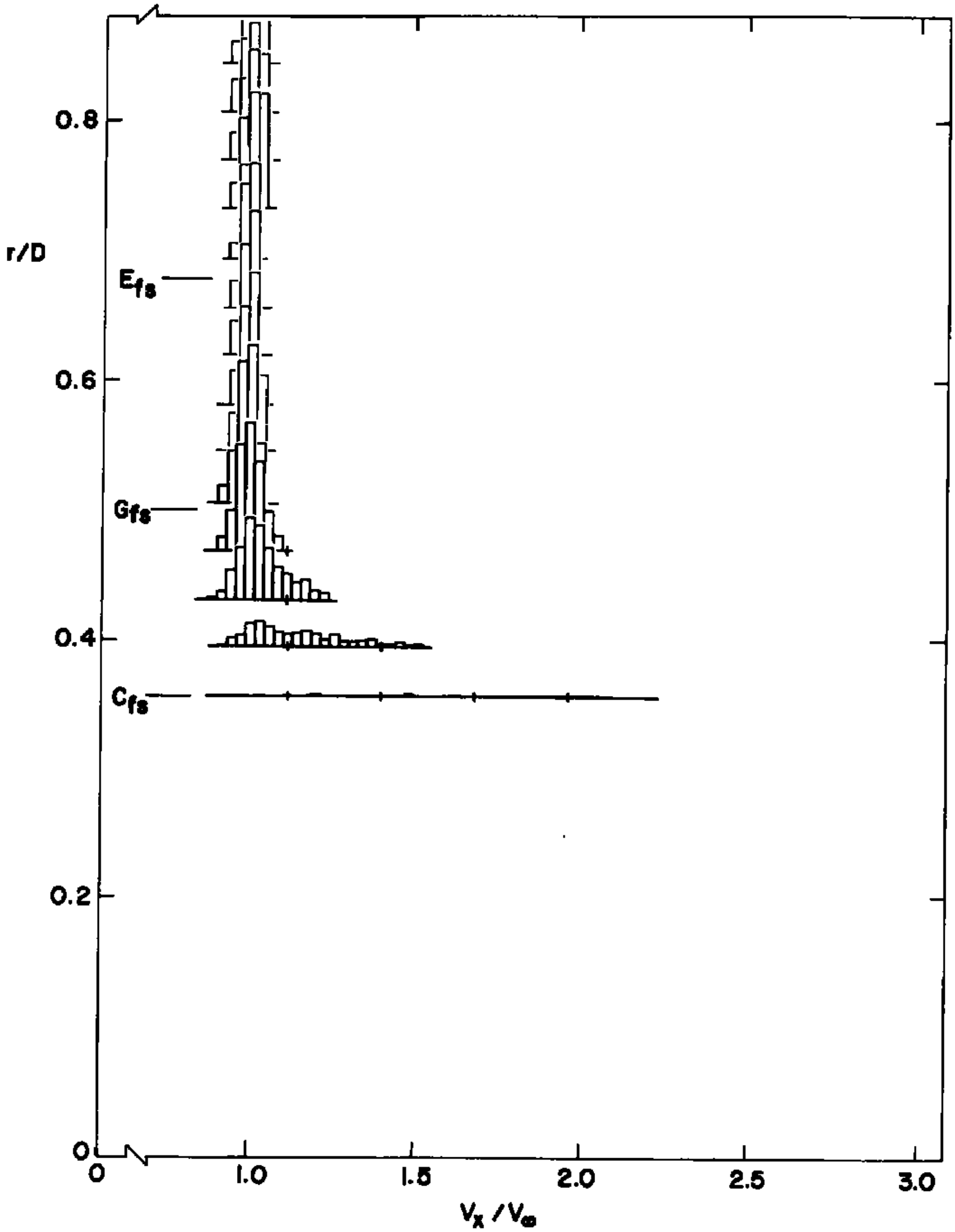

a. Free-stream seeded

Figure 17. Axial velocity probability distributions for three seeding conditions, x/D = 3.

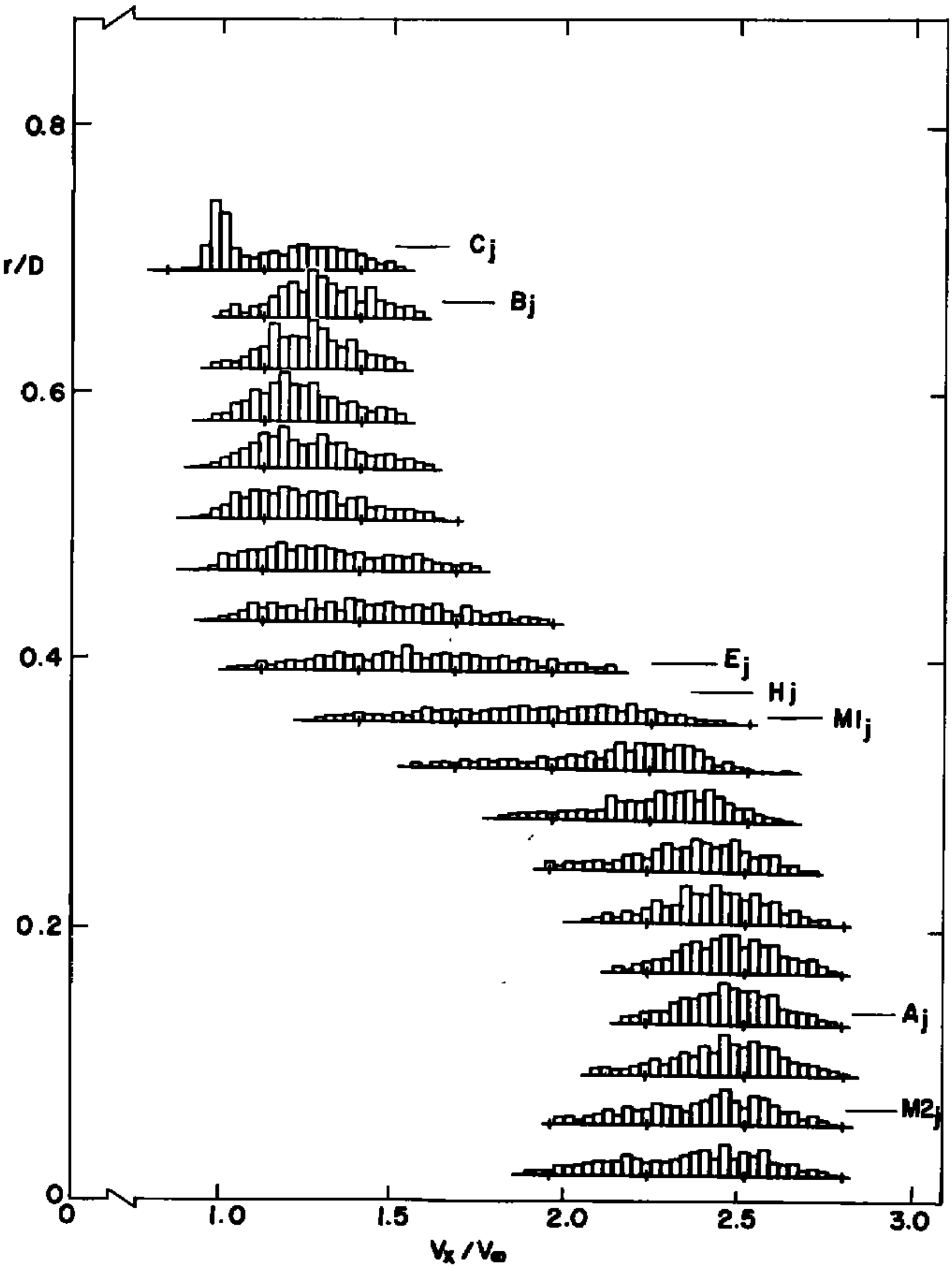

b. Jet seeded
Figure 17. Continued.

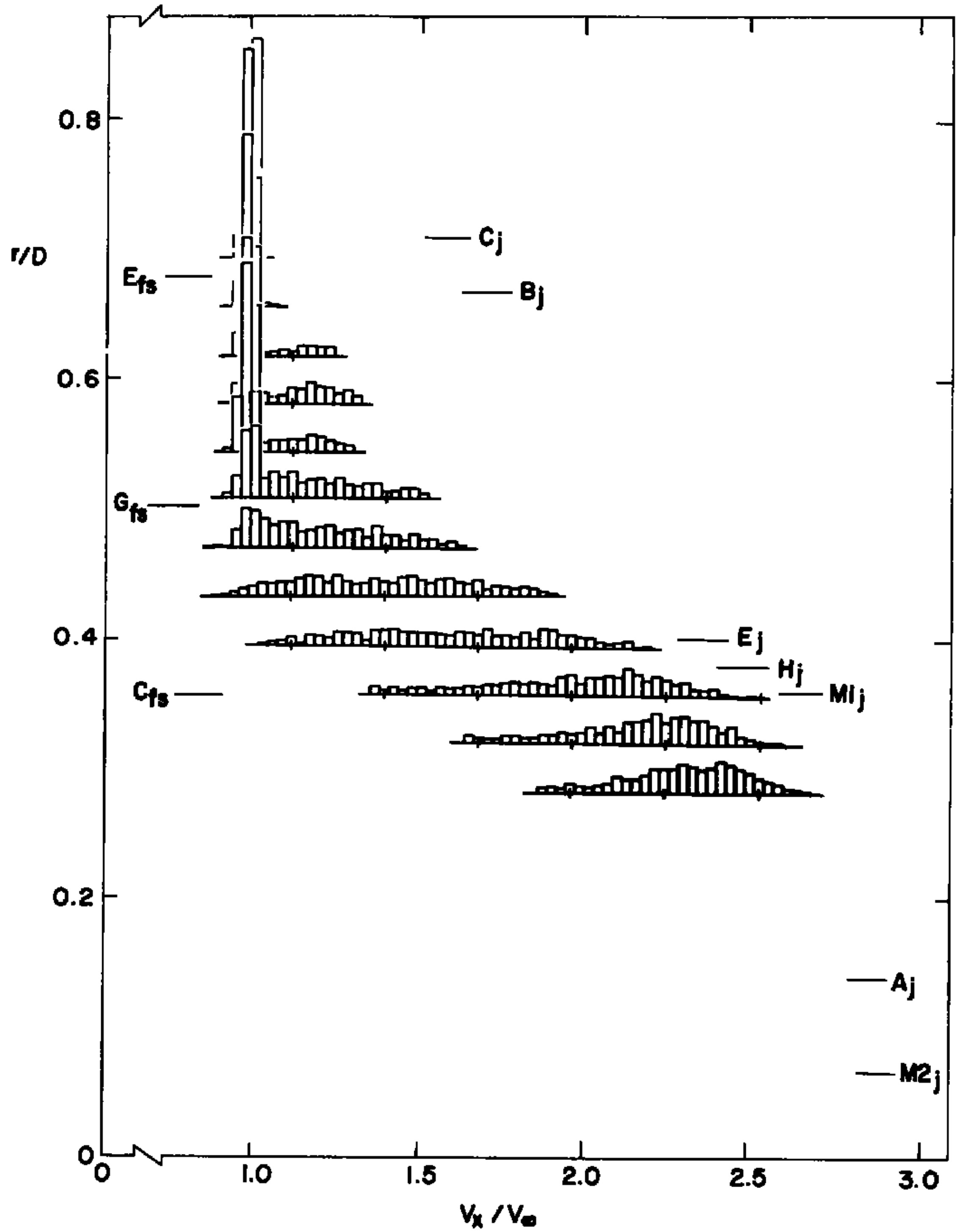

c. Dual seeded

Figure 17. Concluded.

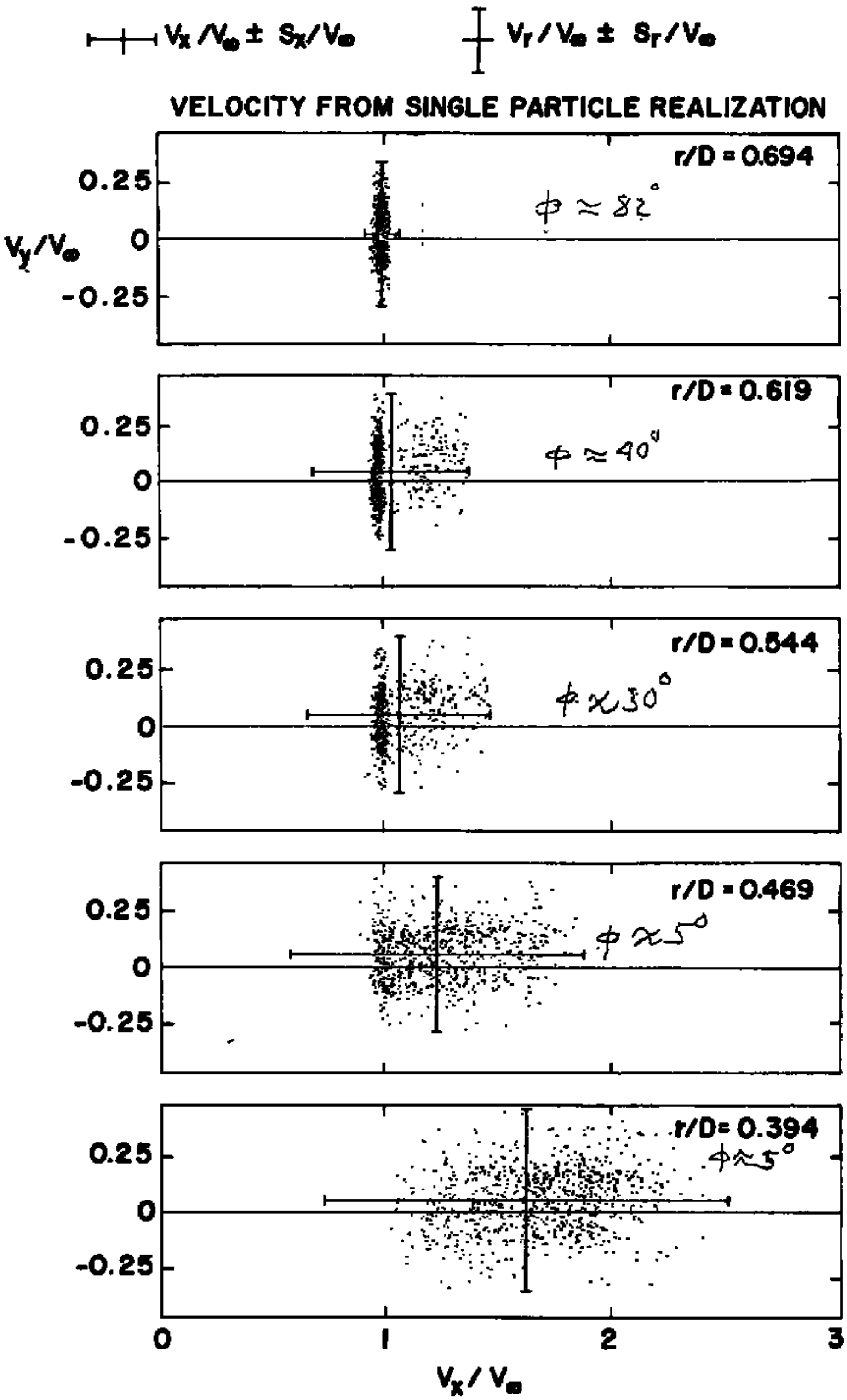

Figure 18. Two-dimensional velocity distribution is the intermittent region for dual seeding, x/D = 3.

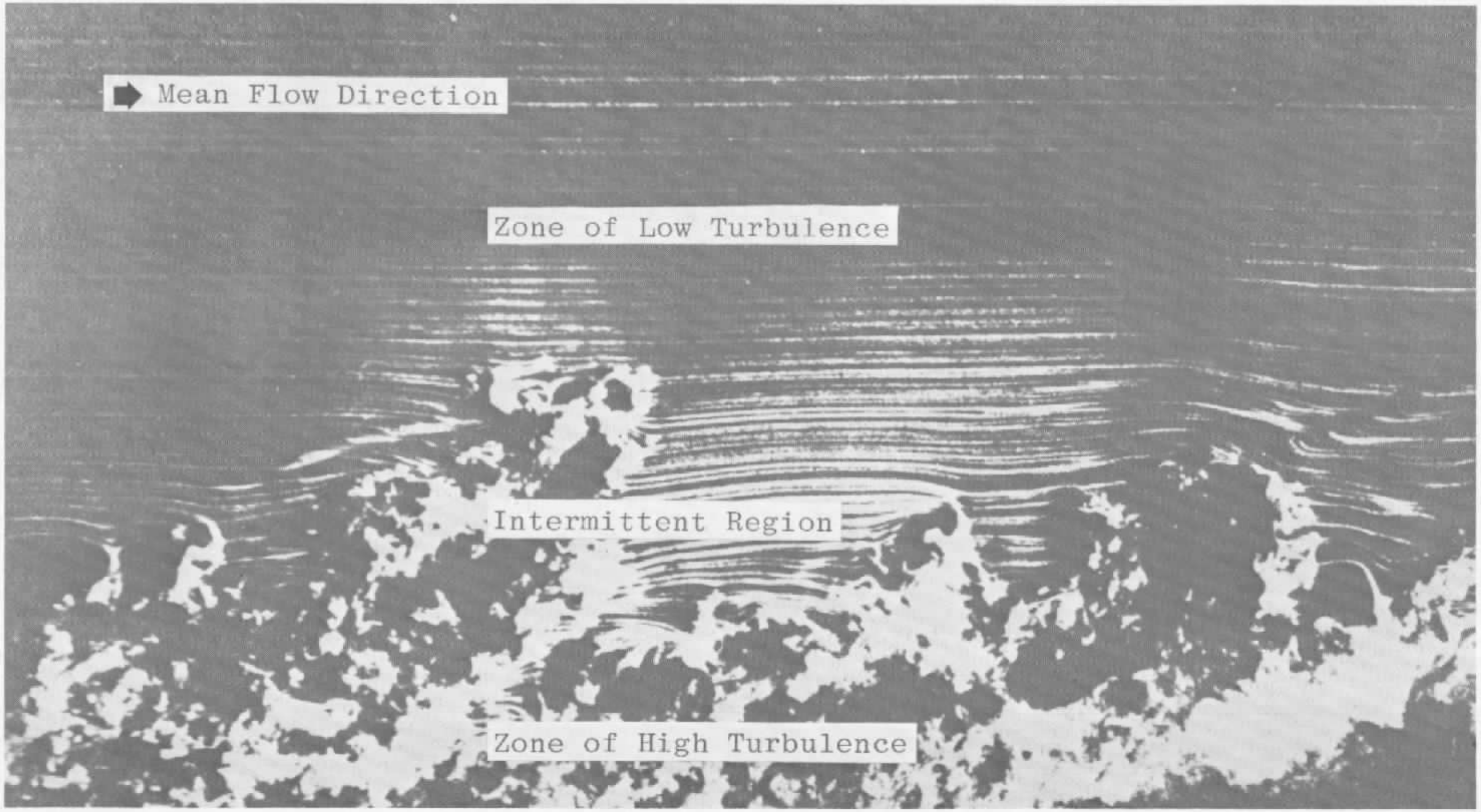

Figure 19. Turbulent shear layer boundary

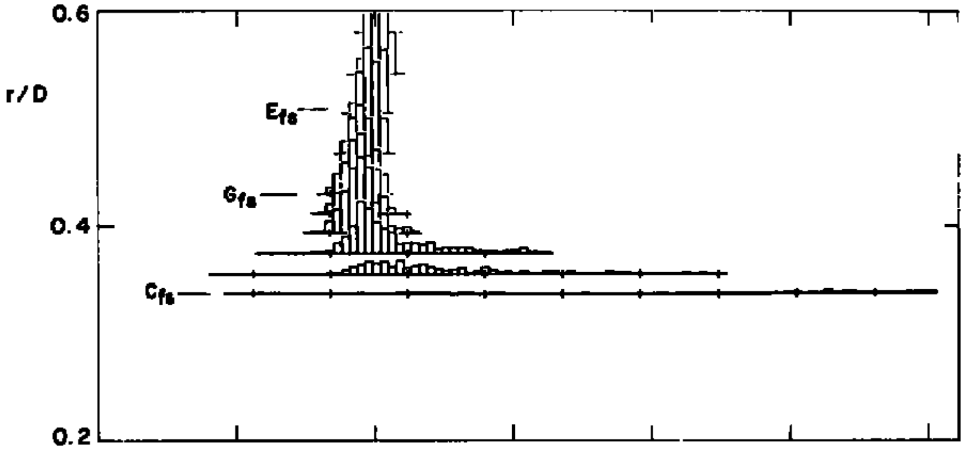

a. Free-stream seeded

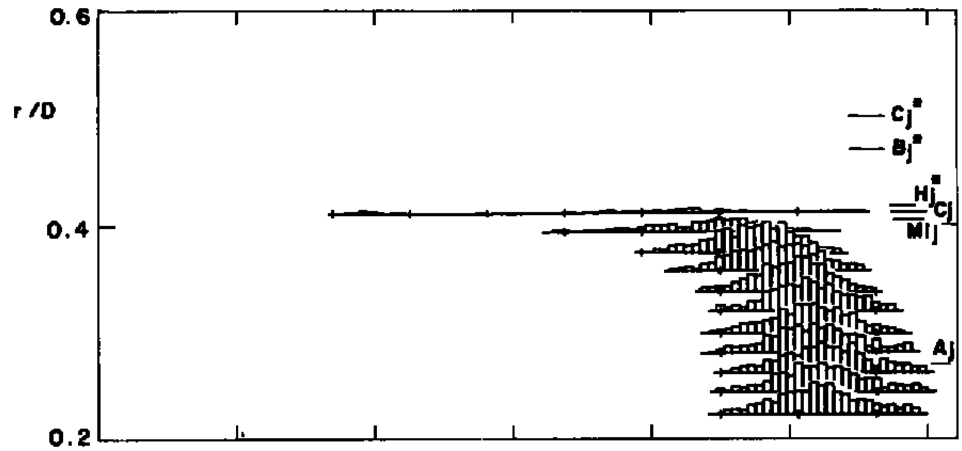

b. Jet seeded

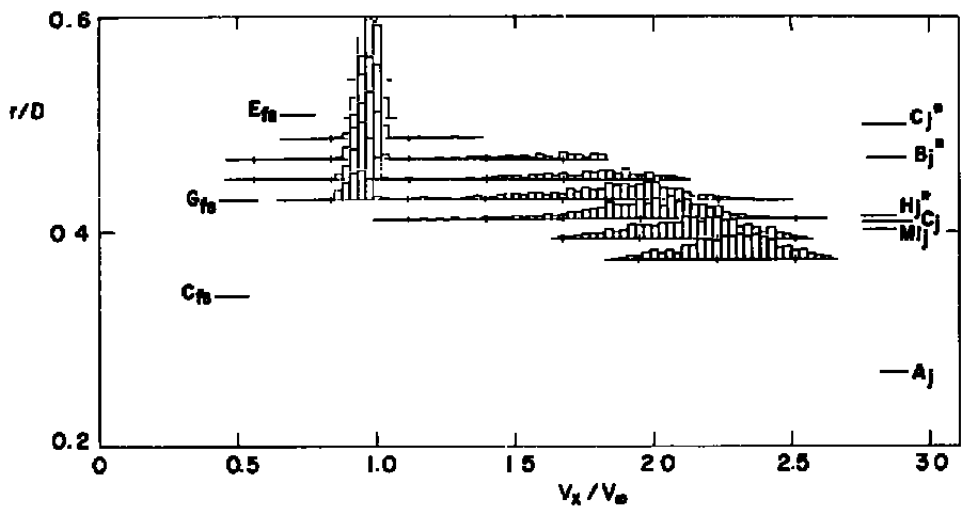

c. Dual seeded

Figure 20. Axial velocity probability distributions for three seed combinations, x/D = 1.

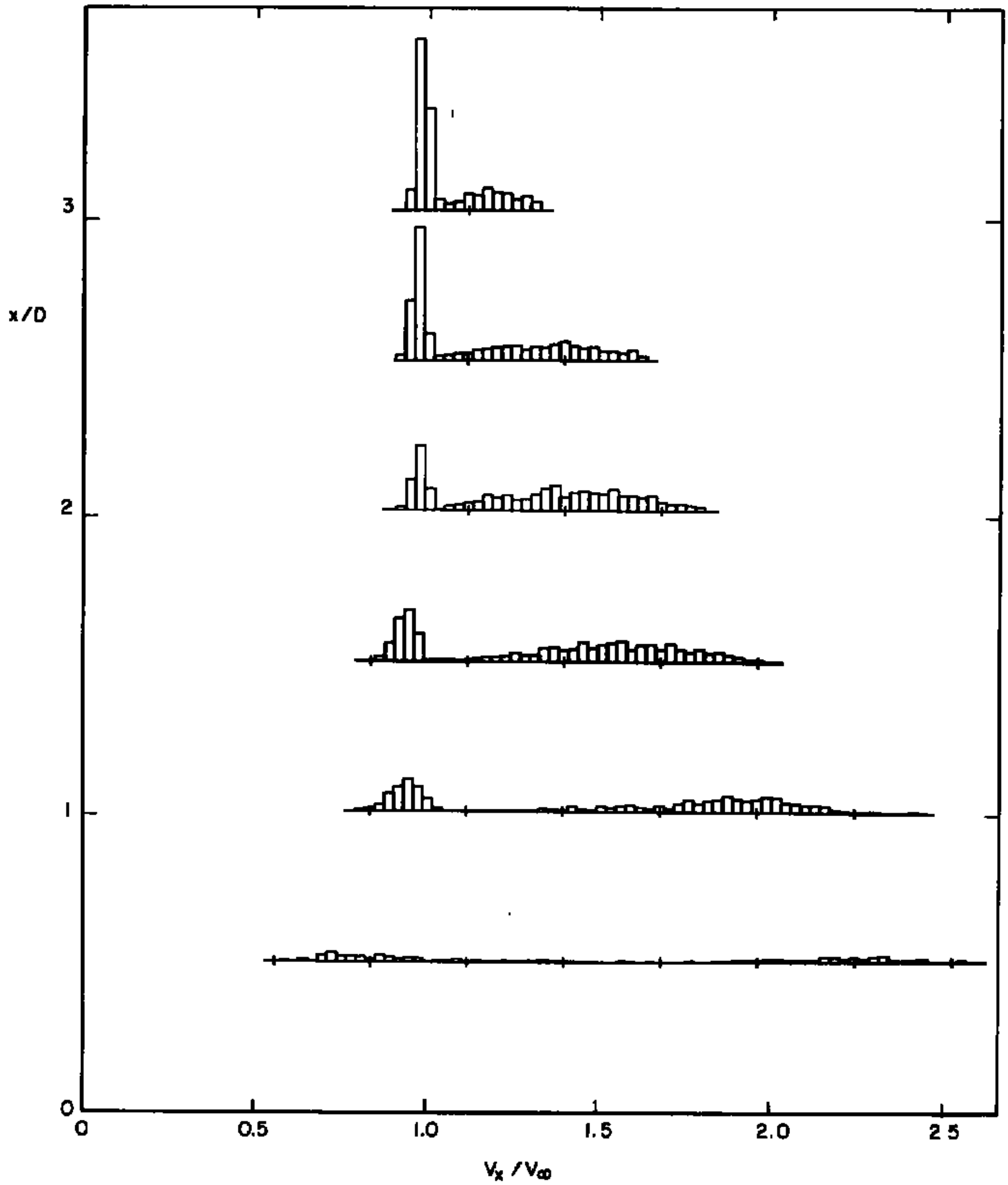

Figure 21. Axial velocity probability distributions within the intermittent region at each x-station for dual seeding.

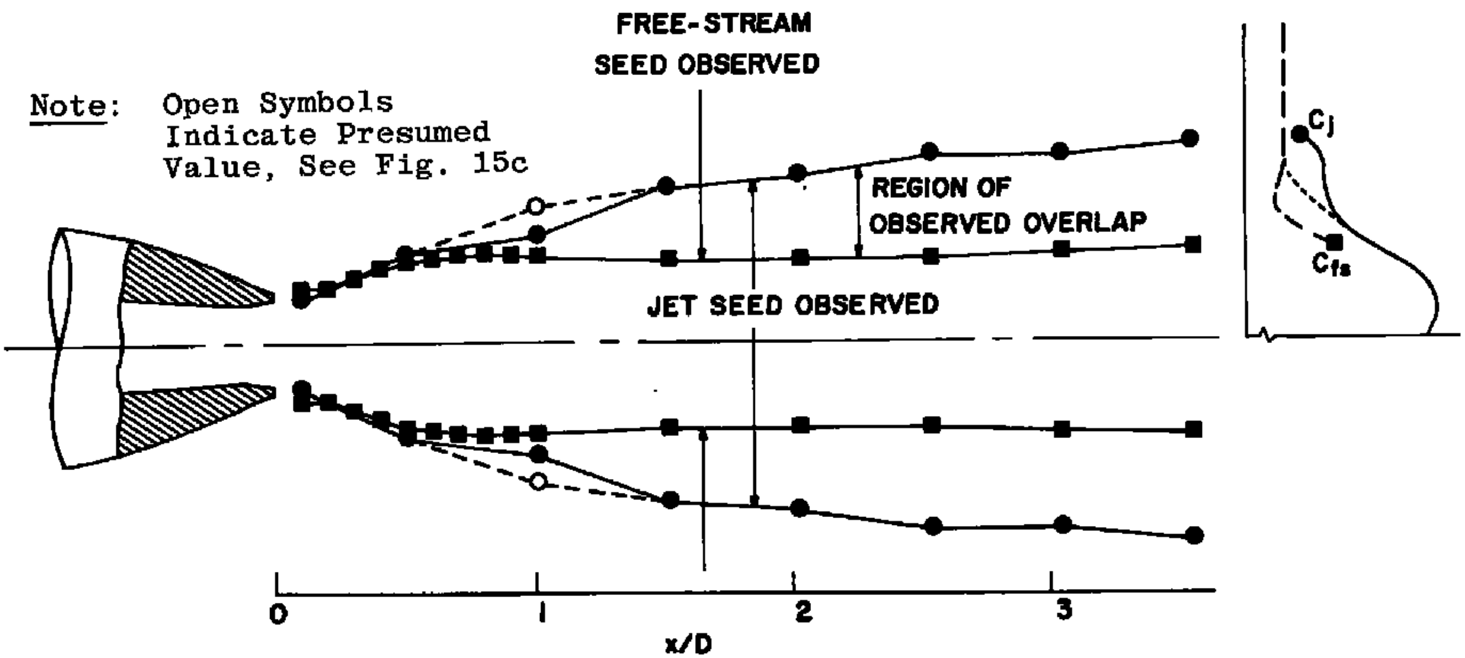

a. C_{fs} and C_j

Figure 22. Axial variation of key characteristics in the jet plume axial velocity profiles.

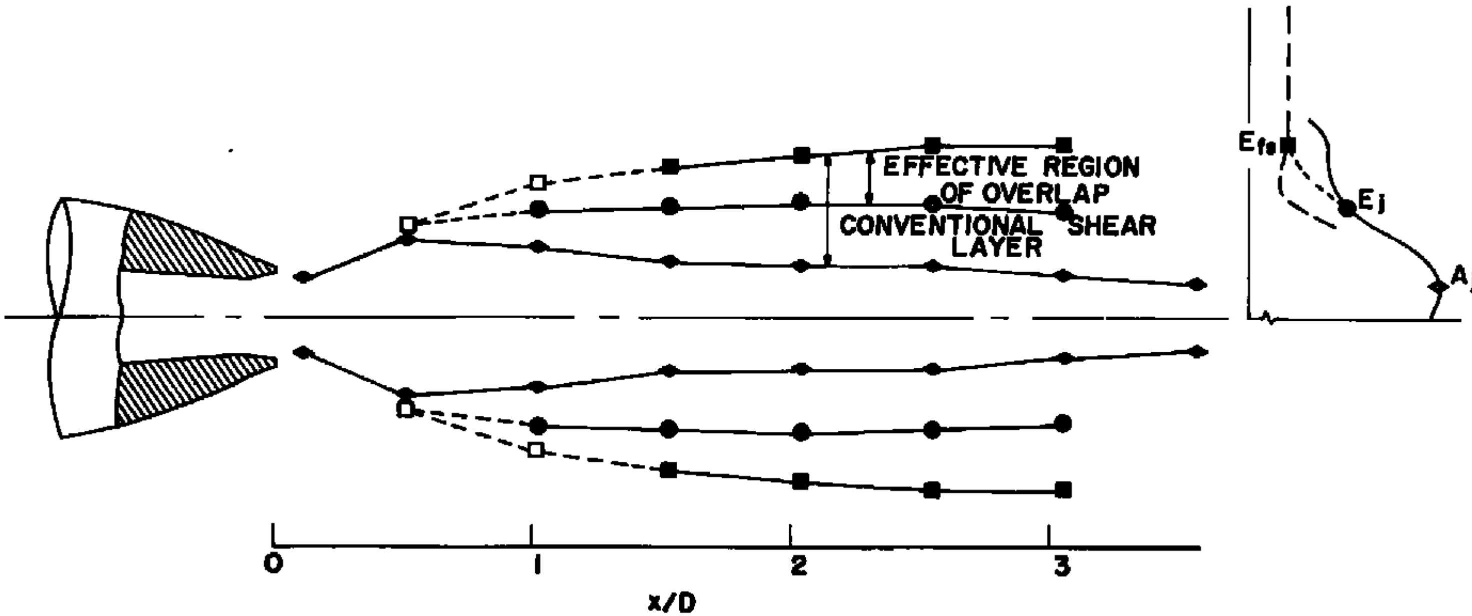

b. E_{fs}, E_j, and A_j
Figure 22. Continued.

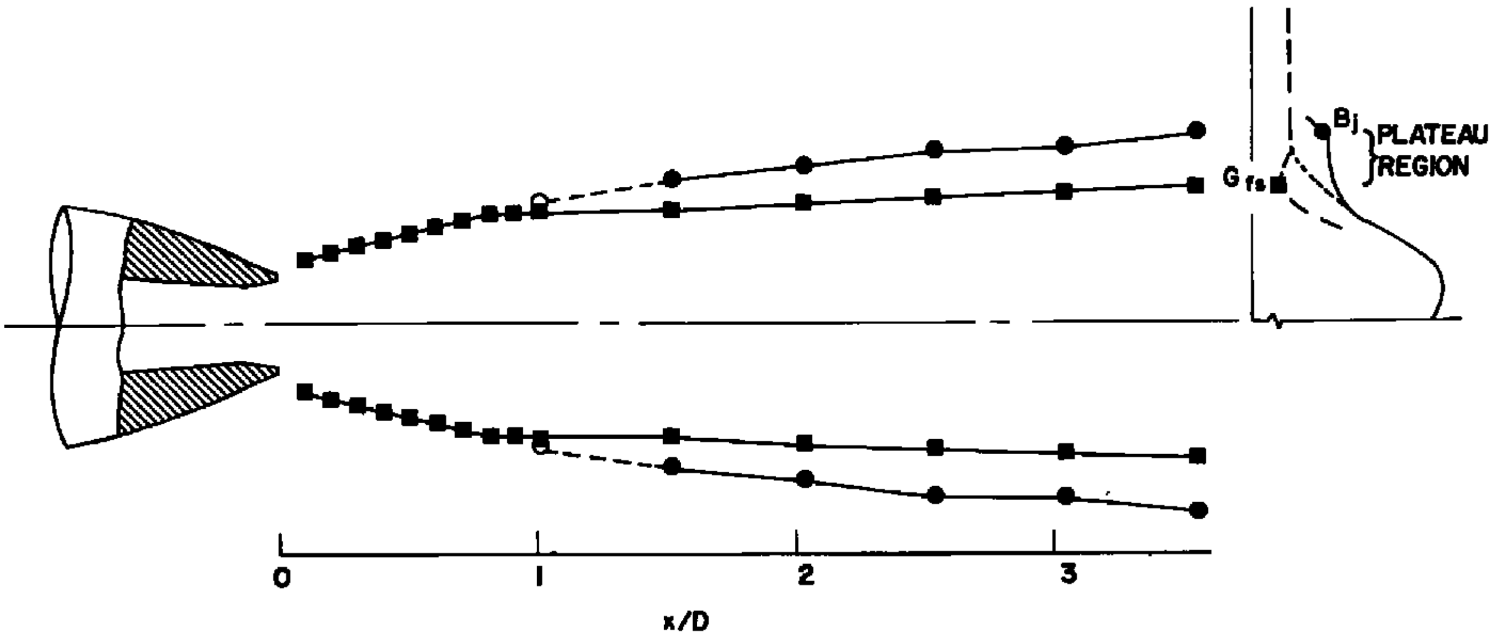

c. B_j and G_{fs}
Figure 22. Concluded.

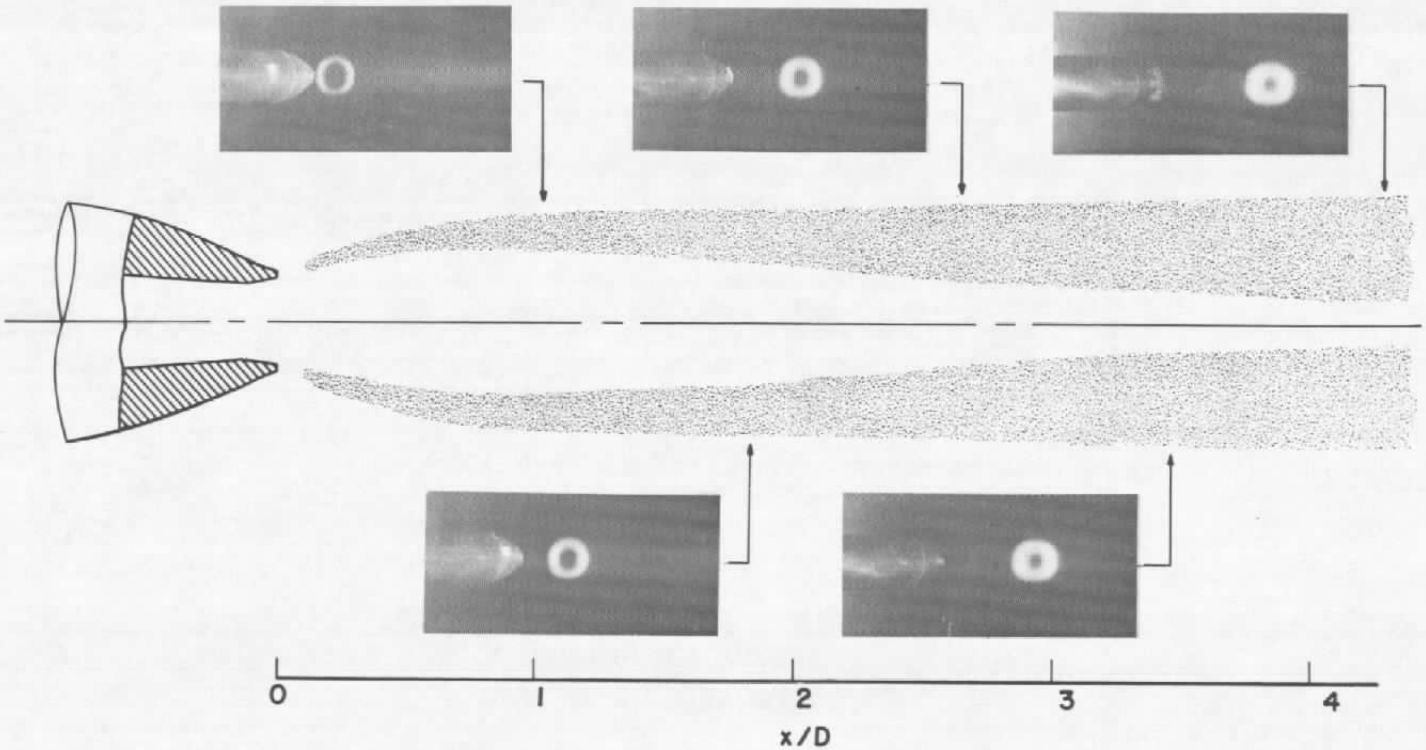

Figure 23. Laser vapor screen flow visualization.

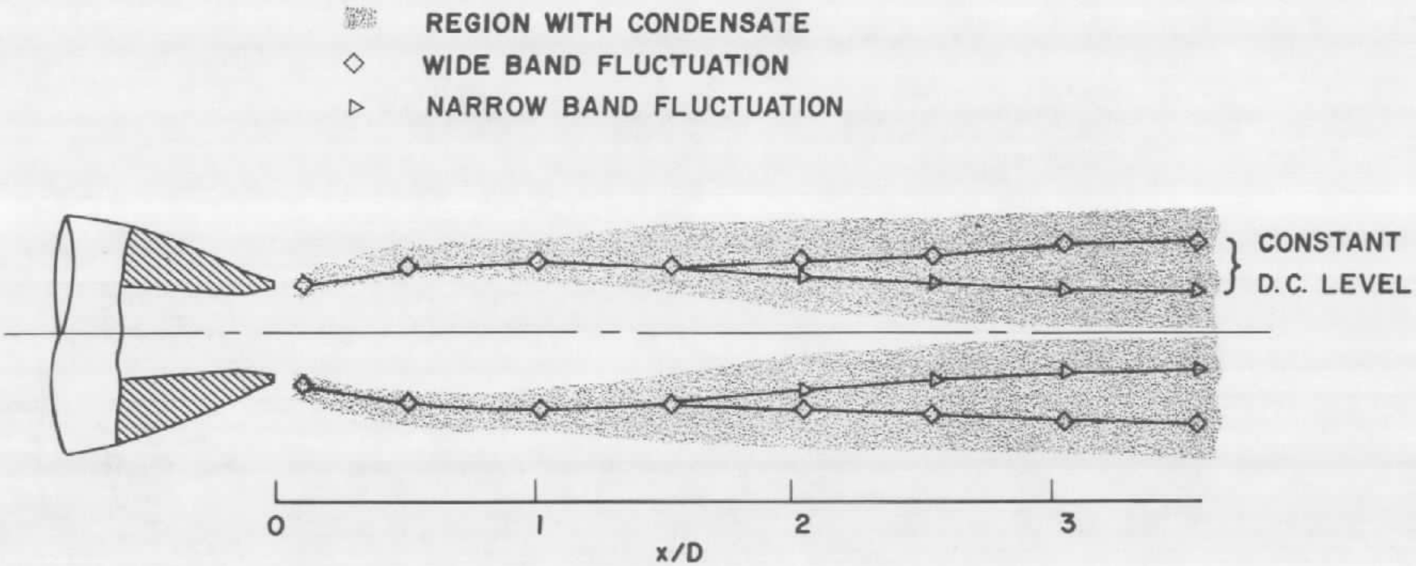

Figure 24. LDV oscilloscope signal "visualization".

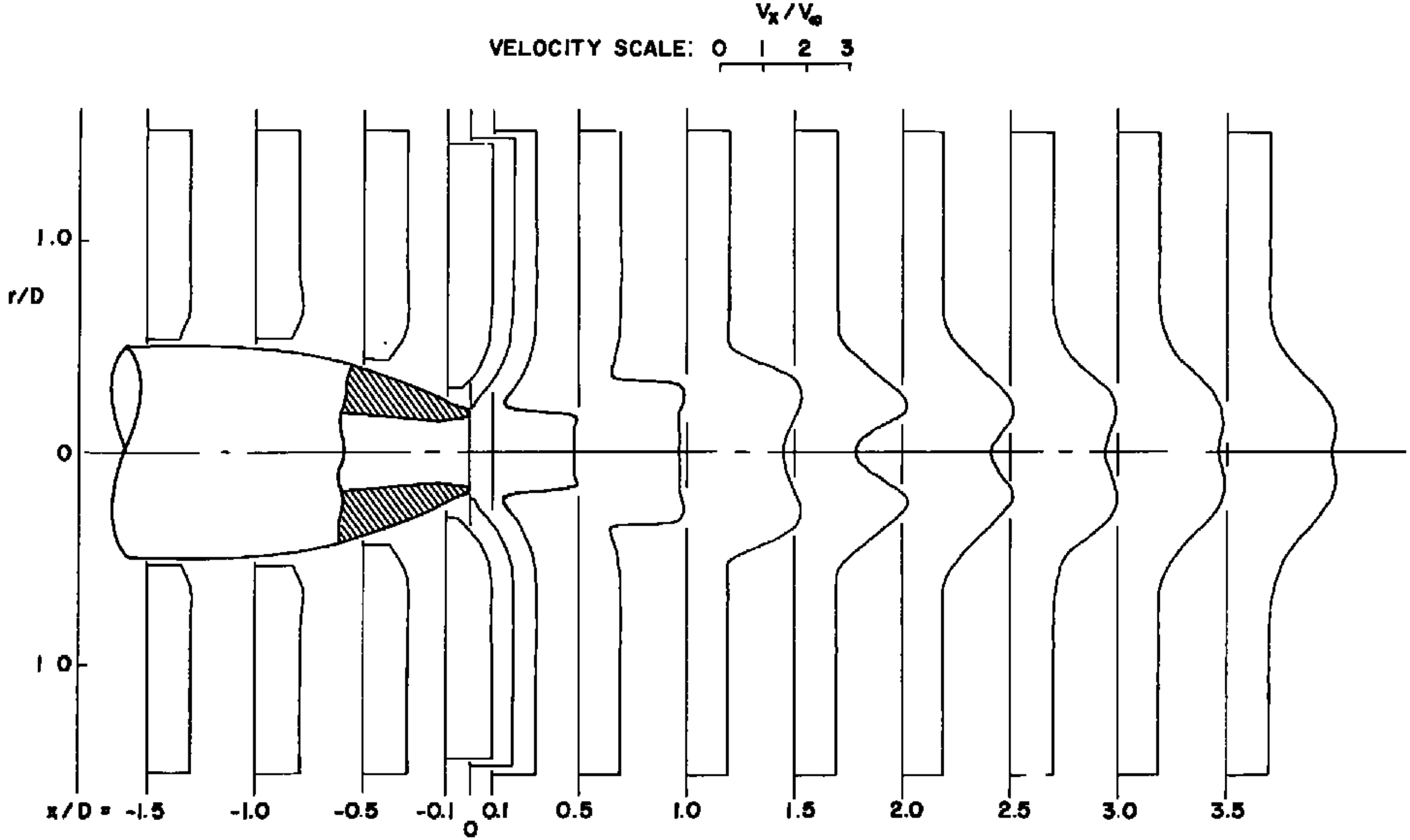

Figure 25. Resolved velocity profiles.

APPENDIX A
Data Reduction Equations

Crocco number squared	$C^2 = \dfrac{\lvert V \rvert^2}{2cpT_t}$
Mach number	$M = \left(\dfrac{5\,C^2}{1 - C^2} \right)^{1/2}$
Sample mean velocity	$V_x = \dfrac{1}{N} \sum_{i=1}^{N} V_{x_i}$
	$V_r = \dfrac{1}{N} \sum_{i=1}^{N} V_{ri}$
Mean velocity magnitude	$V = (V_x^2 + V_r^2)^{1/2}$
Sample variance	$VAR_x = \dfrac{1}{N} \sum_{i=1}^{N} (V_{x_i} - V_x)^2$
	$VAR_r = \dfrac{1}{N} \sum_{i=1}^{N} (V_{r_i} - V_r)^2$
Turbulence intensity (Sample standard deviation)	$S_x = (VAR_x)^{1/2}$
	$S_r = (VAR_r)^{1/2}$
Skewness	$SK_x = \dfrac{1}{N(VAR_x)^{3/2}} \sum_{i=1}^{N} (V_{x_i} - V_x)^3$
	$SK_r = \dfrac{1}{N(VAR_r)^{3/2}} \sum_{i=1}^{N} (V_{r_i} - V_r)^3$
Kurtosis	$KU_x = \dfrac{1}{N(VAR_x)^2} \sum_{i=1}^{N} (V_{x_i} - V_x)^4$
Turbulence kinetic energy (assuming tangetial and radial variences are equal)	$TKE = \dfrac{1}{2} (VAR_x + 2\,VAR_r)$

Reynolds shear stress (covariance)	$R_{xr} = \frac{1}{N} \sum_{i=1}^{N} (V_{x_i} - V_x)(V_{r_i} - V_r)$
Particle realization rate	$PPS = \frac{N}{t}$
Particle number density indicator	$PPL = \frac{N}{t} \frac{V_\infty}{\lvert V \rvert}$

APPENDIX B
Experimental Data

V_∞ = 713.0 ft/sec T_t = 640.3 °R D = 0.986 in.

SEQ	x/D	r/D	V_x/V_∞	V_r/V_∞	$\|V\|/V_\infty$	M	S_x/V_∞	S_r/V_∞	SK_x	SK_r	KU_x	KU_r	RE_{xr}	TKE	N	PPS	PPL	SE	CC
1310	-2.028	1.502	0.994	-0.025	0.994	0.591	0.026	0.127	0.151	-0.092	4.520	3.207	64.4	8319.5	996	41	41	1	1
1311	-1.826	1.502	0.989	-0.036	0.939	0.588	0.044	0.132	0.129	0.017	3.542	3.154	-294.1	9315.3	987	55	56	1	1
1314	-1.623	1.502	0.994	-0.031	0.995	0.591	0.024	0.129	-0.224	0.026	3.568	3.056	-101.9	8664.8	992	48	49	1	1
1315	-1.420	1.502	0.991	-0.021	0.991	0.589	0.035	0.130	-0.209	-0.033	3.681	2.977	105.7	8965.1	989	41	41	1	1
1318	-1.217	1.502	0.999	-0.020	0.999	0.594	0.039	0.125	0.406	-0.070	3.896	2.899	32.3	8325.7	991	32	32	1	1
1319	-1.014	1.502	0.979	-0.019	0.979	0.581	0.036	0.140	-0.460	0.097	3.186	3.253	122.1	10346.5	993	27	28	1	1
1322	-0.811	1.502	0.968	-0.033	0.969	0.575	0.055	0.134	-0.724	-0.016	4.111	3.271	-197.2	9870.2	994	39	40	1	1
1323	-0.609	1.502	0.972	-0.032	0.973	0.577	0.038	0.133	-0.223	-0.050	4.108	3.188	-29.8	9312.2	994	54	55	1	1
1326	-0.406	1.502	0.961	-0.040	0.962	0.571	0.092	0.139	-1.153	0.016	5.899	3.157	540.4	11996.8	992	22	22	1	1
1327	-0.203	1.502	0.975	-0.022	0.976	0.579	0.037	0.132	-0.434	0.085	4.225	3.224	49.0	9224.0	993	27	28	1	1
1330	0.0	1.502	0.973	-0.033	0.974	0.578	0.048	0.130	-0.684	-0.030	4.278	3.109	-68.2	9169.0	992	30	31	1	1
1331	0.203	1.502	0.975	-0.030	0.976	0.579	0.038	0.136	-0.360	0.025	3.466	3.284	-9.9	9803.1	989	31	32	1	1
1334	0.406	1.502	0.990	-0.025	0.990	0.588	0.058	0.138	-0.632	0.070	5.213	3.313	-64.5	10518.1	980	26	26	1	1
1335	0.609	1.502	0.974	-0.015	0.974	0.578	0.041	0.146	-0.441	-0.019	4.826	3.442	-282.6	11289.7	998	24	25	1	1
1338	0.811	1.502	0.970	-0.044	0.971	0.577	0.035	0.135	-0.523	0.097	6.007	3.310	53.1	9617.6	994	37	38	1	1
1339	1.014	1.502	0.975	-0.033	0.976	0.579	0.039	0.136	-0.604	0.157	4.380	3.284	-162.7	9737.0	997	40	41	1	1
1341	1.217	1.502	0.963	-0.025	0.963	0.571	0.043	0.129	-0.501	0.012	4.190	3.329	35.6	8980.6	999	33	34	1	1
1342	1.420	1.502	0.969	-0.027	0.970	0.576	0.037	0.146	-0.535	0.029	6.042	3.066	108.5	11121.0	995	44	45	1	1
1345	1.623	1.502	0.961	-0.032	0.961	0.570	0.038	0.137	-0.181	-0.008	4.142	3.194	56.5	9915.0	993	28	29	1	1
1346	1.826	1.502	0.967	-0.041	0.968	0.574	0.036	0.136	-0.513	-0.052	4.539	3.221	-64.7	9670.9	992	42	43	1	1
1349	2.028	1.502	0.968	-0.044	0.969	0.575	0.037	0.140	-0.030	0.060	5.056	3.150	-132.6	10301.7	994	20	21	1	1
1350	2.231	1.502	0.971	-0.065	0.973	0.578	0.038	0.134	-0.397	-0.075	5.403	3.377	-132.9	9454.6	997	28	29	1	1
1353	2.434	1.502	0.970	-0.046	0.971	0.576	0.037	0.140	-0.311	0.091	4.019	3.179	-79.2	10332.6	995	24	25	1	1
1354	2.637	1.502	0.962	-0.046	0.964	0.572	0.037	0.148	-0.470	0.031	4.270	3.121	-44.4	11452.5	997	33	34	1	1
1357	2.840	1.502	0.966	-0.049	0.967	0.574	0.035	0.139	-0.174	-0.002	3.606	3.382	-113.8	10086.1	996	19	19	1	1
1358	3.043	1.502	0.960	-0.059	0.962	0.571	0.036	0.129	-0.699	0.185	4.839	3.376	212.8	8799.8	997	32	33	1	1
1361	3.245	1.502	0.964	-0.048	0.966	0.573	0.037	0.134	-0.368	-0.104	3.468	3.088	77.4	9532.0	992	21	22	1	1
1362	3.448	1.502	0.972	-0.055	0.974	0.578	0.037	0.143	-0.471	-0.085	5.315	3.115	-80.2	10809.3	994	22	23	1	1
1364	3.550	1.502	0.971	-0.032	0.971	0.576	0.036	0.142	-0.833	-0.021	5.816	3.278	-292.3	10526.6	998	23	24	1	1

V_∞ = 713.0 ft/sec T_t = 640.3 °R D = 0.986 in.

SEQ	x/D	r/D	V_x/V_∞	V_r/V_∞	$\lvert V\rvert/V_\infty$	M	S_x/V_∞	S_r/V_∞	SK_x	SK_r	KU_x	KU_r	RE_{xr}	TKE	N	PPS	PPL	SE	CC
1308	-2.028	1.350	0.992	-0.026	0.992	0.590	0.022	0.129	0.030	0.046	3.384	3.203	-70.7	8524.1	992	150	151	1	1
1312	-1.826	1.350	0.995	-0.017	0.995	0.592	0.020	0.124	-0.149	0.105	3.696	2.966	58.8	7854.7	988	74	74	1	1
1313	-1.623	1.350	1.000	-0.025	1.001	0.595	0.020	0.134	0.070	-0.052	3.873	3.125	-36.1	9171.4	992	73	73	1	1
1316	-1.420	1.350	0.996	-0.028	0.996	0.592	0.029	0.127	-0.551	0.098	4.810	3.167	-153.6	8473.9	991	80	81	1	1
1317	-1.217	1.350	0.992	-0.031	0.993	0.590	0.028	0.129	0.007	-0.022	3.106	3.075	-32.6	8703.9	994	171	173	1	1
1320	-1.014	1.350	0.983	-0.020	0.983	0.584	0.040	0.141	-0.349	0.066	4.160	3.096	-76.3	10523.2	996	74	75	1	1
1321	-0.811	1.350	0.984	-0.040	0.985	0.585	0.032	0.142	0.044	0.166	3.347	3.197	9.5	10504.3	988	78	79	1	1
1324	-0.609	1.350	0.978	-0.031	0.979	0.581	0.030	0.130	-0.050	-0.119	3.198	3.163	-20.7	8879.0	984	53	54	1	1
1325	-0.406	1.350	0.980	-0.039	0.981	0.583	0.035	0.145	-0.048	-0.088	4.013	3.064	-107.8	11058.5	997	44	45	1	1
1328	-0.203	1.350	0.975	-0.035	0.975	0.579	0.052	0.130	-0.705	0.107	4.604	3.225	141.8	9343.5	996	65	67	1	1
1329	0.0	1.350	0.976	-0.048	0.978	0.580	0.035	0.141	-0.339	0.035	3.460	3.219	-27.1	10363.1	991	91	93	1	1
1332	0.203	1.350	0.982	-0.035	0.983	0.584	0.045	0.150	-0.199	0.077	3.397	3.212	98.9	11928.9	991	45	46	1	1
1333	0.406	1.350	0.972	-0.030	0.973	0.577	0.037	0.146	-0.054	-0.102	6.179	3.011	-408.8	11190.6	994	55	56	1	1
1336	0.609	1.350	0.975	-0.033	0.975	0.579	0.039	0.135	0.030	-0.027	5.263	3.047	-194.4	9639.0	999	69	71	1	1
1337	0.811	1.350	0.966	-0.039	0.967	0.574	0.041	0.137	-0.210	0.066	5.241	3.457	-109.9	9950.6	996	64	66	1	1
1340	1.217	1.350	0.981	-0.037	0.982	0.583	0.036	0.140	-0.090	0.031	3.531	3.070	86.7	10347.7	987	61	62	1	1
1343	1.420	1.350	0.967	-0.039	0.968	0.574	0.032	0.127	0.006	0.082	3.383	3.106	63.5	8400.8	991	60	62	1	1
1344	1.623	1.350	0.963	-0.041	0.964	0.572	0.035	0.134	-0.191	-0.003	3.143	3.038	61.2	9484.3	989	70	73	1	1
1347	1.826	1.350	0.968	-0.035	0.969	0.575	0.039	0.133	-0.427	-0.109	5.150	3.265	136.0	9356.2	996	54	55	1	1
1348	2.028	1.350	0.976	-0.055	0.977	0.580	0.035	0.139	-0.199	0.033	3.452	3.267	-10.5	10065.9	995	46	47	1	1
1351	2.231	1.350	0.965	-0.047	0.966	0.573	0.038	0.141	-0.347	0.061	4.954	3.081	145.6	10401.2	997	44	45	1	1
1352	2.434	1.350	0.968	-0.056	0.970	0.576	0.035	0.146	-0.515	0.060	4.650	3.154	152.5	11177.2	995	69	71	1	1
1355	2.637	1.350	0.957	-0.045	0.958	0.568	0.048	0.141	-0.820	-0.036	6.397	3.167	-312.9	10763.7	992	47	49	1	1
1356	2.840	1.350	0.963	-0.050	0.964	0.572	0.045	0.140	-0.546	0.122	3.648	3.111	73.6	10500.8	996	55	57	1	1
1359	3.043	1.350	0.955	-0.048	0.956	0.567	0.039	0.128	-0.613	0.027	4.800	3.315	-15.9	8663.9	994	50	52	1	1
1360	3.245	1.350	0.981	-0.050	0.982	0.584	0.033	0.140	-0.128	0.053	3.616	3.164	34.1	10214.1	988	47	48	1	1
1363	3.448	1.350	0.969	-0.051	0.970	0.576	0.034	0.139	0.173	0.026	3.518	3.538	-60.7	10057.6	982	41	42	1	1
1365	3.550	1.350	0.953	-0.048	0.954	0.565	0.067	0.143	-0.243	0.118	4.254	3.293	-337.1	11504.3	991	35	37	1	1

V_∞ = 713.0 ft/sec　　T_t = 640.3 °R　　D = 0.986 in.

SEQ	x/D	r/D	V_x/V_∞ H	V_r/V_∞ I	$\lvert V\rvert/V_\infty$	M	S_x/V_∞ B	S_r/V_∞ C	SK_x	SK_r	KU_x	KU_r	RE_{xr} A	TKE	N	PPS	PPL	SE	CC
821	0.051	0.0	1.836	0.108	1.839	1.200	0.135	0.132	-0.010	0.016	2.664	2.827	-279.7	13411.8	999	79	43	2	1
822	0.101	0.0	1.980	0.083	1.982	1.324	0.134	0.129	-0.179	0.068	2.696	2.793	-302.9	13086.3	993	183	92	2	1
823	0.152	0.0	2.088	0.073	2.090	1.424	0.006	0.134	0.000	-0.004	0.0	2.992	0.0	9158.5	1000	268	128	2	1
825	0.203	0.0	2.159	0.061	2.160	1.493	0.143	0.134	-0.310	0.025	2.663	3.047	-359.7	14325.1	994	231	107	2	1
826	0.254	0.0	2.218	0.044	2.219	1.552	0.144	0.121	-0.354	-0.135	2.642	2.714	-326.4	12776.7	996	371	167	2	1
827	0.304	0.0	2.217	0.041	2.217	1.551	0.140	0.133	-0.181	-0.038	2.365	3.163	-956.2	13958.0	998	106	48	2	1
828	0.355	0.0	2.276	0.057	2.277	1.613	0.141	0.143	-0.296	-0.016	2.604	3.296	105.4	15500.1	995	154	67	2	1
829	0.406	0.0	2.304	0.014	2.304	1.644	0.129	0.132	-0.227	-0.004	2.478	3.123	-587.7	13077.0	995	296	128	2	1
830	0.456	0.0	2.310	0.012	2.310	1.650	0.126	0.137	-0.242	-0.045	2.599	3.082	-433.7	13506.3	989	377	163	2	1
831	0.507	0.0	2.350	0.020	2.350	1.695	0.129	0.132	-0.366	0.002	2.598	3.041	-657.1	13107.1	998	172	73	2	1
832	0.609	0.0	2.382	0.006	2.382	1.731	0.137	0.139	-0.265	-0.065	2.772	3.132	-196.2	14639.7	995	295	124	2	1
833	0.710	0.0	2.419	0.007	2.419	1.775	0.138	0.136	-0.287	-0.081	2.632	2.752	15.5	14246.8	998	198	82	2	1
834	0.811	0.0	2.461	0.008	2.461	1.826	0.141	0.138	-0.243	-0.125	2.756	3.021	-1030.0	14701.4	994	178	72	2	1
835	0.913	0.0	2.477	0.002	2.477	1.846	0.159	0.144	-0.036	-0.059	2.552	2.975	-606.2	16948.3	997	155	62	2	1
836	1.014	0.0	2.456	0.007	2.456	1.820	0.165	0.165	0.082	-0.013	2.372	3.069	1260.2	20781.4	996	128	52	2	1
837	1.116	0.0	2.196	-0.006	2.196	1.529	0.292	0.145	0.162	-0.035	2.243	2.989	-434.8	32399.2	998	134	61	2	1
838	1.217	0.0	1.909	-0.004	1.909	1.259	0.406	0.154	0.201	-0.114	2.702	3.085	1605.2	53977.3	994	124	65	2	1
839	1.318	0.0	1.781	-0.010	1.781	1.152	0.426	0.154	0.114	0.116	2.910	2.889	1842.4	58168.8	995	138	77	2	1
840	1.420	0.0	1.753	-0.008	1.753	1.129	0.366	0.161	0.043	-0.112	3.098	3.088	-653.1	47379.5	997	186	106	2	1
841	1.521	0.0	1.810	-0.004	1.810	1.175	0.319	0.158	-0.246	-0.069	3.077	2.885	179.3	38588.9	989	151	83	2	1
842	1.623	0.0	1.910	-0.007	1.910	1.260	0.310	0.151	-0.403	0.056	3.137	2.986	1251.6	36050.4	994	103	54	2	1
843	1.724	0.0	1.987	-0.002	1.987	1.329	0.264	0.154	-0.382	-0.092	2.622	2.751	-220.0	29782.1	996	83	41	2	1
844	1.826	0.0	2.088	0.002	2.088	1.422	0.255	0.144	-0.195	-0.022	2.780	3.046	843.9	27048.9	998	85	40	2	1
845	1.927	0.0	2.105	0.003	2.105	1.438	0.255	0.151	-0.144	0.078	2.666	3.002	187.8	28021.2	998	98	46	2	1
846	2.028	0.0	2.144	0.012	2.144	1.477	0.252	0.147	-0.369	0.008	2.908	2.959	822.6	27204.7	992	84	39	2	1
847	2.130	0.0	2.211	-0.005	2.211	1.545	0.238	0.152	-0.352	-0.103	2.626	2.894	436.6	26145.5	995	136	61	2	1
848	2.231	0.0	2.210	0.011	2.210	1.543	0.233	0.155	-0.272	-0.027	2.486	3.045	17.3	25970.9	996	72	33	2	1
849	2.333	0.0	2.233	0.005	2.233	1.568	0.222	0.157	-0.360	0.008	2.627	3.020	222.1	25103.3	996	62	27	2	1
850	2.434	0.0	2.232	0.017	2.232	1.566	0.228	0.152	-0.397	-0.078	2.681	3.106	430.7	25025.2	996	47	21	2	1
851	2.535	0.0	2.302	0.018	2.303	1.642	0.230	0.149	-0.449	-0.063	2.813	2.977	464.6	24685.7	997	70	30	2	1
852	2.637	0.0	2.294	0.017	2.294	1.632	0.226	0.147	-0.342	0.042	2.527	2.911	-305.4	24030.3	996	52	22	2	1
853	2.738	0.0	2.312	0.006	2.312	1.652	0.217	0.149	-0.388	-0.007	2.645	3.005	1220.9	23325.1	995	119	51	2	1
854	2.840	0.0	2.325	0.026	2.325	1.666	0.212	0.142	-0.345	-0.002	2.497	3.184	501.6	21633.5	999	107	46	2	1
855	2.941	0.0	2.323	0.015	2.323	1.665	0.214	0.143	-0.408	-0.137	2.456	2.993	-124.1	22090.5	996	62	26	2	1
856	3.043	0.0	2.339	0.016	2.339	1.682	0.214	0.146	-0.395	-0.076	2.689	2.776	768.4	22587.7	998	85	36	2	1

V_∞ = 713.0 ft/sec T_t = 640.3 °R D = 0.986 in.

SEQ	x/D	r/D	V_x/V_∞	V_r/V_∞	$\lvert V\rvert/V_\infty$	M	S_x/V_∞	S_r/V_∞	SK_x	SK_r	KU_x	KU_r	RE_{xr}	TKE	N	PPS	PPL	SE	CC
857	0.304	0.190	2.233	0.648	2.325	1.667	0.161	0.222	-0.132	-0.021	2.414	2.915	5567.4	31661.5	997	13	5	2	1
858	0.406	0.190	2.311	0.604	2.389	1.740	0.152	0.177	-0.346	-0.058	2.614	3.010	3847.5	21783.5	999	27	11	2	1
859	0.507	0.190	2.377	0.541	2.438	1.798	0.141	0.165	-0.370	0.028	2.560	2.945	3156.8	18811.6	993	41	17	2	1
860	0.609	0.190	2.408	0.482	2.455	1.819	0.140	0.175	-0.361	-0.113	2.575	2.880	2393.3	20608.3	995	168	68	2	1
861	0.710	0.190	2.440	0.429	2.477	1.846	0.143	0.161	-0.249	0.069	2.692	2.962	1533.9	18411.9	996	212	85	2	1
862	0.811	0.190	2.495	0.365	2.522	1.903	0.140	0.164	-0.340	0.018	2.588	2.910	723.3	18626.0	991	371	147	2	1
863	0.913	0.190	2.491	0.306	2.510	1.888	0.148	0.152	-0.283	0.050	2.747	3.105	596.3	17329.9	995	93	37	2	1
864	1.014	0.190	2.518	0.254	2.531	1.915	0.153	0.129	-0.243	0.109	2.641	2.947	-472.6	14359.1	993	126	49	2	1
865	1.116	0.190	2.563	0.189	2.570	1.967	0.145	0.142	-0.183	0.282	2.649	3.124	-69.1	15525.4	997	261	101	2	1
866	1.217	0.190	2.557	0.147	2.561	1.956	0.146	0.139	-0.055	0.117	2.550	2.838	-1080.1	15177.5	996	167	65	2	1
867	1.318	0.190	2.519	0.120	2.521	1.902	0.151	0.160	-0.039	0.118	2.688	3.136	-69.0	18803.6	993	229	90	2	1
868	1.420	0.190	2.526	0.129	2.529	1.913	0.138	0.141	-0.227	-0.164	2.672	3.129	261.2	14956.4	994	130	51	2	1
869	1.521	0.190	2.517	0.127	2.520	1.901	0.141	0.127	-0.203	-0.061	2.640	3.132	970.0	13251.3	993	195	77	2	1
870	1.623	0.190	2.532	0.123	2.536	1.921	0.153	0.131	-0.271	-0.026	2.639	3.248	359.1	14603.5	994	200	79	2	1
871	1.724	0.190	2.530	0.120	2.533	1.918	0.148	0.129	-0.278	-0.082	2.616	3.280	918.9	14063.0	991	194	76	2	1
872	1.826	0.190	2.512	0.104	2.514	1.893	0.157	0.134	-0.311	-0.089	2.722	3.151	266.1	15418.5	994	148	58	2	1
873	1.927	0.190	2.517	0.096	2.519	1.899	0.164	0.129	-0.247	0.083	2.467	2.957	913.9	15358.2	995	201	79	2	1
874	2.028	0.190	2.470	0.085	2.471	1.839	0.171	0.128	-0.206	-0.036	2.690	2.895	-280.4	15763.9	999	178	72	2	1
875	2.130	0.190	2.497	0.080	2.488	1.860	0.163	0.132	-0.029	-0.095	2.363	3.289	-181.8	15649.3	997	118	47	2	1
876	2.231	0.190	2.466	0.061	2.467	1.833	0.163	0.131	-0.152	0.040	2.417	3.096	753.6	15549.5	996	138	56	2	1
877	2.333	0.190	2.496	0.054	2.496	1.871	0.153	0.136	-0.110	0.078	2.461	2.998	-96.5	15350.3	994	113	45	2	1
878	2.434	0.190	2.459	0.045	2.459	1.824	0.158	0.126	-0.260	-0.071	2.916	2.897	-679.8	14411.5	993	72	29	2	1
879	2.535	0.190	2.393	0.041	2.394	1.745	0.165	0.156	-0.206	-0.072	2.886	3.143	333.1	19271.4	992	184	76	2	1
880	2.637	0.190	2.446	0.035	2.447	1.809	0.160	0.154	-0.174	-0.183	2.902	2.962	789.6	18526.5	992	140	57	2	1
881	2.738	0.190	2.458	0.039	2.458	1.823	0.166	0.157	-0.309	-0.056	3.199	2.993	-340.9	19572.6	989	119	48	2	1
882	2.840	0.190	2.433	0.030	2.433	1.792	0.162	0.152	-0.027	-0.090	2.755	2.981	715.6	18497.7	989	116	48	2	1
883	2.941	0.190	2.453	0.039	2.453	1.816	0.156	0.145	-0.226	-0.109	2.760	2.736	176.2	16827.4	990	181	74	2	1
884	3.043	0.190	2.471	0.017	2.471	1.839	0.023	0.153	0.000	0.066	0.0	3.085	0.0	12068.7	1000	417	168	2	1

V_∞ = 713.0 ft/sec T_t = 640.3 °R D = 0.986 in.

SEQ	x/D	r/D	V_x/V_∞	V_r/V_∞	$\|V\|/V_\infty$	M	S_x/V_∞	S_r/V_∞	SK_x	SK_r	KU_x	KU_r	RE_{xr}	TKE	N	PPS	PPL	SE	CC
1307	-2.028	1.274	0.993	-0.039	0.994	0.591	0.023	0.127	-0.010	-0.020	4.605	2.864	74.8	8321.0	997	108	108	1	1
1306	-2.028	1.198	0.992	-0.030	0.992	0.590	0.022	0.132	0.096	0.003	3.909	3.147	-59.5	8987.6	996	174	175	1	1
1305	-2.028	1.122	0.999	-0.025	0.999	0.594	0.019	0.134	-0.114	-0.064	3.392	3.191	21.2	9249.7	992	363	361	1	1
1304	-2.028	1.046	0.993	-0.027	0.993	0.590	0.021	0.129	-0.111	0.137	3.508	3.200	-77.0	8559.1	995	230	230	1	1
1303	-2.028	0.970	0.997	-0.027	0.997	0.593	0.020	0.129	0.035	-0.023	3.332	3.019	10.2	8507.7	995	362	360	1	1
1302	-2.028	0.894	0.994	-0.036	0.994	0.591	0.018	0.134	-0.110	0.003	3.884	2.936	-31.6	9169.4	992	277	277	1	1
1301	-2.028	0.818	0.997	-0.029	0.998	0.593	0.020	0.130	-0.028	-0.093	4.026	2.815	96.5	8714.2	998	388	387	1	1
1300	-2.028	0.780	0.999	-0.023	0.999	0.594	0.020	0.129	0.213	0.087	3.874	3.155	45.5	8584.5	989	307	306	1	1
1299	-2.028	0.742	0.997	-0.024	0.997	0.593	0.018	0.133	0.069	-0.007	3.922	3.156	-61.4	9039.3	988	227	226	1	1
1298	-2.028	0.723	0.996	-0.024	0.997	0.593	0.019	0.132	0.150	-0.094	3.898	3.093	28.3	8890.6	994	233	232	1	1
1297	-2.028	0.704	1.002	-0.023	1.002	0.596	0.022	0.136	0.305	0.014	4.151	2.997	-50.0	9468.0	986	216	214	1	1
1296	-2.028	0.685	0.998	-0.010	0.998	0.593	0.021	0.136	0.358	0.022	4.160	2.807	79.0	9495.4	984	146	146	1	1
1295	-2.028	0.666	0.990	-0.014	0.990	0.589	0.023	0.134	-0.407	-0.024	4.347	2.976	51.1	9200.9	982	102	102	1	1
1294	-2.028	0.647	0.987	-0.015	0.987	0.587	0.028	0.136	0.011	-0.063	4.717	2.694	62.0	9645.3	976	122	123	1	1
1293	-2.028	0.628	0.963	-0.017	0.963	0.571	0.037	0.132	-0.435	0.027	4.292	2.945	113.2	9200.1	979	47	48	1	1
1292	-2.028	0.609	0.951	-0.024	0.951	0.564	0.045	0.138	-0.660	-0.054	3.556	2.903	-106.3	10232.4	989	26	27	1	1
1291	-2.028	0.590	0.918	-0.019	0.919	0.543	0.051	0.142	-0.572	-0.099	3.146	2.981	-167.2	10930.0	990	9	10	1	1
1290	-2.028	0.570	0.887	-0.001	0.887	0.523	0.060	0.141	-0.487	0.001	3.193	3.290	-110.0	10964.6	993	5	6	1	1
1289	-2.028	0.551	0.839	-0.008	0.840	0.494	0.073	0.133	-0.487	0.089	3.134	3.265	-52.1	10391.9	995	4	4	1	1
1288	-2.028	0.532	0.775	-0.013	0.775	0.454	0.086	0.147	-0.271	-0.014	2.632	2.807	-177.3	12811.4	987	3	4	1	1

V_∞ = 713.0 ft/sec T_t = 640.3 °R   D = 0.986 in.

SEQ	x/D	r/D	V_x/V_∞	V_r/V_∞	$\lvert V\rvert/V_\infty$	M	S_x/V_∞	S_r/V_∞	SK_x	SK_r	KU_x	KU_r	RE_{xr}	TKE	N	PPS	PPL	SE	CC
32	-1.521	1.274	0.995	-0.023	0.996	0.592	0.013	0.062	0.167	0.177	5.560	2.857	18.4	1996.7	994	170	169	1	1
31	-1.521	1.198	0.992	-0.023	0.992	0.590	0.029	0.062	-0.244	0.194	3.013	2.904	-61.1	2172.7	990	139	139	1	1
30	-1.521	1.122	0.995	-0.020	0.995	0.591	0.012	0.062	0.391	0.233	5.264	2.692	-15.6	1994.8	984	108	108	1	1
29	-1.521	1.046	0.995	-0.029	0.995	0.592	0.014	0.062	0.043	0.180	5.012	2.872	11.2	1981.3	991	169	169	1	1
28	-1.521	0.970	0.999	-0.022	0.999	0.594	0.013	0.062	0.080	0.221	4.532	2.655	-25.6	1985.9	991	67	66	1	1
27	-1.521	0.932	0.990	-0.031	0.990	0.589	0.023	0.063	-0.396	0.061	3.472	3.038	11.0	2148.2	989	223	224	1	1
26	-1.521	0.894	1.000	-0.036	1.000	0.595	0.015	0.066	-0.239	0.169	4.728	2.991	20.2	2260.4	990	1282	1273	1	1
25	-1.521	0.856	0.996	-0.032	0.996	0.592	0.015	0.061	0.091	0.178	4.726	3.127	4.3	1955.1	988	970	967	1	1
24	-1.521	0.818	0.999	-0.029	1.000	0.594	0.014	0.062	-0.048	0.063	5.836	2.877	22.0	2006.0	993	822	817	1	1
23	-1.521	0.780	1.002	-0.032	1.002	0.596	0.013	0.061	0.193	0.052	5.739	2.909	8.6	1914.6	989	688	682	1	1
22	-1.521	0.742	1.006	-0.047	1.007	0.599	0.012	0.060	-0.170	-0.028	6.096	3.137	1.8	1864.5	983	403	398	1	1
21	-1.521	0.704	1.003	-0.042	1.004	0.597	0.013	0.061	0.121	-0.169	5.349	3.506	7.5	1968.3	993	159	158	1	1
20	-1.521	0.685	1.004	-0.047	1.005	0.598	0.014	0.072	-0.009	-0.478	6.161	4.120	18.8	2697.3	978	132	130	1	1
19	-1.521	0.666	1.001	-0.040	1.002	0.596	0.016	0.064	-0.242	-0.153	4.925	3.668	-27.7	2130.6	981	84	83	1	1
18	-1.521	0.647	0.992	-0.040	0.993	0.590	0.024	0.061	-0.686	-0.093	4.234	3.387	-25.1	2014.8	983	44	44	1	1
17	-1.521	0.628	0.976	-0.041	0.977	0.580	0.034	0.059	-0.818	-0.027	3.834	3.544	43.3	2076.0	981	26	27	1	1
16	-1.521	0.609	0.949	-0.045	0.950	0.563	0.045	0.065	-0.715	-0.204	3.418	3.912	7.0	2659.9	993	16	16	1	1
15	-1.521	0.590	0.921	-0.048	0.922	0.545	0.053	0.061	-0.586	0.178	3.121	3.234	-56.0	2596.6	990	6	6	1	1
14	-1.521	0.570	0.875	-0.048	0.877	0.517	0.061	0.054	-0.297	0.321	2.674	3.027	22.3	2427.4	238	3	4	1	1
13	-1.521	0.551	0.819	-0.054	0.821	0.482	0.069	0.064	-0.194	0.064	2.465	3.118	-49.0	3256.3	207	1	2	1	1
12	-1.521	0.532	0.736	-0.059	0.738	0.432	0.092	0.056	-0.363	-0.120	2.893	3.429	-325.8	3769.2	114	1	1	1	1

V_∞ = 713.0 ft/sec T_t = 640.3 °R D = 0.986 in.

SEQ	x/D	r/D	V_x/V_∞	V_r/V_∞	$\lvert V\rvert/V_\infty$	M	S_x/V_∞	S_r/V_∞	SK_x	SK_r	KU_x	KU_r	RE_{xr}	TKE	N	PPS	PPL	SE	CC
56	-1.014	1.274	0.992	-0.041	0.992	0.590	0.011	0.066	-0.024	0.309	6.243	2.977	-36.4	2249.8	984	421	420	1	1
55	-1.014	1.198	0.993	-0.041	0.994	0.591	0.013	0.064	0.091	0.166	5.331	3.046	-9.9	2109.4	987	718	715	1	1
54	-1.014	1.122	0.994	-0.041	0.995	0.592	0.014	0.061	0.116	0.137	5.510	3.050	20.1	1924.2	993	1260	1253	1	1
53	-1.014	1.046	0.994	-0.038	0.994	0.591	0.015	0.065	-0.181	-0.058	4.854	2.978	21.7	2213.3	988	912	907	1	1
52	-1.014	0.970	0.988	-0.029	0.989	0.587	0.025	0.066	-0.454	0.338	3.773	3.172	-12.9	2384.5	985	187	188	1	1
51	-1.014	0.932	0.997	-0.041	0.998	0.593	0.014	0.062	0.293	0.205	5.295	3.047	-10.4	1986.3	988	963	956	1	1
50	-1.014	0.894	0.994	-0.038	0.995	0.592	0.016	0.065	0.205	0.165	4.402	2.994	-17.1	2201.6	987	861	857	1	1
49	-1.014	0.856	0.998	-0.042	0.998	0.594	0.019	0.062	0.040	0.171	4.161	3.207	-42.3	2069.7	989	904	896	1	1
48	-1.014	0.818	1.010	-0.043	1.011	0.602	0.016	0.061	0.226	0.087	4.046	2.950	-9.8	1931.9	990	725	710	1	1
47	-1.014	0.780	1.014	-0.031	1.015	0.604	0.016	0.062	-0.077	0.120	4.271	2.839	-2.6	2024.2	993	320	312	1	1
46	-1.014	0.742	1.018	-0.041	1.019	0.607	0.016	0.058	0.302	0.127	4.550	3.086	35.7	1760.6	983	239	232	1	1
45	-1.014	0.704	1.022	-0.039	1.023	0.609	0.016	0.061	-0.034	0.018	5.061	3.533	34.7	1929.7	987	109	105	1	1
44	-1.014	0.685	1.023	-0.039	1.024	0.610	0.016	0.059	0.168	0.146	4.745	3.156	18.2	1819.1	986	88	85	1	1
43	-1.014	0.666	1.020	-0.037	1.020	0.608	0.020	0.060	-0.076	0.066	4.260	3.228	17.2	1913.4	985	48	46	1	1
42	-1.014	0.647	1.012	-0.043	1.013	0.603	0.026	0.058	-0.537	0.116	4.272	3.317	-33.6	1860.3	980	24	23	1	1
41	-1.014	0.628	1.001	-0.046	1.002	0.596	0.032	0.059	-0.878	0.187	4.284	3.248	97.6	2039.9	995	14	14	1	1
40	-1.014	0.609	0.985	-0.047	0.986	0.586	0.041	0.059	-0.536	0.225	3.425	3.080	13.1	2188.4	995	9	9	1	1
39	-1.014	0.590	0.957	-0.049	0.958	0.568	0.045	0.060	-0.468	0.222	2.671	3.740	-161.6	2338.2	261	5	5	1	1
38	-1.014	0.570	0.922	-0.044	0.923	0.546	0.057	0.060	-0.448	0.168	2.937	2.870	136.7	2642.0	299	3	3	1	1
37	-1.014	0.551	0.883	-0.053	0.885	0.522	0.061	0.052	-0.166	0.352	2.444	2.942	125.5	2300.5	168	1	1	1	1
36	-1.014	0.532	0.838	-0.062	0.840	0.494	0.067	0.065	0.030	-0.213	2.981	2.976	51.8	3274.2	113	0	0	1	1

V_∞ = 713.0 ft/sec T_t = 640.3 °R D = 0.986 in.

SEQ	x/D	r/D	V_x/V_∞	V_r/V_∞	$\|V\|/V_\infty$	M	S_x/V_∞	S_r/V_∞	SK_x	SK_r	KU_x	KU_r	RE_{xr}	TKE	N	PPS	PPL	SE	CC
437	-0.913	1.274	0.984	-0.031	0.984	0.585	0.017	0.095	0.072	0.080	4.321	3.025	9.2	4611.9	992	527	522	1	1
436	-0.913	1.198	0.983	-0.026	0.983	0.584	0.023	0.097	-0.060	0.262	7.717	3.051	-83.1	4943.1	997	49	48	1	1
435	-0.913	1.122	0.985	-0.042	0.986	0.586	0.017	0.099	-0.178	-0.017	4.310	3.411	15.8	5064.1	990	154	152	1	1
434	-0.913	1.046	0.985	-0.040	0.986	0.586	0.020	0.103	-0.047	0.016	3.972	3.285	38.2	5542.5	993	589	582	1	1
433	-0.913	0.970	0.985	-0.042	0.986	0.586	0.018	0.095	0.036	0.206	4.311	2.874	10.8	4713.7	995	911	899	1	1
432	-0.913	0.932	0.990	-0.050	0.992	0.589	0.037	0.139	-0.464	0.060	5.546	2.870	-157.9	10220.3	993	989	971	1	1
431	-0.913	0.894	0.995	-0.059	0.997	0.593	0.025	0.147	-0.075	-0.039	3.707	2.918	78.2	11104.0	990	814	795	1	1
430	-0.913	0.856	0.994	-0.042	0.995	0.591	0.029	0.147	0.010	-0.100	3.531	2.841	166.1	11243.3	987	803	786	1	1
429	-0.913	0.818	1.000	-0.052	1.002	0.596	0.029	0.140	-0.234	0.079	3.550	2.863	43.0	10223.5	984	478	465	1	1
428	-0.913	0.780	1.004	-0.044	1.005	0.598	0.028	0.142	-0.144	-0.014	3.805	2.896	39.4	10410.0	993	560	542	1	1
427	-0.913	0.742	1.010	-0.047	1.011	0.602	0.023	0.135	0.147	0.020	3.986	2.975	-135.4	9433.5	985	473	456	1	1
426	-0.913	0.704	1.014	-0.046	1.015	0.605	0.022	0.144	0.234	-0.039	3.640	2.850	-53.8	10622.7	991	224	215	1	1
425	-0.913	0.685	1.017	-0.046	1.018	0.606	0.026	0.143	0.702	0.026	6.295	2.874	-45.0	10586.0	999	215	206	1	1
424	-0.913	0.666	1.021	-0.045	1.022	0.609	0.025	0.146	0.280	0.009	4.065	3.131	-38.3	10918.8	997	175	167	1	1
423	-0.913	0.647	1.021	-0.050	1.022	0.609	0.024	0.146	-0.093	-0.064	3.874	3.181	-13.5	10966.1	985	124	118	1	1
422	-0.913	0.628	1.025	-0.050	1.026	0.611	0.026	0.142	-0.204	-0.068	3.530	2.847	99.6	10426.7	985	87	83	1	1
421	-0.913	0.609	1.011	-0.049	1.013	0.603	0.033	0.141	-0.781	0.033	4.627	2.916	-34.3	10441.6	996	72	70	1	1
420	-0.913	0.590	0.997	-0.058	0.999	0.594	0.040	0.142	-0.615	-0.217	3.628	3.030	148.9	10650.6	997	41	40	1	1
419	-0.913	0.570	0.972	-0.060	0.974	0.578	0.046	0.145	-0.586	0.014	3.696	3.195	13.0	11177.4	996	35	35	1	1
418	-0.913	0.551	0.951	-0.063	0.953	0.565	0.051	0.146	-0.457	0.106	3.092	2.887	-206.1	11535.9	997	39	40	1	1
417	-0.913	0.532	0.918	-0.059	0.920	0.544	0.057	0.148	-0.214	-0.160	3.064	3.003	406.5	11974.4	992	26	27	1	1
416	-0.913	0.513	0.914	-0.091	0.919	0.543	0.071	0.146	-0.284	-0.066	3.185	2.967	-217.2	12095.3	989	12	12	1	1
415	-0.913	0.494	0.821	-0.068	0.824	0.485	0.078	0.142	0.027	0.100	2.473	2.971	310.5	11836.4	306	2	3	1	1

V_∞ = 713.0 ft/sec T_t = 640.3 °R D = 0.986 in.

SEQ	x/D	r/D	V_x/V_∞	V_r/V_∞	$\lvert V\rvert/V_\infty$	M	S_x/V_∞	S_r/V_∞	SK_x	SK_r	KU_x	KU_r	RE_{xr}	TKE	N	PPS	PPL	SE	CC
398	-0.811	1.274	0.983	-0.038	0.983	0.584	0.013	0.079	-0.175	0.411	5.153	3.408	17.2	3230.4	994	497	490	1	1
397	-0.811	1.198	0.982	-0.039	0.983	0.584	0.010	0.083	-0.104	0.358	7.314	3.299	-17.0	3529.7	995	684	676	1	1
396	-0.811	1.122	0.983	-0.044	0.984	0.584	0.013	0.078	-0.216	0.369	5.780	3.526	50.0	3097.6	992	663	654	1	1
395	-0.811	1.046	0.981	-0.043	0.982	0.583	0.017	0.085	-0.134	0.420	4.486	3.624	-3.0	3760.2	992	1397	1380	1	1
394	-0.811	0.970	0.984	-0.039	0.985	0.585	0.013	0.084	-0.304	0.413	4.957	3.567	-5.5	3673.1	989	826	813	1	1
393	-0.811	0.932	0.988	-0.044	0.989	0.588	0.012	0.081	-0.131	0.470	6.223	3.355	-1.7	3360.0	991	1016	996	1	1
392	-0.811	0.894	0.989	-0.045	0.990	0.588	0.014	0.077	-0.172	0.211	4.940	3.323	6.7	3039.1	993	1311	1285	1	1
391	-0.811	0.856	0.992	-0.043	0.993	0.590	0.013	0.072	-0.002	0.341	5.575	3.281	3.6	2703.7	992	743	725	1	1
390	-0.811	0.818	1.004	-0.035	1.004	0.597	0.013	0.079	-0.385	0.388	5.790	3.503	6.2	3222.7	993	240	232	1	1
389	-0.811	0.780	1.005	-0.053	1.006	0.599	0.019	0.115	-0.176	0.152	3.816	3.013	-34.6	6772.1	995	370	357	1	1
388	-0.811	0.742	1.001	-0.046	1.002	0.596	0.021	0.118	0.084	0.130	3.780	3.042	2.2	7135.5	997	308	299	1	1
387	-0.811	0.704	1.015	-0.046	1.016	0.605	0.015	0.120	0.091	0.192	4.774	2.944	-22.0	7383.7	993	352	336	1	1
385	-0.811	0.685	1.016	-0.045	1.017	0.606	0.018	0.123	-0.167	-0.030	4.910	2.945	20.3	7718.5	993	220	210	1	1
384	-0.811	0.666	1.018	-0.044	1.019	0.607	0.022	0.118	-0.384	0.116	4.713	3.096	-26.7	7230.1	992	296	282	1	1
383	-0.811	0.647	1.011	-0.047	1.012	0.602	0.024	0.115	-0.541	0.041	4.182	3.101	-22.7	6829.4	992	153	146	1	1
382	-0.811	0.628	1.003	-0.051	1.005	0.598	0.030	0.119	-0.623	-0.182	3.967	3.100	-13.7	7447.8	992	83	80	1	1
381	-0.811	0.609	0.981	-0.052	0.982	0.584	0.036	0.121	-0.593	-0.006	3.397	3.256	-75.6	7832.1	991	57	56	1	1
380	-0.811	0.590	0.964	-0.062	0.966	0.573	0.041	0.128	-0.409	0.020	3.060	2.866	34.1	8720.6	995	72	72	1	1
379	-0.811	0.570	0.941	-0.067	0.943	0.559	0.047	0.117	-0.328	-0.015	2.797	3.299	-40.6	7500.0	995	32	33	1	1
378	-0.811	0.551	0.904	-0.073	0.907	0.536	0.054	0.123	-0.271	-0.039	2.721	3.019	38.4	8374.2	987	27	29	1	1
377	-0.811	0.532	0.868	-0.082	0.872	0.514	0.058	0.124	-0.269	-0.062	2.752	3.100	-145.4	8644.1	993	15	17	1	1
376	-0.811	0.513	0.822	-0.091	0.827	0.487	0.065	0.128	0.118	-0.071	2.735	2.968	-296.9	9456.1	994	17	20	1	1
375	-0.811	0.494	0.742	-0.083	0.747	0.437	0.069	0.137	0.107	0.026	2.684	2.923	-32.9	10690.0	989	11	15	1	1

V_∞ = 713.0 ft/sec T_t = 640.3 °R   D = 0.986 in.

SEQ	x/D	r/D	V_x/V_∞	V_r/V_∞	$\lvert V\rvert/V_\infty$	M	S_x/V_∞	S_r/V_∞	SK_x	SK_r	KU_x	KU_r	RE_{xr}	TKE	N	PPS	PPL	SE	CC
351	-0.710	1.274	0.988	-0.038	0.989	0.588	0.010	0.085	-0.084	0.319	8.281	3.740	-51.4	3725.6	989	375	370	1	1
352	-0.710	1.198	0.981	-0.038	0.982	0.583	0.013	0.082	-0.254	0.572	6.144	3.669	17.5	3428.1	989	819	814	1	1
353	-0.710	1.122	0.987	-0.036	0.988	0.587	0.014	0.083	-0.087	0.212	5.210	3.614	-5.8	3521.3	991	1223	1208	1	1
354	-0.710	1.046	0.977	-0.038	0.978	0.581	0.052	0.080	-0.495	0.335	3.180	3.600	-3.3	3900.7	997	1353	1350	1	1
355	-0.710	0.970	0.990	-0.031	0.990	0.588	0.014	0.082	-0.197	0.420	4.367	3.490	-35.8	3442.3	993	765	754	1	1
356	-0.710	0.932	0.989	-0.041	0.990	0.588	0.015	0.076	-0.293	0.357	5.229	3.837	2.9	3027.8	991	1497	1475	1	1
357	-0.710	0.894	0.997	-0.037	0.998	0.593	0.027	0.077	-0.092	0.340	3.256	3.514	-88.0	3175.0	997	860	841	1	1
358	-0.710	0.856	0.998	-0.038	0.998	0.594	0.018	0.080	-0.650	0.467	5.112	3.600	-98.8	3302.1	990	943	922	1	1
359	-0.710	0.818	0.998	-0.032	0.999	0.594	0.015	0.074	-0.879	0.408	9.922	3.569	50.6	2822.3	999	372	364	1	1
360	-0.710	0.780	1.012	-0.025	1.012	0.603	0.016	0.079	-0.188	0.177	4.080	3.136	-22.6	3243.2	996	213	205	1	1
361	-0.710	0.742	1.010	-0.023	1.010	0.601	0.013	0.085	-0.055	0.256	5.401	3.227	7.8	3685.3	996	127	122	1	1
362	-0.710	0.704	1.015	-0.027	1.016	0.605	0.014	0.081	-0.023	0.360	5.689	3.331	12.2	3406.7	992	59	57	1	1
363	-0.710	0.685	1.018	-0.045	1.019	0.607	0.015	0.118	0.172	-0.079	5.054	3.159	-24.9	7163.3	992	170	162	1	1
364	-0.710	0.666	1.023	-0.053	1.024	0.610	0.018	0.119	-0.153	0.065	4.527	3.180	-20.8	7287.3	991	166	158	1	1
365	-0.710	0.647	1.015	-0.052	1.017	0.605	0.021	0.126	-0.599	-0.098	4.556	3.020	-70.1	8134.8	993	97	93	1	1
366	-0.710	0.628	1.011	-0.057	1.012	0.602	0.026	0.118	-0.510	-0.032	4.048	3.160	40.2	7303.3	991	81	78	1	1
367	-0.710	0.609	0.990	-0.064	0.992	0.589	0.039	0.119	-0.844	-0.002	4.434	3.194	-164.3	7561.7	994	67	66	1	1
368	-0.710	0.590	0.976	-0.067	0.978	0.581	0.039	0.123	-0.438	-0.165	3.351	2.971	55.9	8094.6	992	36	36	1	1
369	-0.710	0.570	0.961	-0.085	0.965	0.572	0.050	0.126	-0.338	-0.052	2.930	3.077	-219.5	8715.3	992	32	32	1	1
370	-0.710	0.551	0.930	-0.074	0.933	0.552	0.051	0.126	-0.303	-0.096	3.199	2.964	-254.8	8749.6	994	32	33	1	1
371	-0.710	0.532	0.895	-0.089	0.899	0.531	0.057	0.125	-0.222	-0.077	2.699	3.065	-137.7	8810.3	991	17	18	1	1
372	-0.710	0.513	0.854	-0.097	0.859	0.506	0.057	0.132	-0.192	0.064	2.793	2.875	97.9	9719.1	994	16	18	1	1
373	-0.710	0.494	0.800	-0.100	0.807	0.474	0.062	0.124	-0.030	-0.031	2.803	3.170	-57.8	8792.4	996	10	13	1	1
374	-0.710	0.475	0.729	-0.106	0.737	0.431	0.071	0.137	-0.071	0.051	2.661	2.888	-164.9	10822.3	989	7	9	1	1

V_∞ = 713.0 ft/sec T_t = 640.3 °R D = 0.986 in.

SEQ	x/D	r/D	V_x/V_∞	V_r/V_∞	$\lvert V\rvert/V_\infty$	M	S_x/V_∞	S_r/V_∞	SK_x	SK_r	KU_x	KU_r	RE_{xr}	TKE	N	PPS	PPL	SE	CC
344	-0.609	1.274	0.983	-0.031	0.983	0.584	0.012	0.081	0.069	0.292	5.641	3.494	-3.4	3354.3	992	354	351	1	1
343	-0.609	1.198	0.984	-0.036	0.985	0.585	0.011	0.076	-0.043	0.485	6.004	3.734	-5.3	2978.7	992	453	448	1	1
342	-0.609	1.122	0.980	-0.038	0.981	0.583	0.013	0.079	0.054	0.414	5.516	3.782	-21.2	3238.0	989	893	885	1	1
341	-0.609	1.046	0.987	-0.028	0.987	0.587	0.013	0.079	-0.418	0.409	5.788	3.362	0.6	3256.8	991	736	725	1	1
340	-0.609	0.970	0.989	-0.036	0.989	0.588	0.012	0.081	-0.187	0.382	6.991	3.643	-8.0	3356.1	992	799	786	1	1
339	-0.609	0.932	0.986	-0.042	0.987	0.586	0.026	0.076	-0.722	0.463	3.584	3.731	-84.2	3145.4	993	917	904	1	1
338	-0.609	0.894	0.987	-0.034	0.987	0.587	0.016	0.079	-0.306	0.364	4.810	3.774	-22.3	3273.1	992	841	829	1	1
337	-0.609	0.856	0.992	-0.032	0.992	0.590	0.013	0.073	-0.406	0.556	6.348	3.453	10.9	2763.5	992	635	623	1	1
336	-0.609	0.818	0.999	-0.052	1.000	0.595	0.018	0.110	-0.143	0.143	3.966	3.031	72.2	6203.2	991	536	521	1	1
335	-0.609	0.780	1.003	-0.046	1.004	0.597	0.017	0.116	-0.019	0.043	3.901	3.244	16.3	6951.5	994	350	339	1	1
334	-0.609	0.742	1.009	-0.050	1.011	0.601	0.015	0.119	-0.074	-0.026	5.117	3.036	-32.7	7264.2	995	540	520	1	1
333	-0.609	0.704	1.007	-0.054	1.008	0.600	0.015	0.119	-0.039	-0.022	4.622	3.065	-3.5	7244.3	991	319	308	1	1
332	-0.609	0.685	1.009	-0.059	1.011	0.602	0.016	0.116	0.076	-0.012	6.159	3.192	11.7	6866.3	992	171	165	1	1
331	-0.609	0.666	1.009	-0.041	1.010	0.601	0.017	0.126	-0.017	-0.007	4.737	3.109	30.5	8175.3	991	167	161	1	1
330	-0.609	0.647	1.000	-0.059	1.002	0.596	0.021	0.120	-0.174	0.036	4.124	3.081	-61.6	7481.0	989	131	127	1	1
329	-0.609	0.628	1.003	-0.078	1.007	0.599	0.027	0.117	-0.436	-0.025	5.669	3.172	-191.2	7095.7	993	137	132	1	1
328	-0.609	0.609	0.984	-0.071	0.986	0.586	0.031	0.122	-0.604	0.008	3.378	3.290	-52.9	7778.4	993	96	95	1	1
327	-0.609	0.590	0.971	-0.078	0.974	0.578	0.039	0.121	-0.530	-0.076	3.103	3.122	64.8	7850.0	991	45	45	1	1
326	-0.609	0.570	0.947	-0.090	0.952	0.564	0.044	0.124	-0.459	-0.045	3.419	2.965	-189.9	8281.5	997	41	42	1	1
325	-0.609	0.551	0.916	-0.098	0.921	0.545	0.050	0.124	-0.280	-0.019	2.811	3.127	-108.4	8517.7	994	31	32	1	1
324	-0.609	0.532	0.884	-0.095	0.889	0.525	0.050	0.126	-0.313	0.042	3.021	3.111	-67.5	8756.1	991	26	28	1	1
323	-0.609	0.513	0.851	-0.101	0.857	0.505	0.060	0.123	-0.180	-0.051	2.575	2.987	-211.5	8623.6	996	17	20	1	1
322	-0.609	0.494	0.811	-0.108	0.818	0.481	0.062	0.120	-0.303	0.029	2.868	2.971	-208.1	8244.0	995	10	12	1	1
321	-0.609	0.475	0.768	-0.113	0.777	0.456	0.067	0.122	-0.087	-0.012	2.837	2.916	-287.2	8719.0	991	12	15	1	1
320	-0.609	0.456	0.673	-0.130	0.686	0.400	0.077	0.128	-0.558	-0.139	3.648	2.986	-150.0	9831.2	593	7	10	1	1
319	-0.609	0.453	0.654	-0.120	0.665	0.388	0.078	0.139	0.021	0.027	2.829	2.849	-156.2	11435.2	330	5	7	1	1

V_∞ = 713.0 ft/sec T_t = 640.3 °R D = 0.986 in.

SEQ	x/D	r/D	V_x/V_∞	V_r/V_∞	$\lvert V\rvert/V_\infty$	M	S_x/V_∞	S_r/V_∞	SK_x	SK_r	KU_x	KU_r	RE_{xr}	TKE	N	PPS	PPL	SE	CC
102	-0.507	1.274	0.976	-0.030	0.977	0.580	0.012	0.094	-0.343	0.198	5.393	2.960	0.1	4543.8	981	770	770	1	1
101	-0.507	1.198	0.979	-0.033	0.979	0.582	0.011	0.086	-0.401	0.077	6.877	3.194	66.7	3801.8	983	593	591	1	1
100	-0.507	1.122	0.978	-0.022	0.978	0.581	0.010	0.090	0.074	0.225	8.404	3.010	16.8	4154.4	978	960	959	1	1
99	-0.507	1.084	0.980	-0.019	0.980	0.582	0.013	0.084	-0.464	0.218	7.625	3.114	-99.9	3644.7	997	613	612	1	1
98	-0.507	1.046	0.982	-0.034	0.982	0.583	0.012	0.088	-0.251	0.123	6.051	3.035	42.9	4003.0	988	556	553	1	1
97	-0.507	1.008	0.982	-0.037	0.983	0.584	0.014	0.088	-0.249	0.165	5.166	3.199	29.4	4011.6	986	696	692	1	1
96	-0.507	0.970	0.981	-0.030	0.982	0.583	0.012	0.093	-0.066	0.133	6.203	3.175	52.5	4441.4	980	742	739	1	1
95	-0.507	0.932	0.981	-0.028	0.982	0.583	0.014	0.089	-0.749	0.152	7.683	3.099	28.7	4055.8	998	691	688	1	1
94	-0.507	0.894	0.983	-0.029	0.984	0.584	0.011	0.084	-0.033	0.216	6.664	3.060	57.2	3624.8	981	727	722	1	1
93	-0.507	0.856	0.983	-0.029	0.984	0.584	0.011	0.087	-0.218	0.277	7.049	3.148	-5.5	3853.7	984	893	887	1	1
92	-0.507	0.818	0.988	-0.033	0.989	0.588	0.009	0.093	-0.184	0.111	9.585	2.990	-36.2	4462.1	981	455	450	1	1
91	-0.507	0.780	0.992	-0.037	0.992	0.590	0.009	0.086	-0.080	0.139	8.785	3.277	1.2	3758.2	979	401	395	1	1
90	-0.507	0.742	0.994	-0.055	0.996	0.592	0.010	0.087	0.120	0.093	8.444	3.101	-13.1	3858.6	975	369	362	1	1
89	-0.507	0.704	0.997	-0.067	0.999	0.594	0.009	0.089	0.155	0.041	9.535	3.233	5.8	4083.1	971	150	146	1	1
88	-0.507	0.685	0.999	-0.059	1.001	0.595	0.008	0.082	-0.444	-0.006	12.975	3.315	12.3	3408.5	971	98	95	1	1
87	-0.507	0.666	1.003	-0.058	1.004	0.598	0.010	0.087	-0.264	-0.041	8.490	3.258	-9.3	3856.8	979	76	73	1	1
86	-0.507	0.647	1.002	-0.067	1.004	0.597	0.010	0.091	-0.008	-0.040	8.174	3.272	0.6	4192.2	978	54	52	1	1
85	-0.507	0.628	0.998	-0.088	1.002	0.596	0.013	0.095	-0.902	-0.210	6.840	3.489	-2.9	4588.4	982	40	39	1	1
84	-0.507	0.609	0.990	-0.091	0.994	0.591	0.019	0.095	-0.635	0.020	5.044	3.501	19.7	4713.9	978	23	23	1	1
83	-0.507	0.590	0.978	-0.104	0.983	0.584	0.028	0.092	-1.265	-0.291	7.139	3.644	24.1	4524.1	995	19	19	1	1
82	-0.507	0.570	0.959	-0.102	0.965	0.572	0.033	0.094	-0.669	-0.052	3.430	3.442	6.8	4727.6	986	12	12	1	1
81	-0.507	0.551	0.938	-0.110	0.944	0.559	0.040	0.091	-0.643	-0.157	3.516	3.356	74.4	4626.2	994	9	9	1	1
80	-0.507	0.532	0.908	-0.126	0.916	0.542	0.047	0.102	-0.390	-0.317	2.745	3.525	145.8	5901.8	996	4	4	1	1
79	-0.507	0.513	0.882	-0.129	0.892	0.527	0.052	0.090	-0.243	-0.505	2.557	3.748	-140.8	4772.8	564	1	1	1	1
77	-0.507	0.494	0.828	-0.109	0.835	0.492	0.063	0.052	-0.284	-0.092	2.479	3.083	-6.3	2356.9	214	0	1	1	1
76	-0.507	0.475	0.780	-0.111	0.787	0.462	0.065	0.055	-0.002	-0.024	2.466	3.597	-71.7	2643.3	239	0	1	1	1
75	-0.507	0.456	0.731	-0.121	0.741	0.434	0.073	0.060	0.099	-0.854	2.957	3.801	158.8	3158.7	110	0	0	1	1
74	-0.507	0.436	0.661	-0.151	0.678	0.396	0.085	0.083	0.086	-0.750	2.410	3.659	1.5	5322.6	115	0	0	1	1

V_∞ = 713.0 ft/sec $\qquad$ T_t = 640.3 °R $\qquad$ D = 0.986 in.

SEQ	x/D	r/D	V_x/V_∞	V_r/V_∞	$\lvert V\rvert/V_\infty$	M	S_x/V_∞	S_r/V_∞	SK_x	SK_r	KU_x	KU_r	RE_{xr}	TKE	N	PPS	PPL	SE	CC
290	-0.406	1.274	0.986	-0.035	0.987	0.586	0.014	0.089	-0.297	0.222	4.942	3.573	9.0	4064.5	991	843	835	1	1
291	-0.406	1.198	0.988	-0.038	0.988	0.587	0.010	0.081	-0.147	0.139	7.838	3.642	-61.4	3337.5	994	518	513	1	1
292	-0.406	1.122	0.991	-0.036	0.992	0.590	0.015	0.083	-0.396	0.257	5.048	3.841	58.1	3532.7	994	736	726	1	1
293	-0.406	1.046	0.986	-0.041	0.987	0.586	0.013	0.084	-0.092	0.009	5.181	3.785	68.5	3633.1	994	956	947	1	1
294	-0.406	0.970	0.987	-0.046	0.989	0.587	0.017	0.086	-0.766	0.236	6.633	3.557	111.2	3798.2	998	1343	1328	1	1
295	-0.406	0.932	0.987	-0.042	0.988	0.587	0.018	0.083	-0.642	0.173	4.337	3.520	80.6	3562.2	996	1065	1053	1	1
296	-0.406	0.894	0.989	-0.038	0.989	0.588	0.027	0.081	-0.263	0.167	4.364	3.673	104.7	3531.5	992	871	860	1	1
297	-0.406	0.856	0.992	-0.044	0.993	0.590	0.011	0.081	-0.518	0.093	7.211	3.578	-22.5	3350.1	992	905	891	1	1
298	-0.406	0.818	0.997	-0.037	0.997	0.593	0.016	0.080	-0.379	0.296	4.441	3.765	-35.1	3345.9	995	567	556	1	1
299	-0.406	0.780	0.991	-0.035	0.992	0.590	0.011	0.083	-0.114	0.229	6.643	3.223	41.1	3503.7	992	333	328	1	1
300	-0.406	0.742	0.998	-0.044	0.998	0.594	0.010	0.080	-0.178	0.150	8.648	3.582	-6.9	3294.0	995	131	129	1	1
301	-0.406	0.704	0.998	-0.068	1.000	0.595	0.018	0.115	-0.409	-0.059	4.401	3.282	-8.5	6843.6	991	383	374	1	1
302	-0.406	0.685	0.998	-0.066	1.000	0.594	0.017	0.117	-0.509	-0.158	4.426	3.237	-44.1	7062.7	997	229	224	1	1
303	-0.406	0.666	0.999	-0.075	1.001	0.596	0.016	0.119	-0.116	0.027	4.571	2.949	-33.2	7294.0	992	221	215	1	1
304	-0.406	0.647	0.997	-0.079	1.000	0.595	0.019	0.124	-0.272	-0.077	4.180	2.948	21.9	7881.9	991	142	138	1	1
306	-0.406	0.628	0.988	-0.076	0.991	0.589	0.024	0.118	-1.136	-0.029	8.902	3.116	-48.0	7225.8	997	116	115	1	1
307	-0.406	0.609	0.980	-0.089	0.984	0.584	0.026	0.128	-0.438	-0.083	3.694	2.866	-52.2	8468.3	995	114	113	1	1
308	-0.406	0.590	0.967	-0.090	0.971	0.576	0.032	0.120	-0.438	-0.025	3.372	2.853	-132.0	7516.0	990	72	73	1	1
309	-0.406	0.570	0.946	-0.088	0.950	0.563	0.038	0.117	-0.507	-0.173	3.255	3.176	51.9	7334.1	989	47	48	1	1
310	-0.406	0.551	0.923	-0.097	0.928	0.549	0.043	0.120	-0.509	-0.178	3.175	3.028	-73.0	7801.5	992	35	37	1	1
311	-0.406	0.532	0.899	-0.098	0.905	0.535	0.055	0.120	-0.524	-0.019	3.175	2.968	-84.0	8030.3	989	29	31	1	1
312	-0.406	0.513	0.862	-0.104	0.868	0.512	0.056	0.120	-0.641	-0.212	3.369	3.067	229.7	8128.9	993	28	31	1	1
313	-0.406	0.494	0.837	-0.112	0.844	0.497	0.058	0.128	-0.433	-0.103	3.037	3.045	30.5	9158.9	992	20	24	1	1
314	-0.406	0.475	0.798	-0.115	0.806	0.474	0.059	0.121	-0.182	-0.074	2.739	2.962	-31.2	8344.6	991	18	22	1	1
315	-0.406	0.456	0.759	-0.116	0.767	0.450	0.059	0.121	-0.111	-0.067	2.788	3.033	-80.1	8377.5	993	13	16	1	1
316	-0.406	0.437	0.711	-0.116	0.720	0.421	0.067	0.125	-0.060	-0.003	2.805	3.124	-142.4	9125.6	994	7	10	1	1
317	-0.406	0.418	0.637	-0.120	0.648	0.378	0.073	0.132	-0.163	-0.056	2.626	2.645	-542.8	10170.4	524	3	5	1	1
318	-0.406	0.403	0.526	-0.128	0.542	0.314	0.086	0.127	-0.012	-0.083	2.827	3.160	-1071.8	10040.3	214	1	2	1	1

V_∞ = 713.0 ft/sec T_t = 640.3 °R D = 0.986 in.

SEQ	x/D	r/D	V_x/V_∞	V_r/V_∞	$\lvert V\rvert/V_\infty$	M	S_x/V_∞	S_r/V_∞	SK_x	SK_r	KU_x	KU_r	RE_{xr}	TKE	N	PPS	PPL	SE	CC
283	-0.304	1.274	0.984	-0.035	0.985	0.585	0.011	0.082	0.147	0.150	6.080	3.441	-11.5	3488.4	990	493	489	1	1
282	-0.304	1.198	0.980	-0.032	0.980	0.582	0.016	0.084	-0.353	0.084	4.284	3.469	34.9	3657.5	993	669	666	1	1
280	-0.304	1.122	0.982	-0.038	0.983	0.584	0.014	0.084	-0.218	0.251	4.394	3.674	-20.3	3616.4	994	1337	1329	1	1
279	-0.304	1.046	0.987	-0.039	0.988	0.587	0.019	0.083	-0.361	0.148	4.334	3.873	-19.9	3617.9	990	1933	1912	1	1
278	-0.304	0.970	0.982	-0.043	0.983	0.584	0.019	0.083	-0.725	0.125	6.403	3.664	145.6	3617.9	998	1376	1366	1	1
277	-0.304	0.932	0.984	-0.041	0.984	0.585	0.015	0.083	0.031	0.078	5.047	3.740	-13.1	3536.7	989	1338	1327	1	1
276	-0.304	0.894	0.981	-0.056	0.983	0.584	0.023	0.116	-0.265	0.012	5.183	3.397	149.2	6916.2	998	1514	1504	1	1
275	-0.304	0.856	0.987	-0.060	0.989	0.588	0.015	0.111	-0.141	0.019	4.959	3.545	1.9	6285.7	987	869	858	1	1
274	-0.304	0.818	0.989	-0.063	0.991	0.589	0.017	0.119	-0.067	0.139	4.497	3.373	-118.3	7313.1	996	653	644	1	1
273	-0.304	0.780	0.986	-0.068	0.989	0.587	0.018	0.122	-0.714	-0.064	6.365	3.300	-179.4	7675.6	998	475	469	1	1
272	-0.304	0.742	0.989	-0.066	0.991	0.589	0.018	0.124	-0.281	-0.049	4.423	2.904	-47.7	7925.9	993	365	359	1	1
271	-0.304	0.704	0.987	-0.067	0.990	0.588	0.020	0.125	-0.353	-0.067	5.311	3.071	-49.2	8079.1	998	458	451	1	1
270	-0.304	0.685	0.988	-0.073	0.991	0.589	0.018	0.122	-0.271	-0.083	4.193	3.052	-61.5	7687.5	993	241	237	1	1
269	-0.304	0.666	0.986	-0.072	0.988	0.587	0.017	0.125	-0.358	-0.052	4.364	3.138	-13.9	7957.5	995	199	196	1	1
268	-0.304	0.647	0.985	-0.078	0.989	0.587	0.020	0.122	-0.341	-0.052	4.629	3.168	-41.6	7687.2	993	180	178	1	1
266	-0.304	0.628	0.977	-0.080	0.980	0.582	0.019	0.121	-0.517	-0.073	4.170	3.092	28.7	7543.6	995	138	138	1	1
265	-0.304	0.609	0.970	-0.077	0.973	0.577	0.027	0.124	-0.629	-0.044	3.740	3.224	-63.3	7995.9	992	115	115	1	1
264	-0.304	0.590	0.955	-0.094	0.960	0.569	0.032	0.119	-0.550	-0.069	3.812	2.988	-181.5	7502.5	998	99	100	1	1
263	-0.304	0.570	0.938	-0.083	0.942	0.558	0.034	0.126	-0.463	-0.080	3.214	3.014	-34.2	8318.6	988	65	67	1	1
262	-0.304	0.551	0.919	-0.089	0.924	0.546	0.042	0.118	-0.434	-0.141	3.018	2.938	-64.8	7474.8	993	62	65	1	1
261	-0.304	0.532	0.888	-0.108	0.894	0.528	0.049	0.123	-0.505	0.074	3.440	2.948	-208.6	8293.1	994	47	52	1	1
260	-0.304	0.513	0.868	-0.097	0.874	0.515	0.051	0.123	-0.369	-0.079	2.976	3.151	-194.2	8359.9	989	20	23	1	1
259	-0.304	0.494	0.832	-0.102	0.839	0.494	0.056	0.121	-0.432	-0.139	2.953	2.787	-468.8	8206.4	989	24	27	1	1
258	-0.304	0.475	0.798	-0.110	0.805	0.473	0.059	0.129	-0.162	-0.081	2.848	2.978	149.1	9302.4	995	12	14	1	1
257	-0.304	0.456	0.762	-0.117	0.771	0.452	0.061	0.123	-0.096	-0.100	2.557	2.735	-264.6	8672.7	992	16	20	1	1
256	-0.304	0.437	0.716	-0.112	0.725	0.424	0.063	0.129	-0.107	-0.110	2.685	3.049	-28.4	9464.3	990	9	13	1	1
255	-0.304	0.418	0.670	-0.113	0.679	0.396	0.066	0.125	-0.010	-0.026	2.750	3.108	-3.2	9010.0	997	7	10	1	1
254	-0.304	0.399	0.593	-0.117	0.605	0.352	0.075	0.135	-0.276	-0.049	3.475	2.697	-70.5	10728.7	534	3	6	1	1
253	-0.304	0.380	0.477	-0.110	0.489	0.284	0.096	0.137	-0.238	-0.079	2.909	3.046	-245.0	11925.3	507	1	2	1	1
252	-0.304	0.369	0.378	-0.119	0.397	0.229	0.105	0.137	0.030	0.205	2.674	3.115	-159.0	12390.6	204	0	1	1	1

V_∞ = 713.0 ft/sec T_t = 640.3 °R D = 0.986 in.

SEQ	x/D	r/D	V_x/V_∞	V_r/V_∞	$\lvert V\rvert/V_\infty$	M	S_x/V_∞	S_r/V_∞	SK_x	SK_r	KU_x	KU_r	RE_{xr}	TKE	N	PPS	PPL	SB	CC
248	-0.203	1.274	0.977	-0.024	0.977	0.580	0.014	0.086	-0.395	0.315	5.341	3.128	72.1	3844.9	993	892	887	1	1
247	-0.203	1.198	0.974	-0.030	0.974	0.578	0.014	0.082	-0.299	0.076	5.614	3.602	43.0	3463.9	989	1261	1256	1	1
246	-0.203	1.122	0.981	-0.031	0.982	0.583	0.018	0.093	-0.230	0.025	3.924	3.595	56.3	4522.9	998	818	809	1	1
245	-0.203	1.046	0.979	-0.038	0.980	0.582	0.018	0.084	-0.442	0.060	4.014	3.620	-7.4	3694.2	991	1184	1173	1	1
244	-0.203	0.970	0.978	-0.039	0.979	0.581	0.015	0.088	-0.172	0.064	4.711	3.588	-77.7	4012.7	993	958	950	1	1
243	-0.203	0.932	0.972	-0.039	0.973	0.577	0.020	0.091	-0.211	0.442	5.991	3.420	-24.1	4270.3	998	1714	1710	1	1
242	-0.203	0.894	0.976	-0.044	0.977	0.580	0.017	0.084	-0.209	0.054	4.417	4.050	-20.0	3687.5	990	1445	1436	1	1
241	-0.203	0.856	0.973	-0.041	0.974	0.578	0.016	0.084	-0.225	0.070	4.361	3.665	27.2	3630.3	994	1119	1115	1	1
240	-0.203	0.818	0.974	-0.041	0.975	0.579	0.016	0.086	-0.264	0.071	5.098	3.614	-11.5	3866.9	995	688	685	1	1
239	-0.203	0.780	0.988	-0.060	0.990	0.588	0.022	0.123	-0.240	0.054	3.491	3.159	-66.8	7801.6	994	804	789	1	1
238	-0.203	0.742	0.976	-0.066	0.979	0.581	0.020	0.126	-0.287	0.011	4.156	3.157	71.2	8224.4	995	819	812	1	1
237	-0.203	0.704	0.976	-0.068	0.978	0.581	0.018	0.122	0.164	0.012	4.127	3.006	-9.2	7625.2	992	315	312	1	1
236	-0.203	0.685	0.973	-0.075	0.975	0.579	0.018	0.123	-0.117	0.096	4.984	3.243	-72.3	7738.6	989	297	295	1	1
235	-0.203	0.666	0.974	-0.070	0.976	0.580	0.020	0.129	-0.433	-0.026	4.385	2.988	-66.6	8568.1	995	228	226	1	1
234	-0.203	0.647	0.977	-0.070	0.979	0.581	0.031	0.126	0.353	0.026	4.312	2.966	179.9	8327.0	995	283	281	1	1
233	-0.203	0.628	0.955	-0.084	0.959	0.569	0.020	0.125	-0.308	-0.038	4.244	2.933	-43.9	8048.3	995	241	244	1	1
232	-0.203	0.609	0.953	-0.072	0.955	0.566	0.023	0.123	-0.449	0.084	3.511	2.996	-71.4	7781.0	993	176	179	1	1
231	-0.203	0.590	0.943	-0.092	0.948	0.562	0.027	0.123	-0.413	-0.043	3.845	3.028	-109.0	7904.5	992	120	123	1	1
230	-0.203	0.570	0.928	-0.086	0.932	0.552	0.035	0.124	-0.772	-0.143	4.029	2.963	-134.0	8185.3	998	106	110	1	1
229	-0.203	0.551	0.907	-0.080	0.911	0.538	0.044	0.122	-0.717	-0.074	3.995	3.039	-58.4	8113.0	997	69	73	1	1
228	-0.203	0.532	0.889	-0.094	0.892	0.527	0.045	0.123	-0.456	-0.059	2.992	3.250	-67.9	8192.7	995	69	75	1	1
227	-0.203	0.513	0.857	-0.090	0.861	0.508	0.049	0.128	-0.644	-0.012	3.502	3.128	-265.5	8936.6	990	46	52	1	1
226	-0.203	0.494	0.830	-0.091	0.835	0.491	0.052	0.127	-0.306	-0.003	2.680	3.185	-149.7	8819.4	994	26	30	1	1
225	-0.203	0.475	0.800	-0.094	0.805	0.473	0.059	0.122	-0.221	-0.062	2.792	3.055	-223.6	8515.4	989	27	33	1	1
224	-0.203	0.456	0.762	-0.098	0.769	0.451	0.059	0.130	-0.032	-0.105	2.557	2.986	-33.9	9489.5	990	22	28	1	1
223	-0.203	0.437	0.735	-0.100	0.742	0.434	0.060	0.128	-0.226	-0.141	2.851	2.980	-59.5	9246.9	995	16	21	1	1
222	-0.203	0.418	0.681	-0.114	0.691	0.403	0.061	0.100	-0.031	-0.215	2.789	3.163	-79.4	6069.0	987	5	7	1	1
221	-0.203	0.399	0.639	-0.118	0.650	0.379	0.069	0.104	-0.074	-0.104	2.892	3.179	-296.4	6738.2	983	3	5	1	1
219	-0.203	0.380	0.636	-0.132	0.649	0.379	0.074	0.128	-0.233	-0.072	3.146	2.962	-79.4	9749.2	989	11	16	1	1
218	-0.203	0.361	0.576	-0.121	0.589	0.342	0.086	0.138	-0.152	-0.256	3.029	3.126	-20.3	11543.2	985	4	7	1	1
217	-0.203	0.342	0.500	-0.095	0.509	0.295	0.104	0.159	-0.156	-0.095	2.601	2.489	231.8	15608.4	199	0	1	1	1
216	-0.203	0.338	0.480	-0.100	0.490	0.284	0.117	0.171	-0.438	-0.229	3.129	3.191	172.6	18243.6	118	0	1	1	1

V_∞ = 713.0 ft/sec T_t = 640.3 °R D = 0.986 in.

SEQ	x/D	r/D	V_x/V_∞	V_r/V_∞	$\lvert V\rvert/V_\infty$	M	S_x/V_∞	S_r/V_∞	SK_x	SK_r	KU_x	KU_r	RE_{xr}	TKE	N	PPS	PPL	SE	CC
182	-0.101	1.274	0.976	-0.034	0.977	0.580	0.012	0.069	-0.314	0.233	6.561	3.306	-0.6	2454.3	994	1068	1069	1	1
183	-0.101	1.198	0.980	-0.027	0.980	0.582	0.009	0.069	-0.291	0.367	9.409	3.069	12.0	2418.8	993	755	753	1	1
184	-0.101	1.122	0.981	-0.037	0.981	0.583	0.011	0.065	-0.239	0.337	7.577	3.155	-24.3	2156.6	992	1143	1139	1	1
185	-0.101	1.046	0.979	-0.040	0.979	0.582	0.012	0.065	-0.517	0.257	6.573	3.038	29.3	2195.9	991	1703	1699	1	1
186	-0.101	0.970	0.978	-0.050	0.980	0.582	0.012	0.069	-0.391	0.393	6.824	3.463	21.9	2446.0	991	1849	1844	1	1
187	-0.101	0.932	0.973	-0.054	0.975	0.579	0.015	0.068	-0.689	0.283	5.770	3.500	5.3	2437.4	990	2313	2319	1	1
188	-0.101	0.894	0.979	-0.050	0.980	0.582	0.013	0.068	-0.597	0.375	6.210	3.332	96.2	2389.5	993	1441	1437	1	1
189	-0.101	0.856	0.991	-0.043	0.991	0.589	0.017	0.070	-0.531	0.371	4.823	3.198	22.2	2543.0	987	1282	1264	1	1
190	-0.101	0.818	0.983	-0.039	0.984	0.584	0.008	0.064	-0.342	0.287	10.418	3.308	9.3	2122.9	987	545	542	1	1
191	-0.101	0.780	0.983	-0.055	0.984	0.585	0.011	0.060	-0.651	0.288	6.942	3.566	-11.1	1862.4	992	514	511	1	1
192	-0.101	0.742	0.981	-0.057	0.983	0.584	0.010	0.055	-0.810	0.301	9.671	3.275	19.7	1575.6	987	290	289	1	1
193	-0.101	0.704	0.977	-0.062	0.979	0.582	0.015	0.065	-0.755	0.253	6.752	3.349	27.3	2179.8	990	200	199	1	1
194	-0.101	0.685	0.983	-0.076	0.986	0.586	0.013	0.060	-0.449	0.025	7.417	3.766	10.9	1898.6	989	87	86	1	1
195	-0.101	0.666	0.976	-0.079	0.979	0.581	0.014	0.058	-0.955	0.040	8.813	3.452	14.9	1757.4	980	44	43	1	1
196	-0.101	0.647	0.968	-0.083	0.971	0.577	0.018	0.060	-0.235	-0.020	6.003	3.555	65.1	1920.7	994	28	29	1	1
197	-0.101	0.628	0.972	-0.085	0.976	0.579	0.016	0.061	-0.307	-0.008	6.601	3.820	-23.3	1922.9	988	13	13	1	1
198	-0.101	0.609	0.961	-0.085	0.965	0.573	0.019	0.061	-0.424	0.137	5.341	3.583	43.8	1967.6	983	8	8	1	1
199	-0.101	0.590	0.950	-0.088	0.954	0.566	0.020	0.096	-0.063	0.144	4.209	3.425	-19.0	4788.4	982	133	136	1	1
200	-0.101	0.570	0.938	-0.098	0.944	0.559	0.028	0.096	-0.839	0.028	6.100	3.232	57.7	4909.2	993	89	92	1	1
201	-0.101	0.551	0.924	-0.103	0.930	0.550	0.031	0.097	-0.744	-0.107	4.195	3.282	-123.0	5062.2	993	54	57	1	1
202	-0.101	0.532	0.901	-0.118	0.909	0.537	0.038	0.106	-0.546	-0.153	3.258	3.327	-47.7	6049.9	988	36	39	1	1
203	-0.101	0.513	0.889	-0.126	0.898	0.530	0.040	0.099	-0.508	-0.181	3.109	3.332	-12.0	5422.0	991	25	28	1	1
204	-0.101	0.494	0.861	-0.128	0.871	0.513	0.049	0.099	-0.567	-0.259	3.200	3.455	-59.8	5550.3	995	19	22	1	1
205	-0.101	0.475	0.838	-0.127	0.847	0.499	0.050	0.100	-0.329	-0.006	2.897	3.290	-175.1	5690.2	991	13	15	1	1
206	-0.101	0.456	0.810	-0.132	0.821	0.482	0.053	0.096	-0.266	-0.191	2.784	3.580	61.0	5367.3	995	11	13	1	1
207	-0.101	0.437	0.775	-0.129	0.786	0.461	0.056	0.099	-0.231	-0.197	2.657	3.662	-173.1	5752.7	994	9	11	1	1
208	-0.101	0.418	0.743	-0.141	0.756	0.443	0.060	0.095	-0.071	-0.266	2.943	3.134	-247.4	5490.8	987	5	7	1	1
209	-0.101	0.399	0.703	-0.131	0.715	0.418	0.061	0.101	-0.115	-0.282	2.682	3.341	-116.4	6177.9	997	4	6	1	1
210	-0.101	0.380	0.677	-0.130	0.690	0.403	0.064	0.102	-0.050	-0.110	2.720	3.177	200.7	6330.5	991	3	5	1	1
211	-0.101	0.361	0.624	-0.137	0.639	0.372	0.066	0.107	-0.247	0.087	2.709	3.198	105.3	6972.1	517	1	2	1	1
212	-0.101	0.342	0.573	-0.130	0.588	0.342	0.074	0.109	-0.155	-0.330	2.758	3.285	92.2	7460.8	519	1	1	1	1
213	-0.101	0.323	0.504	-0.106	0.515	0.299	0.091	0.130	0.003	0.332	2.334	3.466	742.5	10728.4	198	0	0	1	1
214	-0.101	0.304	0.367	-0.061	0.372	0.215	0.125	0.138	-0.237	0.382	3.173	3.191	-2025.9	13601.6	126	0	1	1	1
215	-0.101	0.285	0.262	-0.060	0.269	0.155	0.141	0.113	0.045	-0.594	2.434	3.240	-957.9	11534.5	57	0	0	1	1

V_∞ = 713.0 ft/sec T_t = 640.3 °R D = 0.986 in.

SEQ	x/D	r/D	V_x/V_∞	V_r/V_∞	$\lvert V \rvert/V_\infty$	M	S_x/V_∞	S_r/V_∞	SK_x	SK_r	KU_x	KU_r	RE_{xr}	TKE	N	PPS	PPL	SE	CC
174	0.0	1.274	0.979	-0.035	0.980	0.582	0.011	0.066	-0.267	0.435	6.494	2.997	-23.6	2221.6	994	1166	1165	1	1
173	0.0	1.198	0.976	-0.029	0.976	0.580	0.011	0.069	-0.426	0.277	6.184	3.176	24.6	2423.0	993	1574	1578	1	1
172	0.0	1.122	0.975	-0.043	0.976	0.580	0.013	0.074	-0.211	0.409	6.081	3.365	26.9	2823.5	991	2400	2407	1	1
171	0.0	1.046	0.979	-0.043	0.980	0.582	0.013	0.068	-0.464	0.337	5.224	3.338	-33.8	2399.9	989	1978	1977	1	1
170	0.0	0.970	0.979	-0.041	0.980	0.582	0.011	0.073	-0.391	0.303	6.557	3.230	-8.6	2717.3	993	2035	2033	1	1
169	0.0	0.932	0.981	-0.036	0.982	0.583	0.010	0.067	-0.491	0.364	9.063	3.241	-24.6	2318.0	991	1149	1146	1	1
168	0.0	0.894	0.982	-0.036	0.983	0.584	0.010	0.065	-0.210	0.465	6.797	3.182	14.2	2163.3	995	1272	1268	1	1
167	0.0	0.856	0.981	-0.046	0.982	0.583	0.010	0.063	-0.540	0.342	8.622	3.421	-27.7	2022.0	991	1595	1591	1	1
166	0.0	0.818	0.979	-0.066	0.982	0.583	0.010	0.094	-0.697	0.070	7.653	3.306	41.0	4488.1	992	1161	1159	1	1
165	0.0	0.780	0.979	-0.068	0.981	0.583	0.013	0.090	-0.802	0.071	8.181	3.399	-103.7	4157.3	999	714	713	1	1
164	0.0	0.742	0.976	-0.064	0.978	0.581	0.012	0.092	-0.271	-0.023	6.546	3.560	-12.6	4344.4	992	724	725	1	1
163	0.0	0.704	0.968	-0.056	0.970	0.575	0.015	0.087	-0.499	0.186	4.663	3.214	51.2	3919.0	985	749	757	1	1
162	0.0	0.685	0.969	-0.064	0.972	0.577	0.014	0.089	-0.585	0.037	5.467	3.372	-22.6	4058.4	989	487	491	1	1
161	0.0	0.666	0.968	-0.072	0.971	0.576	0.017	0.094	-0.615	-0.002	10.649	3.507	91.9	4603.6	999	364	367	1	1
160	0.0	0.647	0.963	-0.077	0.966	0.573	0.015	0.094	-0.273	-0.019	4.348	3.359	31.0	4570.3	990	308	312	1	1
159	0.0	0.628	0.962	-0.081	0.965	0.573	0.016	0.092	-0.157	0.022	4.504	3.474	92.4	4411.9	989	348	354	1	1
158	0.0	0.590	0.950	-0.084	0.954	0.566	0.018	0.093	-0.416	-0.084	4.588	3.504	3.2	4488.5	985	147	151	1	1
157	0.0	0.570	0.940	-0.091	0.944	0.559	0.022	0.097	-0.268	-0.060	4.338	3.214	-10.6	4878.3	985	102	105	1	1
156	0.0	0.551	0.924	-0.092	0.928	0.549	0.030	0.095	-0.507	-0.002	3.516	3.505	23.8	4778.9	986	130	138	1	1
155	0.0	0.513	0.883	-0.096	0.888	0.524	0.041	0.095	-0.605	-0.005	3.531	3.457	-311.1	4996.8	994	68	75	1	1
154	0.0	0.494	0.860	-0.094	0.865	0.510	0.046	0.099	-0.412	-0.093	2.898	3.380	-52.1	5483.4	996	44	49	1	1
153	0.0	0.475	0.838	-0.101	0.844	0.497	0.046	0.099	-0.239	-0.128	2.732	3.551	-141.0	5556.8	993	30	34	1	1
152	0.0	0.456	0.805	-0.109	0.813	0.478	0.053	0.101	-0.425	-0.006	2.972	3.517	-113.3	5889.9	997	26	32	1	1
151	0.0	0.437	0.772	-0.111	0.780	0.457	0.056	0.107	-0.170	-0.167	2.737	3.155	-328.5	6618.8	994	20	25	1	1
150	0.0	0.418	0.740	-0.115	0.749	0.439	0.055	0.100	-0.099	-0.232	2.616	3.279	27.5	5854.4	991	14	18	1	1
149	0.0	0.399	0.701	-0.118	0.710	0.415	0.058	0.100	-0.072	-0.105	2.651	3.279	-186.2	5985.6	990	14	20	1	1
148	0.0	0.380	0.665	-0.114	0.675	0.394	0.060	0.100	-0.048	-0.155	3.006	3.349	-87.5	5996.9	993	6	10	1	1
147	0.0	0.361	0.611	-0.120	0.623	0.363	0.061	0.102	0.026	-0.041	2.553	2.923	-2.3	6211.9	556	7	11	1	1
146	0.0	0.342	0.562	-0.123	0.575	0.334	0.070	0.103	-0.100	-0.110	2.925	3.016	-332.0	6662.6	535	4	7	1	1
145	0.0	0.323	0.475	-0.111	0.488	0.283	0.090	0.111	-0.344	-0.044	3.195	3.106	-640.6	8311.2	521	2	4	1	1
144	0.0	0.304	0.332	-0.096	0.346	0.199	0.129	0.113	-0.058	-0.184	2.503	3.212	-1850.4	10652.4	508	1	4	1	1
143	0.0	0.285	0.192	-0.060	0.201	0.116	0.081	0.101	0.462	0.170	2.871	3.252	-608.8	6876.5	542	3	17	1	1
142	0.0	0.266	0.130	-0.055	0.141	0.081	0.061	0.096	0.291	-0.026	2.883	3.275	-529.4	5661.5	593	4	30	1	1
140	0.0	0.247	0.096	-0.056	0.112	0.064	0.055	0.096	0.323	-0.017	3.110	3.163	-252.0	5406.7	525	4	37	1	1
138	0.0	0.236	0.078	-0.056	0.095	0.055	0.045	0.111	0.200	-0.072	3.667	3.478	-403.1	6809.8	301	2	24	1	1

V_∞ = 713.0 ft/sec T_t = 640.3 °R D = 0.986 in.

SEQ	x/D	r/D	V_x/V_∞	V_r/V_∞	$\lvert V\rvert/V_\infty$	M	S_x/V_∞	S_r/V_∞	SK_x	SK_r	KU_x	KU_r	RE_{xr}	TKE	N	PPS	PPL	SE	CC
115	0.051	0.190	0.299	0.131	0.326	0.188	0.635	0.219	1.859	0.202	4.733	2.771	38950.6	126784.0	28	0	1	2	1
114	0.051	0.152	1.787	0.182	1.796	1.164	0.130	0.132	-0.273	0.012	2.912	3.609	1443.7	13178.5	985	7	4	2	1
113	0.051	0.114	1.756	0.156	1.763	1.137	0.115	0.101	-0.165	-0.069	2.892	3.053	1148.7	8570.4	994	60	33	2	1
112	0.051	0.076	1.764	0.140	1.770	1.142	0.105	0.101	-0.350	-0.063	3.103	2.865	693.5	7952.1	994	99	55	2	1
111	0.051	0.038	1.789	0.135	1.794	1.162	0.098	0.099	-0.237	-0.152	2.776	2.907	470.4	7480.3	993	127	69	2	1
110	0.051	0.0	1.801	0.100	1.804	1.170	0.106	0.094	-0.304	-0.040	3.075	2.491	369.1	7310.5	993	85	46	2	1
109	0.051	-0.038	1.812	-0.103	1.815	1.180	0.109	0.095	-0.229	0.094	2.880	2.699	-448.6	7586.4	993	89	48	2	1
108	0.051	-0.076	1.872	0.014	1.872	1.227	0.096	0.151	-0.180	0.029	3.054	2.944	-606.9	13881.5	979	86	45	2	1
107	0.051	-0.114	1.855	0.099	1.857	1.215	0.116	0.149	-0.274	0.148	3.086	2.818	-246.3	14768.5	983	42	22	2	1
106	0.051	-0.152	1.856	0.255	1.874	1.229	0.161	0.168	-0.948	0.330	4.665	3.577	2229.0	20961.5	269	2	1	2	1

NOTE: NEGATIVE R/D INDICATES MEASUREMENT ON OPPOSITE SIDE OF JET CENTERLINE (I.E. -Z/D)

V_∞ = 713.0 ft/sec T_t = 640.3 °R D = 0.986 in.

SEQ	x/D	r/D	V_x/V_∞	V_r/V_∞	$\lvert V \rvert/V_\infty$	M	S_x/V_∞	S_r/V_∞	SK_x	SK_r	KU_x	KU_r	RE_{xr}	TKE	N	PPS	PPL	SE	CC
446	0.101	1.274	0.972	-0.037	0.973	0.577	0.017	0.100	-0.098	0.271	4.345	3.005	-11.9	5174.6	995	287	285	1	1
447	0.101	1.198	0.973	-0.039	0.973	0.578	0.017	0.092	-0.036	0.205	4.050	3.066	-37.5	4421.1	995	311	308	1	1
448	0.101	1.122	0.974	-0.036	0.974	0.578	0.016	0.101	0.044	0.091	4.574	3.296	-13.9	5210.3	991	438	434	1	1
449	0.101	1.046	0.975	-0.040	0.976	0.579	0.016	0.101	0.165	0.193	4.134	3.205	-35.6	5253.7	991	688	682	1	1
450	0.101	0.970	0.976	-0.047	0.977	0.580	0.015	0.101	0.097	0.102	4.339	3.617	-27.0	5286.2	992	802	794	1	1
451	0.101	0.932	0.976	-0.044	0.977	0.580	0.018	0.099	0.159	0.111	4.146	3.314	49.8	5096.4	992	656	649	1	1
452	0.101	0.894	0.974	-0.043	0.975	0.579	0.019	0.101	0.249	0.040	3.772	3.222	63.9	5277.0	995	861	853	1	1
453	0.101	0.856	0.973	-0.048	0.974	0.578	0.015	0.095	-0.068	0.237	4.508	3.174	49.0	4655.7	995	675	670	1	1
454	0.101	0.818	0.973	-0.056	0.975	0.579	0.017	0.095	0.052	0.177	4.602	3.285	14.6	4658.9	990	644	638	1	1
455	0.101	0.780	0.969	-0.051	0.970	0.576	0.017	0.098	-0.166	0.071	4.151	3.365	65.7	4988.8	992	390	389	1	1
456	0.101	0.742	0.967	-0.054	0.969	0.575	0.016	0.100	-0.265	0.156	4.966	3.334	-8.6	5108.9	994	269	269	1	1
457	0.101	0.704	0.964	-0.059	0.966	0.573	0.018	0.095	-0.173	-0.060	4.324	3.490	31.5	4659.4	990	195	195	1	1
458	0.101	0.685	0.962	-0.065	0.964	0.572	0.018	0.095	-0.145	-0.053	5.075	3.317	-21.5	4667.2	995	135	136	1	1
459	0.101	0.666	0.961	-0.063	0.963	0.571	0.017	0.094	-0.486	-0.022	4.381	3.321	17.8	4600.2	992	93	93	1	1
460	0.101	0.647	0.957	-0.061	0.959	0.569	0.021	0.093	-0.211	0.138	3.805	3.343	1.5	4550.0	993	63	63	1	1
461	0.101	0.628	0.952	-0.061	0.954	0.566	0.020	0.089	-0.198	0.175	3.818	3.546	-53.9	4084.9	989	48	49	1	1
462	0.101	0.609	0.945	-0.070	0.947	0.561	0.020	0.093	-0.650	-0.038	6.224	3.407	-56.5	4511.3	997	45	46	1	1
463	0.101	0.590	0.937	-0.076	0.940	0.557	0.026	0.150	-0.168	0.053	4.012	2.977	36.3	11629.2	998	119	123	1	1
464	0.101	0.570	0.925	-0.075	0.928	0.549	0.026	0.138	-0.129	-0.104	6.081	2.963	-155.9	9880.8	997	77	80	1	1
465	0.101	0.551	0.921	-0.083	0.924	0.547	0.027	0.145	-0.633	-0.062	5.437	3.084	-207.7	10846.9	991	57	60	1	1
466	0.101	0.532	0.909	-0.086	0.913	0.540	0.033	0.141	-0.367	-0.021	3.292	3.045	24.5	10410.0	989	50	53	1	1
467	0.101	0.513	0.901	-0.069	0.904	0.534	0.046	0.138	-0.606	-0.040	3.677	2.953	72.9	10227.2	992	33	35	1	1
468	0.101	0.494	0.870	-0.082	0.874	0.516	0.043	0.137	-0.557	-0.046	3.074	2.856	-149.1	9979.7	994	34	38	1	1
469	0.101	0.475	0.847	-0.083	0.851	0.501	0.047	0.145	-0.382	0.055	3.083	3.007	-17.0	11298.4	989	28	32	1	1
470	0.101	0.456	0.834	-0.086	0.839	0.494	0.053	0.137	-0.252	-0.057	2.944	2.866	39.0	10271.2	995	22	25	1	1
471	0.101	0.437	0.797	-0.083	0.801	0.470	0.053	0.139	-0.299	0.127	2.865	2.866	47.3	10518.3	989	26	31	1	1
472	0.101	0.418	0.770	-0.079	0.774	0.454	0.059	0.139	-0.245	0.017	2.933	2.857	-37.1	10652.5	984	6	7	1	1
473	0.101	0.399	0.740	-0.083	0.745	0.436	0.061	0.147	-0.292	-0.135	3.088	3.168	-176.1	11889.9	996	3	5	1	1
474	0.101	0.380	0.696	-0.103	0.704	0.411	0.065	0.151	-0.102	-0.071	2.960	2.977	94.0	12639.9	988	5	7	1	1
475	0.101	0.361	0.663	-0.084	0.668	0.390	0.069	0.148	-0.261	0.071	3.159	2.975	-587.2	12335.1	976	15	22	1	1
476	0.101	0.342	0.612	-0.095	0.619	0.361	0.073	0.148	-0.282	0.006	2.865	2.990	-110.9	12540.0	974	23	36	1	1
477	0.101	0.323	0.559	-0.099	0.568	0.330	0.086	0.151	-0.281	0.048	3.160	3.001	-100.9	13507.7	973	11	18	1	1
478	0.101	0.304	0.490	-0.091	0.498	0.289	0.095	0.151	-0.315	-0.123	3.081	2.870	-359.8	13967.7	966	4	8	1	1
479	0.101	0.285	0.402	-0.106	0.415	0.240	0.108	0.177	-0.178	-0.153	2.773	3.230	-437.6	18867.4	966	3	7	1	1
480	0.101	0.266	0.305	-0.098	0.321	0.185	0.102	0.196	0.006	0.027	2.676	3.251	-387.5	22259.6	953	3	9	1	1
481	0.101	0.247	0.226	-0.084	0.241	0.139	0.110	0.198	0.245	0.029	2.911	2.921	-1597.4	23010.0	902	4	17	1	1
482	0.101	0.228	0.252	-0.084	0.266	0.153	0.219	0.195	1.727	0.082	9.499	2.894	1523.2	31615.9	813	1	3	1	1
483	0.101	0.209	0.325	-0.028	0.326	0.188	0.493	0.241	0.769	0.296	3.633	2.078	8983.0	91287.1	15	0	0	1	1

V_∞ = 713.0 ft/sec T_t = 640.3 °R D = 0.986 in.

SEQ	x/D	r/D	V_x/V_∞	V_r/V_∞	$\lvert V\rvert/V_\infty$	M	S_x/V_∞	S_r/V_∞	SK_x	SK_r	KU_x	KU_r	RE_{xr}	TKE	N	PPS	PPL	SE	CC
493	0.101	0.171	1.870	0.416	1.916	1.265	0.138	0.326	0.148	0.194	2.044	2.685	4120.9	58718.9	19	0	0	2	1
494	0.101	0.152	1.958	0.233	1.971	1.314	0.181	0.237	-0.039	-0.112	2.672	2.871	6470.6	36791.8	104	0	0	2	1
495	0.101	0.133	1.988	0.177	1.996	1.337	0.172	0.236	-0.184	0.133	3.037	3.021	5948.1	35883.3	994	5	2	2	1
496	0.101	0.114	1.935	0.142	1.940	1.286	0.173	0.199	-0.063	0.080	2.780	2.994	5258.9	27757.5	995	12	6	2	1
497	0.101	0.095	1.909	0.139	1.915	1.264	0.151	0.183	-0.143	0.088	2.620	2.931	2479.7	22890.6	998	31	16	2	1
498	0.101	0.076	1.919	0.126	1.923	1.271	0.150	0.185	-0.253	0.025	2.559	3.031	1727.8	23052.1	993	36	19	2	1
499	0.101	0.057	1.910	0.110	1.913	1.263	0.152	0.190	-0.294	-0.041	2.762	2.992	2087.2	24173.5	996	68	35	2	1
500	0.101	0.038	1.937	0.088	1.939	1.285	0.158	0.177	-0.520	-0.111	3.021	2.982	1602.9	22314.7	997	47	24	2	1
501	0.101	0.019	1.898	0.092	1.900	1.252	0.148	0.134	-0.255	0.141	2.737	3.108	572.7	14651.4	994	202	106	2	1
502	0.101	0.0	1.898	0.081	1.900	1.251	0.157	0.137	-0.265	-0.023	2.654	2.881	1080.5	15847.9	997	37	19	2	1
503	0.101	-0.019	1.920	-0.062	1.921	1.269	0.155	0.136	-0.309	0.133	2.721	3.156	-1213.6	15595.7	997	12	6	2	1
504	0.101	-0.038	1.917	-0.043	1.918	1.267	0.160	0.137	-0.396	-0.011	2.910	2.903	-673.6	16072.9	994	9	5	2	1
505	0.101	-0.057	1.915	-0.015	1.915	1.265	0.157	0.122	-0.283	0.153	2.677	3.049	-564.0	13896.6	992	8	4	2	1
506	0.101	-0.076	1.956	0.034	1.957	1.301	0.160	0.169	-0.404	0.069	3.002	2.993	167.0	21034.4	990	14	7	2	1
507	0.101	-0.095	1.951	0.062	1.952	1.297	0.166	0.172	-0.548	0.064	2.845	2.958	456.7	22077.0	987	6	3	2	1
508	0.101	-0.114	1.937	0.085	1.939	1.286	0.185	0.172	-0.187	0.101	2.817	2.997	1197.5	23704.4	997	4	2	2	1
509	0.101	-0.133	1.967	0.178	1.975	1.317	0.182	0.174	-0.087	-0.018	2.844	2.790	1550.3	23809.4	990	1	0	2	1
510	0.101	-0.152	1.947	0.260	1.964	1.308	0.185	0.183	0.091	-0.132	2.530	2.962	-196.4	25733.8	170	2	1	2	1

NOTE: NEGATIVE R/D INDICATES MEASUREMENT ON OPPOSITE SIDE OF JET CENTERLINE (I.E. -Z/D)

V_∞ = 713.0 ft/sec T_t = 640.3 °R D = 0.986 in.

SEQ	x/D	r/D	V_x/V_∞	V_r/V_∞	$\lvert V\rvert/V_\infty$	M	S_x/V_∞	S_r/V_∞	SK_x	SK_r	KU_x	KU_r	RE_{xr}	TKE	N	PPS	PPL	SE	CC
1138	0.203	0.894	0.974	-0.043	0.975	0.579	0.028	0.120	0.096	0.040	2.875	3.249	26.2	7534.0	994	30	30	1	1
1139	0.203	0.856	0.971	-0.049	0.972	0.577	0.022	0.121	-0.182	-0.093	3.721	3.370	63.1	7534.8	989	30	30	1	1
1140	0.203	0.818	0.968	-0.045	0.969	0.575	0.024	0.122	-0.313	0.072	3.644	3.116	-48.7	7705.8	998	27	27	1	1
1141	0.203	0.780	0.966	-0.039	0.967	0.574	0.024	0.125	-0.255	0.022	3.711	2.889	49.8	8103.1	996	21	21	1	1
1142	0.203	0.742	0.955	-0.054	0.956	0.567	0.025	0.128	-0.167	-0.015	3.825	3.250	51.5	8506.7	992	19	19	1	1
1143	0.203	0.704	0.959	-0.044	0.960	0.569	0.024	0.124	-0.127	-0.055	3.389	3.200	-83.1	7933.0	993	19	19	1	1
1144	0.203	0.666	0.950	-0.042	0.951	0.564	0.020	0.129	-0.095	0.072	3.365	3.014	46.2	8584.3	984	15	16	1	1
1145	0.203	0.628	0.944	-0.041	0.945	0.560	0.026	0.132	-0.202	-0.115	3.538	3.221	9.8	9086.4	991	10	11	1	1
1146	0.203	0.590	0.933	-0.057	0.934	0.553	0.028	0.129	0.100	-0.087	3.599	2.803	55.7	8628.0	982	7	7	1	1
1147	0.203	0.551	0.931	-0.069	0.934	0.553	0.043	0.143	-0.322	0.025	3.272	2.966	2.4	10916.8	998	4	4	1	1
1148	0.203	0.513	0.889	-0.054	0.891	0.526	0.042	0.150	-0.509	-0.071	3.178	3.036	-151.2	11859.8	989	2	2	1	1
1149	0.203	0.475	0.855	-0.045	0.857	0.505	0.052	0.152	-0.417	-0.057	2.810	3.512	-43.5	12450.1	511	1	1	1	1
1150	0.203	0.437	0.796	-0.045	0.797	0.468	0.070	0.153	-0.251	-0.121	2.739	3.260	-339.2	13079.0	537	0	1	1	1
1151	0.203	0.399	0.749	-0.064	0.752	0.440	0.076	0.133	-0.119	-0.078	3.009	3.114	267.6	10481.8	513	1	1	1	1
1152	0.203	0.361	0.680	-0.061	0.682	0.398	0.080	0.134	-0.186	-0.074	2.962	3.055	238.8	10741.4	491	1	1	1	1

V_∞ = 713.0 ft/sec T_t = 640.3 °R D = 0.986 in.

SEQ	x/D	r/D	V_x/V_∞	V_r/V_∞	$\lvert V\rvert/V_\infty$	M	S_x/V_∞	S_r/V_∞	SK_x	SK_r	KU_x	KU_r	RE_{xr}	TKE	N	PPS	PPL	SE	CC
1180	0.304	0.894	1.001	-0.041	1.002	0.596	0.010	0.065	-0.511	0.560	8.411	3.761	-11.2	2141.7	991	109	108	1	1
1181	0.304	0.856	1.003	-0.048	1.004	0.597	0.011	0.059	-1.410	0.606	13.558	3.732	7.7	1796.5	999	108	107	1	1
1182	0.304	0.818	1.004	-0.048	1.005	0.598	0.008	0.063	-0.452	0.439	11.637	3.365	-2.1	2052.3	990	59	58	1	1
1183	0.304	0.780	1.000	-0.047	1.001	0.595	0.009	0.063	-0.449	0.632	8.253	3.837	-17.5	2026.2	991	32	32	1	1
1184	0.304	0.742	1.000	-0.048	1.001	0.595	0.014	0.079	0.124	0.297	6.827	3.653	-8.5	3240.2	995	22	22	1	1
1185	0.304	0.704	0.994	-0.055	0.996	0.592	0.014	0.095	-0.090	0.131	5.944	3.279	-34.7	4597.4	997	94	94	1	1
1186	0.304	0.666	0.989	-0.062	0.991	0.589	0.016	0.094	-0.198	0.089	5.058	3.410	-9.8	4540.7	993	47	47	1	1
1187	0.304	0.628	0.980	-0.070	0.982	0.583	0.018	0.104	-0.080	-0.099	4.680	3.410	-26.6	5574.7	997	11	11	1	1
1188	0.304	0.590	0.964	-0.050	0.965	0.573	0.019	0.091	-0.388	0.275	4.779	3.286	14.9	4280.6	988	240	248	1	1
1189	0.304	0.551	0.945	-0.050	0.946	0.561	0.026	0.088	-0.735	0.224	4.676	3.263	16.7	4127.0	986	183	193	1	1
1190	0.304	0.513	0.924	-0.053	0.926	0.548	0.035	0.093	-0.662	0.063	3.355	3.304	-142.5	4754.0	991	114	122	1	1
1191	0.304	0.475	0.873	-0.044	0.874	0.516	0.044	0.096	-0.424	0.127	2.895	3.075	76.7	5163.3	994	41	47	1	1
1192	0.304	0.437	0.816	-0.049	0.818	0.481	0.055	0.101	-0.250	-0.016	2.825	3.393	-105.6	5928.8	985	8	10	1	1
1193	0.304	0.399	0.758	-0.042	0.759	0.445	0.057	0.133	-0.026	-0.106	2.966	2.943	-243.7	9764.9	996	30	40	1	1
1194	0.304	0.361	0.679	-0.033	0.680	0.397	0.066	0.141	-0.166	0.036	2.837	2.883	-536.2	11204.9	994	20	30	1	1
1195	0.304	0.323	0.577	-0.018	0.577	0.335	0.082	0.138	-0.265	0.061	2.814	2.896	-662.9	11440.4	998	13	22	1	1
1196	0.304	0.285	0.597	-0.015	0.597	0.347	0.138	0.167	1.829	0.221	7.650	3.181	144.3	18969.9	481	0	1	1	1
1197	0.304	0.266	0.679	0.017	0.680	0.397	0.225	0.194	0.951	-0.206	4.620	3.254	228.9	32029.9	222	0	0	1	0
1198	0.304	0.247	0.689	0.052	0.691	0.403	0.416	0.271	-0.750	0.411	4.155	3.277	2290.8	81208.9	32	0	0	1	0

V_∞ = 713.0 ft/sec T_t = 640.3 °R D = 0.986 in.

SEQ	x/D	r/D	V_x/V_∞	V_r/V_∞	$\lvert V\rvert/V_\infty$	M	S_x/V_∞	S_r/V_∞	SK_x	SK_r	KU_x	KU_r	RE_{xr}	TKE	N	PPS	PPL	SE	CC
1200	0.406	0.894	0.972	-0.038	0.973	0.578	0.012	0.091	-0.115	0.268	5.951	3.423	17.1	4263.5	994	375	375	1	1
1201	0.406	0.856	0.970	-0.046	0.971	0.577	0.011	0.096	-0.306	0.124	5.941	3.469	23.2	4669.7	993	370	370	1	1
1202	0.406	0.818	0.970	-0.047	0.971	0.577	0.011	0.088	0.222	0.191	6.402	3.415	23.9	3961.0	993	389	390	1	1
1203	0.406	0.780	0.967	-0.042	0.967	0.574	0.012	0.090	0.116	0.311	6.114	3.297	7.6	4111.1	995	402	404	1	1
1204	0.406	0.742	0.964	-0.046	0.966	0.573	0.013	0.085	-0.379	0.164	5.315	3.276	-14.6	3716.6	991	353	356	1	1
1205	0.406	0.704	0.961	-0.039	0.962	0.571	0.014	0.087	-0.295	0.318	5.628	3.250	-14.0	3866.4	997	151	153	1	1
1206	0.406	0.666	0.957	-0.048	0.958	0.568	0.014	0.086	-0.198	0.192	4.967	3.473	-11.4	3788.2	994	77	79	1	1
1207	0.406	0.628	0.949	-0.047	0.950	0.563	0.017	0.112	0.321	0.016	5.353	3.103	26.1	6451.2	993	39	40	1	1
1208	0.406	0.590	0.937	-0.040	0.938	0.555	0.018	0.096	-0.083	0.197	3.998	2.824	-67.3	4803.4	984	252	262	1	1
1209	0.406	0.551	0.920	-0.032	0.920	0.544	0.024	0.100	-0.691	0.179	4.273	3.119	-1.5	5230.7	984	141	149	1	1
1210	0.406	0.513	0.888	-0.040	0.888	0.525	0.036	0.098	-0.448	0.103	3.039	3.051	-37.3	5225.4	989	105	116	1	1
1211	0.406	0.475	0.849	-0.044	0.850	0.500	0.043	0.095	-0.306	0.152	2.616	3.415	-44.7	5109.1	993	61	70	1	1
1212	0.406	0.437	0.797	-0.034	0.798	0.469	0.051	0.101	-0.408	0.149	3.044	2.956	-555.7	5816.7	996	26	32	1	1
1213	0.406	0.399	0.740	-0.025	0.741	0.434	0.056	0.106	-0.254	0.145	2.792	3.216	-290.2	6515.0	993	18	24	1	1
1214	0.406	0.361	0.669	-0.015	0.669	0.390	0.064	0.105	-0.258	-0.007	2.780	3.050	-157.6	6696.7	993	7	11	1	1
1215	0.406	0.323	0.686	0.036	0.687	0.401	0.128	0.175	1.367	0.243	4.975	3.187	2978.1	19680.8	944	1	2	1	0
1216	0.406	0.304	0.859	0.073	0.862	0.508	0.229	0.231	0.973	0.014	3.917	3.125	12740.2	40511.4	125	0	0	1	0
1217	0.406	0.285	0.866	0.096	0.872	0.514	0.302	0.275	-0.260	0.762	5.294	3.979	15356.8	61718.4	103	0	0	1	0

V_∞ = 713.0 ft/sec T_t = 640.3 °R D = 0.986 in.

SEQ	x/D	r/D	V_x/V_∞	V_r/V_∞	$\lvert V\rvert/V_\infty$	M	S_x/V_∞	S_r/V_∞	SK_x	SK_r	KU_x	KU_r	RE_{xr}	TKE	N	PPS	PPL	SE	CC
1033	0.507	0.894	0.989	-0.037	0.990	0.588	0.014	0.096	0.149	0.254	5.132	3.467	-39.7	4767.4	996	71	70	1	1
1034	0.507	0.856	0.987	-0.031	0.987	0.586	0.018	0.098	0.043	0.173	4.294	3.151	59.1	4953.7	994	78	78	1	1
1035	0.507	0.818	0.984	-0.033	0.985	0.585	0.023	0.093	0.523	0.253	4.838	3.265	5.5	4499.3	993	66	66	1	1
1036	0.507	0.780	0.982	-0.029	0.982	0.583	0.027	0.102	-0.235	0.168	4.071	3.133	94.5	5423.6	997	47	47	1	1
1037	0.507	0.742	0.978	-0.044	0.979	0.582	0.020	0.130	0.047	0.060	3.720	2.999	-29.0	8751.5	994	88	89	1	1
1038	0.507	0.704	0.975	-0.035	0.975	0.579	0.017	0.141	0.101	-0.007	4.178	3.118	-79.9	10130.2	994	100	101	1	1
1039	0.507	0.666	0.972	-0.045	0.973	0.578	0.021	0.140	0.220	0.092	6.252	3.069	73.9	10122.2	997	114	115	1	1
1040	0.507	0.628	0.968	-0.035	0.968	0.575	0.020	0.140	0.195	-0.040	3.751	2.896	6.0	10000.7	996	74	75	1	1
1041	0.507	0.590	0.959	-0.035	0.959	0.569	0.021	0.147	-0.107	0.110	4.329	2.945	-1.2	11033.5	987	66	68	1	1
1042	0.507	0.551	0.949	-0.020	0.949	0.562	0.027	0.156	-0.227	0.144	4.369	2.884	-71.7	12599.7	995	39	41	1	1
1043	0.507	0.513	0.924	-0.017	0.924	0.547	0.033	0.158	-0.437	-0.019	3.649	2.941	-101.5	12947.6	994	29	31	1	1
1044	0.507	0.475	0.892	0.001	0.892	0.527	0.042	0.157	-0.273	0.066	2.943	2.974	-91.8	13025.0	996	15	17	1	1
1045	0.507	0.437	0.842	0.010	0.842	0.496	0.052	0.158	-0.204	0.013	2.838	2.902	-111.7	13334.8	993	10	11	1	1
1046	0.507	0.399	0.782	-0.002	0.782	0.459	0.060	0.140	-0.050	0.006	2.835	3.065	-171.4	10812.6	996	22	28	1	1
1047	0.507	0.380	0.755	-0.003	0.755	0.442	0.061	0.140	-0.117	-0.120	2.861	2.914	72.1	10860.1	997	21	28	1	1
1048	0.507	0.361	0.727	0.012	0.728	0.426	0.067	0.143	0.417	-0.082	3.891	3.227	-48.3	11500.0	980	13	18	1	0
1049	0.507	0.342	0.777	0.039	0.778	0.456	0.110	0.164	1.312	0.048	4.899	2.880	183.6	16683.8	573	2	2	1	0
1050	0.507	0.323	0.980	0.113	0.987	0.586	0.255	0.192	0.293	0.831	3.188	4.499	22474.5	35385.6	102	0	0	1	0

V_∞ = 713.0 ft/sec T_t = 640.3 °R D = 0.986 in.

SEQ	x/D	r/D	V_x/V_∞	V_r/V_∞	$\lvert V\rvert/V_\infty$	M	S_x/V_∞	S_r/V_∞	SK_x	SK_r	KU_x	KU_r	RE_{xr}	TKE	N	PPS	PPL	SE	CC
1512	0.507	0.361	0.728	0.019	0.728	0.426	0.095	0.266	1.900	0.890	10.277	5.016	12148.7	38162.6	581	1	1	3	1
1511	0.507	0.342	1.436	0.600	1.556	0.976	0.667	0.388	0.188	-0.556	1.292	2.666	46102.1	189752.5	315	0	0	3	1
1510	0.507	0.323	2.319	0.797	2.452	1.815	0.172	0.207	-0.720	0.237	4.887	3.061	1159.8	29417.0	660	2	1	3	1
1509	0.507	0.304	2.384	0.790	2.511	1.890	0.151	0.186	-0.314	0.132	2.512	3.069	2699.3	23325.3	918	4	1	3	0
1508	0.507	0.285	2.368	0.785	2.494	1.868	0.134	0.186	-0.506	0.120	2.790	3.119	1656.0	22192.4	970	6	2	3	0
1507	0.507	0.266	2.343	0.773	2.467	1.834	0.124	0.174	-0.396	0.146	2.668	2.801	1369.4	19244.5	988	9	3	3	0
1506	0.507	0.247	2.307	0.695	2.409	1.764	0.135	0.159	-0.515	0.061	3.043	2.867	2277.3	17497.5	992	9	3	3	0
1505	0.507	0.228	2.276	0.630	2.362	1.708	0.131	0.163	-0.356	0.131	2.799	3.196	1286.2	17855.5	991	13	5	3	0
1504	0.507	0.209	2.256	0.564	2.325	1.667	0.133	0.149	-0.355	-0.063	2.777	3.012	1808.1	15706.2	991	20	8	3	0

V_∞ = 713.0 ft/sec T_t = 640.3 °R D = 0.986 in.

SEQ	x/D	r/D	V_x/V_∞	V_r/V_∞	$\lvert V\rvert/V_\infty$	M	S_x/V_∞	S_r/V_∞	SK_x	SK_r	KU_x	KU_r	RE_{xr}	TKE	N	PPS	PPL	SE	CC
513	0.507	0.342	2.263	0.728	2.377	1.726	0.131	0.221	-0.773	-0.216	3.844	4.152	1982.3	29285.6	100	0	0	2	0
514	0.507	0.323	2.345	0.764	2.466	1.832	0.162	0.209	-0.145	-0.216	3.160	3.310	5138.7	28979.9	442	1	0	2	0
515	0.507	0.304	2.420	0.775	2.541	1.929	0.169	0.214	-0.361	-0.016	2.877	3.074	4903.0	30522.3	985	2	0	2	1
516	0.507	0.285	2.430	0.793	2.556	1.948	0.156	0.210	-0.327	0.059	2.900	3.010	4095.7	28577.2	987	5	2	2	1
517	0.507	0.266	2.425	0.779	2.547	1.937	0.164	0.221	-0.589	-0.063	3.451	2.880	5276.2	31657.8	987	12	4	2	1
518	0.507	0.247	2.404	0.722	2.510	1.888	0.175	0.224	-0.326	0.254	2.790	3.043	4003.6	33190.7	991	19	7	2	1
519	0.507	0.228	2.377	0.670	2.469	1.837	0.170	0.223	-0.171	0.101	2.996	2.916	2923.2	32576.8	993	31	12	2	1
520	0.507	0.209	2.377	0.606	2.453	1.816	0.173	0.197	-0.179	0.043	2.896	2.851	2827.0	27391.6	992	49	20	2	1
521	0.507	0.190	2.361	0.542	2.422	1.779	0.169	0.207	-0.212	-0.048	3.016	3.148	3667.0	29108.8	996	94	38	2	1
522	0.507	0.171	2.355	0.477	2.403	1.756	0.168	0.206	-0.056	-0.062	2.692	2.789	3219.4	28723.3	994	101	41	2	1
523	0.507	0.152	2.350	0.424	2.388	1.738	0.166	0.203	-0.098	-0.044	2.846	2.987	2601.7	28022.4	996	149	62	2	1
524	0.507	0.133	2.344	0.360	2.372	1.720	0.166	0.192	0.033	0.072	2.989	2.913	937.5	25797.8	991	154	64	2	1
525	0.507	0.114	2.330	0.306	2.350	1.695	0.183	0.191	-0.017	-0.094	2.666	3.078	1566.3	27069.6	992	194	82	2	1
526	0.507	0.095	2.341	0.258	2.355	1.701	0.174	0.181	-0.048	0.018	2.736	2.926	572.9	24290.9	995	161	68	2	1
527	0.507	0.076	2.325	0.212	2.335	1.678	0.179	0.176	0.116	0.043	2.728	3.268	1304.3	23783.9	996	143	61	2	1
528	0.507	0.057	2.335	0.158	2.341	1.684	0.170	0.159	-0.018	0.046	2.873	3.183	1966.1	20184.4	997	126	53	2	1
529	0.507	0.038	2.362	0.126	2.366	1.712	0.192	0.171	0.108	-0.079	2.640	3.018	1893.3	24214.9	996	84	35	2	1
530	0.507	0.019	2.353	0.055	2.354	1.699	0.182	0.167	0.080	-0.085	2.644	2.909	776.5	22599.6	993	68	28	2	1
531	0.507	0.0	2.369	0.006	2.369	1.717	0.175	0.161	-0.069	0.004	2.820	3.195	753.6	20996.6	993	64	27	2	1
533	0.507	-0.019	2.369	0.030	2.369	1.716	0.184	0.164	-0.049	0.012	2.810	2.948	-457.3	22311.0	990	108	45	2	1
534	0.507	-0.038	2.380	0.070	2.381	1.730	0.182	0.163	0.060	-0.045	2.893	2.737	-561.4	21923.8	991	76	31	2	1
535	0.507	-0.057	2.378	0.149	2.382	1.732	0.185	0.169	0.015	0.089	3.201	3.129	45.1	23226.4	990	72	30	2	1
536	0.507	-0.076	2.323	0.179	2.330	1.672	0.200	0.164	-0.120	-0.012	3.195	2.963	335.6	23781.3	989	64	27	2	1
537	0.507	-0.095	2.361	0.237	2.373	1.721	0.168	0.167	0.119	0.048	3.116	2.873	528.0	21242.6	990	113	47	2	1
538	0.507	-0.114	2.382	0.293	2.400	1.753	0.181	0.172	0.044	-0.061	3.271	2.947	166.8	23307.6	994	74	30	2	1
539	0.507	-0.133	2.353	0.360	2.380	1.729	0.168	0.164	-0.019	0.176	2.925	2.982	1036.2	20866.3	995	63	26	2	1
540	0.507	-0.152	2.369	0.405	2.403	1.756	0.169	0.166	0.123	0.127	2.838	2.858	-757.8	21245.2	990	48	20	2	1

NOTE: NEGATIVE R/D INDICATES MEASUREMENT ON OPPOSITE SIDE OF JET CENTERLINE (I.E. -Z/D)

V_∞ = 713.0 ft/sec T_t = 640.3 °R D = 0.986 in.

SEQ	x/D	r/D	V_x/V_∞	V_r/V_∞	$\|V\|/V_\infty$	M	S_x/V_∞	S_r/V_∞	SK_x	SK_r	KU_x	KU_r	RE_{xr}	TKE	N	PPS	PPL	SE	CC
1218	0.609	0.894	0.971	-0.036	0.972	0.577	0.013	0.096	0.026	0.161	5.134	3.322	-21.0	4756.4	987	409	410	1	1
1219	0.609	0.856	0.970	-0.035	0.970	0.576	0.013	0.092	-0.151	0.033	5.977	3.321	-15.2	4328.9	991	310	311	1	1
1220	0.609	0.818	0.968	-0.028	0.968	0.575	0.013	0.097	0.217	0.062	5.143	3.350	-40.3	4807.1	990	264	266	1	1
1221	0.609	0.780	0.968	-0.032	0.969	0.575	0.014	0.090	0.259	0.242	5.943	3.408	20.7	4165.2	993	236	237	1	1
1222	0.609	0.742	0.965	-0.034	0.965	0.573	0.012	0.094	0.024	0.168	5.363	3.229	4.4	4522.1	991	157	158	1	1
1223	0.609	0.704	0.956	-0.032	0.956	0.567	0.015	0.092	0.553	0.222	5.017	3.400	-28.7	4355.0	991	100	101	1	1
1224	0.609	0.666	0.956	-0.031	0.956	0.567	0.014	0.090	0.154	0.005	5.718	3.183	-72.2	4174.9	993	59	60	1	1
1225	0.609	0.628	0.953	-0.023	0.953	0.565	0.021	0.106	1.565	0.111	21.817	3.181	-92.7	5845.6	998	24	24	1	1
1226	0.609	0.590	0.952	-0.022	0.952	0.564	0.017	0.096	-0.097	0.232	4.697	3.054	-55.9	4776.0	985	191	196	1	1
1227	0.609	0.551	0.943	-0.025	0.943	0.559	0.025	0.102	-0.493	0.160	4.026	3.172	-11.5	5418.0	986	114	118	1	1
1228	0.609	0.513	0.920	-0.012	0.920	0.544	0.032	0.103	-0.607	0.067	3.654	3.117	59.9	5605.8	990	72	76	1	1
1229	0.609	0.475	0.878	-0.011	0.879	0.518	0.041	0.096	-0.322	0.255	2.959	2.978	-131.4	5143.8	992	31	35	1	1
1230	0.609	0.437	0.838	-0.003	0.839	0.493	0.047	0.106	-0.223	-0.142	2.855	3.122	-97.8	6272.7	997	17	20	1	1
1231	0.609	0.399	0.789	-0.010	0.789	0.463	0.052	0.108	-0.024	0.164	3.042	2.971	-164.5	6620.0	982	9	11	1	0
1232	0.609	0.380	0.778	-0.017	0.779	0.457	0.062	0.113	0.538	0.056	4.610	3.013	-116.4	7473.3	964	3	4	1	0
1233	0.609	0.361	0.821	-0.007	0.821	0.482	0.107	0.133	1.059	0.028	4.297	3.043	626.5	11845.9	493	1	1	1	0
1234	0.609	0.342	0.983	0.039	0.984	0.585	0.265	0.218	0.791	0.136	4.167	3.467	2997.4	42020.0	113	0	0	1	0
1235	0.609	0.323	1.264	0.006	1.264	0.768	0.396	0.180	1.102	-0.084	3.797	2.508	39546.8	56174.8	35	0	0	1	0

V_∞ = 713.0 ft/sec T_t = 640.3 °R D = 0.986 in.

SEQ	x/D	r/D	V_x/V_∞	V_r/V_∞	$\lvert V\rvert/V_\infty$	M	S_x/V_∞	S_r/V_∞	SK_x	SK_r	KU_x	KU_r	RB_{xr}	TKE	N	PPS	PPL	SE	CC
1238	0.710	0.894	0.971	-0.031	0.971	0.576	0.010	0.106	0.325	0.248	7.044	3.515	-23.1	5783.3	989	227	228	1	1
1239	0.710	0.856	0.969	-0.037	0.970	0.576	0.010	0.103	0.626	0.033	7.310	3.631	-26.9	5423.9	986	302	304	1	1
1240	0.710	0.818	0.969	-0.036	0.969	0.575	0.009	0.102	0.260	0.181	7.232	3.487	-30.9	5265.7	986	239	240	1	1
1241	0.710	0.780	0.965	-0.037	0.966	0.573	0.009	0.107	0.130	0.112	7.856	3.519	-5.1	5843.2	989	135	137	1	1
1242	0.710	0.742	0.963	-0.035	0.964	0.572	0.010	0.108	0.189	0.216	7.181	3.529	-70.7	5963.1	988	107	109	1	1
1243	0.710	0.704	0.962	-0.033	0.963	0.571	0.010	0.105	-0.200	0.179	6.733	3.546	-71.8	5647.0	988	55	55	1	1
1244	0.710	0.666	0.959	-0.035	0.960	0.569	0.010	0.108	0.194	-0.078	6.782	3.414	-27.6	6003.7	993	22	23	1	1
1245	0.710	0.628	0.954	-0.028	0.954	0.566	0.017	0.110	-2.194	-0.047	19.794	3.160	-98.8	6264.8	999	8	8	1	1
1246	0.710	0.590	0.959	-0.027	0.959	0.569	0.016	0.112	-0.440	-0.043	6.577	3.162	-76.2	6446.7	984	2	2	1	1
1247	0.710	0.551	0.947	-0.018	0.947	0.561	0.023	0.133	-0.403	0.013	4.055	2.979	-111.3	9088.0	986	105	108	1	1
1248	0.710	0.513	0.930	-0.021	0.930	0.551	0.032	0.137	-0.395	-0.075	3.565	3.037	-35.6	9857.6	990	60	62	1	1
1249	0.710	0.475	0.900	-0.017	0.900	0.531	0.038	0.139	-0.256	0.008	2.988	2.968	-44.0	10214.4	990	26	28	1	1
1250	0.710	0.437	0.859	-0.009	0.859	0.506	0.047	0.143	-0.233	-0.049	2.739	2.977	-167.5	11008.1	994	9	11	1	1
1251	0.710	0.399	0.823	0.001	0.823	0.484	0.054	0.153	0.276	0.050	3.632	3.024	122.6	12644.8	972	3	4	1	0
1252	0.710	0.380	0.865	-0.000	0.865	0.510	0.118	0.165	2.059	0.008	8.324	3.225	-602.8	17395.0	490	1	1	1	0
1253	0.710	0.361	0.986	-0.004	0.986	0.586	0.206	0.195	0.911	0.338	3.381	3.289	2348.6	30176.9	160	0	0	1	0
1254	0.710	0.342	1.460	0.084	1.463	0.907	0.525	0.372	0.574	0.263	2.399	2.325	64109.6	140458.8	28	0	0	1	0

V_∞ = 713.0 ft/sec T_t = 640.3 °R D = 0.986 in.

SEQ	x/D	r/D	V_x/V_∞	V_r/V_∞	$\lvert V\rvert/V_\infty$	M	S_x/V_∞	S_r/V_∞	SK_x	SK_r	KU_x	KU_r	RE_{xr}	TKE	N	PPS	PPL	SE	CC
1255	0.811	0.894	0.970	-0.035	0.971	0.576	0.016	0.098	0.492	0.067	4.031	3.811	-6.7	4920.9	991	200	200	1	1
1256	0.811	0.856	0.969	-0.039	0.970	0.576	0.013	0.094	0.298	0.172	4.907	3.814	-4.0	4557.1	990	201	202	1	1
1257	0.811	0.818	0.970	-0.025	0.970	0.576	0.014	0.098	0.004	0.264	5.446	3.429	-1.8	4973.2	990	145	146	1	1
1258	0.811	0.780	0.972	-0.037	0.973	0.578	0.015	0.095	0.304	0.169	4.221	3.666	-13.8	4604.9	988	126	125	1	1
1259	0.811	0.742	0.966	-0.032	0.967	0.574	0.013	0.090	0.299	0.196	5.497	3.579	-23.9	4117.4	989	93	93	1	1
1260	0.811	0.704	0.964	-0.030	0.964	0.572	0.013	0.093	0.518	0.148	5.616	3.259	-32.8	4393.6	992	50	51	1	1
1261	0.811	0.666	0.964	-0.028	0.965	0.572	0.013	0.105	0.152	-0.007	5.645	3.522	36.0	5678.8	985	21	21	1	1
1262	0.811	0.628	0.965	-0.036	0.966	0.573	0.019	0.140	0.448	0.105	4.267	2.755	85.0	10023.5	988	191	193	1	1
1263	0.811	0.590	0.960	-0.033	0.961	0.570	0.020	0.137	-0.627	-0.060	11.767	3.118	-226.8	9614.2	998	132	133	1	1
1264	0.811	0.551	0.961	-0.025	0.961	0.570	0.023	0.129	-0.499	-0.080	4.408	2.936	59.0	8537.9	981	78	79	1	1
1265	0.811	0.513	0.939	-0.013	0.939	0.556	0.032	0.139	-0.399	0.073	4.267	3.112	-54.1	10131.6	984	42	44	1	1
1266	0.811	0.475	0.919	-0.019	0.919	0.543	0.038	0.131	-0.202	-0.022	3.191	3.178	48.0	9142.3	991	19	20	1	0
1267	0.811	0.437	0.887	-0.019	0.887	0.524	0.048	0.142	-0.130	-0.060	2.941	3.024	90.7	10842.9	991	11	13	1	0
1268	0.811	0.399	0.913	-0.006	0.913	0.540	0.099	0.138	1.365	0.079	5.563	3.108	287.7	12181.1	961	2	2	1	0
1269	0.811	0.380	0.952	0.008	0.952	0.565	0.145	0.187	1.139	0.042	4.333	2.664	133.7	23019.0	489	1	1	1	0
1270	0.811	0.361	1.170	0.033	1.170	0.705	0.252	0.197	1.277	0.386	4.239	3.291	5524.5	35821.0	98	0	0	1	0

V_∞ = 713.0 ft/sec T_t = 640.3 °R D = 0.986 in.

SEQ	x/D	r/D	V_x/V_∞	V_r/V_∞	$\|V\|/V_\infty$	M	S_x/V_∞	S_r/V_∞	SK_x	SK_r	KU_x	KU_r	RE_{xr}	TKE	N	PPS	PPL	SE	CC
1271	0.913	0.894	0.968	-0.036	0.968	0.575	0.023	0.131	0.502	0.060	6.138	2.921	-62.6	8856.8	998	328	330	1	1
1272	0.913	0.856	0.974	-0.022	0.974	0.578	0.026	0.129	0.378	0.012	3.595	2.951	-158.3	8672.5	998	406	406	1	1
1273	0.913	0.818	0.970	-0.026	0.970	0.576	0.019	0.136	0.281	-0.011	3.798	3.164	-86.6	9553.0	991	267	268	1	1
1274	0.913	0.780	0.968	-0.027	0.968	0.574	0.019	0.128	0.128	0.003	6.871	2.967	78.2	8359.3	999	319	321	1	1
1275	0.913	0.742	0.968	-0.026	0.968	0.574	0.018	0.117	0.221	-0.074	3.934	3.230	21.8	6979.1	990	238	239	1	1
1276	0.913	0.704	0.963	-0.036	0.963	0.572	0.016	0.115	0.021	0.207	4.121	3.127	-9.4	6758.7	993	637	643	1	1
1277	0.913	0.666	0.960	-0.024	0.961	0.570	0.016	0.128	0.187	0.152	4.610	3.069	17.6	8379.0	992	285	289	1	1
1278	0.913	0.628	0.962	-0.016	0.962	0.570	0.018	0.124	0.167	0.025	4.312	2.801	12.8	7916.1	992	376	381	1	1
1279	0.913	0.590	0.963	-0.021	0.963	0.571	0.018	0.122	-0.084	0.052	5.150	3.170	-39.1	7622.9	993	246	249	1	1
1280	0.913	0.551	0.958	-0.009	0.958	0.568	0.025	0.124	-0.299	0.104	4.555	2.959	30.4	7970.7	989	169	172	1	1
1281	0.913	0.513	0.947	-0.008	0.947	0.561	0.032	0.131	-0.374	-0.109	3.901	2.858	-18.6	8969.6	990	91	93	1	1
1282	0.913	0.475	0.926	-0.014	0.926	0.548	0.039	0.130	-0.234	0.037	4.087	3.022	11.9	9030.9	997	35	37	1	0
1283	0.913	0.437	0.902	-0.008	0.902	0.533	0.047	0.125	-0.080	0.046	2.987	2.976	67.5	8440.1	988	27	30	1	0
1284	0.913	0.399	0.916	-0.000	0.916	0.542	0.078	0.142	1.499	0.072	6.517	3.069	1045.8	11832.9	973	7	8	1	0
1285	0.913	0.380	0.969	-0.004	0.969	0.575	0.136	0.158	1.499	0.071	5.445	3.146	1837.9	17452.8	972	3	3	1	0
1286	0.913	0.361	1.100	-0.014	1.100	0.659	0.237	0.188	1.365	0.401	4.891	3.490	10049.6	32336.9	481	0	0	1	0
1287	0.913	0.342	1.315	0.031	1.316	0.803	0.419	0.276	1.386	0.539	4.492	2.972	26050.0	83422.4	283	0	0	1	0

V_∞ = 713.0 ft/sec T_t = 640.3 °R D = 0.986 in.

SEQ	x/D	r/D	V_x/V_∞	V_r/V_∞	$\lvert V\rvert/V_\infty$	M	S_x/V_∞	S_r/V_∞	SK_x	SK_r	KU_x	KU_r	RE_{xr}	TKE	N	PPS	PPL	SE	CC
1053	1.014	0.818	0.970	-0.032	0.971	0.576	0.016	0.130	-0.267	0.136	4.638	3.235	26.4	8603.2	997	104	104	1	1
1054	1.014	0.780	0.978	-0.028	0.978	0.581	0.033	0.134	0.991	0.121	4.790	2.974	-52.7	9374.2	991	73	73	1	1
1055	1.014	0.742	0.973	-0.032	0.974	0.578	0.013	0.136	0.245	0.103	5.453	3.257	-5.2	9428.2	994	81	80	1	1
1056	1.014	0.704	0.971	-0.035	0.972	0.577	0.020	0.141	0.072	-0.017	3.882	2.978	73.3	10168.6	995	80	80	1	1
1057	1.014	0.666	0.972	-0.024	0.972	0.577	0.018	0.141	-0.080	0.071	4.279	2.926	-28.8	10216.0	989	84	84	1	1
1058	1.014	0.628	0.972	-0.023	0.973	0.577	0.026	0.147	0.162	-0.079	3.528	2.831	-34.6	11169.1	993	73	73	1	1
1059	1.014	0.590	0.967	-0.020	0.968	0.574	0.021	0.147	0.063	0.005	4.008	2.836	63.0	11131.3	991	52	52	1	1
1060	1.014	0.551	0.972	-0.016	0.972	0.577	0.032	0.153	-0.058	-0.029	3.655	2.918	-141.2	12086.5	990	35	35	1	1
1061	1.014	0.513	0.956	-0.009	0.956	0.567	0.030	0.152	-0.266	0.027	4.337	2.944	-164.0	11922.4	990	23	24	1	0
1062	1.014	0.475	0.937	-0.014	0.937	0.555	0.039	0.155	-0.222	-0.051	3.398	2.881	-208.8	12582.6	990	12	12	1	0
1063	1.014	0.437	0.910	-0.006	0.910	0.538	0.053	0.155	-0.120	0.009	5.997	2.796	294.2	12933.0	993	5	6	1	0
1064	1.014	0.418	0.914	0.005	0.914	0.541	0.065	0.157	1.347	0.046	7.948	2.902	465.6	13626.9	982	6	6	1	0
1065	1.014	0.399	0.929	-0.004	0.929	0.550	0.097	0.168	2.427	-0.030	11.756	3.222	896.3	16804.5	977	4	4	1	0
1066	1.014	0.380	1.066	-0.001	1.066	0.637	0.267	0.191	1.926	0.162	7.520	3.358	8055.2	36732.6	942	1	1	1	0
1069	1.014	0.361	1.272	-0.024	1.273	0.774	0.456	0.210	1.463	0.163	4.288	3.027	16569.7	75349.1	493	1	1	1	0
1070	1.014	0.342	1.704	-0.023	1.705	1.090	0.644	0.300	0.141	-0.093	1.614	3.271	28082.9	151014.8	103	0	0	1	0

V_∞ = 713.0 ft/sec T_t = 640.3 °R   D = 0.986 in.

SEQ	x/D	r/D	V_x/V_∞	V_r/V_∞	$\lvert V\rvert/V_\infty$	M	S_x/V_∞	S_r/V_∞	SK_x	SK_r	KU_x	KU_r	RE_{xr}	TKE	N	PPS	PPL	SE	CC
1440	1.014	0.551	0.965	-0.037	0.966	0.573	0.023	0.113	-0.279	-0.048	3.262	3.459	94.0	6634.8	822	7	8	3	0
1439	1.014	0.532	0.966	-0.041	0.967	0.574	0.027	0.106	-0.355	0.032	3.691	3.399	844.0	5875.7	841	6	6	3	1
1438	1.014	0.513	0.957	-0.038	0.958	0.568	0.034	0.135	0.819	0.569	16.713	4.720	3276.1	9620.1	786	4	5	3	1
1437	1.014	0.494	1.000	0.018	1.000	0.595	0.172	0.199	3.192	1.034	12.090	4.040	11772.5	27629.4	851	5	5	3	1
1436	1.014	0.475	1.144	0.159	1.155	0.695	0.344	0.271	1.220	0.348	2.826	2.076	25308.4	67608.0	916	5	4	3	1
1435	1.014	0.456	1.275	0.239	1.298	0.791	0.419	0.271	0.503	0.006	1.513	2.122	19426.9	82145.8	933	7	6	3	1
1434	1.014	0.437	1.563	0.312	1.594	1.004	0.455	0.239	-0.473	-0.278	1.711	2.667	21966.0	81640.8	994	8	5	3	1
1433	1.014	0.418	1.800	0.353	1.834	1.195	0.405	0.215	-1.217	-0.260	3.500	2.921	13642.8	65208.3	993	11	6	3	1
1432	1.014	0.399	2.083	0.366	2.115	1.448	0.227	0.208	-0.636	-0.118	3.548	2.864	7784.1	35166.6	964	17	8	3	1
1431	1.014	0.380	2.231	0.386	2.264	1.600	0.201	0.201	-0.763	-0.148	4.020	2.874	5625.1	30798.1	977	31	13	3	1
1430	1.014	0.361	2.347	0.378	2.377	1.725	0.157	0.204	-0.386	-0.098	2.821	2.835	4707.4	27335.5	983	36	15	3	1
1429	1.014	0.342	2.434	0.386	2.464	1.830	0.144	0.193	-0.285	-0.086	2.681	2.972	1415.4	24183.7	987	45	18	3	1
1428	1.014	0.304	2.530	0.353	2.555	1.947	0.126	0.175	-0.068	-0.096	2.256	2.790	-401.2	19605.9	986	12	4	3	0
1427	1.014	0.266	2.568	0.314	2.587	1.991	0.146	0.175	-0.369	0.100	2.741	2.908	-199.6	21037.8	991	10	4	3	0
1426	1.014	0.228	2.561	0.275	2.576	1.975	0.149	0.159	-0.264	0.199	2.618	3.057	-2.4	18553.5	986	20	7	3	0

V_∞ = 713.0 ft/sec T_t = 640.3 °R D = 0.986 in.

SEQ	x/D	r/D	V_x/V_∞	V_r/V_∞	$\lvert V\rvert/V_\infty$	M	S_x/V_∞	S_r/V_∞	SK_x	SK_r	KU_x	KU_r	RE_{xr}	TKE	N	PPS	PPL	SE	CC
571	1.014	0.418	1.795	0.318	1.823	1.186	0.471	0.299	-1.026	0.139	2.603	2.415	27309.5	101930.9	127	0	0	2	0
570	1.014	0.399	2.117	0.386	2.152	1.485	0.256	0.236	-1.128	0.007	4.073	3.081	11917.3	44936.1	490	2	0	2	0
569	1.014	0.380	2.319	0.429	2.358	1.704	0.165	0.223	-0.587	0.015	3.709	2.769	5139.7	32155.1	975	4	1	2	0
568	1.014	0.361	2.393	0.423	2.430	1.788	0.174	0.195	-0.604	-0.194	4.112	2.942	3212.0	26992.0	981	7	2	2	0
567	1.014	0.342	2.457	0.419	2.492	1.865	0.154	0.184	-0.425	-0.016	3.890	2.825	1482.4	23245.5	977	10	4	2	0
566	1.014	0.323	2.522	0.404	2.554	1.946	0.162	0.188	0.041	-0.004	2.974	2.869	1590.6	24609.5	986	12	4	2	1
565	1.014	0.304	2.531	0.415	2.565	1.960	0.175	0.173	-0.091	0.043	3.369	2.877	241.2	23060.7	993	14	5	2	1
564	1.014	0.285	2.545	0.377	2.572	1.971	0.181	0.189	0.095	0.070	2.973	2.725	1861.5	26548.4	987	30	11	2	1
563	1.014	0.266	2.591	0.363	2.616	2.031	0.177	0.189	0.064	0.062	2.654	2.740	860.5	26180.7	996	48	18	2	1
562	1.014	0.247	2.582	0.345	2.605	2.015	0.188	0.190	0.239	0.170	2.897	2.939	824.0	27327.8	995	74	28	2	1
561	1.014	0.228	2.566	0.336	2.588	1.991	0.182	0.185	0.112	-0.023	2.939	2.923	-137.9	25776.1	994	125	47	2	1
560	1.014	0.209	2.563	0.323	2.583	1.985	0.191	0.183	0.228	0.120	2.711	2.829	1191.0	26222.5	992	62	23	2	1
559	1.014	0.190	2.540	0.298	2.557	1.950	0.214	0.188	-0.395	0.044	3.607	3.180	-1408.2	29724.9	988	74	28	2	1
558	1.014	0.171	2.492	0.294	2.509	1.887	0.190	0.197	0.084	0.108	2.881	3.041	1368.1	29023.5	992	91	36	2	1
557	1.014	0.152	2.421	0.274	2.436	1.796	0.175	0.180	0.175	0.139	2.589	2.981	-129.0	24328.4	992	95	38	2	1
556	1.014	0.133	2.384	0.264	2.398	1.751	0.156	0.180	0.148	0.089	2.957	2.970	2074.5	22773.7	990	87	36	2	1
555	1.014	0.114	2.309	0.217	2.319	1.660	0.130	0.177	-0.341	0.119	2.931	3.057	393.6	20246.6	987	160	68	2	1
554	1.014	0.095	2.295	0.183	2.303	1.642	0.111	0.171	-0.140	0.043	3.191	2.980	-245.5	17950.5	991	63	27	2	1
553	1.014	0.076	2.280	0.158	2.285	1.623	0.112	0.172	-0.609	-0.048	3.845	3.104	-419.9	18167.6	990	47	20	2	1
552	1.014	0.057	2.263	0.113	2.266	1.602	0.106	0.167	-0.349	-0.084	3.045	2.982	239.9	17133.1	986	41	18	2	1
551	1.014	0.038	2.254	0.079	2.256	1.591	0.108	0.182	-0.603	-0.068	3.810	3.101	689.6	19743.5	987	66	28	2	1
550	1.014	0.019	2.246	0.042	2.246	1.581	0.099	0.176	-0.496	-0.039	2.920	3.207	-194.1	18244.9	985	60	26	2	1
549	1.014	0.0	2.184	-0.005	2.184	1.516	0.176	0.160	-0.987	-0.038	4.186	2.819	-1581.8	20923.6	981	52	23	2	1
548	1.014	-0.019	2.252	0.010	2.252	1.587	0.104	0.168	-0.646	0.042	3.569	3.046	963.1	17137.1	980	70	31	2	1
547	1.014	-0.038	2.270	0.053	2.270	1.607	0.103	0.184	-0.446	-0.042	3.393	3.101	527.6	19992.4	982	83	36	2	1
546	1.014	-0.057	2.298	0.079	2.299	1.638	0.109	0.180	-0.284	0.037	2.809	2.699	511.3	19491.9	986	136	58	2	1
545	1.014	-0.076	2.315	0.118	2.318	1.659	0.122	0.181	-0.568	0.101	4.063	2.929	-239.4	20466.8	990	31	13	2	1
544	1.014	-0.095	2.365	0.154	2.370	1.718	0.147	0.183	-0.785	0.015	4.380	2.876	142.7	22527.7	984	27	11	2	1
543	1.014	-0.114	2.394	0.193	2.402	1.755	0.163	0.179	0.225	-0.002	3.445	2.943	-672.1	23077.6	989	49	20	2	1
542	1.014	-0.133	2.428	0.219	2.438	1.798	0.181	0.181	0.159	0.030	2.849	2.877	-75.4	25007.1	982	63	25	2	1
541	1.014	-0.152	2.460	0.243	2.472	1.840	0.200	0.180	0.092	0.096	2.707	2.870	-56.4	26688.5	984	18	7	2	1

NOTE: NEGATIVE R/D INDICATES MEASUREMENT ON OPPOSITE SIDE OF JET CENTERLINE (I.E. -Z/D)

V_∞ = 713.0 ft/sec T_t = 640.3 °R D = 0.986 in.

SEQ	x/D	r/D	V_x/V_∞	V_r/V_∞	$\|V\|/V_\infty$	M	S_x/V_∞	S_r/V_∞	SK_x	SK_r	KU_x	KU_r	RE_{xr}	TKE	N	PPS	PPL	SE	CC
1075	1.521	0.894	0.965	-0.040	0.966	0.573	0.012	0.101	0.266	0.359	5.331	3.630	46.1	5253.2	989	47	47	1	1
1076	1.521	0.856	0.968	-0.034	0.969	0.575	0.015	0.103	0.236	0.066	3.985	3.458	52.5	5493.1	988	52	52	1	1
1077	1.521	0.818	0.956	-0.021	0.957	0.567	0.013	0.097	0.172	0.205	4.760	3.539	-13.8	4777.1	992	41	41	1	1
1078	1.521	0.780	0.965	-0.031	0.965	0.573	0.017	0.122	0.021	0.006	4.284	3.100	80.6	7608.9	992	38	39	1	1
1079	1.521	0.742	0.955	-0.043	0.956	0.567	0.019	0.143	0.065	0.032	3.547	2.763	-68.7	10535.4	994	63	63	1	1
1080	1.521	0.704	0.960	-0.029	0.961	0.570	0.021	0.149	0.250	0.022	3.637	2.858	52.8	11448.0	995	62	62	1	1
1081	1.521	0.666	0.955	-0.020	0.956	0.567	0.020	0.144	0.189	0.028	3.919	3.104	-8.6	10688.1	992	58	59	1	1
1082	1.521	0.628	0.953	-0.024	0.954	0.565	0.019	0.145	0.054	0.013	3.812	2.999	13.8	10717.4	984	67	68	1	1
1083	1.521	0.590	0.953	-0.031	0.953	0.565	0.023	0.145	-0.156	0.021	3.613	2.958	41.9	10886.8	990	55	56	1	0
1084	1.521	0.551	0.946	-0.015	0.946	0.561	0.028	0.151	0.033	-0.023	3.777	2.739	-86.6	11823.4	988	40	40	1	0
1085	1.521	0.513	0.930	-0.032	0.931	0.551	0.032	0.144	-1.007	0.029	5.683	3.052	167.1	10797.4	997	25	26	1	0
1086	1.521	0.475	0.912	-0.018	0.912	0.539	0.038	0.158	-0.477	0.049	3.634	2.846	-464.9	13095.5	989	19	20	1	0
1087	1.521	0.437	0.889	0.001	0.889	0.525	0.056	0.156	0.960	-0.015	10.118	3.092	992.0	13169.4	976	11	12	1	0
1088	1.521	0.399	0.904	-0.005	0.904	0.534	0.107	0.157	2.135	0.012	9.269	2.927	696.0	15364.1	970	3	4	1	0
1089	1.521	0.361	1.258	0.033	1.259	0.765	0.416	0.197	0.972	0.176	3.030	3.080	7888.1	63772.1	483	1	0	1	0
1090	1.521	0.323	1.824	0.038	1.825	1.187	0.511	0.236	-0.396	-0.093	1.833	3.573	11494.5	94591.1	77	0	0	1	0

V_∞ = 713.0 ft/sec T_t = 640.3 °R   D = 0.986 in.

SEQ	x/D	r/D	V_x/V_∞	V_r/V_∞	$\lvert V\rvert/V_\infty$	M	S_x/V_∞	S_r/V_∞	SK_x	SK_r	KU_x	KU_r	RE_{xr}	TKE	N	PPS	PPL	SE	CC
1491	1.521	0.704	0.957	-0.042	0.958	0.568	0.011	0.109	0.005	-0.066	5.506	2.890	26.4	6121.8	979	25	26	3	0
1492	1.521	0.666	0.953	-0.045	0.954	0.566	0.020	0.105	0.278	-0.127	3.656	3.332	-13.1	5733.1	995	75	77	3	0
1493	1.521	0.628	0.955	-0.042	0.956	0.567	0.014	0.101	-0.039	0.056	4.652	3.155	-17.8	5262.6	986	70	72	3	0
1494	1.521	0.590	0.947	-0.036	0.948	0.562	0.019	0.122	2.162	0.145	31.749	3.597	1387.9	7653.3	983	25	26	3	1
1495	1.521	0.551	0.962	0.023	0.962	0.571	0.084	0.170	4.488	0.579	23.938	3.322	7485.5	16474.5	948	14	14	3	1
1496	1.521	0.513	1.169	0.144	1.178	0.711	0.318	0.193	0.770	0.116	1.976	2.583	12072.7	44745.1	999	19	15	3	1
1497	1.521	0.475	1.329	0.167	1.339	0.820	0.330	0.164	-0.121	0.098	1.669	2.718	7898.4	41299.8	996	28	21	3	1
1498	1.521	0.437	1.523	0.166	1.532	0.958	0.311	0.151	-0.565	0.082	2.696	2.891	4503.0	36171.3	989	57	37	3	1
1499	1.521	0.399	1.774	0.177	1.783	1.153	0.242	0.139	-0.440	0.044	2.888	3.050	4855.5	24705.8	974	38	21	3	0
1500	1.521	0.361	2.009	0.168	2.016	1.355	0.241	0.146	-0.672	0.152	3.244	2.816	5795.2	25555.5	982	38	18	3	0
1501	1.521	0.323	2.196	0.154	2.202	1.535	0.192	0.144	-0.706	-0.011	3.473	3.093	3048.8	19884.0	944	80	35	3	0
1502	1.521	0.285	2.338	0.126	2.341	1.685	0.176	0.146	-0.794	0.060	3.554	3.011	2347.6	18752.3	961	74	31	3	0
1503	1.521	0.247	2.454	0.151	2.458	1.823	0.141	0.140	-0.221	-0.093	2.375	3.106	-46.8	15023.9	994	69	27	3	0

V_∞ = 713.0 ft/sec T_t = 640.3 °R D = 0.986 in.

SEQ	x/D	r/D	V_x/V_∞	V_r/V_∞	$\lvert V\rvert/V_\infty$	M	S_x/V_∞	S_r/V_∞	SK_x	SK_r	KU_x	KU_r	RE_{xr}	TKE	N	PPS	PPL	SE	CC
630	1.521	0.609	1.275	0.190	1.289	0.785	0.270	0.221	0.207	0.190	1.742	2.524	14358.2	43397.0	165	0	0	2	0
629	1.521	0.590	1.316	0.203	1.331	0.814	0.284	0.230	0.081	0.087	1.575	2.634	14515.2	47413.5	293	2	1	2	0
628	1.521	0.570	1.449	0.223	1.466	0.909	0.231	0.201	-0.515	0.092	2.586	2.721	8353.1	34155.1	1000	3	2	2	0
627	1.521	0.551	1.474	0.229	1.492	0.928	0.232	0.198	-0.513	0.160	2.767	2.896	7171.0	33651.0	998	7	4	2	0
626	1.521	0.532	1.489	0.235	1.507	0.939	0.221	0.193	-0.430	0.086	2.833	2.958	5313.0	31463.8	997	9	6	2	0
625	1.521	0.513	1.518	0.219	1.533	0.959	0.209	0.193	-0.316	0.117	2.751	2.977	4562.4	30000.9	999	29	19	2	0
624	1.521	0.494	1.516	0.204	1.530	0.956	0.216	0.187	-0.101	0.193	2.481	2.950	6185.7	29562.1	1000	38	25	2	0
623	1.521	0.475	1.493	0.186	1.504	0.938	0.231	0.187	0.062	0.043	2.527	3.178	5303.3	31356.5	998	83	55	2	0
622	1.521	0.456	1.520	0.162	1.528	0.955	0.251	0.182	-0.091	0.146	2.579	2.970	7015.3	32904.9	1000	163	107	2	0
621	1.521	0.437	1.506	0.147	1.513	0.944	0.273	0.175	-0.025	-0.029	2.275	2.947	6257.4	34515.6	1000	345	228	2	0
620	1.521	0.418	1.563	0.133	1.569	0.985	0.300	0.187	-0.015	0.089	2.374	3.004	8399.5	40601.5	1000	406	259	2	1
619	1.521	0.399	1.613	0.121	1.617	1.022	0.325	0.188	-0.080	0.070	2.265	2.920	9391.7	44918.6	999	455	281	2	1
618	1.521	0.380	1.763	0.134	1.768	1.140	0.363	0.207	-0.121	0.166	2.190	2.993	11393.9	55329.6	999	430	244	2	1
617	1.521	0.361	1.919	0.128	1.923	1.272	0.336	0.201	-0.418	0.020	2.490	3.023	9808.2	49154.3	997	408	212	2	1
616	1.521	0.342	2.087	0.125	2.091	1.425	0.321	0.198	-0.670	0.135	2.875	2.869	10201.9	46067.5	998	532	255	2	1
615	1.521	0.323	2.200	0.126	2.204	1.537	0.280	0.193	-0.707	-0.003	3.007	3.116	7850.4	38887.0	994	489	222	2	1
614	1.521	0.304	2.317	0.136	2.321	1.662	0.250	0.201	-0.722	-0.076	3.096	3.043	6400.1	36480.8	988	411	177	2	1
613	1.521	0.285	2.416	0.123	2.419	1.775	0.217	0.196	-0.716	0.034	3.230	3.022	5987.6	31445.6	987	362	149	2	1
612	1.521	0.266	2.494	0.129	2.497	1.872	0.194	0.193	-0.654	-0.183	3.247	3.195	2451.1	28473.7	989	454	182	2	1
611	1.521	0.247	2.551	0.134	2.555	1.947	0.175	0.198	-0.677	-0.110	3.174	2.953	2641.0	27817.1	979	420	164	2	1
610	1.521	0.228	2.610	0.149	2.614	2.028	0.161	0.191	-0.585	0.019	3.065	3.060	2893.7	25224.8	987	442	169	2	1
609	1.521	0.209	2.629	0.134	2.633	2.055	0.160	0.195	-0.781	-0.003	3.322	3.195	1745.7	25860.2	985	454	172	2	1
608	1.521	0.190	2.570	0.123	2.573	1.971	0.204	0.185	-0.742	-0.176	2.894	2.927	1524.8	27912.1	994	458	178	2	1
607	1.521	0.171	2.420	0.094	2.422	1.779	0.268	0.182	-0.277	-0.063	2.187	2.897	2440.9	35030.8	996	374	154	2	1
606	1.521	0.152	2.256	0.060	2.257	1.593	0.315	0.193	-0.055	-0.070	2.214	3.004	5039.7	44267.6	995	344	152	2	1
605	1.521	0.133	2.052	0.020	2.052	1.389	0.323	0.205	0.129	-0.150	2.918	3.182	3799.2	47896.8	999	293	143	2	1
604	1.521	0.114	1.883	-0.008	1.883	1.237	0.331	0.196	-0.143	-0.064	2.542	2.812	2842.6	47394.6	998	369	196	2	1
603	1.521	0.095	1.741	-0.022	1.741	1.119	0.360	0.204	-0.014	-0.025	2.455	3.002	487.1	54131.6	998	447	256	2	1
602	1.521	0.076	1.614	-0.030	1.615	1.020	0.366	0.219	-0.000	-0.177	2.261	2.986	1020.0	58546.2	999	326	202	2	1
601	1.521	0.057	1.527	-0.013	1.527	0.954	0.390	0.200	0.162	-0.051	2.362	2.780	-556.5	58997.0	1000	321	210	2	1
600	1.521	0.038	1.421	-0.024	1.422	0.878	0.390	0.218	0.330	-0.152	2.394	3.229	1522.5	62735.8	999	350	246	2	1
599	1.521	0.019	1.428	-0.015	1.428	0.882	0.401	0.203	0.245	-0.173	2.306	3.164	-1306.1	61824.8	998	219	153	2	1
598	1.521	0.0	1.408	-0.007	1.408	0.868	0.401	0.192	0.318	-0.020	2.499	2.961	1392.9	59668.1	998	239	170	2	1
597	1.521	-0.019	1.444	0.001	1.444	0.894	0.413	0.194	0.219	0.043	2.260	3.010	-971.7	62484.3	998	200	138	2	1
596	1.521	-0.038	1.447	0.001	1.447	0.896	0.408	0.200	0.232	0.084	2.246	2.891	-27.8	62765.4	995	172	119	2	1
595	1.521	-0.057	1.509	0.008	1.509	0.941	0.422	0.200	0.306	-0.003	2.288	3.021	-1845.7	65688.7	995	198	131	2	1
594	1.521	-0.076	1.593	-0.009	1.593	1.003	0.413	0.201	0.072	0.048	2.144	2.988	-3613.7	63912.6	998	255	160	2	1
593	1.521	-0.095	1.702	-0.019	1.702	1.088	0.400	0.217	0.021	-0.057	2.214	2.948	-5064.8	64626.1	996	152	89	2	1
592	1.521	-0.133	2.077	0.007	2.077	1.412	0.331	0.198	-0.089	-0.192	2.689	2.949	-2703.0	47678.7	994	188	90	2	1
590	1.521	-0.152	2.180	0.017	2.180	1.512	0.245	0.153	0.428	-0.096	3.103	2.929	-926.5	27154.2	985	104	48	2	1

NOTE: NEGATIVE R/D INDICATES MEASUREMENT ON OPPOSITE SIDE OF JET CENTERLINE (I.E. -Z/D)

V_∞ = 713.0 ft/sec T_t = 640.3 °R D = 0.986 in.

SEQ	x/D	r/D	V_x/V_∞	V_r/V_∞	$\lvert V\rvert/V_\infty$	M	S_x/V_∞	S_r/V_∞	SK_x	SK_r	KU_x	KU_r	RE_{xr}	TKE	N	PPS	PPL	SE	CC
1091	2.028	0.894	0.967	-0.044	0.968	0.574	0.031	0.123	-0.178	0.012	3.252	3.270	-11.3	7993.3	986	51	51	1	1
1092	2.028	0.956	0.968	-0.036	0.969	0.575	0.019	0.123	0.097	0.098	4.114	3.261	-19.7	7842.4	989	36	37	1	1
1093	2.028	0.818	0.971	-0.038	0.972	0.577	0.026	0.129	0.159	0.201	3.314	2.987	-2.8	8618.9	990	48	48	1	1
1094	2.028	0.780	0.972	-0.035	0.972	0.577	0.023	0.127	0.046	0.024	3.347	3.282	-24.7	8397.1	992	56	56	1	1
1095	2.028	0.742	0.967	-0.041	0.967	0.574	0.020	0.124	0.112	0.055	5.329	3.087	-69.9	7973.0	994	47	48	1	1
1096	2.028	0.704	0.963	-0.041	0.964	0.572	0.021	0.130	-0.021	0.016	4.189	3.039	-41.5	8706.3	997	34	35	1	1
1097	2.028	0.666	0.961	-0.038	0.962	0.571	0.018	0.126	0.123	0.167	3.917	3.097	-71.8	8110.4	990	34	35	1	1
1098	2.028	0.628	0.965	-0.032	0.965	0.573	0.023	0.134	0.410	0.167	3.711	2.803	55.7	9219.5	988	30	30	1	1
1099	2.028	0.590	0.962	-0.025	0.962	0.571	0.022	0.123	-0.299	0.028	4.427	2.774	17.0	7747.8	992	21	22	1	0
1100	2.028	0.551	0.957	-0.024	0.958	0.568	0.025	0.139	-0.237	0.021	3.740	2.968	-34.7	9982.7	985	18	18	1	0
1101	2.028	0.513	0.949	-0.020	0.949	0.562	0.034	0.134	-0.225	-0.030	6.213	3.041	153.7	9399.0	989	12	12	1	0
1102	2.028	0.475	0.942	-0.005	0.942	0.558	0.043	0.140	0.229	0.208	6.574	3.010	294.3	10467.5	981	7	7	1	0
1103	2.028	0.437	0.954	0.001	0.954	0.566	0.084	0.139	2.564	-0.009	12.734	3.150	1598.2	11544.5	975	3	4	1	0
1104	2.028	0.399	1.044	0.015	1.044	0.623	0.196	0.152	1.681	0.012	5.858	2.777	2563.7	21575.7	496	1	1	1	0
1105	2.028	0.361	1.418	0.025	1.418	0.875	0.418	0.185	0.458	-0.144	2.058	3.064	5703.3	61625.9	517	0	0	1	0
1106	2.028	0.323	1.842	0.060	1.843	1.203	0.381	0.180	-0.342	0.185	2.153	3.195	14032.7	53348.5	95	0	0	1	0

V_∞ = 713.0 ft/sec T_t = 640.3 °R D = 0.986 in.

SEQ	x/D	r/D	V_x/V_∞	V_r/V_∞	$\lvert V\rvert/V_\infty$	M	S_x/V_∞	S_r/V_∞	SK_x	SK_r	KU_x	KU_r	RE_{xr}	TKE	N	PPS	PPL	SE	CC
1462	2.028	0.742	0.962	-0.034	0.962	0.571	0.011	0.099	-0.189	0.151	4.996	2.741	12.1	4995.1	988	124	127	3	0
1461	2.028	0.704	0.959	-0.025	0.960	0.569	0.011	0.101	-0.299	0.071	6.185	3.057	105.1	5196.2	995	158	162	3	0
1460	2.028	0.666	0.959	-0.038	0.959	0.569	0.011	0.109	-0.288	-0.005	6.652	3.366	58.7	6109.7	995	116	119	3	0
1459	2.028	0.628	0.964	-0.016	0.964	0.572	0.034	0.120	4.461	0.274	39.655	3.563	1555.4	7610.2	967	42	43	3	0
1458	2.028	0.590	1.007	0.031	1.008	0.600	0.144	0.149	2.468	0.527	7.711	3.324	5909.3	16591.1	968	42	41	3	1
1457	2.028	0.551	1.106	0.079	1.109	0.665	0.233	0.149	1.127	0.151	2.859	2.846	6888.4	25116.8	996	54	48	3	1
1456	2.028	0.513	1.279	0.121	1.285	0.782	0.255	0.122	0.017	0.215	1.863	3.299	3629.6	24143.0	998	33	25	3	1
1455	2.028	0.475	1.361	0.116	1.366	0.839	0.264	0.118	-0.129	0.107	2.243	3.274	2961.0	24870.5	1000	40	28	3	1
1454	2.028	0.437	1.472	0.102	1.475	0.916	0.289	0.122	-0.195	0.214	2.316	2.968	4758.2	28787.2	997	68	45	3	1
1453	2.028	0.399	1.686	0.091	1.689	1.077	0.289	0.124	-0.399	0.217	2.519	3.093	5493.3	29106.2	999	81	47	3	0
1452	2.028	0.361	1.911	0.081	1.913	1.263	0.268	0.128	-0.609	-0.060	2.857	3.200	4376.4	26662.3	996	81	41	3	0
1451	2.028	0.323	2.149	0.081	2.171	1.503	0.230	0.141	-0.765	-0.068	3.261	3.021	5191.1	23531.1	984	78	35	3	0
1450	2.028	0.285	2.375	0.097	2.377	1.725	0.170	0.139	-0.857	-0.001	3.673	3.097	2092.6	17169.6	986	136	56	3	0
1449	2.028	0.247	2.440	0.073	2.441	1.802	0.160	0.135	-0.475	0.081	2.949	3.047	-97.6	15843.8	988	92	37	3	0

V_∞ = 713.0 ft/sec T_t = 640.3 °R D = 0.986 in.

SEQ	x/D	r/D	V_x/V_∞	V_r/V_∞	$\lvert V\rvert/V_\infty$	M	S_x/V_∞	S_r/V_∞	SK_x	SK_r	KU_x	KU_r	RE_{xr}	TKE	N	PPS	PPL	SE	CC
673	2.028	0.647	1.073	0.031	1.073	0.642	0.192	0.222	1.709	-0.063	4.551	2.859	8896.0	34411.3	989	5	5	2	0
672	2.028	0.628	1.121	0.074	1.124	0.675	0.228	0.221	1.048	0.061	2.643	2.834	9817.8	38034.2	994	5	4	2	0
671	2.028	0.609	1.297	0.131	1.304	0.795	0.243	0.213	-0.058	-0.019	2.073	2.931	8660.8	38074.2	994	5	4	2	0
670	2.028	0.590	1.255	0.103	1.259	0.765	0.244	0.200	0.139	-0.026	1.824	2.854	8049.4	35444.1	997	9	7	2	0
669	2.028	0.570	1.370	0.138	1.377	0.846	0.203	0.173	-0.289	0.112	2.664	2.818	4013.8	25737.7	1000	23	16	2	0
668	2.028	0.551	1.380	0.139	1.387	0.853	0.189	0.172	-0.068	0.041	2.572	2.966	2585.2	24163.6	996	78	55	2	0
667	2.028	0.532	1.362	0.119	1.367	0.839	0.199	0.175	0.113	-0.046	2.548	2.728	3069.7	25684.5	997	51	37	2	0
666	2.028	0.513	1.355	0.123	1.360	0.835	0.203	0.164	0.269	0.137	2.711	2.958	3833.2	24123.6	999	165	120	2	0
665	2.028	0.494	1.335	0.105	1.339	0.820	0.216	0.165	0.331	-0.044	2.434	3.045	2605.8	25689.9	997	92	68	2	0
664	2.028	0.475	1.328	0.090	1.331	0.814	0.230	0.169	0.373	0.086	2.566	3.082	3198.2	28061.8	999	162	120	2	0
663	2.028	0.456	1.348	0.091	1.351	0.828	0.254	0.166	0.455	-0.104	2.551	3.055	4118.7	30326.1	999	205	150	2	0
662	2.028	0.437	1.472	0.111	1.477	0.917	0.269	0.141	0.204	0.119	2.375	3.035	4465.8	28612.9	999	158	106	2	0
661	2.028	0.418	1.564	0.124	1.569	0.986	0.296	0.148	0.007	0.100	2.349	2.830	6145.3	33354.1	1000	178	112	2	1
660	2.028	0.399	1.648	0.109	1.652	1.048	0.303	0.147	-0.165	0.101	2.167	3.002	7132.6	34300.4	1000	261	156	2	1
659	2.028	0.380	1.781	0.114	1.784	1.154	0.306	0.152	-0.365	0.183	2.389	3.022	7201.8	35549.5	998	211	116	2	1
658	2.028	0.361	1.875	0.107	1.878	1.233	0.303	0.147	-0.578	0.102	2.715	2.900	5871.4	34398.8	996	246	129	2	1
657	2.028	0.342	2.006	0.089	2.008	1.347	0.304	0.155	-0.728	0.172	2.913	2.907	7560.4	35682.9	998	256	125	2	1
656	2.028	0.323	2.112	0.091	2.114	1.447	0.272	0.154	-0.712	0.072	2.991	3.044	6800.2	30899.3	990	222	103	2	1
655	2.028	0.304	2.257	0.098	2.259	1.595	0.235	0.155	-0.903	0.125	3.315	2.987	5673.5	26285.8	988	278	121	2	1
654	2.028	0.285	2.368	0.117	2.371	1.719	0.196	0.158	-0.819	-0.135	3.309	2.944	4102.8	22398.3	985	290	120	2	1
653	2.028	0.266	2.426	0.083	2.428	1.785	0.198	0.179	-0.771	-0.016	3.132	2.886	5079.0	26171.9	986	398	161	2	1
652	2.028	0.247	2.467	0.081	2.468	1.835	0.193	0.201	-0.834	-0.006	3.416	3.018	4966.6	29869.5	989	474	189	2	1
651	2.028	0.228	2.524	0.074	2.525	1.908	0.169	0.188	-0.436	-0.159	2.648	2.692	3090.8	25242.1	995	396	154	2	1
650	2.028	0.209	2.549	0.060	2.550	1.941	0.162	0.190	-0.482	-0.077	2.737	2.845	1842.4	25078.7	985	317	122	2	1
649	2.028	0.190	2.540	0.062	2.541	1.928	0.174	0.194	-0.360	-0.050	2.553	3.051	1804.4	26785.2	994	260	101	2	1
648	2.028	0.171	2.501	0.046	2.502	1.878	0.204	0.192	-0.151	-0.044	2.515	2.926	1490.5	29362.8	997	189	74	2	1
647	2.028	0.152	2.448	0.027	2.448	1.811	0.203	0.187	-0.015	-0.044	2.520	2.904	89.0	28228.0	993	190	76	2	1
646	2.028	0.133	2.393	0.034	2.393	1.745	0.204	0.173	-0.081	-0.058	2.961	3.034	-1223.2	25775.0	993	153	63	2	1
645	2.028	0.114	2.314	0.021	2.314	1.654	0.227	0.183	-0.301	-0.037	2.979	2.801	131.0	30186.3	991	158	67	2	1
644	2.028	0.095	2.235	0.011	2.235	1.569	0.245	0.179	-0.361	-0.092	2.722	3.161	-387.4	31555.1	997	180	79	2	1
643	2.028	0.076	2.180	-0.002	2.180	1.513	0.258	0.185	-0.500	-0.022	2.787	3.050	-31.2	34196.8	995	161	73	2	1
642	2.028	0.057	2.112	-0.013	2.112	1.445	0.284	0.190	-0.290	0.018	2.600	3.073	867.5	38808.1	995	153	71	2	1
641	2.028	0.038	2.095	-0.012	2.095	1.428	0.290	0.197	-0.135	-0.096	2.462	2.999	99.5	41030.5	997	211	99	2	1
640	2.028	0.019	2.043	-0.002	2.043	1.380	0.300	0.198	-0.241	-0.008	2.364	3.016	2075.3	42919.7	997	181	87	2	1
639	2.028	0.0	2.020	0.001	2.020	1.358	0.314	0.194	-0.123	-0.036	2.296	2.835	2992.2	44110.9	998	162	79	2	1
638	2.028	-0.019	2.012	-0.006	2.012	1.351	0.302	0.202	-0.149	0.013	2.254	2.899	-1437.3	43961.1	997	161	79	2	1
637	2.028	-0.038	2.053	-0.010	2.053	1.389	0.307	0.200	-0.194	0.082	2.200	3.064	-4100.0	44317.6	997	151	72	2	1
636	2.028	-0.057	2.089	-0.009	2.089	1.424	0.303	0.191	-0.294	0.080	2.393	2.833	-4739.2	41822.9	997	150	71	2	1
635	2.028	-0.076	2.166	-0.018	2.166	1.498	0.275	0.199	-0.260	0.097	2.461	2.822	-4202.6	39379.3	999	120	54	2	1
634	2.028	-0.095	2.218	-0.025	2.218	1.552	0.264	0.200	-0.378	-0.016	2.655	3.082	-3455.8	38041.1	995	102	45	2	1
633	2.028	-0.114	2.294	-0.011	2.294	1.632	0.244	0.189	-0.268	-0.036	2.699	2.749	-2081.5	33198.8	999	96	41	2	1
632	2.028	-0.133	2.376	-0.017	2.376	1.725	0.229	0.189	-0.195	-0.026	3.012	3.004	-1921.7	31351.3	993	108	44	2	1
631	2.028	-0.152	2.438	-0.009	2.438	1.798	0.202	0.177	0.018	-0.068	2.751	2.877	435.1	26364.1	992	108	43	2	1

NOTE: NEGATIVE R/D INDICATES MEASUREMENT ON OPPOSITE SIDE OF JET CENTERLINE (I.E. -Z/D)

V_∞ = 713.0 ft/sec T_t = 640.3 °R D = 0.986 in.

SEQ	x/D	r/D	V_x/V_∞	V_r/V_∞	$\|V\|/V_\infty$	M	S_x/V_∞	S_r/V_∞	SK_x	SK_r	KU_x	KU_r	RE_{xr}	TKE	N	PPS	PPL	SE	CC
1107	2.535	0.894	0.967	-0.047	0.968	0.574	0.021	0.122	-0.115	0.005	4.176	3.285	-79.3	7679.6	999	38	38	1	1
1108	2.535	0.856	0.964	-0.045	0.965	0.573	0.021	0.121	0.041	0.102	3.706	2.999	72.6	7554.4	995	30	31	1	1
1109	2.535	0.818	0.962	-0.046	0.963	0.571	0.018	0.122	0.093	0.043	3.941	3.052	89.0	7639.7	988	31	31	1	1
1110	2.535	0.780	0.968	-0.036	0.968	0.575	0.021	0.123	0.091	0.253	3.347	3.155	39.9	7816.8	988	36	36	1	1
1111	2.535	0.742	0.966	-0.049	0.967	0.574	0.020	0.123	0.120	0.077	3.796	3.240	-127.3	7741.6	990	31	31	1	1
1112	2.535	0.704	0.948	-0.040	0.949	0.562	0.020	0.122	0.115	-0.061	3.683	3.102	65.5	7617.2	994	20	21	1	0
1113	2.535	0.666	0.960	-0.047	0.962	0.570	0.021	0.130	0.207	0.091	4.031	2.963	27.4	8766.4	995	23	23	1	0
1114	2.535	0.628	0.958	-0.043	0.959	0.568	0.021	0.123	-0.217	0.071	4.159	2.868	19.5	7751.1	999	27	28	1	0
1115	2.535	0.590	0.950	-0.043	0.951	0.563	0.022	0.125	-0.009	-0.002	3.861	2.990	-22.1	8035.3	992	19	20	1	0
1116	2.535	0.551	0.950	-0.028	0.951	0.564	0.028	0.129	-0.549	-0.059	5.746	2.959	-20.3	8694.2	992	15	16	1	0
1117	2.535	0.513	0.941	-0.013	0.941	0.558	0.031	0.133	-0.295	-0.047	4.767	2.930	60.2	9264.8	986	10	11	1	0
1118	2.535	0.475	0.941	-0.019	0.941	0.557	0.043	0.132	0.666	-0.077	6.313	2.997	-160.0	9302.4	994	8	8	1	0
1119	2.535	0.437	0.955	-0.016	0.955	0.566	0.067	0.138	1.625	0.152	8.056	3.103	88.9	10890.6	973	3	3	1	0
1120	2.535	0.399	1.025	-0.001	1.025	0.610	0.136	0.141	1.751	-0.061	6.322	3.033	1295.5	14767.4	963	1	1	1	0
1121	2.535	0.361	1.255	-0.007	1.255	0.762	0.295	0.156	1.065	-0.080	3.517	3.073	1919.6	34460.3	365	0	0	1	0
1122	2.535	0.323	1.676	0.040	1.677	1.068	0.430	0.164	-0.236	-0.307	1.697	2.523	962.8	60629.9	32	0	0	1	0

V_∞ = 713.0 ft/sec T_t = 640.3 °R   D = 0.986 in.

SEQ	x/D	r/D	V_x/V_∞	V_r/V_∞	$\lvert V\rvert/V_\infty$	M	S_x/V_∞	S_r/V_∞	SK_x	SK_r	KU_x	KU_r	RE_{xr}	TKE	N	PPS	PPL	SE	CC
1490	2.535	0.780	0.962	-0.027	0.962	0.571	0.011	0.106	-0.125	0.094	6.151	2.757	0.0	5707.1	997	49	50	3	0
1489	2.535	0.742	0.966	-0.032	0.966	0.573	0.011	0.109	-0.562	0.066	7.555	2.851	386.5	6115.6	992	41	42	3	0
1488	2.535	0.704	0.963	-0.029	0.963	0.571	0.011	0.118	3.310	0.261	53.821	2.659	766.3	7085.1	983	30	31	3	1
1487	2.535	0.666	0.968	-0.012	0.968	0.574	0.039	0.124	6.128	0.230	44.801	3.286	2371.6	8228.7	966	28	28	3	1
1486	2.535	0.628	1.057	0.116	1.063	0.635	0.181	0.134	1.675	0.135	4.425	2.523	3650.7	17358.6	986	9	8	3	1
1485	2.535	0.590	1.098	0.103	1.102	0.661	0.200	0.111	1.141	0.121	3.045	2.932	2271.5	16380.8	996	13	12	3	1
1484	2.535	0.551	1.161	0.102	1.165	0.702	0.229	0.112	0.640	0.113	2.108	2.895	2744.0	19727.4	997	16	14	3	1
1483	2.535	0.513	1.186	0.093	1.190	0.718	0.247	0.107	0.713	-0.130	2.504	3.082	3055.4	21305.5	995	24	20	3	1
1482	2.535	0.475	1.281	0.090	1.285	0.782	0.268	0.106	0.342	0.012	2.145	3.364	2677.2	24046.7	998	32	25	3	1
1481	2.535	0.437	1.407	0.079	1.409	0.869	0.295	0.112	0.034	0.189	2.089	3.157	3721.7	28429.1	997	31	22	3	1
1480	2.535	0.399	1.640	0.065	1.641	1.040	0.299	0.118	-0.329	-0.010	2.338	3.011	3680.1	29757.6	997	42	25	3	0
1479	2.535	0.361	1.890	0.067	1.891	1.244	0.302	0.125	-0.580	0.112	2.591	3.196	5318.0	31077.1	997	48	25	3	0
1478	2.535	0.323	2.154	0.060	2.155	1.488	0.250	0.127	-0.938	-0.158	3.367	2.810	3805.1	24085.6	987	60	27	3	0
1477	2.535	0.285	2.302	0.051	2.303	1.642	0.179	0.129	-0.865	-0.059	3.783	3.228	1670.5	16691.9	982	59	25	3	0

V_∞ = 713.0 ft/sec $\qquad$ T_t = 640.3 °R $\qquad$ D = 0.986 in.

SEQ	x/D	r/D	V_x/V_∞	V_r/V_∞	$\lvert V\rvert/V_\infty$	M	S_x/V_∞	S_r/V_∞	SK_x	SK_r	KU_x	KU_r	RE_{xr}	TKE	N	PPS	PPL	SE	CC
721	2.535	0.723	1.131	0.022	1.131	0.680	0.217	0.224	1.036	-0.010	2.802	3.057	8623.0	37390.9	221	2	2	2	0
720	2.535	0.704	1.113	0.040	1.114	0.668	0.183	0.210	1.064	-0.255	2.868	2.802	6157.8	30866.8	301	3	3	2	0
719	2.535	0.685	1.207	0.062	1.209	0.731	0.210	0.208	0.345	-0.102	1.968	2.656	5784.9	33214.7	997	4	3	2	0
718	2.535	0.666	1.273	0.096	1.277	0.777	0.185	0.207	0.011	0.076	2.449	3.005	4250.4	30524.8	999	5	4	2	0
717	2.535	0.647	1.294	0.082	1.296	0.790	0.172	0.192	0.046	-0.036	2.899	3.082	2272.6	26248.5	995	8	6	2	0
716	2.535	0.628	1.312	0.086	1.315	0.803	0.164	0.192	0.098	-0.019	2.771	2.987	1837.3	25577.7	996	13	9	2	0
715	2.535	0.609	1.301	0.076	1.304	0.795	0.173	0.187	0.236	-0.048	2.921	2.983	2968.2	25458.0	994	18	14	2	0
714	2.535	0.590	1.266	0.061	1.268	0.771	0.159	0.191	0.287	0.037	2.926	2.967	1306.9	25049.5	992	28	22	2	0
713	2.535	0.570	1.313	0.079	1.315	0.803	0.176	0.171	0.387	0.060	2.959	2.902	1585.3	22728.0	998	43	32	2	0
712	2.535	0.551	1.285	0.070	1.287	0.784	0.186	0.163	0.374	0.195	2.807	3.029	1358.5	22300.3	996	91	70	2	0
711	2.535	0.532	1.289	0.060	1.290	0.786	0.182	0.173	0.435	0.096	2.899	2.977	1699.6	23614.0	996	111	85	2	0
710	2.535	0.513	1.322	0.093	1.325	0.810	0.197	0.125	0.438	0.065	2.717	2.988	2078.3	17806.0	1000	73	55	2	0
709	2.535	0.494	1.341	0.082	1.343	0.823	0.233	0.130	0.436	0.076	2.703	2.798	3354.9	22398.3	1000	89	66	2	0
708	2.535	0.475	1.368	0.070	1.370	0.841	0.249	0.129	0.408	0.114	2.414	2.722	4554.6	24228.7	1000	195	141	2	0
707	2.535	0.456	1.389	0.062	1.391	0.856	0.250	0.131	0.249	0.255	2.290	2.956	3617.0	24574.2	999	132	94	2	0
706	2.535	0.437	1.448	0.059	1.449	0.898	0.264	0.142	0.144	0.074	2.297	3.369	4769.3	27889.2	1000	222	153	2	0
705	2.535	0.418	1.537	0.074	1.538	0.963	0.288	0.138	-0.057	0.223	2.311	3.031	5177.0	30752.2	1000	182	118	2	1
704	2.535	0.399	1.622	0.070	1.624	1.027	0.301	0.135	-0.055	0.074	2.142	2.945	5933.9	32312.5	1000	306	188	2	1
703	2.535	0.380	1.730	0.065	1.732	1.111	0.314	0.145	-0.229	0.073	2.170	2.979	5509.7	35674.7	1000	163	93	2	1
702	2.535	0.361	1.890	0.074	1.891	1.244	0.280	0.124	-0.518	0.169	2.734	2.994	5960.4	27689.6	997	89	47	2	1
701	2.535	0.342	2.041	0.074	2.042	1.379	0.268	0.127	-0.745	0.026	3.000	3.043	4941.0	26418.5	996	90	43	2	1
700	2.535	0.323	2.141	0.080	2.142	1.475	0.245	0.132	-0.771	0.074	3.072	2.998	4913.3	24172.6	992	106	49	2	1
699	2.535	0.304	2.253	0.082	2.255	1.590	0.211	0.128	-1.009	-0.119	3.562	3.051	4252.3	19553.1	987	195	86	2	1
698	2.535	0.285	2.336	0.075	2.337	1.680	0.175	0.125	-0.780	-0.041	3.531	2.822	3038.5	15627.9	991	175	74	2	1
697	2.535	0.266	2.371	0.065	2.372	1.720	0.168	0.127	-0.740	0.161	3.174	2.758	2185.4	15388.6	986	126	53	2	1
696	2.535	0.247	2.399	0.050	2.399	1.752	0.172	0.126	-0.834	-0.022	3.658	3.030	2032.9	15612.5	988	129	53	2	1
695	2.535	0.228	2.440	0.031	2.440	1.800	0.173	0.164	-0.464	0.001	3.324	3.061	1389.7	21294.0	989	382	156	2	1
694	2.535	0.209	2.464	0.040	2.465	1.831	0.176	0.157	-0.418	-0.026	3.026	2.989	1322.0	20441.5	993	237	96	2	1
693	2.535	0.190	2.450	0.032	2.450	1.812	0.171	0.149	-0.244	0.008	2.783	2.924	470.6	18656.7	992	170	69	2	1
692	2.535	0.171	2.432	0.030	2.433	1.792	0.169	0.154	-0.057	-0.191	2.825	3.177	490.1	19299.3	993	137	56	2	1
691	2.535	0.152	2.449	0.029	2.450	1.812	0.168	0.153	-0.018	-0.185	2.693	3.146	-303.5	19096.1	991	104	42	2	1
690	2.535	0.133	2.426	0.018	2.426	1.783	0.173	0.148	-0.207	-0.007	3.182	2.999	-841.6	18656.1	991	119	49	2	1
689	2.535	0.114	2.423	0.017	2.423	1.780	0.178	0.151	-0.347	0.085	2.830	2.983	-514.2	19636.9	991	195	80	2	1
688	2.535	0.095	2.353	0.019	2.353	1.699	0.199	0.149	-0.408	0.073	2.950	3.194	-753.3	21412.3	998	100	42	2	1
687	2.535	0.076	2.318	0.019	2.318	1.659	0.218	0.146	-0.518	-0.107	2.718	3.157	-1023.7	22882.9	994	113	48	2	1
686	2.535	0.057	2.286	0.005	2.286	1.624	0.225	0.153	-0.414	0.232	2.929	3.111	-1096.0	24683.4	998	92	40	2	1
685	2.535	0.038	2.254	0.017	2.254	1.589	0.236	0.155	-0.367	0.086	2.490	2.984	-146.3	26381.8	998	105	46	2	1
684	2.535	0.019	2.217	0.008	2.217	1.550	0.239	0.158	-0.258	0.093	2.448	3.146	80.8	27316.8	997	75	33	2	1
683	2.535	0.0	2.202	0.007	2.202	1.535	0.240	0.153	-0.335	-0.030	2.371	3.040	929.0	26518.8	998	69	31	2	1
682	2.535	-0.019	2.209	-0.004	2.209	1.543	0.253	0.149	-0.301	-0.111	2.350	2.954	-2048.0	27602.1	998	139	63	2	1
681	2.535	-0.038	2.235	-0.013	2.235	1.569	0.267	0.152	-0.256	0.035	2.464	2.845	-1242.9	29880.5	1000	60	26	2	1
679	2.535	-0.057	2.274	-0.014	2.274	1.611	0.235	0.159	-0.354	-0.008	2.656	3.073	-1505.4	26830.7	995	73	32	2	1
678	2.535	-0.076	2.313	-0.004	2.313	1.653	0.229	0.162	-0.319	-0.021	2.800	2.867	-2321.4	26738.6	995	54	23	2	1
677	2.535	-0.095	2.347	0.003	2.347	1.692	0.194	0.153	-0.383	-0.065	2.843	3.124	-1588.1	21381.1	989	53	22	2	1
676	2.535	-0.114	2.387	0.009	2.387	1.737	0.199	0.156	-0.350	0.111	3.064	2.678	-1877.9	22396.7	993	61	25	2	1
675	2.535	-0.133	2.428	-0.003	2.428	1.785	0.187	0.149	-0.203	0.099	3.050	2.994	-1842.3	20252.6	994	70	28	2	1
674	2.535	-0.152	2.470	0.002	2.470	1.838	0.167	0.166	-0.094	0.094	2.938	3.013	-1678.6	21058.6	992	31	12	2	1

NOTE: NEGATIVE R/D INDICATES MEASUREMENT ON OPPOSITE SIDE OF JET CENTERLINE (I.E. -Z/D)

V_∞ = 713.0 ft/sec T_t = 640.3 °R D = 0.986 in.

SEQ	x/D	r/D	V_x/V_∞ H	V_r/V_∞ I	$\|V\|/V_\infty$	M	S_x/V_∞ B	S_r/V_∞ C	SK_x	SK_r	KU_x	KU_r	RE_{xr} A	TKE	N	PPS	PPL	SE	CC
1367	3.043	1.274	0.970	-0.046	0.971	0.576	0.046	0.136	-1.344	0.116	7.236	3.127	-298.9	9983.6	993	60	62	1	1
1368	3.043	1.198	0.968	-0.036	0.968	0.575	0.044	0.148	-0.500	0.021	4.350	3.322	-221.6	11689.4	997	94	96	1	1
1371	3.043	1.122	0.962	-0.037	0.962	0.571	0.038	0.151	-0.431	0.026	3.959	3.256	171.7	11926.4	998	88	90	1	1
1372	3.043	1.046	0.969	-0.039	0.970	0.576	0.031	0.144	-0.157	0.026	3.610	3.203	-100.7	10767.0	986	89	92	1	1
1375	3.043	0.970	0.964	-0.033	0.965	0.572	0.034	0.148	-0.828	0.118	5.966	3.339	-181.7	11430.0	998	102	105	1	1
1123	3.043	0.894	0.965	-0.050	0.967	0.573	0.021	0.130	0.147	0.069	3.680	3.087	42.9	8731.1	988	44	44	1	1
1124	3.043	0.856	0.961	-0.049	0.963	0.571	0.023	0.127	-0.183	0.061	3.957	3.059	172.7	8319.3	999	42	42	1	1
1125	3.043	0.818	0.958	-0.042	0.958	0.568	0.021	0.120	-0.017	-0.015	3.479	2.999	-19.8	7475.9	996	37	38	1	1
1126	3.043	0.780	0.963	-0.042	0.964	0.572	0.024	0.123	0.051	0.014	3.330	3.039	11.8	7802.9	997	28	28	1	1
1127	3.043	0.742	0.962	-0.043	0.963	0.571	0.024	0.125	-0.157	0.096	3.346	3.236	-91.5	8075.2	994	29	29	1	1
1128	3.043	0.704	0.961	-0.037	0.961	0.570	0.020	0.128	0.052	0.021	3.628	2.740	-52.6	8446.1	996	25	25	1	1
1129	3.043	0.666	0.958	-0.036	0.959	0.569	0.020	0.128	-0.175	0.007	4.692	3.099	137.8	8491.0	999	26	27	1	0
1130	3.043	0.628	0.955	-0.035	0.956	0.567	0.021	0.128	0.196	0.100	3.547	3.072	-63.9	8490.1	990	22	23	1	0
1131	3.043	0.590	0.956	-0.028	0.956	0.567	0.021	0.127	-0.179	-0.064	3.684	2.904	28.2	8360.4	987	23	23	1	0
1132	3.043	0.551	0.956	-0.023	0.956	0.567	0.026	0.129	-0.230	-0.007	3.772	2.869	-71.2	8565.8	984	17	17	1	0
1133	3.043	0.513	0.953	-0.018	0.953	0.565	0.034	0.127	0.028	-0.069	4.881	2.712	12.0	8486.6	983	13	13	1	0
1134	3.043	0.475	0.969	-0.005	0.969	0.575	0.048	0.136	0.815	0.085	4.971	3.208	443.5	9943.9	975	9	9	1	0
1135	3.043	0.437	1.024	-0.005	1.024	0.610	0.101	0.137	1.241	-0.146	4.298	3.013	595.3	12165.9	974	4	4	1	0
1136	3.043	0.399	1.123	0.002	1.123	0.674	0.178	0.154	1.244	0.063	4.449	3.021	-150.4	20094.9	489	1	1	1	0
1137	3.043	0.361	1.475	0.033	1.475	0.916	0.325	0.148	0.329	0.115	1.936	2.618	12332.7	38048.7	28	0	0	1	0

V_∞ = 713.0 ft/sec　　T_t = 640.3 °R　　D = 0.986 in.

SEQ	x/D	r/D	V_x/V_∞ H	V_r/V_∞ I	$\lvert V\rvert/V_\infty$	M	S_x/V_∞ B	S_r/V_∞ C	SK_x	SK_r	KU_x	KU_r	RE_{xr} A	TKE	N	PPS	PPL	SE	CC
1463	3.043	0.780	0.963	-0.030	0.964	0.572	0.011	0.098	-0.497	0.147	6.851	2.841	11.2	4961.1	995	153	156	3	0
1464	3.043	0.742	0.963	-0.018	0.963	0.572	0.013	0.107	0.902	0.139	17.498	2.884	85.3	5892.7	982	100	103	3	0
1465	3.043	0.704	0.970	-0.007	0.970	0.576	0.023	0.108	3.768	0.193	30.068	3.182	845.0	6029.4	967	122	123	3	0
1466	3.043	0.666	0.976	-0.002	0.976	0.580	0.064	0.112	3.503	0.081	14.929	2.950	528.6	7412.2	974	80	81	3	1
1467	3.043	0.628	1.014	0.012	1.015	0.604	0.115	0.117	1.918	0.192	5.524	2.923	1786.9	10359.3	980	88	85	3	1
1468	3.043	0.590	1.048	0.029	1.049	0.626	0.133	0.118	1.276	0.086	3.583	2.932	1160.8	11507.6	983	108	101	3	1
1469	3.043	0.551	1.028	0.021	1.028	0.613	0.130	0.116	1.611	0.111	4.655	3.215	1920.4	11177.6	982	126	120	3	1
1470	3.043	0.513	1.128	0.034	1.128	0.678	0.188	0.119	0.956	0.093	3.048	2.857	2134.5	16158.5	995	128	112	3	1
1471	3.043	0.475	1.198	0.029	1.199	0.724	0.216	0.117	0.695	-0.024	2.661	2.762	1720.7	18781.8	994	134	109	3	1
1472	3.043	0.437	1.373	0.029	1.373	0.843	0.260	0.131	0.246	0.011	2.244	3.106	3030.7	25879.8	995	123	88	3	1
1473	3.043	0.399	1.589	0.022	1.589	1.001	0.299	0.136	0.110	-0.005	2.229	2.894	3748.9	32031.6	1000	125	77	3	1
1474	3.043	0.361	1.899	0.057	1.899	1.251	0.288	0.121	-0.568	0.014	2.582	3.491	4265.1	28523.9	995	59	30	3	0
1475	3.043	0.323	2.095	0.040	2.095	1.429	0.244	0.114	-0.792	0.036	3.066	3.136	2790.9	21703.9	989	42	20	3	0
1476	3.043	0.285	2.234	-0.002	2.234	1.568	0.202	0.110	-0.623	-0.126	2.986	3.038	1907.6	16536.4	991	12	5	3	0

V_∞ = 713.0 ft/sec T_t = 640.3 °R D = 0.986 in.

SEQ	x/D	r/D	V_x/V_∞	V_r/V_∞	$\lvert V\rvert/V_\infty$	M	S_x/V_∞	S_r/V_∞	SK_x	SK_r	KU_x	KU_r	RE_{xr}	TKE	N	PPS	PPL	SE	CC
769	3.043	0.723	1.196	0.029	1.196	0.723	0.187	0.198	0.328	-0.044	2.147	2.950	5584.0	28888.0	559	5	4	2	0
768	3.043	0.704	1.163	0.021	1.163	0.701	0.181	0.194	0.527	-0.033	2.370	2.911	3755.3	27448.6	994	9	8	2	0
767	3.043	0.685	1.242	0.038	1.242	0.753	0.164	0.188	0.053	0.068	2.673	2.966	3021.5	24918.7	986	14	11	2	0
766	3.043	0.666	1.287	0.085	1.289	0.785	0.151	0.178	0.206	-0.104	2.952	3.099	2961.9	21917.8	996	18	14	2	0
765	3.043	0.647	1.268	0.069	1.270	0.772	0.147	0.171	0.354	-0.108	3.228	3.184	1717.5	20352.4	996	43	33	2	0
764	3.043	0.628	1.252	0.055	1.253	0.761	0.139	0.165	0.380	-0.032	2.951	3.152	483.6	18792.2	995	60	47	2	0
763	3.043	0.609	1.248	0.051	1.249	0.758	0.135	0.173	0.560	0.114	2.930	3.069	1748.4	19787.6	993	67	53	2	0
762	3.043	0.590	1.229	0.040	1.230	0.745	0.145	0.153	0.596	-0.030	2.903	2.893	1212.4	17309.8	997	63	51	2	0
761	3.043	0.570	1.218	0.042	1.218	0.737	0.161	0.162	0.742	0.097	3.075	3.052	1302.1	19889.9	996	143	117	2	0
760	3.043	0.551	1.261	0.044	1.262	0.767	0.173	0.125	0.640	0.100	2.961	3.031	1682.4	15565.6	990	82	65	2	0
759	3.043	0.532	1.271	0.040	1.272	0.773	0.183	0.126	0.529	-0.051	2.632	2.852	1822.7	16606.2	996	102	80	2	0
758	3.043	0.513	1.256	0.040	1.256	0.763	0.187	0.124	0.586	-0.021	2.788	2.915	1733.0	16632.7	998	135	107	2	0
757	3.043	0.494	1.299	0.043	1.300	0.793	0.206	0.124	0.517	-0.012	2.634	2.728	1333.2	18577.1	999	148	114	2	0
756	3.043	0.475	1.320	0.043	1.320	0.807	0.220	0.122	0.505	0.108	2.521	3.014	2537.6	19804.9	997	200	151	2	0
755	3.043	0.456	1.374	0.043	1.374	0.844	0.247	0.134	0.428	0.027	2.350	2.958	2842.4	24691.5	1000	256	186	2	0
754	3.043	0.437	1.442	0.047	1.443	0.893	0.255	0.129	0.298	0.096	2.391	3.122	3307.9	25010.4	1000	105	72	2	0
753	3.043	0.418	1.518	0.042	1.518	0.948	0.279	0.137	0.265	0.094	2.382	2.859	3524.7	29343.9	1000	150	98	2	0
752	3.043	0.399	1.589	0.044	1.589	1.001	0.283	0.138	0.126	0.022	2.309	2.722	4064.4	30044.7	999	282	177	2	0
751	3.043	0.380	1.715	0.044	1.716	1.099	0.306	0.144	-0.055	0.041	2.068	3.019	6206.4	34339.9	999	183	106	2	1
750	3.043	0.361	1.865	0.062	1.866	1.222	0.310	0.141	-0.331	0.099	2.298	3.143	7156.2	34498.6	1000	265	141	2	1
749	3.043	0.342	1.995	0.066	1.997	1.337	0.287	0.150	-0.588	0.142	2.575	2.895	5730.2	32321.3	997	238	119	2	1
748	3.043	0.323	2.090	0.064	2.091	1.425	0.273	0.147	-0.845	0.085	3.194	2.819	3868.6	29953.1	998	214	102	2	1
747	3.043	0.304	2.176	0.052	2.177	1.510	0.246	0.144	-0.697	0.177	2.846	3.040	3599.0	25945.3	996	204	93	2	1
746	3.043	0.285	2.233	0.040	2.233	1.567	0.214	0.137	-0.699	0.021	3.056	3.186	2997.0	21111.5	993	178	79	2	1
745	3.043	0.266	2.307	0.031	2.307	1.646	0.201	0.147	-0.789	-0.269	3.334	3.066	2397.1	21227.7	997	189	82	2	1
744	3.043	0.247	2.337	0.018	2.337	1.680	0.203	0.147	-0.518	0.054	2.879	2.974	1525.0	21541.5	992	293	125	2	1
743	3.043	0.228	2.379	0.019	2.378	1.727	0.180	0.150	-0.330	-0.178	2.895	2.918	1770.8	19612.7	990	194	81	2	1
742	3.043	0.209	2.414	0.037	2.415	1.770	0.174	0.162	-0.213	0.031	2.925	2.941	1844.5	21061.2	989	253	104	2	1
741	3.043	0.190	2.446	0.018	2.446	1.808	0.162	0.164	-0.121	-0.035	2.944	3.026	628.4	20249.2	993	127	52	2	1
740	3.043	0.171	2.464	0.042	2.464	1.830	0.159	0.168	-0.101	-0.119	2.728	2.897	301.4	20743.2	991	135	54	2	1
739	3.043	0.152	2.469	0.031	2.470	1.837	0.151	0.155	-0.049	-0.011	2.915	2.800	-189.5	18042.0	997	94	38	2	1
738	3.043	0.133	2.465	0.032	2.465	1.831	0.155	0.157	0.002	-0.029	2.670	2.875	-188.4	18605.6	996	134	54	2	1
737	3.043	0.114	2.451	0.024	2.451	1.814	0.160	0.167	-0.221	-0.067	2.665	3.207	-504.5	20670.3	995	104	42	2	1
736	3.043	0.095	2.441	0.024	2.441	1.802	0.181	0.161	-0.420	-0.090	2.798	2.950	-1814.7	21555.9	993	91	37	2	1
735	3.043	0.076	2.407	0.030	2.407	1.761	0.191	0.165	-0.495	0.005	2.696	3.193	-989.4	23119.3	998	110	45	2	1
734	3.043	0.057	2.378	0.022	2.379	1.727	0.209	0.154	-0.283	-0.050	2.543	2.943	-305.8	23148.8	998	102	42	2	1
733	3.043	0.038	2.347	0.027	2.347	1.691	0.213	0.159	-0.309	-0.074	2.361	2.916	-463.3	24388.4	996	81	34	2	1
732	3.043	0.019	2.338	0.016	2.338	1.681	0.229	0.154	-0.315	0.022	2.466	2.989	240.1	25359.6	998	94	40	2	1
731	3.043	0.0	2.331	0.018	2.331	1.673	0.213	0.157	-0.132	-0.033	2.328	2.976	-445.0	24021.5	998	83	35	2	1
730	3.043	-0.019	2.317	-0.006	2.317	1.657	0.216	0.160	-0.229	-0.013	2.414	2.914	-1156.4	24890.8	994	74	31	2	1
729	3.043	-0.038	2.330	-0.002	2.330	1.672	0.222	0.159	-0.164	0.104	2.301	2.696	-893.3	25453.8	999	243	104	2	1
728	3.043	-0.057	2.354	-0.004	2.354	1.700	0.220	0.167	-0.216	0.017	2.468	2.976	-1223.4	26525.2	996	245	104	2	1
727	3.043	-0.076	2.369	0.008	2.369	1.716	0.202	0.160	-0.297	-0.017	2.689	3.119	-1545.3	23353.5	996	89	37	2	1
726	3.043	-0.095	2.408	0.023	2.408	1.762	0.194	0.139	-0.338	0.090	2.679	3.040	-179.3	19377.3	996	61	25	2	1
725	3.043	-0.114	2.425	0.025	2.425	1.782	0.189	0.153	-0.305	0.010	2.631	3.006	-1828.4	20942.7	994	43	17	2	1
724	3.043	-0.133	2.451	0.028	2.451	1.813	0.178	0.153	-0.217	0.058	2.772	2.905	-1155.2	19925.3	994	49	20	2	1
723	3.043	-0.152	2.501	0.042	2.502	1.877	0.175	0.185	-0.360	0.056	2.894	3.110	-1976.4	25198.1	987	107	42	2	1

NOTE: NEGATIVE R/D INDICATES MEASUREMENT ON OPPOSITE SIDE OF JET CENTERLINE (I.E. -Z/D)

V_∞ = 713.0 ft/sec T_t = 640.3 °R D = 0.986 in.

SEQ	x/D	r/D	V_x/V_∞	V_r/V_∞	$\|V\|/V_\infty$	M	S_x/V_∞	S_r/V_∞	SK_x	SK_r	KU_x	KU_r	RE_{xr}	TKE	N	PPS	PPL	SE	CC
892	3.550	1.578	0.965	-0.044	0.966	0.573	0.015	0.095	0.260	0.072	4.730	2.732	10.1	4682.5	994	47	46	1	1
893	3.550	1.502	0.959	-0.052	0.960	0.569	0.014	0.097	-0.219	0.076	5.461	3.122	27.9	4805.2	994	206	205	1	1
894	3.550	1.426	0.960	-0.050	0.962	0.570	0.019	0.097	0.014	0.207	4.672	3.034	-11.9	4881.4	993	163	162	1	1
895	3.550	1.350	0.959	-0.050	0.960	0.569	0.012	0.098	-0.466	0.133	6.331	2.958	24.1	4930.7	994	341	341	1	1
896	3.550	1.274	0.961	-0.047	0.962	0.571	0.011	0.096	0.046	0.226	6.795	2.733	-32.8	4711.5	994	338	337	1	1
897	3.550	1.198	0.960	-0.052	0.962	0.570	0.013	0.098	0.069	0.058	6.068	3.055	-29.8	4953.8	994	364	363	1	1
898	3.550	1.122	0.960	-0.046	0.961	0.570	0.011	0.096	0.199	0.162	7.109	2.713	-5.0	4730.2	996	431	430	1	1
899	3.550	1.046	0.962	-0.060	0.964	0.572	0.013	0.093	0.349	0.212	6.016	2.935	105.7	4483.1	991	1120	1115	1	1
900	3.550	0.970	0.962	-0.059	0.963	0.571	0.016	0.097	0.085	0.174	4.961	2.744	-48.3	4881.1	994	1390	1383	1	1
901	3.550	0.932	0.962	-0.057	0.964	0.572	0.013	0.099	0.476	0.085	5.902	2.902	8.5	5071.9	992	1042	1037	1	1
902	3.550	0.894	0.958	-0.055	0.960	0.569	0.013	0.094	0.041	0.182	6.528	2.966	6.5	4527.9	995	1173	1171	1	1
903	3.550	0.856	0.959	-0.059	0.960	0.570	0.013	0.102	-0.133	0.222	6.011	3.058	4.5	5300.6	993	915	913	1	1
904	3.550	0.818	0.958	-0.058	0.959	0.569	0.015	0.099	-0.113	0.107	4.933	2.874	-25.8	5080.0	997	747	746	1	1
905	3.550	0.780	0.959	-0.058	0.960	0.570	0.013	0.099	0.412	0.154	5.353	2.975	3.1	5024.8	993	1053	1051	1	1
906	3.550	0.742	0.960	-0.060	0.962	0.571	0.013	0.098	-0.174	0.127	6.278	2.929	16.5	4916.3	998	610	608	1	1
907	3.550	0.704	0.960	-0.054	0.961	0.570	0.012	0.100	0.195	0.095	5.665	3.029	41.8	5079.5	995	533	532	1	1
908	3.550	0.666	0.959	-0.051	0.960	0.569	0.013	0.096	0.204	0.086	5.285	3.097	40.7	4753.2	994	386	386	1	0
909	3.550	0.647	0.958	-0.055	0.960	0.569	0.012	0.097	-0.080	0.022	5.661	3.067	35.7	4796.2	997	200	200	1	0
910	3.550	0.628	0.958	-0.052	0.960	0.569	0.011	0.095	0.081	0.178	6.470	2.858	37.4	4629.8	994	157	157	1	0
911	3.550	0.609	0.960	-0.056	0.961	0.570	0.013	0.096	-0.119	0.112	5.146	2.880	16.2	4712.9	994	133	132	1	0
912	3.550	0.590	0.958	-0.050	0.959	0.569	0.014	0.096	0.107	0.030	5.469	2.971	38.2	4695.4	992	130	130	1	0
913	3.550	0.570	0.960	-0.051	0.961	0.570	0.016	0.096	0.582	0.088	7.378	3.072	97.4	4769.1	998	64	64	1	0
914	3.550	0.551	0.961	-0.044	0.962	0.570	0.017	0.102	-0.023	-0.051	4.725	2.934	63.2	5372.3	997	46	46	1	0
915	3.550	0.532	0.962	-0.046	0.963	0.571	0.019	0.097	0.199	0.091	4.300	2.970	115.5	4883.8	990	28	28	1	0
916	3.550	0.513	0.964	-0.051	0.965	0.573	0.022	0.102	0.631	-0.002	7.497	3.127	24.3	5409.9	992	15	15	1	0
917	3.550	0.494	0.975	-0.043	0.976	0.580	0.037	0.104	2.087	0.073	11.640	2.887	275.9	5805.4	994	8	8	1	0
918	3.550	0.475	0.995	-0.047	0.996	0.592	0.057	0.145	1.908	-0.106	8.395	2.781	314.5	11568.6	991	39	37	1	0
919	3.550	0.456	1.021	-0.038	1.022	0.608	0.080	0.155	1.698	0.030	6.413	2.894	1952.6	13783.8	978	33	31	1	0
920	3.550	0.437	1.067	-0.060	1.068	0.639	0.116	0.167	1.540	0.001	5.300	3.021	2170.6	17641.9	978	13	11	1	0
921	3.550	0.418	1.114	-0.055	1.116	0.669	0.153	0.170	1.413	0.184	4.818	3.114	4584.5	20642.5	976	8	6	1	0
922	3.550	0.399	1.193	-0.063	1.195	0.722	0.202	0.168	1.289	-0.059	4.473	3.221	5017.4	24633.9	972	3	3	1	0
923	3.550	0.380	1.346	-0.060	1.347	0.826	0.300	0.180	1.045	0.098	3.373	3.007	7492.4	39472.3	994	2	1	1	0
924	3.550	0.361	1.526	-0.026	1.526	0.954	0.333	0.190	0.490	0.063	2.448	2.747	9045.1	46608.6	511	1	0	1	0

V_∞ = 713.0 ft/sec T_t = 640.3 °R   D = 0.986 in.

SEQ	x/D	r/D	V_x/V_∞	V_r/V_∞	$\lvert V\rvert/V_\infty$	M	S_x/V_∞	S_r/V_∞	SK_x	SK_r	KU_x	KU_r	RE_{xr}	TKE	N	PPS	PPL	SE	CC
819	3.550	0.780	1.069	0.002	1.069	0.639	0.148	0.192	1.057	-0.069	3.175	2.910	3843.7	24284.4	728	5	5	2	0
818	3.550	0.761	1.146	0.062	1.148	0.690	0.159	0.194	0.311	0.043	2.389	2.812	3652.5	25618.8	988	5	4	2	0
817	3.550	0.742	1.146	0.043	1.147	0.690	0.157	0.196	0.509	0.079	2.817	3.158	3333.7	25772.6	980	6	5	2	0
816	3.550	0.723	1.176	0.070	1.178	0.711	0.144	0.195	0.180	-0.023	2.722	3.026	1835.4	24511.2	985	7	6	2	0
815	3.550	0.704	1.165	0.055	1.167	0.703	0.143	0.185	0.421	0.001	3.146	2.967	2192.8	22594.7	977	8	6	2	0
814	3.550	0.685	1.190	0.044	1.190	0.719	0.142	0.199	0.526	0.159	3.161	3.065	2197.8	25246.5	984	13	11	2	0
813	3.550	0.666	1.215	0.062	1.217	0.736	0.127	0.171	0.438	0.150	2.940	3.085	2006.4	19045.5	992	19	16	2	0
812	3.550	0.647	1.203	0.063	1.205	0.728	0.132	0.172	0.596	0.130	3.198	3.090	1371.6	19445.3	994	30	25	2	0
811	3.550	0.628	1.204	0.056	1.205	0.728	0.137	0.156	0.624	0.000	3.164	2.958	1561.7	17085.1	991	38	32	2	0
810	3.550	0.609	1.208	0.054	1.209	0.731	0.146	0.158	0.700	0.131	3.116	2.886	851.6	18090.9	994	55	45	2	0
809	3.550	0.590	1.188	0.050	1.189	0.718	0.142	0.152	0.755	-0.111	3.058	3.064	128.2	16907.8	989	85	71	2	0
808	3.550	0.570	1.184	0.044	1.185	0.715	0.144	0.160	0.735	0.038	3.095	2.917	1037.7	18313.5	989	126	106	2	0
807	3.550	0.551	1.227	0.075	1.229	0.744	0.165	0.113	0.744	0.136	2.960	2.841	1441.8	13403.6	995	61	50	2	0
806	3.550	0.532	1.230	0.061	1.232	0.746	0.162	0.120	0.650	0.100	2.945	2.850	1328.1	13976.3	994	136	110	2	0
805	3.550	0.513	1.251	0.063	1.253	0.761	0.191	0.121	0.789	-0.032	3.130	2.943	2125.3	16725.4	994	188	150	2	0
804	3.550	0.494	1.286	0.067	1.287	0.784	0.207	0.126	0.624	0.042	2.694	2.805	2295.8	19006.0	996	127	98	2	0
803	3.550	0.475	1.326	0.063	1.327	0.811	0.215	0.130	0.585	0.039	2.771	2.938	2676.1	20274.1	997	129	97	2	0
802	3.550	0.456	1.386	0.063	1.387	0.853	0.243	0.132	0.461	0.136	2.487	2.913	2871.6	23916.0	999	180	129	2	0
801	3.550	0.437	1.467	0.066	1.468	0.911	0.276	0.133	0.393	-0.006	2.366	2.930	4544.4	28324.5	1000	177	120	2	0
800	3.550	0.418	1.548	0.066	1.549	0.971	0.290	0.134	0.244	-0.026	2.170	2.890	4243.5	30499.9	1000	193	124	2	0
799	3.550	0.399	1.679	0.060	1.680	1.071	0.296	0.137	0.047	0.224	2.101	3.131	6635.6	31866.0	999	285	169	2	0
798	3.550	0.380	1.757	0.080	1.758	1.133	0.292	0.141	-0.178	-0.060	2.142	2.886	3819.6	31673.7	1000	573	325	2	1
797	3.550	0.361	1.892	0.070	1.894	1.246	0.292	0.139	-0.443	-0.101	2.303	2.996	5861.5	31521.3	1000	257	135	2	1
796	3.550	0.342	1.972	0.063	1.973	1.316	0.274	0.138	-0.588	-0.019	2.907	2.926	4940.6	28834.2	997	453	229	2	1
795	3.550	0.323	2.043	0.065	2.044	1.381	0.264	0.145	-0.596	0.044	2.735	3.172	4917.1	28481.4	994	308	150	2	1
794	3.550	0.304	2.134	0.051	2.135	1.468	0.243	0.145	-0.696	0.039	3.151	2.982	3824.6	25686.8	994	309	144	2	1
793	3.550	0.285	2.184	0.054	2.184	1.517	0.226	0.141	-0.668	0.004	2.886	2.882	3672.7	23094.4	996	269	123	2	1
792	3.550	0.266	2.239	0.044	2.239	1.574	0.219	0.138	-0.534	-0.100	2.828	2.856	2500.0	21937.6	994	187	83	2	1
791	3.550	0.247	2.316	0.045	2.317	1.657	0.195	0.143	-0.451	-0.040	2.995	2.937	1926.6	20019.5	995	236	101	2	1
790	3.550	0.228	2.372	0.040	2.372	1.720	0.198	0.148	-0.491	-0.095	2.946	3.016	1843.2	21130.1	996	231	97	2	1
789	3.550	0.209	2.413	0.032	2.413	1.768	0.181	0.156	-0.480	0.033	2.993	3.027	1842.7	20681.6	989	192	79	2	1
788	3.550	0.190	2.449	0.026	2.450	1.812	0.165	0.152	-0.414	-0.142	2.761	3.045	1608.9	18577.6	992	124	50	2	1
787	3.550	0.171	2.486	0.020	2.486	1.858	0.161	0.145	-0.325	0.011	2.882	3.217	1498.9	17258.9	995	203	81	2	1
786	3.550	0.152	2.499	0.030	2.499	1.874	0.156	0.146	-0.292	-0.021	2.785	3.008	107.9	17052.2	991	235	94	2	1
785	3.550	0.133	2.516	0.035	2.516	1.896	0.150	0.144	-0.270	0.008	2.757	2.863	-208.5	16203.2	995	88	35	2	1
784	3.550	0.114	2.514	0.035	2.515	1.894	0.154	0.144	-0.216	0.116	2.967	3.011	-145.7	16624.3	994	73	29	2	1
783	3.550	0.095	2.493	0.029	2.493	1.866	0.166	0.140	-0.426	-0.199	2.654	3.077	-711.8	16998.7	998	117	46	2	1
782	3.550	0.076	2.469	0.022	2.469	1.836	0.178	0.135	-0.478	0.091	2.714	2.934	-305.4	17404.2	997	183	74	2	1
781	3.550	0.057	2.453	0.021	2.453	1.817	0.184	0.141	-0.472	-0.057	2.603	2.775	-432.7	18740.4	994	81	32	2	1
780	3.550	0.038	2.425	0.028	2.425	1.782	0.190	0.140	-0.236	0.002	2.383	2.926	54.6	19136.5	997	61	25	2	1
779	3.550	0.019	2.400	0.021	2.400	1.752	0.198	0.142	-0.292	-0.046	2.536	2.893	-381.9	20200.3	1000	143	59	2	1
778	3.550	0.0	2.410	0.026	2.410	1.764	0.192	0.143	-0.296	-0.049	2.334	3.108	491.8	19735.2	998	99	41	2	1
777	3.550	-0.019	2.403	-0.017	2.403	1.756	0.195	0.143	-0.120	0.064	2.556	3.081	-1289.9	20005.2	999	75	31	2	1
776	3.550	-0.038	2.392	-0.023	2.392	1.743	0.197	0.138	-0.183	0.163	2.515	2.845	-666.4	19488.5	999	57	24	2	1
775	3.550	-0.057	2.410	-0.010	2.410	1.765	0.189	0.137	-0.164	0.013	2.235	3.047	-1662.1	18663.8	999	91	37	2	1
774	3.550	-0.076	2.424	-0.008	2.424	1.781	0.199	0.149	-0.187	0.035	2.580	2.872	-1332.2	21443.4	998	100	41	2	1
773	3.550	-0.095	2.450	-0.010	2.450	1.813	0.189	0.146	-0.351	-0.050	2.561	3.099	-1183.0	19979.2	998	48	19	2	1
772	3.550	-0.114	2.481	-0.011	2.481	1.851	0.181	0.155	-0.251	0.040	2.574	2.813	-1730.5	20565.5	995	82	33	2	1
771	3.550	-0.133	2.490	-0.012	2.490	1.862	0.172	0.147	-0.350	-0.012	2.700	2.828	-1792.5	18430.7	992	51	20	2	1
770	3.550	-0.152	2.483	-0.009	2.483	1.854	0.176	0.140	-0.257	-0.029	2.647	2.799	-1525.9	17817.9	997	58	23	2	1

NOMENCLATURE

A	Area under a velocity probability distribution curve, Eq. (4)
A_j, B_j, C_j, E_j, C_{fs}, G_{fs}, E_{fs}, H_j, $M1_j$, $M2_j$	Velocity profile characteristic notation, (Fig. 15)
C^2	Crocco number squared, ft^2/sec^2
CC	Data condition code
C_p	Afterbody pressure coefficient, $(P - P_\infty)/q_\infty$
cp	Specific heat at constant pressure, ft-lbf/slug °R
D	Maximum model diameter, in. (Fig. 2b)
KU	Sample Kurtosis parameter
ℓ	Afterbody contour coordinate, in. (Fig. 2a), and pressure orifice coordinate, in. (Fig. 6)
M	Mach number
N	Number of particle realizations in a sample
NSPR	Nozzle exit static-to-free-stream static pressure ratio, P_e/P_∞
P	Static pressure, psia
PPL	Particle number density parameter
PPS	Particle realization rate
q	Dynamic pressure, psi
R	Reynolds shear stress, ft^2/sec^2

r	Afterbody contour coordinate, in. (Fig. 2a)
S	Sample standard deviation, ft/sec
SE	Seeding condition code
SEQ	File sequence number for data point identification
SK	Sample skewness parameter
t	Time required to obtain sample, sec
Tt	Total temperature, °R
TKE	Turbulence kinetic energy, per unit mass
$\overline{V}$	Mean velocity vector
$\|V\|$	Magnitude of $\overline{V}$, ft/sec
VAR	Sample variance, ft²/sec²
V_k	Mean of the kth component velocity sample, kth component of $\overline{V}$, ft/sec
V_{k_i}	Magnitude of the kth component of velocity obtained from the ith particle realization, ft/sec
V_∞	Free-stream velocity, ft/sec
x, y, z	Tunnel coordinates, rectangular Cartesian (Figs. 7-8)
x, r	Cylindrical body coordinates corresponding to x and $\|z\|$ tunnel coordinates when y = 0
σ	Turbulent mixing similarity parameter
ϕ	Angle of pressure orifice, deg (Fig. 6)
Ω	Intermittency factor [Eqs. (1-4)]

Subscripts

e, e1, e2	Experimentally determined [Eqs. (2-4)] and nozzle exit conditions
fs	Free-stream seeded
i	Associated with ith particle realization
j	Jet seeded
ℓ	Local condition
x, y, z, r	Coordinate direction
∞	Tunnel free-stream condition

Superscripts

a	Indicated average value [Eq. (1)]
d	Dual seeded [Eqs. (2-3)]
fs	Free-stream seeded [Eqs. (1-2)]
fsm	Dual seeded free-stream mode [Eqs. (3-4)]
j	Jet seeded [Eqs. (1-2)]
jm	Dual seeded jet mode [Eqs. (3-4)]